MICROELECTRONIC APPROACHES

TO

TRANSDUCERS FOR CHEMICAL ACTIVITY MEASUREMENT

ROBERT GRAHAM KELLY

A Thesis Submitted for
the Degree of Doctor of Philosophy

to

The University of Edinburgh

April 1979

To my wife, Jean,

and

To the memory of my late Father
who sadly was not spared to see its completion

ABSTRACT:

Conventional ion selective electrodes are briefly reviewed, with particular reference to the pH sensitive glass electrode, and the benefits which might result from the application of microelectronic techniques to electrode manufacture are noted. It is shown that microelectronic 'transducers' may conveniently be classified into two general categories, described as the 'potentiometric' type and the 'field effect' type, and certain constructional and operational advantages of the former type are suggested.

The theory of membrane potentials is critically reviewed and the relationship between such well known phenomena as the 'Donnan potential', the 'liquid junction potential' and the 'glass membrane potential' is discussed. A model is proposed for the operation of the 'Ion Sensitive Field Effect Transistor' (a transducer of the 'field effect' type) by drawing upon the theories of the glass electrode and the conventional 'Insulated Gate Field Effect Transistor'.

The fabrication of 'field effect' type devices is described and the results of measurements on them are reported.

It is noted that a clear understanding of the mechanism and stability of solid state contacts to ion selective materials is necessary for the development of sensors of the 'potentiometric' type. To this end, an experimental structure has been devised to allow measurement of the pH sensitivity and stability of metal connected glass electrode cells. Severe problems are caused by

electrical leakage effects but a satisfactory structure has been achieved and might have application in the manufacture of conventional glass membrane electrodes. The results of measurements on metal connected devices show that Nernstian pH responses are obtainable and that cell potentials are fairly stable over periods of several weeks. Improvements to the measurement techniques are required in order to investigate further the long term stability and temperature sensitivity of the devices. Suggestions are made for further research into the mechanism of the solid contact and into fabrication methods for the devices. It is expected that the method of construction developed here will be applicable to this work.

DECLARATION:

This thesis has been composed by myself and, with the exception of Appendix 4, its content has not been submitted for any other degree or publication. The work of which it is a record has been carried out by myself except where specific reference has been made to other authors.

R.G. Kelly

ACKNOWLEDGEMENTS:

I wish to thank all those members of the academic and technical staff of the Department of Electrical Engineering, University of Edinburgh, who have given advice and assistance in the course of this work. I am especially grateful to my supervisors, Dr J R Jordan and Dr A E Owen, for their support and encouragement throughout and to Mr J Gow for the construction of glass disc electrodes and for his thoroughly reliable and meticulous assistance in carrying out the experimental work of Chapter 9.

I am grateful to the Water Research Centre, Stevenage, Hertfordshire, for the financial support which made the project possible and to the Director of the Wolfson Microelectronics Institute for permitting me to register as a part-time post graduate student whilst in the employment of the Institute.

My thanks are also due to Miss Jean Clarke for her expert typing of the manuscript.

Finally, I would like to thank my wife for her support and tolerance and my parents, whose past sacrifices on my behalf have ultimately made this work possible.

CONTENTS:

LIST OF SYMBOLS:

a	activity
C	capacitance
c	concentration
D	diffusion constant
d	membrane thickness
E	electromotive force
E_{as}	glass electrode asymmetry potential
E_F	Fermi energy
E_j	liquid junction potential
E_o	standard potential of a cell or half-cell
e	electronic charge
F	Faraday's constant
$\overline{F}$	driving force for particle transport
I	current
J	flux density
K	equilibrium constant
K_{sp}	solubility product
K^{pot}	selectivity coefficient
K^+, K^-	*see text, p 46*
k	Boltzmann's constant
$\overline{k}$	*see text, p 46*
L	channel length of IGFET or ISFET device
N	Avogadro's constant
n	*see text, p 56*
p	*see text, p 56*

q	charge density
R	gas constant
R	resistance
r	Donnan distribution ratio
T	absolute temperature
t	transport number
U	*see text, p 51*
u	ionic mobility
V	*see text, p 51*
V	electrical potential difference
V_T	threshold voltage of IGFET or ISFET device
v	velocity
W	channel width of IGFET or ISFET device
x	distance
z	ionic charge number (valency)
β	gain constant of IGFET or ISFET device
γ	activity coefficient
ε	relative permittivity (dielectric constant)
ε_o	permittivity of free space
μ	mobility (of electrons or holes)
μ	chemical potential
μ_o	standard chemical potential
$\tilde{\mu}$	electrochemical potential
ξ	*see text, p 45*
ρ	resistivity
ψ	electrical potential

ℓn	natural logarithms
$\log_{10}$	logarithms to the base of 10

In the cases of those symbols which have alternative meanings, the distinction will be clear from the context.

Some of the symbols from the above list are used with different meanings in certain parts of the text. In such cases the alternative meaning is defined locally.

Subscripts to the above symbols are defined in the text.

NOTATION

The system of notation to be described was chosen with the objectives of achieving consistency through the thesis while, as far as possible, retaining a degree of similarity with the several systems which have been used in the literature, especially in the analyses which are reviewed in some detail in Chapters 3 and 4.

Individual ions are labelled by means of subscripts. Cations are denoted by subscript i, anions by j and ions of unspecified charge by k, so that $\Sigma\ c_i$, for example, indicates the sum of the concentrations of all cations. For simplicity, in cases where only a limited number of monovalent species are involved, they are denoted by upper case subscripts, eg c_A, c_B. Species indicated in this way are assumed to be cations, unless a superscript (eg c_A^-) is used to denote an anion. Much of the analysis is restricted to singly charged species however and the superscripts have usually been omitted in these circumstances. They have been included only where it was felt that a specific indication of the charge would assist the reader. Chemical symbols are also employed as subscripts where appropriate, eg c_{Na}; the meaning will be clear from the context.

Distinct phases within an electrochemical system are denoted by the use of single primes (') and double primes ("). In cases where the analysis is concerned with equilibria between two solution phases, the single and double primes are used to distinguish between the solutions. (Examples are the analyses of the liquid junction and the Donnan membrane equilibrium). Where phase boundary processes are involved, the primes distinguish between the interior of the membrane

phase and the adjacent solution phase. In the latter case, the single prime (') is used for the membrane phase and the double prime (") for the aqueous phase. The subscripts o and d are used to denote the membrane-solution interfaces which are situated at x = o and x = d respectively, where x represents distance measured along the co-ordinate direction perpendicular to the surfaces of a parallel sided, planar membrane. As an example, ψ_o' denotes the electrical potential at a point just inside the membrane phase at the phase boundary situated at x = o. The potential in the solution phase adjacent to this membrane surface is denoted by $\psi_o"$. (The subscript o is also used in other symbols such as μ_o and E_o, for the standard chemical potential and standard cell potential, but the distinction will be clear from the context).

CHAPTER 1: INTRODUCTION

The quantitative measurement of ionic species, especially in aqueous solution, is important in such diverse fields as process control[1], pollution monitoring[2] and biomedical[3] and oceanographic research[4]. Ion selective electrode measurements have been found to be valuable in many such analytical situations because the electrode is a 'transducer' which directly converts ionic activity into an electrical potential which may be read on a suitable voltmeter. The technique allows quick and simple measurement when used in the laboratory and also lends to adaptation for on-line measurements[1].

The advantages of electrode measurement are many. Their rapid response time (as compared with sampling and laboratory analysis) is essential in many process control applications and even allows direct measurement of participating species in studies of reaction kinetics[5]. Electrode measurements are non-destructive and virtually non-contaminating to the sample and are simple and convenient to use. The characteristic logarithmic response of the ion selective electrode allows measurements to be made with constant precision over a wide range of concentration which makes feasible the analysis of trace quantities, in pollution monitoring for example. Electrodes respond essentially to the activity of a species, not to its total concentration (Section 2.1). In many situations this is an advantage (eg where the rate of a reaction is dependent on pH). Even when total concentration is required, electrode techniques may be employed if the test solution is appropriately pre-treated to eliminate the effects of complexation or of variations in ionic strength.

Alternatively the electrode may be used as the indicator in a potentiometric titration[6]. Other analytical techniques such as 'known addition'[6] and 'linear null point potentiometry'[6] have been devised to extend the usefulness of electrode measurements.

The best known ion selective electrode is the glass membrane pH electrode first discovered by Cremer[7] in 1906 and characterised by Haber and Klemensiewicz[8] in 1909 and greatly refined in its modern form in respect of both glass composition and associated instrumentation. More recently, a wide range of materials other than glass have been employed in devising electrodes sensitive to ions other than H^+ and new techniques for electrode construction have been developed for use with them. For general reviews, see references 9, 10 and 11. Electrodes are now available commercially[12] which are sensitive to a wide range of anions and cations including Ag^+, NH_4^+, Br^-, Cd^{++}, Ca^{++}, $C\ell^-$, Cu^{++}, CN^-, F^-, I^-, Pb^{++}, NO_3^-, $C\ell O_4^-$, K^+, Na^+ and S^{--}.

The object of this thesis is to investigate the application of the techniques of microelectronic circuit manufacture to the production of ion selective transducers.

An essential characteristic of microcircuit technology is the deposition or growth of planar films of material in an all solid state structure. The term 'microelectronics' embraces a family of techniques including 'silicon integrated circuits'[13] and 'thick film' and 'thin film' hybrid circuits[14,15]. These techniques involve the preparation and evaluation of films of material between about 50 nm and 50 μm thick in the crystalline or amorphous state. Good control of dimensional tolerances is achieved by the use of photolithography (eg line widths and spacings of less than 10 μm) and chemical purity is sufficiently accurately controlled that doping levels of 1 per 10^7 atoms are used,

in silicon technology for example. The operations involved are largely capital intensive so that low costs are achievable in large scale production.

It is clear that any 'microelectronic electrode' will necessarily employ solid phase connection to the ion sensitive material instead of the more common membrane configuration with liquid phase filling solution. It is therefore necessary to establish that satisfactory stable connection to ion sensitive materials can be made in the solid phase and, if possible, to develop a theoretical model for the mechanism of such connection. The experimental work of this thesis is concerned with the development of techniques for the investigation of this problem for the case of ion sensitive glasses, using a pH glass of the well known composition of 'Corning 015' as an example.

Several advantages may result from the successful application of microcircuit techniques to the development of novel forms of electrochemical sensor. Experience in microelectronics suggests that the small size, light-weight and all solid state construction will lead to a mechanically robust device and the absence of a filling solution will allow operation over a wide temperature range. The small size of the sensor and the possibility of incorporating an in situ amplifier of low output impedance will minimise the problems associated with the transmission of high impedance level signals. A temperature sensor could be included in close thermal contact with the sensor material enabling correction to be made for temperature sensitivity of the electrode output. It remains to be seen whether any improvement in the stability or reproducibility of the sensor materials themselves will be achieved. It is noted however that microcircuit film deposition techniques are expected to be more controllable, both dimensionally and

thermally, than methods such as flame working which are used in the construction of conventional glass bulb electrodes. The use of much thinner films of material than would be practical with a membrane configuration may lead to a simplification in instrumentation and/or allow the use of sensor materials of high resistivity. It is recognised that the chemical durability of the sensor material will place a lower limit on film thickness but it is interesting to note that, in the case of glasses, those compositions having higher resistivity frequently exhibit greater durability[16]. An attractive possibility sometimes claimed for the microelectronic approach is the integration of 'arrays' of materials, sensitive to different ions, into a single sensor[17]. It must be noted however that the adequate characterisation of such an array will require a greater degree of stability in the selectivity constants of the individual sensors than has so far been achieved[18]. Finally, the possibilities for cost reduction by the use of the microelectronic approach are obvious although their realisation will depend on many commercial factors, especially the market requirement for the devices and hence the level of production which can be employed.

Conventional ion selective electrodes are reviewed in the following chapter, with particular reference to pH measurement using the glass electrode. Certain theoretical concepts which are relevant to the study of ion selective electrodes are reviewed in Chapter 3 and the existing theories of the glass membrane electrode are summarised in Chapter 4. An important feature of the latter two chapters is a comparison of the theoretical models used for such well known phenomena as 'Donnan potentials', 'liquid junction potentials', 'permselective membrane potentials' and 'glass electrode potentials'.

The microelectronic approach to ion sensitive transducers is discussed in Chapter 5 and two alternative kinds of device, described as the 'potentiometric' type and the 'field effect' type, are identified. Device construction, with particular reference to the problems associated with electrical leakage effects, is discussed in Chapter 6. The fabrication of both field effect and potentiometric sensors is described. The latter devices employ solid phase contacts to glass membranes. The results of measurements on the field effect devices are presented in Chapter 7 and arguments are proposed in favour of the alternative, potentiometric connection. The experimental techniques which were used in making measurements on the potentiometric devices are described in Chapter 8 and the results of these measurements are presented in Chapter 9. It is concluded that satisfactory devices may be made by fusing discs of ion sensitive glass to glass-ceramic substrates and this structure is recommended for further studies of the mechanism and stability of solid phase contacts to ion sensitive glass.

CHAPTER 2 : ION SELECTIVE ELECTRODES

2.1 INTRODUCTION

The terms 'sensitive', 'selective' and 'specific' have been used interchangeably and sometimes imprecisely in the literature on electrodes. It is clear that any practical electrode must be 'sensitive' to the ion which it is intended to measure. Most electrodes however are sensitive to several ions and the relative sensitivity to one particular species is described by the 'selectivity' of the electrode to that species. Few, if any, electrodes can be regarded as 'specific' (ie uniquely selective) to one ion, although the modern glass pH electrode may be regarded as almost so for many purposes. In this thesis, the generic term 'ion selective electrode' is used for those devices which are sensitive to a limited number of ions and which, by the use of suitable analytical techniques, can be used to measure a particular species.

The techniques of ion selective electrode measurement are introduced in the following section with particular reference to the pH sensitive glass electrode. Factors which affect the performance of glass pH electrode cells are then discussed in Section 2.3. The emphasis placed on the glass pH electrode in this chapter reflects the use of pH glass as the ion sensitive material in most of the experimental work to be described. Glass electrodes sensitive to ions other than H^+ are also discussed in Section 2.3 however and the modern 'non-glass' ion selective electrodes are briefly reviewed in Section 2.4.

2.2 ION SELECTIVE ELECTRODE MEASUREMENT TECHNIQUES

The oldest and best known ion selective electrode is the glass membrane pH electrode, the usual form of which is illustrated in Figure 2.2.1. It comprises a bulb of a special pH sensitive glass blown on the end of a tube of inert 'stem-glass' which has a thermal expansion coefficient similar to that of the pH glass. The electrode contains a filling solution which is 'buffered' to a constant pH and an internal reference electrode to make electrical contact to the filling solution. When the membrane is placed in a solution containing hydrogen ions an exchange of ions takes place between the solution and the surface layer of the glass resulting in the development of an electrical potential difference across the glass-solution interface. The magnitude of the potential difference depends on the activity of hydrogen ions in the test solution. A similar effect takes place at the inner surface of the membrane but the associated potential is constant because the hydrogen ion activity of the inner filling solution is constant. The total potential difference developed across the membrane may be measured if contact is made to the test solution by means of a suitable 'external' reference electrode as shown in Figure 2.2.2. The input resistance of the voltmeter must be large compared with the resistance of the glass membrane.

The total potential across the glass membrane is the sum of phase boundary potentials at the membrane-solution interfaces and diffusion potentials in the membrane interior[19]. It can be shown that, in the case of a pH electrode responding to only one ion (H^+), the non-equilibrium diffusion potentials sum to zero (Chapter 4). The membrane potential is therefore determined by the phase boundary processes which are assumed to be in thermodynamic equilibrium.

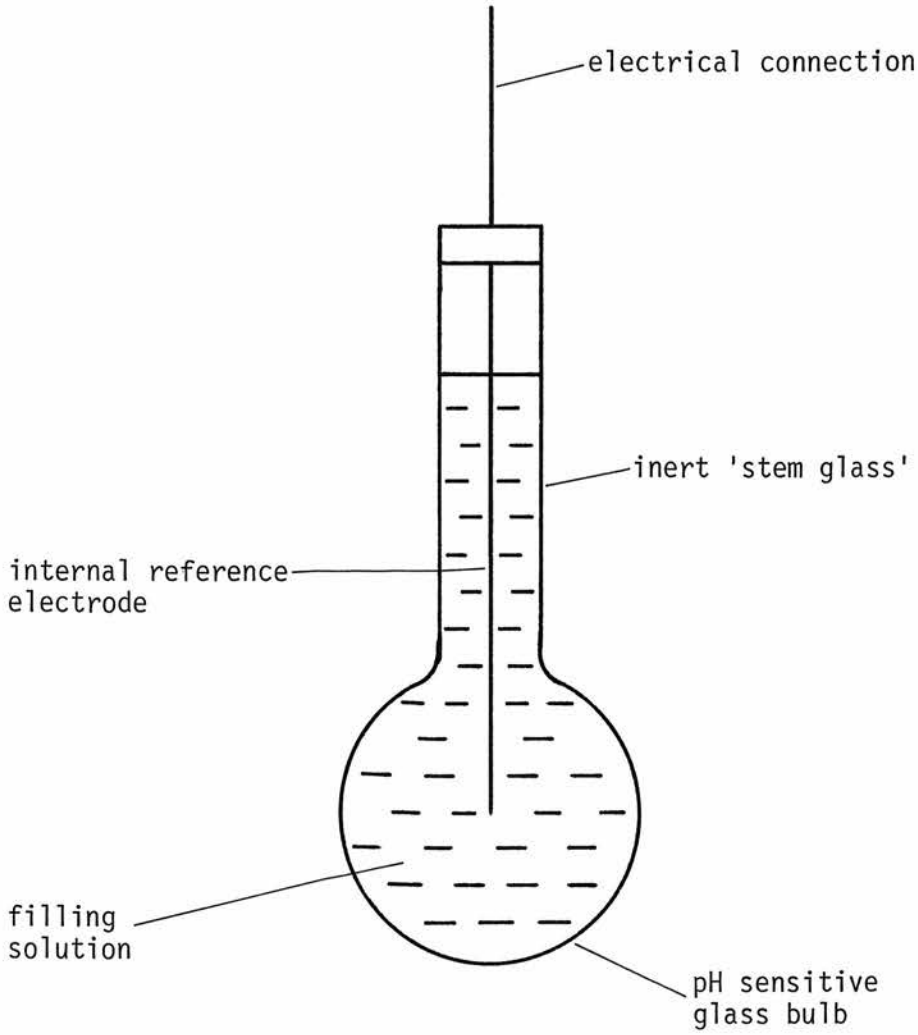

Figure 2.2.1 Glass membrane pH electrode

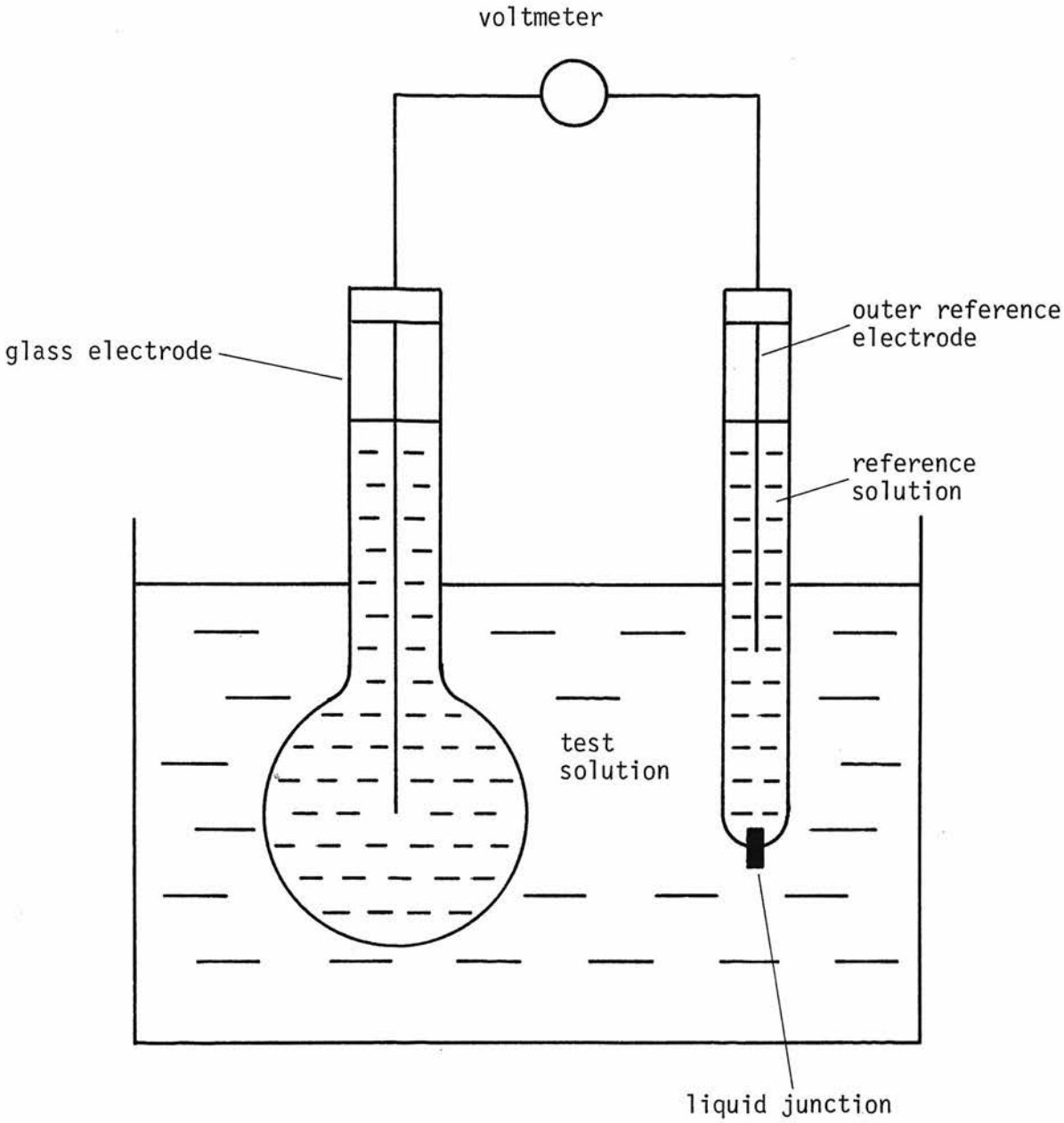

Figure 2.2.2 Glass electrode cell

The system of Figure 2.2.2 may be represented by the cell

outer reference electrode	reference solution	‖ test solution (a_H')	glass membrane	filling solution (a_H'')	inner reference electrode

The total potential of this cell (E) is described by the well known Nernst equation[20] which is characteristic of a single process in thermodynamic equilibrium

$$E = E_{R1} + E_{as} + \frac{RT}{F} \ln \frac{a_H'}{a_H''} + E_j - E_{R2} \qquad (2.2.1)$$

where E_{R1} and E_{R2} represent the potentials at the inner and outer reference electrodes and E_j is the 'liquid junction potential' (Appendix 1) associated with the outer reference electrode. E_{as} is the so-called 'asymmetry potential' of the glass membrane. These potentials are usually regarded as being approximately constant as is a_H'', the hydrogen ion activity of the buffered inner filling solution. The cell potential may then be written as

$$E = E_o + \frac{RT}{F} \ln a_H' \qquad (2.2.2)$$

where E_o is a constant, the 'standard potential' of the cell.

The pH of a solution[21] is defined by

$$pH = -\log_{10} a_H \qquad (2.2.3)$$

After substituting numerical values for the constants R and F and for the conversion factor between $\log_{10}$ and ln, Equation 2.2.2 becomes

$$E = E_o - 0.1984\ T\ (pH) \qquad (2.2.4)$$

where E and E_o are in millivolts. The quantity 0.1984T is the 'electrode response', usually expressed in mV/pH , which has the values

58.16 mV/pH at 20°C
59.15 mV/pH at 25°C
60.15 mV/pH at 30°C

By differentiation of Equation 2.2.2 it can be shown that

$$\frac{da_H'}{dE} = \frac{F}{RT} a_H'$$

ie $$\frac{\Delta a_H'}{a_H'} \approx \frac{F}{RT} \Delta E \qquad (2.2.5)$$

which illustrates the important consequence of logarithmic response that measurements can be made to constant precision over a wide dynamic range. For example, an uncertainty of ±0.6 mV in the measurement of the cell potential corresponds to approximately ±1% uncertainty in pH value at 30°C. This represents an uncertainty of ±2.3% in the hydrogen ion activity whether the measurement is made at (say) pH1 or pH10, ie at activities of 10^{-1} or 10^{-10} mole/litre. It must be understood of course that uncertainties other than that in the measurement of potential will also affect the overall accuracy of measurement.

In general, for any electrode which is responding selectively to one species, the Nernst equation may be written

$$E = E_o + \frac{RT}{z_k F} \ln a_k \qquad (2.2.6)$$

where z_k is the valency of the species in equilibrium. A more complex equation obtains in the case of mixed response to more than one species

as will be described in Section 2.3 with reference to cation sensitive glass electrodes.

It will be noticed that it is the *activity* of the ion in question which appears in the Nernst equation and in the definition of pH. An understanding of the concept of activity and its relation to concentration is essential to the intelligent interpretation of pH and other ion selective electrode measurements. The activity of a species, to which an electrode responds, may differ from its concentration in solution for several reasons. Firstly, interaction between ions tends to reduce their effectiveness to take part in a chemical process. An activity coefficient, γ, defined by

$$a = \gamma c$$

may be used to relate the activity of an ion, a, to its concentration, c. The value of γ depends on the total ionic strength of the solution involved and tends to unity for very dilute solutions but decreases with increasing concentration[22]. Secondly, the ion being measured may exist partly as an unionised or undissociated neutral species and thirdly, it may be bound in a complex.

In many applications, such as the monitoring of industrial or biological processes for instance, activities may be of greater significance than concentrations since it is the former which determine reaction rates and the positions of equilibria. Similarly, in reaction rate studies, corrosion research and the measurement of water hardness, activity is of fundamental significance. No other technique allows the measurement of activity with the simplicity of the electrode method. If, on the other hand, a measurement of total concentration is required then steps must be taken to ensure that all complexes etc

are fully dissociated before making the electrode measurement and that errors do not arise due to differences in ionic strength between the test solutions and those used to standardise the electrode. The use of ionic strength adjusters for this purpose is noted, a particularly elegant example being the 'TISAB' (Total Ionic Strength Adjustment Buffer)[23] marketed by Orion Research especially for use in fluoride ion measurement. This reagent contains a pH buffer, to free any fluoride which is bound as HF, and CDTA or citrate to break down complexes of F^- with aluminium and other cations. It also has high ionic strength to control the fluoride ion activity coefficient. Concentration data may also be obtained by means of analytical techniques, such as 'linear null point potentiometry'[6], 'known addition'[6] or 'potentiometric titration'[6], though these methods do lack the simplicity of the direct electrode measurement.

It is important to recognise that the glass 'electrode' is strictly speaking not an 'electrode' insofar as the processes taking place through the glass membrane involve only ionic species. It is at the inner and outer reference electrodes that electrode processes, involving interaction between ions and electrons, take place. In this way the reference electrodes make electrical connection between the ionically conducting aqueous solutions and the electronically conducting external circuitry. The ideal reference electrode would be one which made 'ohmic' contact to the solution without developing an electrical potential difference. In practice any electrode process involves a free energy change and the practical requirement is that the associated potential difference must remain substantially constant in test solutions of different composition and ionic strength over the operating temperature range and lifetime of

the system.

Inner and outer reference electrodes are also employed in conjunction with non-glass ion selective electrodes of the membrane configuration. Certain other types of electrode (Chapter 5) use solid state connection instead of an internal reference electrode but the external reference is always required in order to make connection to the test solution.

Reference electrode systems may be classified into those with and without liquid junction. In the latter case the solution must contain (at constant activity) an ion to which the reference electrode is reversible. A common example is the use of a silver-silver chloride electrode in a solution containing a constant concentration of $C\ell^-$ ions. This technique is often used in accurate work but the need to add a reagent to the test solution may be inconvenient in many applications and may even be impossible owing to, for example, precipitation of insoluble salts from the test solution. A further problem is that the reference electrode potential may be affected by species in the unknown test solution, by the establishment of a 'redox potential' for example.

The use of an electrode with liquid junction is sometimes more convenient. In this arrangement (Figure 2.2.2) the reference electrode itself is in contact with a solution of constant composition which helps to ensure a constant electrode potential. There is of course a liquid junction potential associated with the interface between the reference electrode's internal solution and the test solution and this potential contributes to the total cell potential. Although the liquid junction potential is in general a function of the test solution composition, it can be shown that it is small if certain

conditions concerning the concentrations and mobilities of the diffusing species are met[24]. If the solution on the reference electrode side of the junction is a single binary electrolyte for instance, then the required conditions are that the concentration of this electrolyte is much greater than that of the test solution (which comprises the opposite side of the junction) and that the mobilities of the two ions are similar. A concentrated (typically 3.5 molar) solution of potassium chloride is usually employed in practice. It must be understood however that a precise calculation of the liquid junction potential would require the knowledge of single activity coefficients which are thermodynamically undefined. Furthermore, as observed by Covington[25], the evidence in support of using the 3.5 M KCℓ salt bridge is somewhat flimsy. Ives and Janz[26] have estimated however that the use of a salt bridge is acceptable when an absolute uncertainty of 1 or 2 mV (corresponding to approximately 0.02 to 0.04 pH units) can be tolerated.

In practice a silver-silver chloride electrode is often used as the internal reference in pH cells, the electrode filling solution having a fairly high (and therefore stable) $C\ell^-$ concentration as well as being buffered to constant pH. The outer reference electrode is usually a calomel (mercury-mercurous chloride) electrode incorporating a liquid junction of the ceramic plug or ground glass sleeve type.

In summary it may be said that a satisfactory reference electrode arrangement can be easily and cheaply implemented in most practical applications provided standard practice is followed. In certain applications however, and whenever high accuracy is sought, the stability and accuracy of the reference electrode may well be of greater significance than the performance of the pH or ion selective

electrode itself. Both the theoretical problems of interpreting single activity coefficients and the practical problems and techniques associated with reference electrode systems have been extensively reviewed[26].

It is well known that the electrical resistance of glass electrode membranes is high (10 MΩ to 1000 MΩ is typical, depending on the glass composition). A high input impedance electrometer voltmeter must therefore be used to measure the cell potential and suitable precautions must be taken to prevent electrical leakage effects in parallel with the meter input. Surface leakage across insulators can be especially troublesome with devices which are necessarily in close proximity to highly conductive electrolytic solutions. Due care must also be taken to ensure adequate electrostatic screening of the high impedance level signals to prevent spurious meter indications due to electrical 'pick-up' or 'body capacitance'.

The resistances of non-glass ion selective electrodes are typically of the order of 50 MΩ[10] so that a high quality digital voltmeter may be used for the measurement of cell potential. Care is still required with regard to leakage and screening however.

2.3 PERFORMANCE OF GLASS ELECTRODES

The expression for the total glass electrode cell potential (Equation 2.2.1) includes a constant term, E_{as}, due to the glass asymmetry potential. This represents the small potential (typically 10 mV) which is usually observed in an otherwise entirely symmetrical cell having identical inner and outer reference electrodes and

solutions. The origin of the asymmetry potential is uncertain but it clearly indicates some inhomogeneity in the bulk membrane or difference between the properties of the two surfaces. Possible causes[27] include strains in the glass (especially in a bulb, where the outer surface is in tension and the inner surface is in compression), differential loss of alkali during flame working or storage and poisoning of one surface (eg by a film of grease) during its working life. The magnitude of the asymmetry potential may vary somewhat from day to day over a range of a few millivolts. This effect is usually not distinguished from instabilities originating in the reference electrodes and liquid junction, the summed effects being regarded as a change in E_o (Equation 2.2.2) which is usually compensated for by adjustment of the appropriate offset control of the pH meter while the electrode is exposed to a suitable calibrating solution.

Temperature effects are significant in glass electrode measurements. The first order dependence of the electrode response is apparent from the RT/F term in the Nernst equation (2.2.2). Less obvious is the temperature dependence of the E_o term. The glass asymmetry potential, liquid junction potential and even the pH of the filling buffer solution are all temperature dependent although the effects are not usually significant over small (10 to 20 deg C) temperature ranges[21]. The temperature coefficients of the inner and outer reference electrodes may well be significant however, and will result in an overall temperature dependence of the cell emf if they are not of the same type. Furthermore it must always be recognised that the pH of the test solution itself is a function of temperature. It is therefore imperative either to standardise the electrode and pH

meter at the temperature of measurement or to employ some system of compensation, either manual or automatic. Such techniques, including the concept of the 'isopotential point' have been discussed by Mattock[21] and by Covington[10,25].

In practice, the response of pH and other ion selective electrodes seldom corresponds precisely to the slope factor (RT/F term) of the Nernst equation, even after account has been taken of temperature and activity coefficients etc. An electrode must always be standardised in at least two solutions having known pH so that the E_0 value and slope factor of the electrode cell may be determined. Such standardisation requires buffer solutions of accurately known pH which may be reasonably easily made up and which maintain their pH for a reasonable period of time under normal laboratory conditions. The best known range of pH buffer solutions is probably that recommended by the US National Bureau of Standards (see Mattock and Band[24]). In accurate work it is necessary to calibrate the electrode using two buffers having pH values close to and bracketing that which is expected for the unknown solution[21]. It is also advisable that the calibrating solution should be similar in ionic strength and composition to the unknown in order to reduce errors due to liquid junction potentials and variations in activity coefficients[21]. Calibration should always be carried out before measurement as the E_0 value of an electrode cell is susceptible to a drift of several millivolts from day to day.

The high resistance of glass electrode membranes was noted in the previous section. The measurement of membrane resistance is complicated by dielectric and space charge polarisation effects as described by Eckfeldt and Perley[28] who conclude that the true ohmic resistance of a glass electrode membrane is that observed in a dc measurement,

although the true dc value of membrane current may not be reached for several hours after the application of a voltage across the membrane (at room temperature). More recently, expressions for the complex impedance of glass membranes have been derived by Buck[29,30] in the light of the ion exchange - diffusion theory and experimental results have been reported by Buck and Krull[31] and by Brand and Rechnitz[32].

The resistance of glass membranes is also strongly dependent on temperature and, according to Eckfeldt and Perley[28], obeys the equation

$$\log R = A + \frac{B}{T} \qquad (2.3.1)$$

where A and B are constants of the particular glass. For Corning 015 glass the dc resistance approximately halves for a 7 deg C increase in temperature at around room temperature. It follows that the input resistance of any voltmeter which is used for the measurement of cell potentials must be specified with regard to the lowest anticipated operating temperature.

The resistivity of a glass is also dependent on its thermal history so that a carefully annealed sample may have a value several times higher than that of a quenched sample of the same chemical composition.

The use of very thin membranes to achieve lower resistance is limited by considerations of mechanical and chemical durability. A thickness of 50 to 100 μm would appear to be the reasonable lower limit for many applications but this is of course greatly dependent on operating conditions, glass composition and required lifetime and

membranes as thin as 1 to 4 μm have been used in glass microelectrodes[33]. It should be noted here that it has been suggested in the literature[34] that there is a maximum thickness of 50 to 130 μm above which electrode response declines. It seems certain that such observations are due entirely to inadequate resistance levels in the experimental arrangement or at the meter input. The present author has observed nearly Nernstian pH responses with glass membranes up to 450 μm thick (Chapter 9).

It is generally observed that those glass compositions which exhibit the greatest resistance to chemical attack also have the highest electrical resistance[16]. The modern lithia based pH glasses for instance have generally higher resistivities than soda glasses and their use as electrodes has been made possible only by corresponding improvements in instrumentation.

It has already been shown that the precision of electrode measurements is constant, independent of the activity of the measured species. In the case of pH measurement using the glass electrode, the operational range of pH is limited by other factors. An acid error[35] has been noted by many workers at pH values of zero or less although there are many apparently conflicting observations. It has been suggested that the effect may be due to the lowering of water activity or to anion penetration of the glass. The long known alkaline error[36] at high pH (greater than 9, typically) is now understood, in terms of the ion exchange theory, to be a response to alkali metal cations rather than a true alkaline error. Furthermore, some glasses (eg Corning 015) are appreciably attacked in strongly alkaline solutions[37].

Systematic studies of the responses to several cations of electrodes made from glasses of different composition were carried out in the late 1950s and early 1960s, notably by G. Eisenman and co-workers[19]. This work led both to a clearer theoretical understanding of the glass electrode and to the development of 'sodium sensitive' and 'cation sensitive' electrodes.

Eisenman, Rudin and Casby[38] proposed an empirical equation to describe the mixed ion response

$$E = E_o + \frac{nRT}{F} \ell n \left[a_A^{\frac{1}{n}} + (K_{AB}^{pot}\, a_B)^{\frac{1}{n}}\right] \qquad (2.3.2)$$

where a_A, a_B represent activities of ions A and B in the test solution. K_{AB}^{pot} is defined as the selectivity coefficient between the ions A and B, and n is a constant for a given glass and pair of cations ($n \leq 1$). The internal filling solution is assumed to be of constant composition. This equation was found to describe the potential for mixtures of two metal cations at constant pH as well as for mixtures of H^+ and one other cation.

Clearly, if $\frac{a_A}{a_B} >> K_{AB}^{pot}$ or if $\frac{a_A}{a_B} << K_{AB}^{pot}$, Equation 2.3.2 reduces to the Nernst equation (2.2.2), the value of n being immaterial. When $a_A \sim K_{AB}^{pot}$ however the electrode exhibits a mixed response, the relative effect of each species on the potential being determined by K_{AB}^{pot}. This is shown graphically in Figure 2.3.1, in which the exact shape of the curved part of the response depends on n. A theoretical derivation of Equation 2.3.2 has since been proposed by Eisenman and others (see Chapter 4).

A pH glass composition which was widely used for many years was that originally suggested by McInnes and Dole[39] and later marketed by

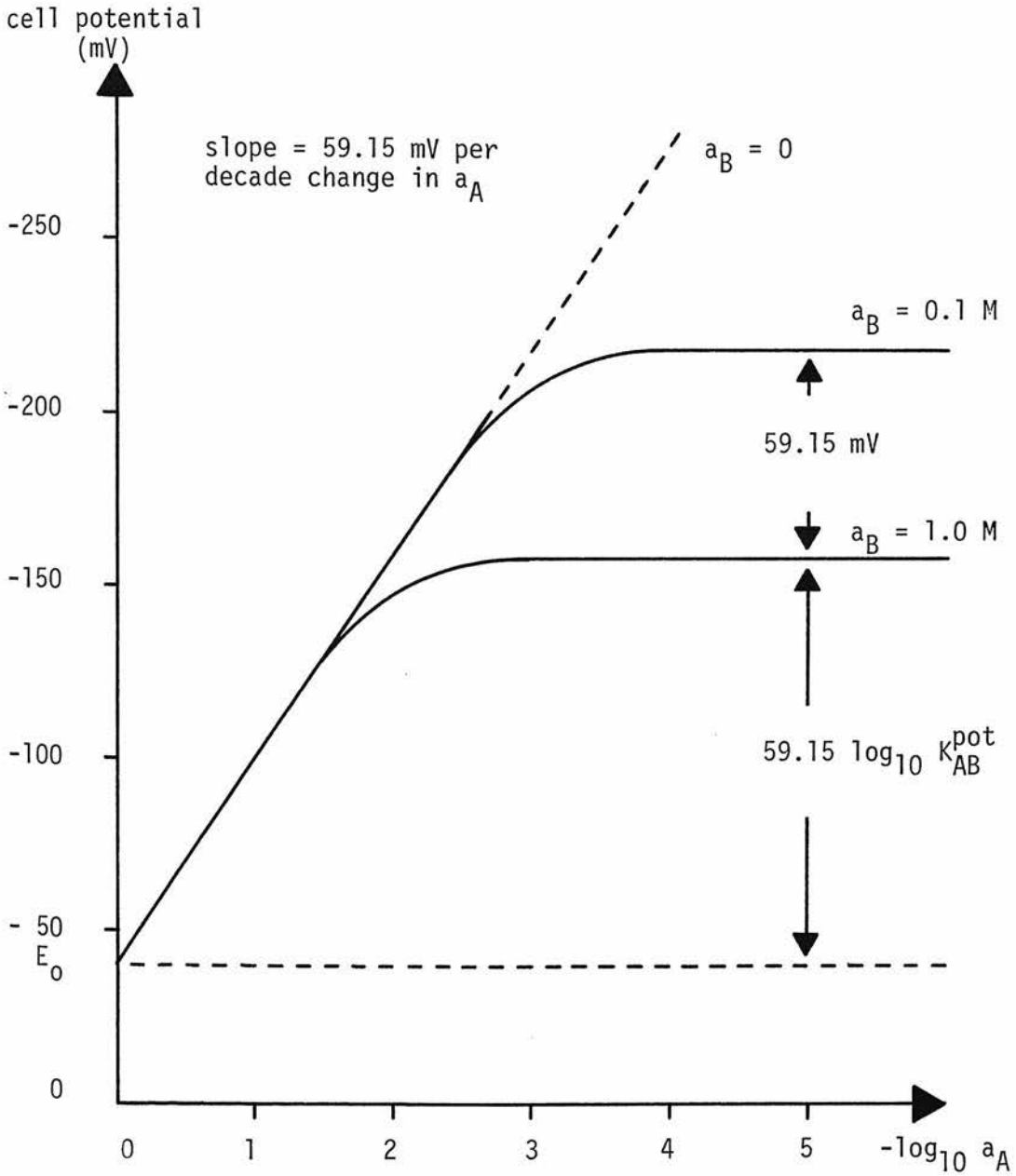

Figure 2.3.1 Form of the mixed ion response equation (Equation 2.3.2) for $K_{AB}^{pot} = 10^{-2}$ (at 25°C)

Corning Glass Works as 'Corning 015' (later re-numbered '0150'). The composition of this glass is 72.2 mole % SiO_2, 21.4 mole % Na_2O, 6.4 mole % CaO and has the lowest melting point of the soda-lime-silica system. K_{H-Na}^{pot} for this glass is about 10^{11} so that alkaline errors due to for example an 0.1 molar concentration of Na^+ become significant at a pH greater than about 9.

The more modern lithia based pH glasses[40] have better H^+ selectivity than Corning 015 and are commonly used up to pH14. It should be noted however that measurements of such high pH values (corresponding to exceedingly small H^+ activities) is only possible as a result of the buffering action of the water equilibrium and the presence of correspondingly high activities of OH^-. The lower limit of detection in the case of ion selective measurements is determined mainly by the practicality of working at concentrations of unbuffered species of less than about 10^{-8} molar.

A systematic study of the dependence of selectivity on glass composition was carried out by Eisenman[19]. It was shown that the relative selectivities to different cations follow a general pattern for a wide variety of glass compositions drawn from the various alkali metal alumino-silicate systems. Thus the selectivity to Na^+ over K^+ indicates directly the relative selectivity of the composition in question to other cations such as Li^+, Rb^+, Cs^+ and H^+. The relative selectivities are explained theoretically in terms of the 'anionic field strengths' of the ion exchange sites in the different compositions.

It must be remembered that the H^+ selectivities of good pH glasses are many orders of magnitude greater than the typical relative

selectivities between cations of the cation selective glasses. Furthermore, all cation sensitive compositions are also responsive to H^+. Meaningful measurement of cation activities therefore requires a careful consideration of the composition of the test solution with regard to its pH and concentrations of interfering cations. The selection of suitable glass compositions selective to Li^+, Na^+, K^+, Rb^+, Cs^+, Ag^+, Tl^+, NH^+_4 and to the alkaline earth cations has been discussed in detail by Eisenman[19]. In the case of Na^+ sensitive compositions (such as NAS 11-18) selectivities over K^+ and other alkali metal cations of typically 300:1 are observed. Hence, apart from the need to buffer to a fairly high pH, electrodes made from these compositions may be regarded for many applications as 'specific' for Na^+. The selectivity constants of electrodes for K^+ and other cations are generally much smaller (typically 10 or less) so that their use is correspondingly less straightforward. It is interesting to note that, although glass 'K^+-electrodes' have in the past been marketed commercially, current practice seems to be to restrict the description of glass electrodes to the terms 'sodium sensitive' and 'cation sensitive'. Furthermore K^+ electrodes of the liquid membrane variety, having much higher selectivities over Na^+ than the glass type, are now gaining acceptance[10,12].

Surprisingly little information has been found in the literature concerning the response time of pH or cation sensitive glass electrodes. Disteche and Dubuisson[41] showed that steady state was reached in less than one second after a step change in pH. It must be understood however that the observed response time in a simple 'dipping'experiment may be due to mixing times in the solution rather than to the electrode itself and may be of the order of minutes,

especially in poorly stirred solutions.

In the case of cation sensitive glass electrodes transient behaviour distinctly different from the steady state performance is sometimes observed, especially when the electrode is responding to a mixture of ions. Rechnitz and Kugler[42] investigated the response times of commercially available cation sensitive and sodium sensitive electrodes. The measurements were first carried out in solutions of a single cation to which the electrode in question showed equilibrium specificity. The response was sufficiently rapid to be unmeasurable with the experimental arrangement used (for which the half-time response due to mixing and electronic time constants was estimated as less than 15 ms). The sodium electrode however showed a transient response to concentration changes of ions such as K^+ and NH_4^+ to which its equilibrium response is negligible. The transient was fast (less than 15 ms half-time) and nearly Nernstian in magnitude. It decayed to the equilibrium value in about 30 s. Further experiments were carried out on the sodium electrode using mixtures of ions. The presence of a 'background' concentration of those ions which had produced transient responses (K^+ and NH_4^+) had a severe effect on the electrode's response to Na^+, the time required for attainment of the equilibrium potential being about 100 times that for the single ion solution. Isard[43] has proposed an explanation for these time dependent effects based on the well established existence of a hydrated layer at the electrode surface. The selectivity constant of this layer is assumed to be different from the bulk glass (due partly to the great differences in ionic mobilities between the bulk and hydrated material). The decay to the equilibrium value is then explained by diffusion of the ions through the hydrated layer which

is consistent with Rechnitz and Krugler's observation[42] of a square root variation of the transient potential with time. The final steady state potential corresponds to equilibrium between the solution, hydrated layer and bulk glass, the selectivity order being that of the latter. Isard[43] admits however that some reported results are inconsistent with this theory. Eisenman's work[44] on the sodium alumino-silicate glass (NAS 27-4) for example revealed no evidence of transient response or time dependence despite the certain existence of a deep hydrated layer in his well leached electrodes.

The most common method of constructing glass electrodes is by the flame working technique in which a bulb of the ion sensitive glass is blown on to a tube of an electrically insulating, inert 'stem glass' which must of course have a thermal expansion coefficient similar to that of the sensitive glass. This and alternative techniques have been reviewed by Portnoy[45]. These include the use of organic adhesives, such as epoxy resins or silicone rubbers, to bond a flat membrane of the ion sensitive glass to an insulating tube. The use of O-ring seals is also suggested. The disadvantage of such techniques is the difficulty of maintaining a sufficiently high level of electrical insulation through the seal for a prolonged period, a problem which seems to have been satisfactorily overcome only with the blown bulb type of construction.

The properties of glass electrodes are known to be affected by the surface condition of the glass as well as by its chemical composition. In particular, the development of a hydrated surface layer appears to be a necessary condition for electrode response[21]. The effects of annealing and etching treatments have been briefly reviewed by Bates[46]. Mechanical lapping of the electrode surface

using fairly coarse (280 grit) abrasive does not appear to affect the electrode response as reported by Portnoy[45] and confirmed by the present author (Chapter 9). Mattock[21] has noted however that the presence of surface films of oil or grease can seriously impair electrode performance. It is worth noting that the flame working method of electrode construction is itself likely to cause volatilization of alkali from the glass surface and this has been suggested as a cause of the asymmetry potential[27]. The thermal history of electrodes made in this way is also inevitably ill-defined so that the degree of annealing and crystallisation in the glass may vary between devices. It remains to be seen whether microelectronic techniques will offer any advantages in this respect.

The construction of microelectrodes for biomedical application involves additional difficulties. The techniques have been reviewed by Hinke[33] and Khuri[47].

In summary it may be said that the glass electrode permits the rapid, convenient and non-contaminating measurement of pH. Provided care is taken regarding the effect on total cell potential of such factors as reference electrodes, liquid junctions, ionic strength, solution composition, temperature and electrical leakage, the measurements may be reproducible to better than 0.01 pH[21]. Modern pH glasses have high chemical durability and almost total selectivity to H^+ over a wide range of pH. Variants are also available for use at extreme temperatures. Sodium sensitive glass electrodes similarly allow the direct measurement of Na^+ provided allowance is made for the interfering effect of H^+ and, to a lesser extent, other cations. Cation sensitive glass electrodes show usable selectivities to various monovalent (and some divalent) cations but great care must be taken to eliminate interferences.

2.4 OTHER ION SELECTIVE ELECTRODES

Research into the suitability of materials other than glass for electrode use culminated, in the late 1960s, in the commercial availability of electrodes sensitive to a wide range of anions and cations[12]. The ion sensitive materials used in these electrodes may be divided into two classes viz organic ion exchangers and insoluble inorganic salts. An alternative classification into 'solid state', 'liquid ion exchange' and 'heterogeneous' electrodes is also used and reflects the physical configuration of the electrode. The devices have been extensively reviewed[10,11,48] and will be considered only briefly here.

Examples of organic ion exchange materials are the synthetic 'crown' compounds and certain antibiotics (which act as complexing agents) and the salts of long chain organic acids and bases. To be suitable for electrode use, the material must have a low vapour pressure to minimise evaporation and a low solubility in water. It is usually dissolved in a water-immiscible organic solvent. A phase boundary potential is established at the interface between the organic phase and an aqueous solution as a consequence of ion exchange between the phases. The selectivity of the exchange process depends on the relative stabilities of the complexes formed between the ion exchange material and the various ions present in the aqueous phase. The process of ion exchange between the solution and 'sites' in the membrane phase is similar to that in the case of the glass electrode, discussed in greater detail in Chapter 4. An important difference however is that the sites in the glass are fixed whereas those in the liquid ion exchanger are mobile. Ross[48] has noted that the general theory of liquid membranes is difficult if two or more exchanging ions are

involved. In practice however it is the region of single ion (Nernstian) response which is of principal interest and an empirical equation is available[48] for estimating the acceptable levels of interfering species.

Organic ion exchangers have been employed in both the 'liquid ion exchange' and the 'heterogeneous' types of electrode. The liquid membrane electrodes sold by Orion Research[12] are an example of the former construction. In these devices the ion exchanger is absorbed in a 'Millipore' filter which is fitted at the tip of a specially designed probe body. This incorporates an inner filling solution, in contact with the 'reference' side of the membrane, and an internal reference electrode. The body also contains a reservoir of the ion exchange solution which is in contact with the periphery of the membrane and maintains the necessary degree of saturation of the membrane pores. Heterogeneous membranes may be made by evaporating a mixture of the ion exchanger and pvc dissolved in a suitable organic solvent. The resulting solid polymer film is sealed to the end of a tube which contains the filling solution and reference electrode.

Electrodes which use insoluble inorganic salts as the active material include the well known fluoride electrode, which employs a single crystal of lanthanum fluoride as the membrane, and the silver sensitive electrodes based on membranes of silver sulphide or halide. The main requirements for electrode application are that the salt must be chemically inert, insoluble in water and have sufficiently high electrical conductivity. Conduction in these crystalline materials is ionic and proceeds by a lattice defect mechanism. According to Ross[48], the selectivity of these materials is due to the nature of the vacancies which are 'tailored' with respect to size, shape and charge distribution

to admit only the mobile ion. All other ions are unable to move. This situation may be contrasted with that of the liquid membrane electrodes in which any ion inside the membrane may move (as a site-ion complex) and selectivity therefore depends mainly on the phase boundary processes. The inorganic salt electrodes are basically selective to the ion which is mobile in the crystal lattice; a silver sulphide membrane is selective to silver ions for example. Sensitivity to other ions can be indirectly obtained however, as a consequence of solubility products. The silver sulphide membrane for example will respond to sulphide activity (provided the test solution is saturated with respect to silver sulphide and contains no additional source of silver ions) as a consequence of the relationship

$$(a_{Ag})^2(a_S) = K_{sp}$$

where K_{sp} is the solubility product of silver sulphide. Although these electrodes have very high selectivities, they are nevertheless prone to interferences resulting from chemical reactions between the membrane and the test solution. Dissolution of the membrane and precipitation of insoluble species on to it are examples of such reactions. The lower limit of detection is ultimately determined by the solubility of the membrane itself but the practical limit in many cases arises out of the difficulties of working with very low concentrations of unbuffered species.

Membrane electrodes have been fabricated using both single crystal and compacted discs of the insoluble inorganic salts. Heterogeneous forms have also been made, eg by dispersing the salt in a silicone rubber matrix. They also require the usual internal filling solution and reference electrode.

Membranes using mixtures of salts may also be formed by the compacted disc method. A mixed silver sulphide-silver halide membrane for example is selective to halide but has several advantages over a simple silver halide membrane, including higher conductivity and reduced photosensitivity. This technique is especially useful where the halide itself cannot be formed into a pressed pellet (eg silver iodide). In a similar way, a membrane comprising a mixture of silver sulphide with the sulphide of another metal is sensitive to that metal. Electrodes for Cu^{++}, Cd^{++} and Pb^{++} have been made in this way.

The techniques of measurement using ion selective electrodes are in principle the same as those used for pH measurement with the glass electrode. In practice however, selectivities are generally poorer so greater care is required in eliminating interfering species from the test solution. In the case of measurements of divalent ions, the Nernstian response is half that obtained with monovalent ions (Equation 2.2.6). A given uncertainty in the measurement of the cell potential is therefore more serious and improvements in technique may be required. An example is the use of 'double junction' reference electrodes incorporating an 'equitransferent' filling solution[49] in order to minimise the liquid junction potential.

It was decided to use pH sensitive glass as the ion sensitive material for the experimental work described in this thesis. There is a large market for pH sensors and the theory and practice of glass electrodes are well established. It is recognised however that the ion sensitive materials described in this section may well be equally suitable for application in microelectronic devices.

CHAPTER 3: THEORY OF MEMBRANE POTENTIALS

3.1 INTRODUCTION

The theory of the operation of ion selective electrodes involves an understanding of the equilibria of charged species between adjacent aqueous and solid phases and of the transport mechanism of the charged species within those phases.

Many of the relevant concepts were first introduced by workers concerned with the more general field of membrane theory and especially by physiologists attempting to understand and model the functions of the living cell membrane. Much of the literature is therefore written in the terminology of biological science and places emphasis on explaining those aspects of membrane behaviour which are most significant to living systems. To the biologist for example, the fluxes of ions in and out of the cell are of equal or greater significance than the membrane potential which is the most important quantity in ion selective electrode work.

The purpose of this chapter is to review the basic concepts and early theories of membrane potentials which contributed to the development, by Eisenman[44] and others, of the ion exchange theory of the glass electrode which is discussed in Chapter 4. An attempt will be made to show the relationship between phenomena such as the 'liquid junction potential', the 'Donnan potential' and the potentials developed across 'fixed charge' and 'ion-exchange' membranes.

3.2 THE ELECTROCHEMICAL POTENTIAL

The concept of electrochemical potential[50] is fundamental to the analysis of both equilibrium and non-equilibrium (transport) phenomena in membranes.

The chemical potential, μ_k', of species, k, which is 'dissolved' in a solid or liquid phase (') is defined by

$$\mu_k' = \mu_{ok}' + RT \ln a_k'$$

where μ_{ok}' is the standard chemical potential of species k in phase (') and a_k' is the activity of species k in phase (').

The difference between the chemical potentials of species k at different states (activity levels) in phase (') is equal to the work done by an external agent (against purely 'chemical' forces) in reversibly transferring one mole of k between the states. If interest were restricted merely to changes in the activity of the species in the one phase (') then the definition of the standard potential, μ_{ok}', would be purely arbitrary. The usefulness of the chemical potential concept however lies in its ability to handle situations in which the species in question are free to move between different phases (eg aqueous solution and solid membrane) or to undergo chemical reaction (eg the formation of a compound from its elements). For this reason, standard states such as μ_{ok}' are all referred by convention to an agreed scale of standard states of the elements. (For convenience, the reference forms of the elements are those in which they commonly occur at $25^{o}C$ and one atmosphere pressure). The standard chemical potential of, say, a compound dissolved in aqueous solution is then derived from the standard potentials of the elements by addition of the work done in converting

the appropriate quantities of the elements, by a reversible process, into 1 mole of the compound in the aqueous solution at unit activity. It must be noted that standard potentials are functions of temperature.

When the transfer of *charged* particles between phases is considered it is necessary to take into account the work done against electrostatic forces as well as 'chemical' forces. The total work is then defined by the electrochemical potential, $\tilde{\mu}_k'$.

$$\tilde{\mu}_k' = \mu_{ok}' + RT \ln a_k' + z_k F \psi' \qquad (3.2.1)$$

where ψ' is the electrical potential of phase (') referred to the standard state in which $\tilde{\mu}_k' = \mu_{ok}'$.

The condition for equilibrium of a charged species between two phases, (') and ("), is then described by the equality of electrochemical potentials between the phases,

$$\tilde{\mu}_k' = \tilde{\mu}_k''$$

$$\text{hence } \mu_{ok}' + RT \ln a_k' + z_k F \psi' = \mu_{ok}'' + RT \ln a_k'' + z_k F \psi'' \qquad (3.2.2)$$

This equation is the starting point for all analyses of the equilibria of charged species between phases. It is completely rigorous, being derived by purely thermodynamic reasoning, although it is of course restricted to situations in which the only forces involved are chemical and electrostatic. If other forces (eg due to hydrostatic pressure gradients) are involved then the reversible work done against them in transferring the particles between the states must be accounted for by additional terms in the equation.

Although the electrochemical potential is a thermodynamic quantity, strictly applicable only to equilibrium situations, the

concept is also commonly used in the analysis of essentially non-equilibrium transport phenomena. The difference between the electrochemical potentials of a species in two states is clearly a measure of the tendency for change to take place towards the equilibrium situation. This idea may be quantified by the introduction of the concept of a 'driving force' for change, related to the gradient of the electrochemical potential. Consider a system in which the electrical potential, the activity of species k and the standard potential of species k are functions of spatial coordinates. (A variation of μ_{ok} within the system could result from the existence of distinct phases or from chemical inhomogeneity). For simplicity we will assume a one dimensional situation in which these quantities are a function of x only. The electrochemical potential is then a function of x. Suppose one mole of k is moved reversibly a short distance, Δx, along the x axis. The work done by the external agent (equal to the change in electrochemical potential $\Delta\tilde{\mu}_k$) may be regarded as work done against a notional driving force, $\bar{F}_k$, where

$$\bar{F}_k \, \Delta x = -\Delta\tilde{\mu}_k$$

Hence, in the limit as $\Delta x \to 0$,

$$\bar{F}_k = -\frac{d\tilde{\mu}_k}{dx}$$

$$= -\frac{d}{dx} (\mu_{ok} + RT \, \ell n \, a_k + z_k \, F \, \psi) \qquad (3.2.3)$$

Again, extra terms must be introduced if other forces, such as pressure gradients, are involved. For a homogeneous phase, in which μ_{ok} is not a function of x, Equation 3.2.3 becomes

$$\bar{F}_k = -\frac{d}{dx}\ (RT\ \ell n\ a_k + z_k\ F\ \psi)$$

$$= -\frac{d}{dx}\ (RT\ \ell n\ \gamma_k\ c_k + z_k\ F\ \psi)$$

where γ_k and c_k are respectively the activity coefficient and concentration of species k. The velocity, v_k, of the particles is related to the driving force by

$$v_k = \bar{F}_k\ u_k$$

where u_k is defined as the mobility of the species. The flux density, J_k, of the species is then given by

$$J_k = v_k\ c_k$$

$$= -u_k\ c_k\ \frac{d}{dx}\ (RT\ \ell n\ \gamma_k\ c_k + z_k\ F\ \psi)$$

$$\text{hence } J_k = -RT\ u_k\ \left(\frac{dc_k}{dx} + c_k\ \frac{d\ \ell n\ \gamma_k}{dx} + z_k\ c_k\ \frac{F}{RT}\ \frac{d\psi}{dx}\right) \qquad (3.2.4)$$

For the special case of unity activity coefficient, Equation 3.2.4 reduces to the Nernst-Planck equation[51]

$$J_k = -RT\ u_k \frac{dc_k}{dx} - u_k\ c_k\ z_k\ F\ \frac{d\psi}{dx} \qquad (3.2.5)$$

We note that J_k and c_k in the above equations are expressed in terms of *molar* quantities, as a consequence of the original definition of the electrochemical potential on a 'per mole' basis.

It is interesting to note, in passing, the relationship between the above equation for particle flux and the corresponding equations in the form usually used in the semiconductor literature. In the latter case, concentrations and fluxes are usually expressed in terms of

particles rather than moles and the Boltzmann constant, k, and the electronic charge, e, are used instead of the gas constant and the Faraday. Multiplying Equation 3.2.5 by Avogadro's Constant, N, we obtain

$$NJ_k = -RT\, u_k \frac{d}{dx}(Nc_k) - u_k (Nc_k)\, z_k F \frac{d\psi}{dx}$$

hence

$$J_k^* = -RT\, u_k \frac{d}{dx}\, c_k^* - u_k\, c_k^*\, z_k F \frac{d\psi}{dx}$$

where J_k^* and c_k^* are the flux density and concentration expressed in terms of *particles*. Using the relationships

$$R = kN$$

and

$$F = eN$$

we obtain

$$J_k^* = -u_k N kT \frac{dc_k^*}{dx} - u_k\, c_k^*\, Ne \frac{d\psi}{dx} \qquad (3.2.6)$$

in which $z_k = +1$ has been assumed. In the semiconductor literature, the equivalent expression for the flux density of holes usually takes the form

$$J^* = -D \frac{dc^*}{dx} - \mu c^* \frac{d\psi}{dx} \qquad (3.2.7)$$

where D and μ are respectively the 'diffusion constant' and the 'mobility' of holes. By comparison of Equations 3.2.6 and 3.2.7 we

obtain

$$D = N\ kT\ u_k \qquad (3.2.8)$$

and $$\mu = N\ e\ u_k \qquad (3.2.9)$$

which shows the relationship between the constants D and μ usually employed in semiconductor work and the mobility, u_k, used in electrochemistry. Division of Equation 3.2.8 by Equation 3.2.9 leads to the 'Einstein equation'[52]

$$\frac{D}{\mu} = \frac{kT}{e}$$

and shows that its validity depends on the assumption of unity activity coefficient, made in using Equation 3.2.5 in the above derivation, and also on the assumption which was tacitly made that the same mobility term, u_k, may be used in relating particle velocity to the chemical and electrostatic components of the driving force. This assumption is by no means universally valid[53].

We conclude this section by observing that a considerable parallelism exists between the theory of electrolytes and semiconductors[54] although this is not always recognised. An interesting example is the relationship between the Fermi energy, E_F, and the electrochemical potential, $\tilde{\mu}_e$, of electrons[55],

$$E_F = \frac{\tilde{\mu}_e}{N}$$

3.3 PERMEABLE MEMBRANES AND THE DONNAN POTENTIAL

The simplest membrane which can be conceived is a fully permeable membrane through which all anions and all cations may pass. The function of the membrane is purely to prevent convection between the

solutions on either side of it.

The condition for thermodynamic equilibrium in such a system is that the electrochemical potential of each species is constant across the membrane (Equation 3.2.2). It follows that the equilibrium membrane potential, $\psi'' - \psi'$, is given by

$$\psi'' - \psi' = \frac{1}{z_k F} (\mu_{ok}' - \mu_{ok}'' + RT \ln \frac{a_k'}{a_k''}) \qquad (3.3.1)$$

Since we have assumed aqueous solutions on both sides of the membrane, we may write

$$\mu_{ok}' = \mu_{ok}''$$

$$\text{therefore } \psi'' - \psi' = \frac{RT}{F} \ln \left(\frac{a_k'}{a_k''} \right)^{\frac{1}{z_k}}$$

It follows that

$$\left(\frac{a_k'}{a_k''}\right)^{\frac{1}{z_k}} = r \qquad (3.3.2)$$

for all species, k, where r, the 'Donnan distribution ratio' is given by

$$r = \exp \frac{F}{RT} (\psi'' - \psi')$$

$$\text{and } \psi'' - \psi' = \frac{RT}{F} \ln r \qquad (3.3.3)$$

Equation 3.3.2 may be alternatively written, for a mixture of any number of anions and cations of different valencies,

$$\left(\frac{a_i'}{a_i''}\right)^{\frac{1}{z_i}} = \left(\frac{a_j''}{a_j'}\right)^{\frac{1}{|z_j|}} = r \qquad (3.3.4)$$

For the particular case in which there is only one univalent cation (A^+) and one univalent anion (B^-) in equilibrium across the membrane, Equation 3.3.4 reduces to

$$\frac{a_A^{+'}}{a_A^{+''}} = \frac{a_B^{-''}}{a_B^{-'}} = r$$

$$\text{hence } a_A^{+'}\, a_B^{-'} = a_A^{+''}\, a_B^{-''} \qquad (3.3.5)$$

which is usually referred to as the basic relationship for the Donnan equilibrium[56].

Assuming charge neutrality in both solutions (ie only a negligible amount of charge requires to cross the membrane in order to sustain the potential, $\psi'' - \psi'$) we may write

$$\left.\begin{aligned} c_A^{+'} &= c_B^{-'} \\ \text{and } c_A^{+''} &= c_B^{-''} \end{aligned}\right\} \qquad (3.3.6)$$

By combining Equations 3.3.5 and 3.3.6, under the assumption that activity is equal to concentration, it can be shown that

$$c_A^{+''} = c_A^{+'}$$

It follows from Equation 3.3.3 that

$$\psi'' - \psi' = 0$$

These results express the commonsense deduction that equilibrium will be reached in this system only after sufficient mass transfer has taken place that the concentrations of each ion are equal on each side of the

membrane. It follows that the equilibrium membrane potential is zero.

It is most important to recognise that systems which are met with in practice may not in fact be in equilibrium and may exist in a non-equilibrium state for extended periods of time. Under these conditions a membrane potential due to the different mobilities of diffusing species may be developed (the 'diffusion potential' or 'liquid junction potential'). Such potentials may be very stable despite their essentially non-equilibrium nature, an important illustration being the salt bridge incorporated into certain reference electrode systems in which potentials stable to within a few millivolts may be maintained for many months. The usual derivation of the equations for the liquid junction potential are given in Appendix 1 and will also be derived in Section 3.4 as a special case of the analysis of the 'fixed charge membrane'.

We notice that the basic relationship for the Donnan equilibrium (Equation 3.3.5) does not by itself yield an expression for the electrical potential. A further condition imposed by charge neutrality is required, the trivial case of Equation 3.3.6 being an example.

In order to derive the classical 'Donnan potential' it is necessary to assume that the membrane is impermeable to at least one of the ions present in the solution on one side of it. The mechanism of this semi-permeability need not be known in order to derive equations for the equilibrium potential.

We will consider as an example a simple case in which there is one monovalent cation (A^+) and one monovalent anion (B^-), both being permeable through the membrane, together with one other singly charged negative species, S^-, present at concentration $c_S^{-'}$ on one side of the membrane only.

The basic relationship of Equation 3.3.5 may be applied to the permeable species, under equilibrium conditions, as before

$$a_A^{+'}\ a_B^{-'} = a_A^{+''}\ a_B^{-''} \tag{3.3.5}$$

The charge neutrality conditions in this case are

$$\left.\begin{aligned} c_A^{+'} &= c_B^{-'} + c_S^{-'} \\ \text{and}\quad c_A^{+''} &= c_B^{-''} = c'' \end{aligned}\right\} \tag{3.3.7}$$

where c'' represents the concentration of A^+ or B^- in phase ("). By combining Equations 3.3.7 and Equation 3.3.5 (assuming unity activity coefficients) we obtain

$$(c_B^{-'} + c_S^{-'})\, c_B^{-'} = (c'')^2$$

$$\text{hence}\quad c_B^{-'} = c_S^{-'} \left[\left\{ \left(\frac{c''}{c_S^{-'}}\right)^2 + \frac{1}{4} \right\}^{\frac{1}{2}} - \tfrac{1}{2} \right]$$

From Equations 3.3.3 and 3.3.4 the 'Donnan membrane potential', $\psi'' - \psi'$, is given by

$$\psi'' - \psi' = \frac{RT}{F} \ln \frac{c_B^{-''}}{c_B^{-'}}$$

$$= -\frac{RT}{F} \ln \frac{c_S^{-'}}{c''} \left[\left\{ \left(\frac{c''}{c_S^{-'}}\right)^2 + \frac{1}{4} \right\}^{\frac{1}{2}} - \tfrac{1}{2} \right] \tag{3.3.8}$$

It must be understood that Equation 3.3.8 refers to the thermodynamic equilibrium values of $\psi'' - \psi'$ and c''. In general however, given arbitrary initial concentrations in the solutions, considerable mass transfer may need to take place before the equilibrium condition

is reached. An example is given in Appendix 2. This may be contrasted with certain phase boundary phenomena in which, as will be discussed in later sections, the electrical potential is established with only a negligible transfer of mass and charge. The example of Appendix 2 also illustrates the phenomenon of ion accumulation (transport against a concentration gradient) which is of considerable significance in cell biology. While mass transfer is taking place a diffusion potential (similar to the liquid junction potential) will exist, its magnitude being dependent on the relative mobilities of the permeable species.

The foregoing analysis follows the classical treatment of the Donnan membrane potential in which the equilibrium is established between solution phases on opposite sides of the membrane, no model being invoked for the detailed structure of the membrane or for the mechanisms of processes within it. In the more complete theory of fixed charge membranes, to be dealt with in the following section, the term 'Donnan potential' is used to describe phase boundary processes between the solution and the membrane phase itself. In this case the fixed charges in the membrane phase are analogous to the impermeable ion, S^-, of the classical treatment.

3.4 FIXED CHARGE MEMBRANES

The process of transport through membranes was regarded, in classical theories, as being essentially one of diffusion in a confined aqueous phase. The membrane itself served merely as a barrier to convection. It was assumed that the membrane surfaces are always in equilibrium with the solutions and that quantities such as solute

concentrations and electrical potential are continuous across the phase boundaries (Figure 3.4.1a). Teorell[57] has noted that the analysis of this model, using the Nernst-Planck equations for the diffusion potential, yielded results which were in reasonable agreement with experiments in coarse, porous membranes. In many other cases however experiments on both biological membranes and certain types of artificial membrane revealed serious discrepancies with the classical theory. The transport of ions was often observed to be much less than could be explained simply by restrictions on the diffusion area due to the 'sieve' effect. Selective ion permeability for either cations or anions was also noticed and could not be explained by the existing theory.

The need to modify the physical model of the membrane in order to explain these deviations from the classical theory resulted in the 'fixed charge theory' of membranes which was proposed independently by Teorell[58] in 1935 and Meyer and Sievers[59-62] in 1936.

The Teorell-Meyer-Sievers (TMS) theory made an essential contribution to the understanding of membrane processes by the introduction of two new concepts of fundamental significance. Firstly, it was assumed that the membrane itself possesses a fixed charge distributed uniformly through it. (No assumption as to the nature of the fixed charge was made). Secondly, it was assumed that processes analogous to the Donnan equilibrium take place at the interfaces between the membrane and the solution phases. Abrupt discontinuities in concentrations and potential are therefore expected at the interfaces, in addition to the continuous variation of these quantities due to classical diffusion processes in the bulk membrane phase (Figure 3.4.1b).

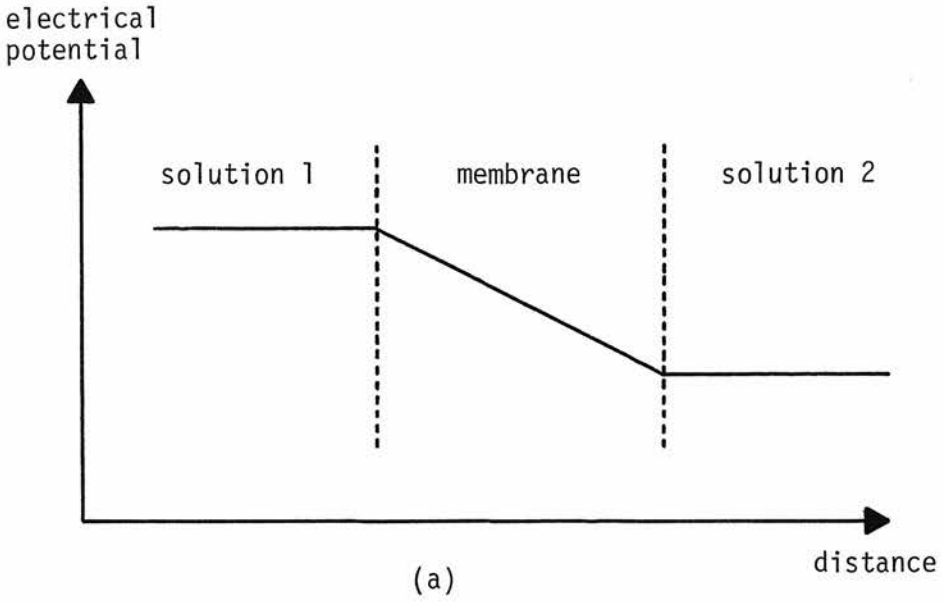

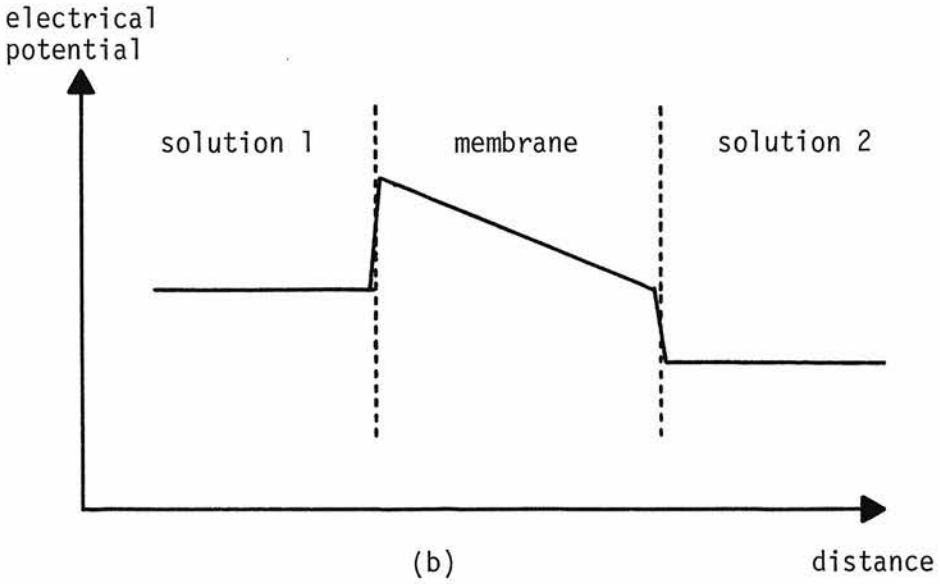

Figure 3.4.1 Variation of electrical potential through a membrane separating two aqueous solutions; (a) classical model, (b) according to the fixed charge theory

The total membrane potential for example is seen as the sum of two phase boundary (or Donnan) potentials and a diffusion potential in the bulk.

An important feature of the TMS theory is that the phase boundary process is assumed to be sufficiently fast that the interfaces may be regarded as being always in thermodynamic equilibrium. The diffusion processes in the membrane interior, on the other hand, are essentially non-equilibrium phenomena in which a continuous (albeit slow) transport of matter is involved. The diffusion process is therefore the rate controlling step of the overall membrane process and quantities such as the diffusion potential rely on non-thermodynamic variables, especially ionic mobilities.

The original TMS theory employed the 'Henderson approximation'[63] which assumes that the ionic concentrations vary linearly with distance through the membrane. The incorrectness of this assumption was subsequently noted by Teorell who published a more rigorous analysis[64] which does not rely upon the Henderson approximation. The revised theory allows expressions to be obtained for the ionic fluxes as well as for the membrane potential (to which the original TMS theory was restricted).

The revised fixed charge theory will now be summarised for comparison with the ion exchange theory of the glass electrode, to be discussed in Chapter 4. The following material is largely based on a review article by Teorell[57].

The model of the fixed charge membrane is defined by the following assumptions:

- The membrane matrix is rigid, of constant volume and behaves as a strongly ionised exchange body with fixed ions or 'charges' of a constant volume density referred to the aqueous interstices (called 'membrane concentration').

- The membrane interstices are permeable to all the cations and anions which are present in the external solutions and are homogeneous throughout the membrane. We note here that in the analysis of the glass electrode, the more restrictive assumption of permeability only to cations may be safely made and the analysis is commonly further restricted to only two exchanging species. This leads to a great simplification in the algebra.

- Osmotic or hydrostatic flow of water is negligible (a very commonly used assumption).

- The membrane surfaces are in a state of permanent instantaneously established Donnan equilibrium with the same distribution ratio for all cations (and the inverse value valid for all anions). This assumption implies that the rates of ion fluxes are entirely controlled by the transport process in the membrane. In terms of electrochemical potentials, the assumption of Donnan equilibria at the phase boundaries is equivalent to the statement that the standard potential of each species in the membrane phase has the same value as in aqueous solution. That is, in physical terms, an ion inside the membrane is in a basically aqueous environment. This must be contrasted with the case of the glass electrode in which the environment of an ion in a silicate lattice site is essentially different from that of one in aqueous solution and hence different standard potentials must be introduced for ions in

these two phases.

- Unity activity coefficients are assumed throughout. Again we contrast with the usual analysis of the glass electrode in which a formal dependence of activity on concentration in the membrane phase is assumed (usually known as 'n-type non-ideal behaviour').

The following additional simplifying assumptions are also used:

- Only monovalent ions are considered.
- Steady state conditions in respect of ion concentrations are assumed throughout (although not, in general, zero current). For the glass electrode, an analysis under non-steady state conditions has been carried out by Conti and Eisenman[65].
- The assumption of macroscopic space charge neutrality within the membrane phase is made. This assumption is commonly made in the mathematical analysis of membrane phenomena and is further discussed in Appendix 3.

The first stage of the analysis is the calculation of the diffusion potential within the membrane using the Nernst-Planck equation for each of the diffusing ions. From Equation 3.2.5 we may write, for a univalent cation species, i,

$$J_i' = - u_i' c_i' \left(\frac{RT}{c_i'} \frac{dc_i'}{dx} + F \frac{d\psi'}{dx}\right) \qquad (3.4.1)$$

where the single primes denote quantities within the membrane phase.

The above mentioned assumptions of homogeneity and unity activity coefficients are implicit in this equation. The corresponding equation for a univalent anion species is

$$J_j' = - u_j' c_j' \left(\frac{RT}{c_j'} \frac{dc_j'}{dx} - F \frac{d\psi'}{dx}\right) \qquad (3.4.2)$$

Charge neutrality within the membrane is expressed by

$$\Sigma c_i' - \Sigma c_j' + z_S c_S' = 0 \qquad (3.4.3)$$

where c_S' is the concentration of membrane sites and $z_S = +1$ for positively charged sites and -1 for negatively charged sites. We note that c_i', c_j' and ψ' in the above equations are functions of x. The assumption of steady state conditions however implies directly that J_i' and J_j' are constant with respect to x.

The set of equations defined by Equations 3.4.1 and 3.4.2 (for all i and j) may then be integrated, using Equation 3.4.3, to give the result derived by Teorell[57]

$$J_i' = -K^+ u_i' (c_{id}' \xi' - c_{io}') \qquad (3.4.4)$$

where the subscripts o and d denote values inside the membrane adjacent to the solution interfaces at x = o and x = d. ξ' is related to the diffusion potential across the membrane, ψ_D, by

$$\xi' = \exp \frac{F}{RT} \psi_D \qquad (3.4.5)$$

where $\psi_D = \psi_d' - \psi_o'$.

K^+ is a factor common to all cation species and is given by

$$K^+ = \frac{RT}{d}\left(\frac{\Sigma c_{id}' - \Sigma c_{io}' - 0.5\, z_S\, c_S'\, \ell n\, \xi'}{\xi'\, \Sigma c_{id}' - \Sigma c_{io}'}\right) \frac{\ell n\, \bar{k}\, \xi'}{\ell n\, \bar{k}} \qquad (3.4.6)$$

$$\text{where } \bar{k} = \frac{\Sigma c_{id}' + 0.5\, z_S\, c_S'\, \frac{\ell n\, \bar{k}\, \xi'}{\ell n\, k}}{\Sigma c_{io}' + 0.5\, z_S\, c_S'\, \frac{\ell n\, \bar{k}\, \xi'}{\ell n\, \bar{k}}} \qquad (3.4.7)$$

$$\text{or} \quad \bar{k} = \frac{\Sigma c_{jd}' - 0.5\, z_S\, c_S'\, \frac{\ell n\, \bar{k}/\xi'}{\ell n\, k}}{\Sigma c_{jo}' - 0.5\, z_S\, c_S'\, \frac{\ell n\, \bar{k}/\xi'}{\ell n\, \bar{k}}} \qquad (3.4.8)$$

The corresponding expression for anion species is

$$J_j' = -K^-\, u_j'\left(\frac{c_{jd}'}{\xi'} - c_{jo}'\right) \qquad (3.4.9)$$

$$\text{where } K^- = \frac{RT}{d}\left(\frac{\Sigma c_{jd}' - \Sigma c_{jo}' - 0.5\, z_S\, c_S'\, \ell n\, \xi'}{\frac{1}{\xi'}\, \Sigma c_{jd}' - \Sigma c_{jo}'}\right) \frac{\ell n\, \bar{k}/\xi'}{\ell n\, k} \qquad (3.4.10)$$

The transcendental form of these equations is a consequence of not using the simplifying Henderson approximation.

Equations 3.4.4 and 3.4.9 pertain solely to the diffusion process taking place within the membrane phase. They relate the flux of each species to the concentrations of anions and cations at planes just beneath the membrane surfaces and to the electrical potential difference between these planes. The equations are valid for the case of non-zero current (ie when an external source of emf is impressed

across the membrane) as well as in the free diffusion (zero current) case. In order to obtain solutions of these equations in terms of directly measurable quantities (such as solution concentrations) and to derive an expression for the total membrane potential, it is necessary to introduce a model for the processes taking place across the phase boundaries between the membrane and the adjacent solutions.

It is often stated in the literature that Donnan potentials are set up at the interfaces. This can be a little confusing in view of the traditional interpretation of the Donnan potential as a total membrane effect, as described in Section 3.3. It must be recognised however that the model used in Section 3.3 (equilibrium between two phases with at least one charged species restricted to one of the phases) can also be applied in the present case to the phase boundary between the membrane and the adjacent solutions. In this case every ion in the solution phase is assumed to be in equilibrium across the boundary and the fixed charge on the membrane sites is analogous to the concentration of the impermeable ion, S^-, of Section 3.3. It was assumed, in the derivation of the Donnan potential, that the standard chemical potential of each species is the same in both phases. This is physically equivalent, in the present case, to assuming that the environment within the membrane is 'aqueous'.

Using Equation 3.3.4, under the assumption of unity activity coefficients, we may write

$$c_i' = rc_i'' \qquad (3.4.11)$$

and

$$c_j' = \frac{1}{r} c_j'' \qquad (3.4.12)$$

for monovalent cations and anions respectively, where the double primes denote the solution phase. Summation of Equations 3.4.11 and 3.4.12 over all i and all j respectively gives

$$\Sigma c_i' = r \Sigma c_i'' \tag{3.4.13}$$

and $$\Sigma c_j' = \frac{1}{r} \Sigma c_j'' \tag{3.4.14}$$

By substitution of Equations 3.4.13 and 3.4.14 into Equation 3.4.3 (the condition for charge neutrality in the membrane phase) we obtain

$$r \Sigma c_i'' - \frac{1}{r} \Sigma c_j'' + z_S c_S' = 0 \tag{3.4.15}$$

Charge neutrality in the solution phase is expressed by

$$\Sigma c_i'' = \Sigma c_j'' = c'' \tag{3.4.16}$$

where c" represents the total concentration of positive or negative species in the solution phase ("). Substituting Equation 3.4.16 into Equation 3.4.15 and solving for r, we obtain

$$r = \left[1 + \left(\frac{z_S c_S'}{2c''}\right)^2\right]^{\frac{1}{2}} - \frac{z_S c_S'}{2c''} \tag{3.4.17}$$

where r is the Donnan distribution ratio between the membrane and the adjacent aqueous phase and is a function of the fixed charge density in the membrane and the total ionic concentration in the aqueous solution. The Donnan potentials associated with the phase boundary processes are then given, by Equation 3.3.3, as

$$\psi_o'' - \psi_o' = \frac{RT}{F} \ln r_o \qquad (3.4.18)$$

and $$\psi_d'' - \psi_d' = \frac{RT}{F} \ln r_d \qquad (3.4.19)$$

where r_o and r_d are the values of r at the interfaces at x = o and x = d respectively ($r_o \neq r_d$ in general). $\psi_o'' - \psi_o'$ and $\psi_d'' - \psi_d'$ are the phase boundary potentials at these interfaces. The summed effect of the two phase boundary potentials, ψ_{PB}, is then given by

$$\psi_{PB} = (\psi_d'' - \psi_d') + (\psi_o' - \psi_o'')$$

$$\text{hence } \psi_{PB} = \frac{RT}{F} \ln \frac{r_d}{r_o} \qquad (3.4.20)$$

The total membrane potential, ψ_M, is the sum of the phase boundary potentials, ψ_{PB}, and the diffusion potential, ψ_D, in the membrane interior which was derived previously. Hence, from Equations 3.4.5 and 3.4.20

$$\psi_M = \frac{RT}{F} \ln \frac{r_d}{r_o} + \frac{RT}{F} \ln \xi'$$

$$\text{hence } \psi_M = \frac{RT}{F} \ln \frac{r_d}{r_o} \xi' \qquad (3.4.21)$$

Using Equations 3.4.11 and 3.4.12, the ionic fluxes (Equations 3.4.4 and 3.4.9) may now be expressed in terms of the ionic concentrations in the aqueous solution phases.

$$J_i' = -K^+ u_i' (r_d c_{id}'' \xi' - r_o c_{io}'') \qquad (3.4.22)$$

and $$J_j' = -K^- u_j' \left(\frac{c_{jd}''}{r_d \xi'} - \frac{c_{jo}''}{r_o}\right) \qquad (3.4.23)$$

The application of the above theory is cumbersome in general, owing to the transcendental nature of Equations 3.4.4 to 3.4.10, and has already been dealt with in detail by Teorell[57]. The present objective is not to discuss the properties of fixed charge membranes but to show that certain commonly occurring phenomena may be regarded as limiting cases of the fixed charge membrane and to indicate the relationship between the fixed charge theory and the theory of the glass electrode. For this purpose the discussion will be restricted to the case of zero membrane current (which is the usual measurement condition in electrode work) and attention will be directed mainly to the membrane potential.

The zero current condition may be expressed by

$$\Sigma J_i' = \Sigma J_j'$$

since all the ions involved are assumed to be monovalent. Hence, using Equations 3.4.4 and 3.4.9,

$$-K^+ \Sigma u_i' (c_{id}' \xi' - c_{io}') = -K^- \Sigma u_j' \left(\frac{c_{jd}'}{\xi'} - c_{jo}'\right)$$

By substituting for K^+ and K^- (from Equations 3.4.6 and 3.4.10) and rearranging, it can be shown that

$$\frac{\xi' U_d' - U_o'}{V_d' - \xi' V_o'} = \frac{\xi' \Sigma c_{id}' - \Sigma c_{io}'}{\Sigma c_{jd}' - \xi' \Sigma c_{jo}'} \frac{\ell n \bar{k} - \ell n \xi'}{\ell n \bar{k} + \ell n \xi'} \qquad (3.4.24)$$

where $U_o' = \Sigma c_{io}' u_i'$,

$U_d' = \Sigma c_{id}' u_i'$,

$V_o' = \Sigma c_{jo}' u_j'$

and $V_d' = \Sigma c_{jd}' u_j'$.

Equation 3.4.24 is the 'extended Planck formula' of Teorell[57].

We now consider the limiting case of a membrane with zero fixed charge ($c_S' \to 0$). In physical terms, this is equivalent to reducing the fixed charge membrane to the simple convection barrier of Section 3.3. It then follows, from Equation 3.4.17, that

$$r_o = r_d = 1$$

and hence that the phase boundary potentials at each interface are zero (Equation 3.4.18 and 3.4.19). The total membrane potential is therefore due solely to the diffusion potential which is obtainable from Equation 3.4.24. It has further been noted by Teorell[57] that the latter equation reduces, when $c_S' = 0$, to

$$\frac{\xi' U_d' - U_o'}{V_d' - \xi' V_o'} = \frac{\xi' c_d' - c_o'}{c_d' - \xi' c_o'} \frac{\ell n \frac{c_d'}{c_o'} - \ell n \xi'}{\ell n \frac{c_d'}{c_o'} + \ell n \xi'} \qquad (3.4.25)$$

where $c_o' = \Sigma c_{io}' = \Sigma c_{jo}'$

and $c_d' = \Sigma c_{id}' = \Sigma c_{jd}'$.

Using Equations 3.4.11 to 3.4.14, together with the condition $r_o = r_d = 1$,

we may re-write Equation 3.4.25 in terms of solution concentrations,

$$\frac{\xi' \Sigma c_{id}'' u_i' - \Sigma c_{io}'' u_i'}{\Sigma c_{jd}'' u_j' - \xi' \Sigma c_{jo}'' u_j'} = \frac{\xi' c_d'' - c_o''}{c_d'' - \xi' c_o''} \frac{\ell n \frac{c_d''}{c_o''} - \ell n \xi'}{\ell n \frac{c_d''}{c_o''} + \ell n \xi'} \quad (3.4.26)$$

where $c_o'' = \Sigma c_{io}'' = \Sigma c_{jo}'' = c_o'$

and $c_d'' = \Sigma c_{id}'' = \Sigma c_{jd}'' = c_d'$

Equation 3.4.26 is equivalent to Equation A1.2 for the liquid junction potential as discussed in Appendix 1. The liquid junction potential may therefore be regarded as a limiting case of the fixed charge membrane potential when the membrane charge, c_S', tends to zero.

The other limiting case of the fixed charge membrane is that for which the membrane fixed charge concentration is large compared with the concentration of ions in the solutions. Explicit equations for the ionic fluxes and membrane potential in the highly charged membrane are not obtainable in general but Teorell[57] has illustrated its properties by reference to certain special cases. One such case (of particular importance in biology) is that of equal total concentrations in the solutions adjacent to the membrane. For this condition, it follows from Equation 3.4.17 that the Donnan distribution ratios, r_o and r_d, at the two interfaces are equal and hence that the sum of the phase boundary potentials, ψ_{PB}, is zero (Equation 3.4.20). The total membrane potential is then equal to the diffusion potential which is obtainable from Equations 3.4.5 and 3.4.24. According to Teorell[57], the latter equation reduces to

$$\xi' = \frac{U_o' + V_d'}{U_d' + V_o'}$$

in the particular case of equal total solution concentrations. The total membrane potential (known as the 'bi-ionic' potential in this particular case) may then be written, in terms of solution concentrations

$$\psi_M = \frac{RT}{F} \ln \left(\frac{r \Sigma u_i' c_{io}'' + \frac{1}{r} \Sigma u_j' c_{jd}''}{r \Sigma u_i' c_{id}'' + \frac{1}{r} \Sigma u_j' c_{jo}''} \right) \qquad (3.4.27)$$

where r is the Donnan distribution ratio at either interface. It can be seen from Equation 3.4.17 that $r \to \infty$ for a membrane with large negative fixed charge and Equation 3.4.27 for the total membrane potential then becomes

$$\psi_M = \frac{RT}{F} \ln \frac{\Sigma u_i' c_{io}''}{\Sigma u_i' c_{id}''} \qquad (3.4.28)$$

in which ψ_M is a function of the concentrations of the cations only. Anion species are in fact effectively excluded from the membrane in this particular case, as a consequence of the limiting value of r (see Equation 3.4.12). It follows that only cations pass through the membrane. In the case of a membrane with large positive fixed charge, it is the cations which are excluded and the potential is determined solely by anionic species. The excluded ions, which have the same sign of charge as the membrane fixed charge, are known as 'co-ions' and membranes which differentiate in this way between positive and negative species are termed 'permselective'.

Equation 3.4.28 introduces the concept of the selectivity of the [illegible]for different ions. For the case of two cations, A^+ and B^+, in a highly negative membrane for example, Equation 3.4.28 becomes

$$\psi_M = \frac{RT}{F} \ln \frac{c_{Ao}'' + \frac{u_B'}{u_A'} c_{Bo}''}{c_{Ad}'' + \frac{u_B'}{u_A'} c_{Bd}''} \qquad (3.4.29)$$

In the limiting cases of $u_B' >> u_A'$ and $u_B' << u_A'$, the membrane potential has a Nernstian dependence on the solution concentrations of A and B respectively. In intermediate cases ($u_B' \approx u_A'$), the concentrations of both species affect the potential to an extent dependent on the mobility ratio, u_B'/u_A'. The selectivity of the potential to each species therefore depends only on the mobility ratio.

Teorell[57] has discussed in detail the predictions of the fixed charge theory, with particular reference to the ionic fluxes and membrane potentials in several special cases of particular interest in biology. The main objective of this section has been to illustrate the origin of selectivity in the fixed charge membrane, for comparison with the glass electrode theory described in Chapter 4. It will be shown that a theoretical model for the glass electrode may be developed from the TMS theory by introducing the concept of a difference between the standard chemical potentials of a species in the membrane phase and the solution phase.

CHAPTER 4: THEORY OF THE GLASS ELECTRODE

A comprehensive theory of the glass electrode was formulated in a series of papers by Eisenman and others in the early 1960s[19,65-68]. The theory is founded on the concept of phase boundary and diffusion processes which was first employed in the TMS theory of fixed charge membranes (Chapter 3). The exact nature of the phase boundary process however is assumed to be an ion exchange mechanism instead of the Donnan equilibrium of the TMS theory. A thermodynamic analysis of the ion exchange process was proposed by Nicolsky in 1937 (see summaries in English by Dole[69] and by Eisenman[66]) but the 'ion exchange' and 'diffusion' mechanisms were for many years regarded as alternative theories. The contribution of Eisenman and his co-workers was their synthesis into a single model, following the original example of the TMS theory.

We shall repeat the approach of Section 3.4 by considering first the diffusion process in the bulk membrane. The boundary conditions for ionic concentrations just inside the membrane will then be determined, using an ion exchange model for the interfacial process.

The glass membrane is defined by the following assumptions, which may be compared with those used in the analysis of the fixed charge membrane (Section 3.4):

- The glass membrane is assumed to be rigid and of constant volume. The sites on which the fixed charge resides are distributed homogeneously through the membrane.

- Anions are completely excluded from the membrane phase and are therefore not in equilibrium across the phase boundaries and the analysis is further restricted to the case of only two exchanging cations, A^+ and B^+.

- Osmotic and hydrostatic flow of water is negligible.

- The ion exchange model for the interfacial process may be defined by the inequality of the standard chemical potentials of a species in the glass and aqueous phases. The equilibrium condition for cation, i, is then given by Equation 3.2.2,

$$\mu_{oi}' + RT \ln a_i' + z_i F\psi' = \mu_{oi}'' + RT \ln a_i'' + z_i F\psi''$$

where $\mu_{oi}' \neq \mu_{oi}''$.

The membrane is therefore regarded as having 'chemical' properties in addition to the properties of fixed charge and prevention of convection which were assumed in the TMS theory of the fixed charge membrane. The environment of an ion in the glass phase is quite different from that in aqueous solution. The phase boundary process is assumed to be fast compared with the bulk (diffusion) process.

- The glass is assumed to exhibit 'n-type non-ideal behaviour'[67] in which the activity of a species in the glass phase has a power law dependence on its concentration,

ie $$a = \gamma c = pc^n \qquad (4.1)$$

where γ is the activity coefficient of the species in the glass phase and p and n are constants.

The following additional simplifying assumptions are also used:

- Only monovalent ions are considered.

- Macroscopic space charge neutrality exists in the glass phase. (This assumption is discussed in Appendix 3).

Equations for the diffusion potential and ionic fluxes in the membrane have been derived by Karreman and Eisenman[67] under the additional assumptions of steady state ionic concentrations (also used in the TMS theory) and zero membrane current. Like the TMS theory, the analysis rests upon a statement of the Nernst-Planck equation for each of the diffusing ions. From Equation 3.2.4, we may write for the present case,

$$J_A' = -RT\, u_A' \left(\frac{dc_A'}{dx} + c_A' \frac{d\, \ell n\, \gamma_A'}{dx} + c_A' \frac{F}{RT} \frac{d\psi'}{dx}\right) \qquad (4.2)$$

and $$J_B' = -RT\, u_B' \left(\frac{dc_B'}{dx} + c_B' \frac{d\, \ell n\, \gamma_B'}{dx} + c_B' \frac{F}{RT} \frac{d\psi'}{dx}\right) \qquad (4.3)$$

where J_A' and J_B' are the fluxes of the two diffusing monovalent cations, A^+ and B^+, to which the analysis is restricted. The single primes again denote the membrane phase. The assumption of homogeneity in the glass phase is implicit in Equations 4.2 and 4.3. (This restriction has been removed in more general analysis by Conti and Eisenman[68], in which the spacing of sites in the glass is assumed to be variable and the standard chemical potentials of ions in the glass phase are therefore functions of x). By solving Equations 4.2 and 4.3 under the above mentioned conditions of charge neutrality, steady state and zero current, Karreman and Eisenman[67] showed that the electrical potential gradient, $\frac{d\psi'}{dx}$, in the membrane is given by

$$\frac{d\psi'}{dx} = -n\frac{RT}{F} \frac{d}{dx} \ell n(u_A' c_A' + u_B' c_B') \qquad (4.4)$$

in which c_A' and c_B' are functions of x. Integration of Equation 4.4 over the entire thickness of the membrane (ie from x = o to x = d) then gives the diffusion potential ψ_D.

$$\psi_D = \psi_d' - \psi_o' = n \frac{RT}{F} \ln \left(\frac{u_A' c_{Ao}' + u_B' c_{Bo}'}{u_A' c_{Ad}' + u_B' c_{Bd}'}\right) \qquad (4.5)$$

where c_{Ao}', c_{Ad}', c_{Bo}' and c_{Bd}' are the ionic concentrations just inside the membrane at each interface. This expression for the diffusion potential is much simpler than the transcendental equations obtained in the TMS theory, as a consequence of the more restrictive assumptions which were employed.

In Karreman and Eisenman's analysis[67] (as in the TMS theory) the mobilities, u_A' and u_B' were assumed to be constants. It has since been shown however[43,65] that it is sufficient to assume that the *ratio* u_B'/u_A' is independent of x, in order to obtain an explicit solution for the diffusion potential. The validity of this assumption has recently been questioned by Isard[43], as discussed later in this chapter.

The zero current condition used in Karreman and Eisenman's analysis[67] was removed in a more general treatment by Conti and Eisenman[68] in which current-voltage relationships (again under steady state conditions) were derived.

Eisenman[66] has related the ionic concentrations just inside the membrane (c_{Ao}', c_{Bo}' etc, in Equation 4.5) to the concentrations of species in the adjacent aqueous solutions. The analysis follows the earlier treatment by Nicolsky, with modifications to account for 'n-type non-ideal behaviour'. Using Equation 3.2.2 we may write

$$\mu_{oA}' + RT \ln a_A' + F\psi' = \mu_{oA}'' + RT \ln a_A'' + F\psi'' \qquad (4.6)$$

and

$$\mu_{oB}' + RT \ln a_B' + F\psi' = \mu_{oB}'' + RT \ln a_B'' + F\psi'' \qquad (4.7)$$

where A^+ and B^+ are the two monovalent cations in equilibrium between a glass phase (') and a solution phase ("). It follows from Equation 4.6 that the phase boundary potential, $\psi'' - \psi'$, is given by

$$\psi'' - \psi' = \frac{\mu_{oA}' - \mu_{oA}''}{F} + \frac{RT}{F} \ln \frac{a_A'}{a_A''} \qquad (4.8)$$

Similarly, from Equation 4.7,

$$\psi'' - \psi' = \frac{\mu_{oB}' - \mu_{oB}''}{F} + \frac{RT}{F} \ln \frac{a_B'}{a_B''} \qquad (4.9)$$

Combining Equations 4.8 and 4.9

$$\mu_{oA}' - \mu_{oA}'' - \mu_{oB}' + \mu_{oB}'' = RT \ln \frac{a_A'' a_B'}{a_A' a_B''} \qquad (4.10)$$

Writing $\mu_{oA}' - \mu_{oA}'' - \mu_{oB}' + \mu_{oB}'' = RT \ln K_{AB}$ where K_{AB} is a constant we obtain

$$K_{AB} = \frac{a_A'' a_B'}{a_A' a_B''} \qquad (4.11)$$

so that K_{AB} may be regarded as the equilibrium constant of an ion exchange reaction, $A' + B'' \leftrightharpoons A'' + B'$, in which species B, initially in solution, replaces species A, initially on a site in the glass phase.

Using Equation 4.1 we may rewrite Equation 4.11 in terms of the concentrations of ions in the glass phase.

$$K_{AB} = \frac{a_A''}{a_B''} \left(\frac{c_B'}{c_A'}\right)^n \tag{4.12}$$

Charge neutrality in the glass is expressed by

$$c_A' + c_B' - c_S' = 0 \tag{4.13}$$

where c_S' is the concentration of negatively charged sites. Combining Equations 4.12 and 4.13 and rearranging, we obtain

$$\frac{(c_A')^n}{a_A''} = \frac{(c_S')^n}{\left[(a_A'')^{\frac{1}{n}} + K_{AB}^{\frac{1}{n}} (a_B'')^{\frac{1}{n}}\right]^n} \tag{4.14}$$

Equation 4.8 for the phase boundary potential may be written (using Equation 4.1) as

$$\psi'' - \psi' = \frac{\mu_{oA}' - \mu_{oA}''}{F} + \frac{RT}{F} \ln \frac{p\,(c_A')^n}{a_A''} \tag{4.15}$$

Combining Equations 4.14 and 4.15 we obtain

$$\psi'' - \psi' = \psi^o - \frac{nRT}{F} \ln \left[(a_A'')^{\frac{1}{n}} + K_{AB}^{\frac{1}{n}} (a_B'')^{\frac{1}{n}}\right] \tag{4.16}$$

where ψ^o is a constant given by

$$\psi^o = \frac{\mu_{oA}' - \mu_{oA}'' + RT \ln p\,(c_S')^n}{F} \tag{4.17}$$

Using Equation 4.16, the phase boundary potentials associated with the

glass solution interfaces at x = o and x = d may be written respectively as

$$\psi_o'' - \psi_o' = \psi^o - \frac{nRT}{F} \ln \left[(a_{Ao}'')^{\frac{1}{n}} + K_{AB}^{\frac{1}{n}} (a_{Bo}'')^{\frac{1}{n}}\right] \tag{4.18}$$

and

$$\psi_d'' - \psi_d' = \psi^o - \frac{nRT}{F} \ln \left[(a_{Ad}'')^{\frac{1}{n}} + K_{AB}^{\frac{1}{n}} (a_{Bd}'')^{\frac{1}{n}}\right] \tag{4.19}$$

The summed effect of the two phase boundary potentials, ψ_{PB}, is given by

$$\psi_{PB} = (\psi_d'' - \psi_d') + (\psi_o' - \psi_o'')$$

hence

$$\psi_{PB} = \frac{nRT}{F} \ln \frac{\left[(a_{Ao}'')^{\frac{1}{n}} + K_{AB}^{\frac{1}{n}} (a_{Bo}'')^{\frac{1}{n}}\right]}{\left[(a_{Ad}'')^{\frac{1}{n}} + K_{AB}^{\frac{1}{n}} (a_{Bd}'')^{\frac{1}{n}}\right]} \tag{4.20}$$

We note that the constant, ψ^o, does not appear in Equation 4.20.

Using Equation 4.14, the concentration of A^+ just inside the glass phase at x = o may be written in terms of the concentrations of A^+ and B^+ in the adjacent solution.

$$C_{Ao}' = \frac{c_S' (a_{Ao}'')^{\frac{1}{n}}}{(a_{Ao}'')^{\frac{1}{n}} + K_{AB}^{\frac{1}{n}} (a_{Bo}'')^{\frac{1}{n}}} \tag{4.21}$$

It can be shown that the corresponding equation for c_{Bo}' is

$$c_{Bo}' = \frac{c_S' \, K_{AB}^{\frac{1}{n}} \, (a_{Bo}")^{\frac{1}{n}}}{(a_{Ao}")^{\frac{1}{n}} + K_{AB}^{\frac{1}{n}} \, (a_{Bo}")^{\frac{1}{n}}} \qquad (4.22)$$

The corresponding expressions for c_{Ad}' and c_{Bd}' (at x = d) may be obtained by replacing the subscript o by d throughout Equations 4.21 and 4.22. It can then be shown that the diffusion potential, ψ_D, of Equation 4.5 may be written, in terms of solution concentrations, as

$$\psi_D = \frac{nRT}{F} \ln \frac{u_A' \, (a_{Ao}")^{\frac{1}{n}} + u_B' \, K_{AB}^{\frac{1}{n}} \, (a_{Bo}")^{\frac{1}{n}}}{u_A' \, (a_{Ad}")^{\frac{1}{n}} + u_B' \, K_{AB}^{\frac{1}{n}} \, (a_{Bd}")^{\frac{1}{n}}} + \frac{nRT}{F} \ln \frac{(a_{Ad}")^{\frac{1}{n}} + K_{AB}^{\frac{1}{n}} \, (a_{Bd}")^{\frac{1}{n}}}{(a_{Ao}")^{\frac{1}{n}} + K_{AB}^{\frac{1}{n}} \, (a_{Bo}")^{\frac{1}{n}}} \qquad (4.23)$$

The total membrane potential, ψ_M, is the sum of the phase boundary potentials, ψ_{PB}, and the diffusion potential, ψ_D. Hence, from Equations 4.20 and 4.23,

$$\psi_M = \frac{nRT}{F} \ln \frac{(a_{Ao}")^{\frac{1}{n}} + \frac{u_B'}{u_A'} K_{AB}^{\frac{1}{n}} \, (a_{Bo}")^{\frac{1}{n}}}{(a_{Ad}")^{\frac{1}{n}} + \frac{u_B'}{u_A'} K_{AB}^{\frac{1}{n}} \, (a_{Bd}")^{\frac{1}{n}}} \qquad (4.24)$$

As described in Chapter 2, the solution on one side of the glass membrane is usually a reference solution of constant composition. In

these circumstances, Equation 4.24 simplifies to

$$\psi_M = E_o + \frac{nRT}{F} \ln \left[(a_A")^{\frac{1}{n}} + \frac{u_B'}{u_A'} K_{AB}^{\frac{1}{n}} (a_B")^{\frac{1}{n}}\right] \qquad (4.25)$$

where E_o is a constant. Equation 4.25 is identical to the empirical equation proposed by Eisenman, Rudin and Casby[38] (Equation 2.3.2) which is represented graphically in Figure 2.3.1. The empirical constant, K_{AB}^{pot}, is now identified with the term $K_{AB} (\frac{u_B'}{u_A'})^n$ from which it is seen that the selectivity coefficient is a function of both the mobility ratio, $\frac{u_B'}{u_A'}$, and the equilibrium constant, K_{AB}, of the phase boundary ion exchange reaction.

It is interesting to compare the origin of the selectivity of the glass electrode with that of the fixed charge membrane of Section 3.4. For a glass electrode exhibiting ideal behaviour (n = 1), Equation 4.24 reduces to

$$\psi_M = \frac{RT}{F} \ln \frac{c_{Ao}" + \frac{u_B'}{u_A'} K_{AB}\, c_{Bo}"}{c_{Ad}" + \frac{u_B'}{u_A'} K_{AB}\, c_{Bd}"} \qquad (4.26)$$

in which concentrations have been used in place of activities in the aqueous phase. We now recall Equation 3.4.4 for the cation flux in the fixed charge membrane

$$J_i' = -K^+ u_i' (c_{id}'\ \xi' - c_{io}') \qquad (3.4.4)$$

The formal relationship between the two theories may be shown by considering a hypothetical fixed charge membrane in which only two cation species, and no anions, are mobile. That is,

$$J_A' = -K^+ u_A'(c_{Ad}' \xi' - c_{Ao}')$$

and $$J_B' = -K^+ u_B'(c_{Bd}' \xi' - c_{Bo}')$$

where $J_A' = -J_B'$

for the zero current condition. Solving these equations for ξ' (and hence for ψ_D) we obtain

$$\psi_D = \frac{RT}{F} \ln \frac{u_A' c_{Ao}' + u_B' c_{Bo}'}{u_A' c_{Ad}' + u_B' c_{Bd}'}$$

which is identical to Equation 4.5 for the diffusion potential of the glass electrode assuming ideal behaviour (ie n = 1). In a similar way, starting from Equation 3.4.22, it can be shown that

$$\xi' = \frac{c_{Ao}'' + \frac{u_B'}{u_A'} c_{Bo}''}{c_{Ad}'' + \frac{u_B'}{u_A'} c_{Bd}''} \quad \frac{r_o}{r_d}$$

for the case of two cations and zero current. Hence, using Equation 3.4.21,

$$\psi_M = \frac{RT}{F} \ln \frac{c_{Ao}'' + \frac{u_B'}{u_A'} c_{Bo}''}{c_{Ad}'' + \frac{u_B'}{u_A'} c_{Bd}''}$$

which is identical to Equation 4.26 for the total potential of the glass electrode, apart from the factor K_{AB} which describes the selectivity of the phase boundary ion exchange process.

It must be understood that the foregoing analysis of the glass electrode potential (like the TMS theory discussed previously) is restricted to *steady state* conditions. Expressions for the concentrations and fluxes of the exchanging species in the membrane have also been derived by Karreman and Eisenman[67], again for steady state conditions. The steady state concentration, $c_A'(x)$, of species A^+ for example is shown to be an exponential function of distance which may be expressed, in the present notation, by

$$c_A'(x) = \frac{\left[c_{Ao}' + \frac{u_B'}{u_A'} c_{Bo}'\right]\left[\frac{u_A' c_{Ad}' + u_B' c_{Bd}'}{u_A' c_{Ao}' + u_B' c_{Bo}'}\right]^{\frac{x}{d}} - \frac{u_B'}{u_A'} c_S'}{1 - \frac{u_B'}{u_A'}} \qquad (4.27)$$

Consider the case of a glass for which K_{AB} is sufficiently small that the potential has a Nernstian dependence on species A^+ (Equation 4.24). A pH electrode responding selectively to H^+ is an important example of this case. It follows from Equation 4.14 that

$$c_{Ao}' = c_S'$$

and $$c_{Ad}' = c_S'$$

and hence, from Equation 4.13, that

$$c_{Bo}' = o$$

and $$c_{Bd}' = o.$$

By substituting these boundary conditions into Equation 4.27, it can be shown that

$$c_A'(x) = c_S'$$

and hence, using Equation 4.13, that

$$c_B'(x) = o$$

so that, in the steady state, all sites throughout the glass phase are occupied by species A^+. For typical pH responsive soda-lime glasses, this implies the complete replacement of the Na^+ ions in the glass by H^+. It is generally accepted[70] that such a situation does not arise and it is clear that glass electrodes can never in practice reach the steady state situation. Conti and Eisenman have shown however[65] that the total membrane *potential* is in fact independent of time (once the phase boundary equilibria are established) and has the value predicted by the steady state analysis, even though the ionic concentrations and electrical potential profile within the membrane are changing with time. In order to obtain this result it is necessary to recognise that the derivation of Equation 4.4, for the electrical potential gradient, does not in fact require the assumption of steady state conditions which was made by Karreman and Eisenman[67]. Since Equation 4.4 is valid for non-steady state conditions, it follows directly from Equation 4.5 that the diffusion potential is time independent because it is a function of the boundary concentrations, c_{Ao}' etc, which are themselves determined by the equilibrium processes at the phase boundaries. Isard[43] has further clarified this matter by integrating Equation 4.4 from the interior of the glass, where all

sites are taken to be occupied by the species which was a constituent of the original material (eg Na^+ in a soda-lime pH glass), to the phase boundary, where exchange with species from the solution phase (eg H^+) has taken place. The diffusion potential, ψ_{si}, between the surface and the interior is then given by

$$\psi_{si} = - \frac{nRT}{F} \ln \frac{u_A'}{u_B'} \frac{(a_A'')^{\frac{1}{n}} + \frac{u_B'}{u_A'} K_{AB}^{\frac{1}{n}} (a_B'')^{\frac{1}{n}}}{(a_A'')^{\frac{1}{n}} + K_{AB}^{\frac{1}{n}} (a_B'')^{\frac{1}{n}}} \qquad (4.28)$$

In the case of glass giving a Nernstian response to ion A^+, Equation 4.28 becomes

$$\psi_{si} = \frac{nRT}{F} \ln \frac{u_A'}{u_B'} \qquad (4.29)$$

Equation 4.29 shows that a significant diffusion potential is developed between the surface and the bulk glass phase, a result which would be expected from a consideration of the concentration gradients which are developed when extensive ion exchange takes place at the surface, as in the case of the pH electrode. Another diffusion potential will clearly exist at the opposite interface of a conventional membrane electrode. In the single ion exchange case of Equation 4.29, this potential is equal in magnitude and opposite in sense to that of the first interface so that the total diffusion potential is zero, as predicted by the steady state theory. In the general case of 'mixed response' to both ions, a net diffusion potential results and contributes to the total membrane potential, again as predicted by the steady state theory. The total potential at one side of the membrane

(ie between the solution and the interior of the glass phase) is then obtained by adding Equation 4.16 for the phase boundary potential and Equation 4.28 for the diffusion potential at one surface. We then obtain

$$\psi'' - \psi_i = \psi^o - \frac{nRT}{F} \ln \frac{u_A'}{u_B'} \left[(a_A'')^{\frac{1}{n}} + \frac{u_B'}{u_A'} K_{AB}^{\frac{1}{n}} (a_B'')^{\frac{1}{n}}\right] \qquad (4.30)$$

where ψ_i is the potential in the interior of the glass phase.

It has been shown that the steady state theory gives correct results for the *total* membrane potential, even under non-steady state conditions. It should be noted however that the foregoing observations about the diffusion potential at a single interface are relevant to consideration of microelectronic electrodes which have asymmetrical structures involving only one glass-solution interface.

It is now generally accepted that the total electrical potential developed across a glass membrane is the sum of phase boundary and diffusion components as described above. Modifications to certain aspects of the theory have been proposed however and will now be summarised.

The assumption of a constant mobility ratio for the exchanging cations has been questioned by Isard[43] who has noted that the mobility ratio in mixed alkali glasses is known to vary widely as one ion is exchanged for another. Drawing upon experimental evidence that the mobility of an ion decreases steeply as its concentration decreases Isard[43] made the crude approximation that $u_A' \gg u_B'$ when $c_A' > \frac{1}{2}c_S'$ and $u_A' \ll u_B'$ when $c_A' < \frac{1}{2}c_S'$. It can then be shown, by integration of Equation 4.4, that the diffusion potential between the interior and

surface of the glass is zero, and the selectivity of the membrane is therefore entirely associated with the phase boundary process. In practice the mobility variation is more complex than was assumed and the 'mixed alkali effect' may not be exactly symmetrical but, as Isard points out[43], the diffusion potential would still be less than that predicted by the assumption of constant mobilities.

The concept of 'n-type non-ideal behaviour' employed in the analysis of this chapter involved the assumption of a power law relationship between the activity of a cation and its concentration in the glass phase. This model has been shown to predict adequately the steady state potentials of membranes responding to mixtures of pairs of monovalent cations. The factor n however is different for different pairs of species exchanging in the same glass and the equations cannot be extended to mixtures of more than two cations. An alternative approach to the 'n-type' theory has been proposed by Nicolsky et al[71]. Their theory assumes hetereogeneity in the ion exchange sites, the different types of site having different binding strengths to the exchanging ions. (In a variant of the theory, the possibility of incomplete dissociation of cations from the sites is also introduced). Equations describing the electrode potential in mixtures of three cations were obtained and verified experimentally. Even more significant is the ability of the theory to describe the 'step-like' variation of electrode potential with pH which is observed in certain ternary glasses containing small amounts (a few mole per cent)of network forming acid oxides such as Al_2O_3 in addition to SiO_2. More recently, Buck[72,73] has proposed an alternative treatment of heterogeneous site glass membrane potentials using a solid state approach inspired by experimental evidence which

suggests that transport in solid alkali silicates bears more resemblance to ionic transport in crystals than in liquid solutions.

Another shortcoming of the ion-exchange-diffusion theory is that it does not explicitly take account of the hydrated layer which is known to develop on the surface of many glasses when immersed in water. This matter has been discussed by Isard[43] who has noted that the existence of a hydrated layer would not affect the total potential difference between the bulk glass and the solution provided all the phases involved are in equilibrium. When the ion concentrations in the solution phase are changed however, it is likely to be some time before equilibrium is re-established throughout the hydrated layer. During this period, diffusion potentials will be developed across the hydrated layer and will contribute to the total membrane potential. It was noted in Section 2.3 that this might explain the transient responses which are sometimes observed when glasses are exposed to mixtures of ions.

CHAPTER 5: THE MICROELECTRONIC APPROACH

5.1 INTRODUCTION

The potential advantages of employing microelectronic techniques in the construction of ion selective devices were noted in Chapter 1. Microelectronic methods always involve the deposition of films of material on to some form of planar substrate. It follows that the transducer will be planar and will necessarily incorporate solid state connection to the sensor material. The films involved have an upper limit of thickness of about 50 μm and can be as thin as a few tens of nanometres. In the latter case, caution will be required in applying conventional theories of, for example, the glass electrode because hydration layers are likely to penetrate the full thickness of the material. It remains to be seen whether this will prove, in practical terms, to be an advantage or a disadvantage.

Solid state connections to ion sensitive materials may be broadly classified into two types which we will describe as 'potentiometric' and 'field effect'. The former type may be regarded as a development of the conventional membrane arrangement of Figure 2.2.1 in which the functions of the filling solution and internal reference electrode are implemented in solid state form. The electrode potential is still measured directly by a suitable voltmeter connected to the solid contact (Figure 5.1.1). In the field effect device on the other hand, the ion sensitive material is deposited on a semiconductor substrate. Electric fields, which originate in the process taking place at the solution interface,penetrate the semiconductor surface and modify its electrical properties. This effect may be monitored by measuring the variation of a suitable electrical parameter (not necessarily a potential) as a function of solution activity. The output of the field

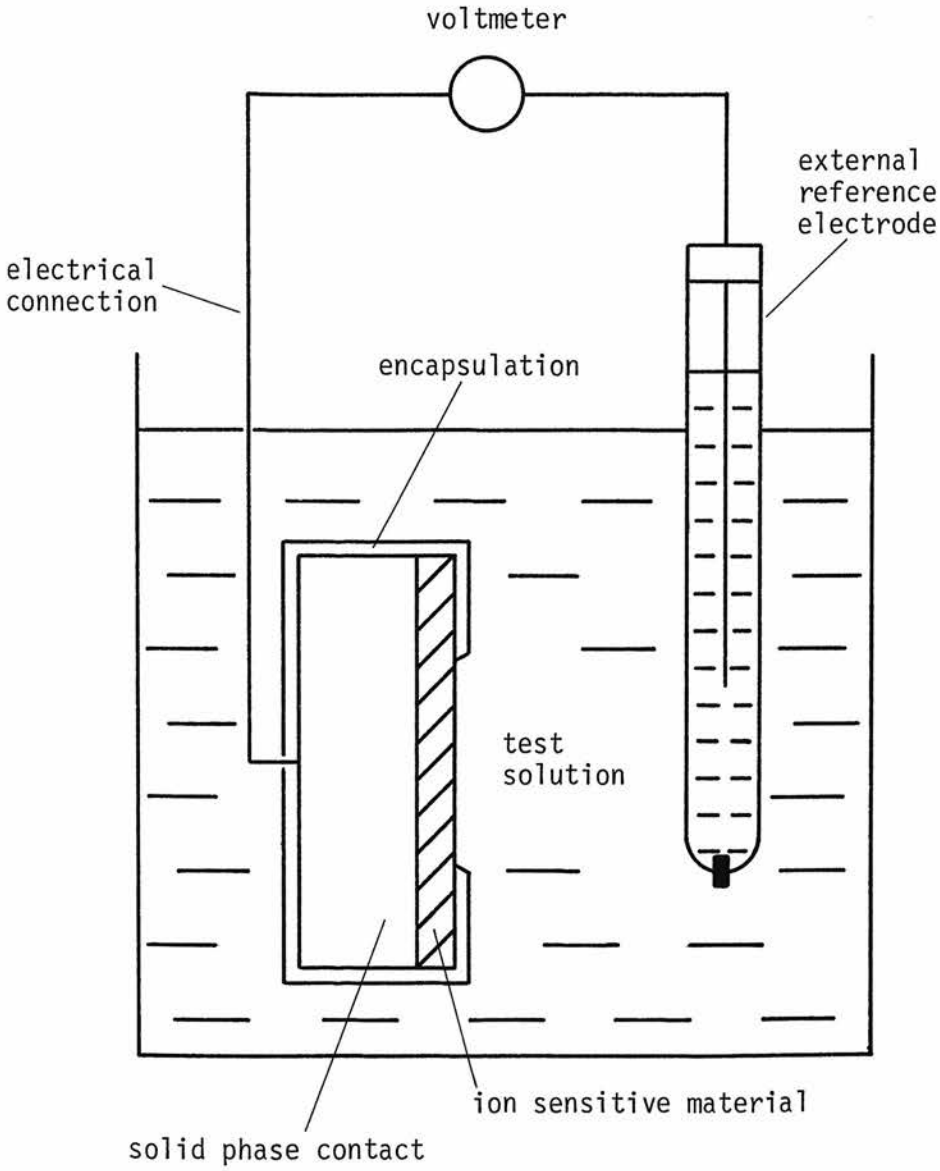

Figure 5.1.1 Solid state connection of the 'potentiometric' type

effect device is therefore obtained indirectly and not as a direct measurement of electrode potential (Figure 5.1.2). It may be useful to regard such a device as a derivative of a conventional semiconductor device. The 'Ion Sensitive Field Effect Transistor' (ISFET) described in Section 5.3, for example, is closely related to the well known 'Insulated Gate Field Effect Transistor' (IGFET).

5.2 POTENTIOMETRIC CONNECTION

Electrodes using solid state connection of the potentiometric type have previously been constructed using conventional, rather than microelectronic, techniques. A simple metallic connection to a glass electrode was reported in 1932 by Thompson[74] who prepared electrodes by blowing a 'test tube' shape from a capillary of Corning 015 pH glass and made contact to them by depositing silver by the Rochelle salts method, followed by electroplating with copper. A Nernstian response of approximately 59 mV/pH was reported but the electrode potential showed considerable drift over a period of about 250 days as shown in Figure 5.2.1. (The pH constant in the figure is the pH value for which the electrode potential was zero, referred to a saturated calomel electrode at 25^{o}C). The 'typical' drift rate was quoted as less than 0.01 pH/day (equivalent to a drift of the standard potential of 0.6 mV/day) although the total range of the pH constant over the period was as much as 1.25 pH units (equivalent to 75 mV). The figure also shows the large differences in pH constant between three electrodes of a nominally similar type and the apparently irreversible effect of

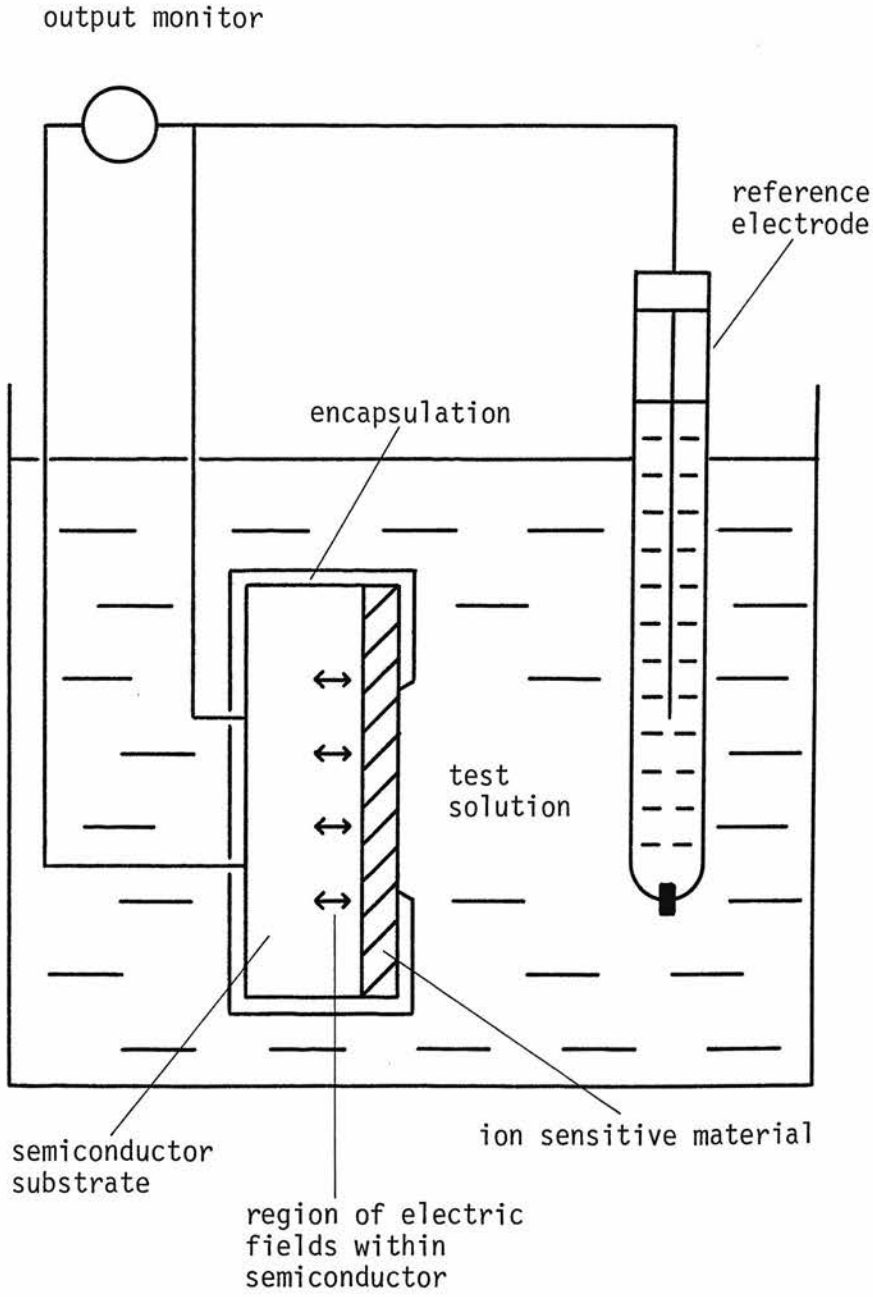

Figure 5.1.2 Solid state connection of the 'field effect' type

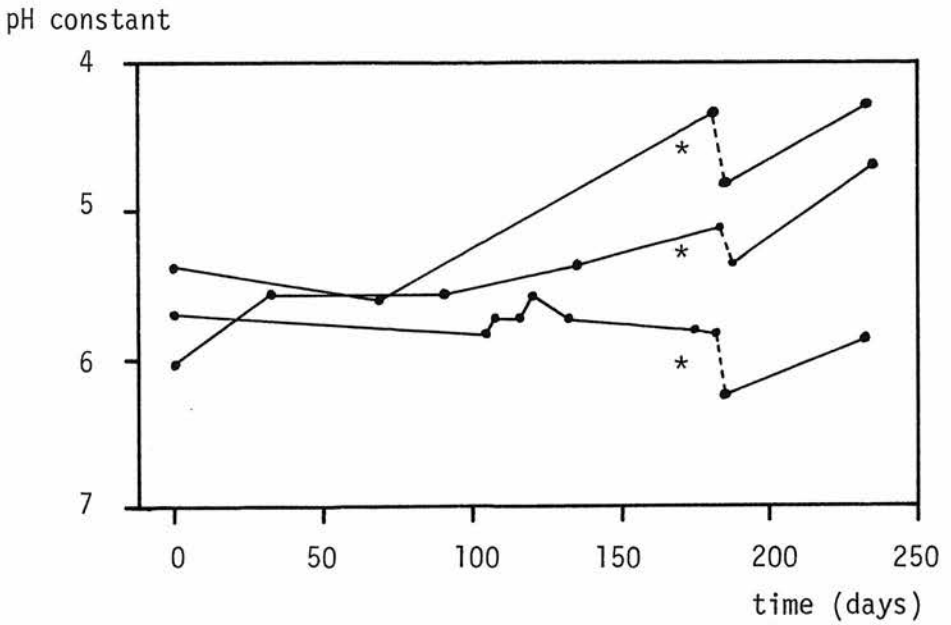

Figure 5.2.1 Variation of pH constant with time for three metal-connected glass electrodes

After Thompson[74].

**denotes effect of applying 1000 V dc for the measurement of resistance.*

current polarisation which took place in the course of making resistance measurements. A similar device comprising a glass bulb, silvered on the inside and filled with wax (or similar material) to give mechanical strength, was patented by Bender and Pye[75]. More recently, Friedman and co-workers have used metal connected glass electrodes for the measurement of pH and cation activities in physiological experiments[76]. Both 'flow-through'[76] and 'spear'[77] designs have been reported. The electrodes were formed either by conventional flame working methods or by using ion selective glass capillaries as supplied by the glass manufacturers, without further working. The metal contacts were formed by the Rochelle salts method or by vacuum evaporation of lead, silver or indium[78]. The high yield of useable devices which was obtained using the latter technique was attributed to the 'quality of the glass-metal contact' and the 'gentle handling' of the glasses in processing, especially the elimination of high temperature operations. pH electrodes made in this way gave Nernstian responses and electrode responses generally remained constant over many months. Standard potential drift rates of typically 0.2 mV/hour were observed (with Na^+ and K^+ sensitive devices) a total range of about 100 mV being observed over 10 months.

It will be clear from Chapter 4 that the mechanism involved at the interface between a glass electrode surface and metal contact is different from that at the glass-solution interface of a conventional membrane electrode. In the latter case purely ionic equilibria are involved and the electrode processes proper (which involve equilibria between ionic and electronic species) take place at the internal reference electrode which might be a silver-silver chloride wire for example. In the metal connected case similar processes must take

place at the metal-glass interface*. It follows that the electrical potentials associated with these processes will have a first order effect on the cell potential and on the stability of the standard potential. The requirement for an electrode process to exist was recognised by Thompson[74] who suggested that a metal-metal oxide or metal-metal silicate electrode may be set up. An alternative mechanism (especially where thin metal films are employed) might involve equilibria between molecular hydrogen (or oxygen) absorbed in the contact metal and ionic species (eg H^+) in the glass, in a manner analogous to the operation of the standard hydrogen electrode in contact with an acid solution. An experimental investigation of the relationship between the cell potential and the partial pressures of gases in the atmosphere would be useful in this connection.

Various elaborations of the simple metal contact to the glass electrode have been proposed, especially in the patent literature. In one case[79] the long term instability and temperature dependence of metal connected electrodes is noted and it is suggested that their performance might be improved by superficial oxidation of the contact metal prior to the application of the ion sensitive glass (in molten form). A more detailed patent claim by Riseman and Wall[80] proposes that a solid, electrically conducting, fused material be interposed between the ion sensitive glass and the contact wire. This material would be chosen to support *electronic* charge transfer between itself and the contacting metal and also permit *ionic* equilibria between itself and the ion sensitive glass. Silver chloride is cited as an

---

*If there were no mechanism for ion-electron interaction then there could be no transfer of charge across the interface which would accordingly be a 'fully polarisable' or 'blocking' interface. Direct measurement of electrical potential across such an interface would not be possible since any real instrument requires a finite input current, however small.

example of such a material. The mechanism of such a contact is easy to visualise in simple terms as an amalgamation of the properties of the silver-silver chloride reference electrode and the glass-solution interface in a conventional, solution filled electrode. An important difference in the latter case however is that H^+ ions are present in the filling solution and it is the equilibrium of H^+ which determines the phase boundary potential at the surface of a pH selective glass. In the case of the solid contact however, it is presumably the equilibrium of silver ions between the solid silver chloride phase and the glass phase which determines the potential. A significant (and subsequently constant) activity of Ag^+ in the glass phase must therefore be determined at manufacture and it is interesting to note in this context that Riseman and Wall[80] have stated that the silver chloride must be held in contact with the membrane at an elevated temperature for some time in order to ensure a good glass-AgCl bond. As in the case of the conventional structure, a non equilibrium potential will also exist due to interdiffusion between Ag^+ and Na^+ in the bulk glass, although this potential should be time invariant since the surface concentrations of Ag^+ and Na^+ are determined in manufacture and are subsequently constant. Riseman and Wall[80] applied this solid contact technique to the manufacture of microelectrodes for biomedical applications and a stability of 0.2 mV over four hours was claimed for the devices.

A slightly modified form of the metal-halide solid contact is described by Beckman Instruments Inc in a more recent patent[81]. In this version, a small proportion (0.05% to 2.0% by weight) of the halide is incorporated into a glass phase which is coated on to the contact metal using high temperature techniques. A coating of the ion selective glass is then deposited on top of the first coating.

Several combinations of contact metal and halide were studied, and copper-cuprous chloride was preferred. For practical reasons of matching thermal expansion coefficients the active contact metal (eg copper) was actually electroplated on to a wire of an electrochemically inert material such as platinum. The performances of four electrodes employing different contact metals were compared with a standard glass electrode and with an electrode using the oxidised metal contact described above. Nernstian responses were generally obtained. Standard potentials were measured over a period of three days,during which time the temperature of the electrodes was varied between 25°C and 40°C. Variations of up to 12 mV were recorded for the cuprous chloride device and up to 22 mV in the case of an electrode using silver chloride. The corresponding figures for the standard glass electrode and for the device with an oxidised copper contact were 8mV and 59mV respectively. It must be remembered however that the quoted results pertain to only one electrode of each type over a fairly short time.

Solid state connection has also been used in conjunction with many of the 'non-glass' ion sensitive materials described in Section 2.4. In some cases it is possible to identify a thermodynamically defined mechanism for these electrodes. Koebel[82], for example, has discussed the case of mixed metal sulphide electrodes which may be connected by means of a silver wire embedded in a pressed pellet of the active material. Buck and Rogers Shepard[83] have compared the mechanism of the membrane metal halide electrode described in Section 2.4 with that of the superficially similar 'all solid state' version and the conventional 'second kind' electrode, and have deduced standard potential values for each type. In other cases however, as

with metal connected glass electrodes, it is not easy to identify the mechanism. The 'coated wire' electrodes developed by Freiser[84] and his co-workers are an example. These devices are the solid connected version of the heterogeneous liquid ion exchange membrane of Section 2.4 and are simply made by dipping a platinum (or even copper) wire into a mixture containing solutions of an organic ion exchanger and polyvinyl chloride and allowing it to air dry. The electrodes are claimed to function as well as the corresponding liquid membrane electrodes. Little indication of the long term stability of the standard potential has been given in the published work although the need for daily restandardisation has been noted by James et al[85]. The theoretical problem of explaining how these devices function has been very succinctly described by Smith et al[86] who have noted the requirement for ion-electron interaction at the back contact as described above for the case of the glass electrode. The practical value of the electrodes has been vigorously defended by Freiser[84] however.

Electrodes which employ the potentiometric type of solid connection are clearly capable of giving useful responses to changes in ion activity. Their operating mechanism is not generally understood however and it is difficult in many cases to identify a single, thermodynamically defined,potential determining process at the solid contact. It seems likely, as a consequence, that the standard potentials of such electrodes will be irreproducible and subject to drift. The published values of standard potential stability are inconsistent, Thompson's simple metal connected glass electrode[74], made in 1932, being apparently more stable than the metal halide devices and the modern glass membrane electrode described in a

patent[81] which was filed in 1970. The development of an experimental structure for the investigation of different techniques of solid connection to ion sensitive glasses is described in subsequent chapters.

Provided a thermodynamically definable process can be identified at the back contact, the operation of the solid connected potentiometric electrode described in this section is very similar to that of a conventional electrode cell consisting of an ion selective membrane together with reference electrodes. In each case, the total cell potential is the sum of several interfacial and diffusion potentials, some of which are determined by purely ionic (membrane) processes while others involve ion-electron interactions. Each of the interfaces involved is essentially non-polarisable so that the complete system is in fact a cell which is capable of continuous conversion of chemical energy into electrical energy. In practice of course, the exchange currents at certain of the interfaces may be small so that the current which may be drawn from the cell without disturbing the equilibrium potentials may be severely limited. It is for this reason that a high impedance voltmeter is usually employed. It is important to recognise however that this limitation on cell current is one of degree and not of principle.

The application of microelectronic techniques to the production of a potentiometric sensor will lead to a planar structure in which films of material constituting the back contact and the ion sensitive medium are deposited on to an inert substrate as shown in Figure 5.2.2. The planar structure may be contrasted with the 'spear', 'bulb' or 'flow through tube' embodiments which usually result when traditional methods are used. Additional ion sensitive elements could be

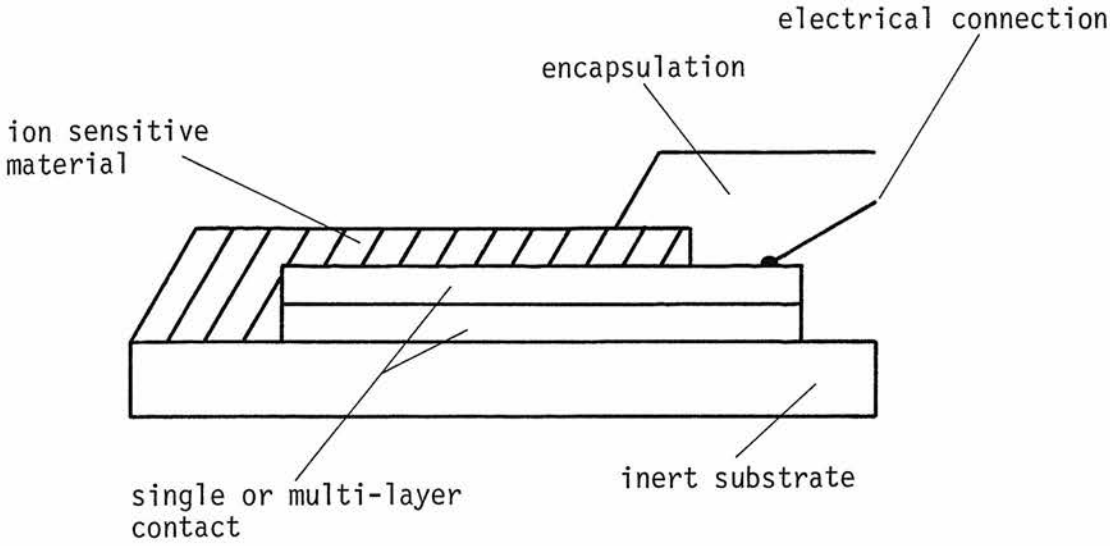

Figure 5.2.2 Cross section of microelectronic potentiometric sensor

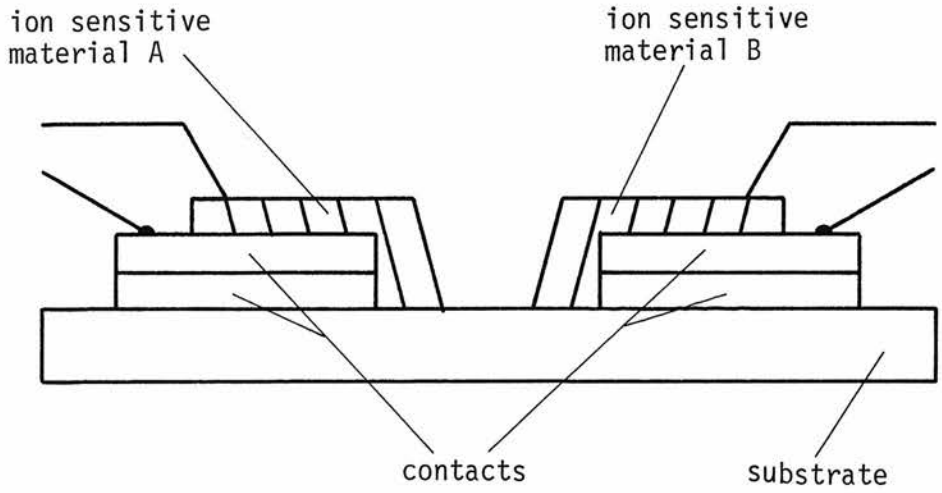

Figure 5.2.3 Sensor incorporating two different ion sensitive materials on the same substrate

incorporated, as shown in Figure 5.2.3, by using masking and selective etching methods. (One of these elements may, in certain applications, function as the reference electrode as described in Section 5.4). The most promising microelectronic technique for the fabrication of this type of device (especially where glass sensing elements are used) is the thick film circuit process[14]. The typical firing temperatures employed in this technology correspond roughly to the softening temperatures of many glasses since the conductor and resistor materials used are commonly incorporated in a glassy phase. The typical film thicknesses of around 10 μm are also similar to the thicknesses of conventional glass membrane electrodes whereas silicon technology, for example, usually involves dimensions an order of magnitude or more smaller. Substrates of ceramic material (eg alumina) are commonly used in thick film work but it is noted that the glass-ceramics described in Section 6.7 would also be suitable and could be chosen to avoid problems of thermal expansion differentials with the ion selective glass layer. The structures of Figures 5.2.2 and 5.2.3 show electrical connections to the 'top' surface of the device as is usual in circuit fabrication. This is likely to prove to be a serious drawback in electrode work because of the difficulty of adequately insulating the contact area from the solution (Section 6.2). A possible solution to this problem involves the use of specially prepared substrates incorporating a metallic wire feed-through (Figure 5.2.4(a)) so that the back contact material on the upper face of the substrate may be entirely covered by the ion sensitive glass. The feed-through could be made by forming a small bead of a suitable glass around an oxidised wire and then fusing the bead into a previously drilled hole in the ceramic substrate to form a metal-glass-ceramic seal. The surface

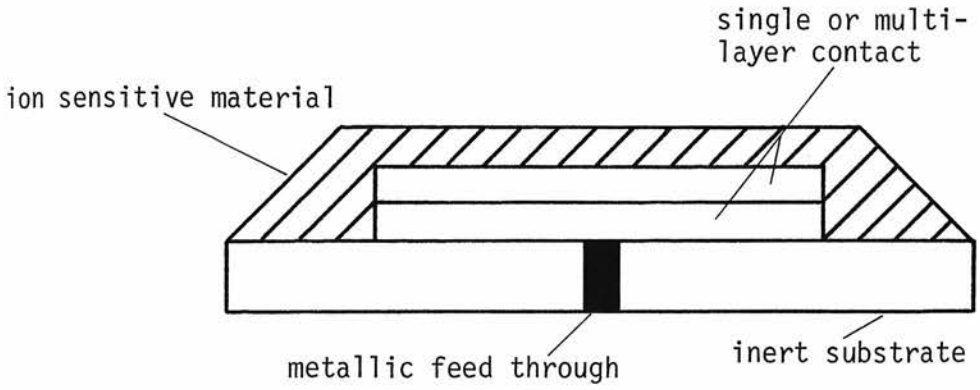

(a)

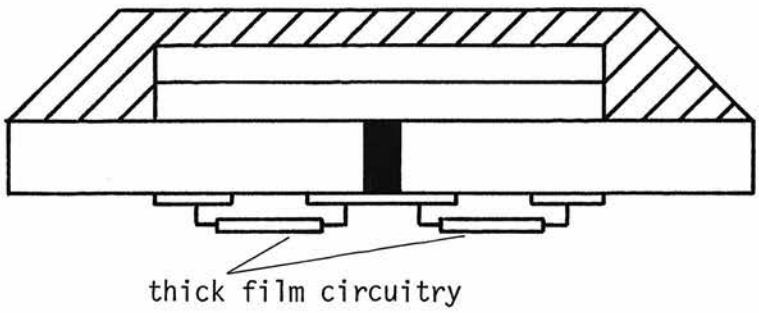

(b)

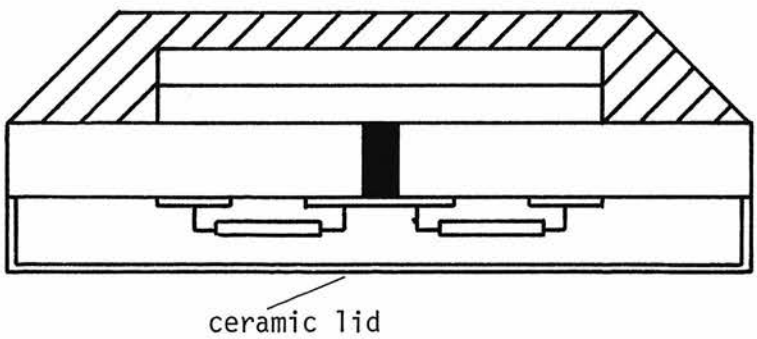

(c)

Figure 5.2.4 Proposed structure for a potentiometric sensor based on thick film circuit techniques

(a) basic structure incorporating feed-through
(b) incorporation of conventional circuitry
(c) encapsulation by standard packaging methods

would then be lapped smooth. It is further envisaged that electronic circuitry for preamplification of the electrode output signal, temperature compensation etc would be deposited by conventional thick film techniques on the reverse side of the substrate as shown in Figure 5.2.4(b). The device would be completed by the attachment of a ceramic 'lid' (Figure 5.2.4(c)), using well known integrated circuit packaging techniques to produce a hermetically sealed device. The package would of course incorporate pins for external electrical connection and these would require to be protected from the aqueous environment. The problems would be greatly reduced however by the incorporation of the internal preamplifier which ensures that the impedance level of the output signal is much lower than that of the electrode itself, making insulation requirements much less stringent. (It may even be possible to include an analogue to digital converter in the assembly so that the output involves purely digital signals which could be optically coupled).

Provided only that a sufficiently stable contact to the ion sensitive glass can be implemented, the foregoing technique will allow all of the advantages claimed for the microelectronic approach to be achieved using substantially standard thick film circuit techniques.

5.3 FIELD EFFECT CONNECTION

A fundamentally different approach to the solid state connection is offered by devices employing field effects to couple the processes taking place at the membrane-solution interface to the external electronic circuitry. The subject has been reviewed by Zemel[87] who has shown that ion sensing devices could in principle be derived from

various conventional semiconductor device structures including the field effect transistor and the gate controlled diode. We note here that the fabrication of any field effect device will involve semiconductor (ie silicon) technology rather than the simple thick film process discussed in the previous section.

The field effect device which has been most widely used is the ISFET (Ion Sensitive Field Effect Transistor). A description of the ISFET device and a review of the published work on the subject are included in a paper by the author which is reproduced in Appendix 4. The structure of a conventional IGFET (Insulated Gate Field Effect Transistor) is shown in Figure 5.3.1. An ISFET device is shown in Figure 5.3.2 for comparison.

IGFET devices are manufactured by the usual methods of silicon integrated circuit fabrication[13,15] in which p-type or n-type dopants, the gate insulator material and the metal contacts are deposited or grown on areas of the semiconductor substrate defined by photolithographic and selective etching techniques. The active area of the device, known as the 'channel', lies beneath the gate insulator and is typically only a few micrometres square but, for convenience in handling the device in manufacture, the silicon chip is usually at least one or two millimetres square. The chip is encapsulated in a metal, plastic or ceramic 'package' for mechanical and environmental protection. The package includes wires or leads for connecting the transistor to a printed circuit board or other electronic assembly.

In operation, the application of an electrical potential between the gate and substrate of the IGFET causes changes in the concentrations of the charge carriers (electrons or holes) in the surface

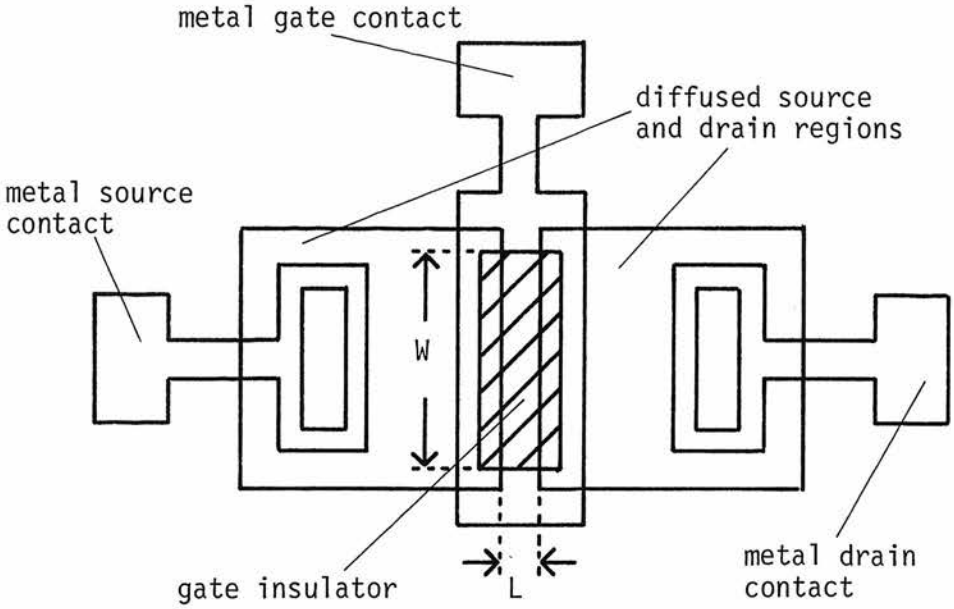

(a)

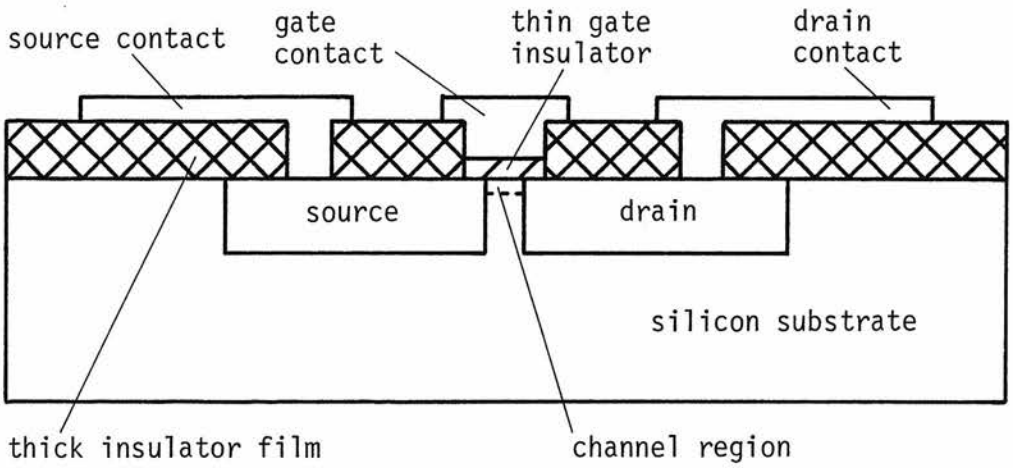

(b)

Figure 5.3.1 Conventional IGFET structure (a) plan, (b) cross-section

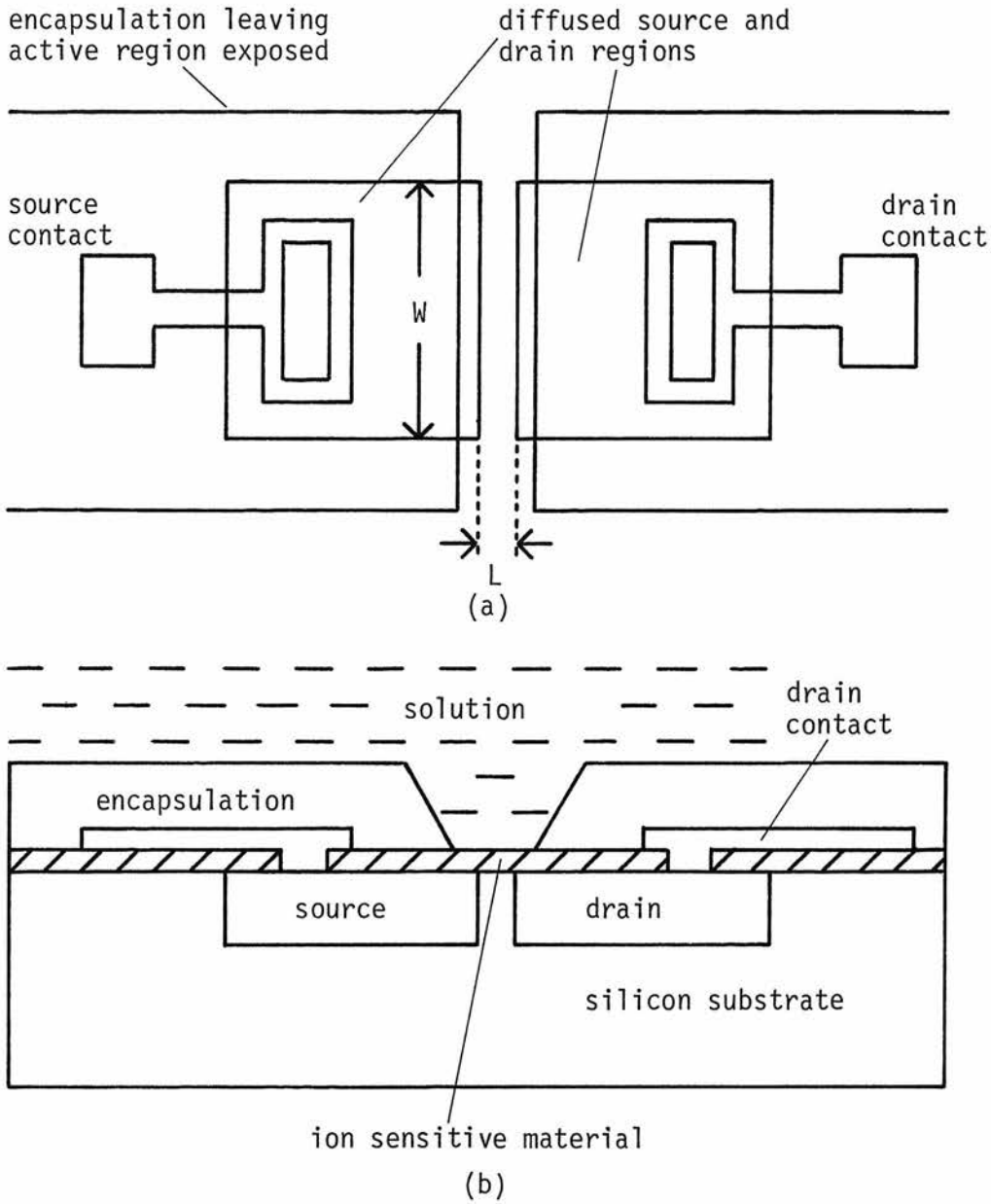

Figure 5.3.2 ISFET structure. (a) plan, (b) cross-section

region of the semiconductor substrate, close to the interface with the gate insulator. The change in carrier concentration alters the conductivity of the channel which in turn changes the current-voltage relationship measured between the 'source' and 'drain' connections to the semiconductor. A change in potential at the input of the transistor (the gate) is thus converted, by means of the field effect, into a change in current at the output (the drain) and the device functions as an amplifier of high input impedance. The electrical performance of the IGFET is described by a set of characteristic curves which show the variation of the drain current of the device with the drain-source voltage for different values of the gate-source voltage (Figure 5.3.3). It is usual to distinguish the 'triode' and 'saturation' regions of operation as shown in the figure. The theoretical derivation of these curves is carried out in standard texts[88,89]. The accurate description of real devices requires complicated and cumbersome analytical expressions which take account of several significant 'second order' effects. For many purposes however a very approximate 'first order' model may be used in which the drain current is assumed to be independent of the drain voltage in the saturation region. The drain current, I_D, of the transistor is then given as a function of the drain-source voltage, V_{DS}, and the gate-source voltage, V_{GS}, by the following equations:

$$I_D = \beta \frac{W}{L} [(V_{GS} - V_T) V_{DS} - \tfrac{1}{2} V_{DS}^2] \qquad (5.3.1)$$

in the triode region and

$$I_D = \frac{\beta}{2} \frac{W}{L} (V_{GS} - V_T)^2 \qquad (5.3.2)$$

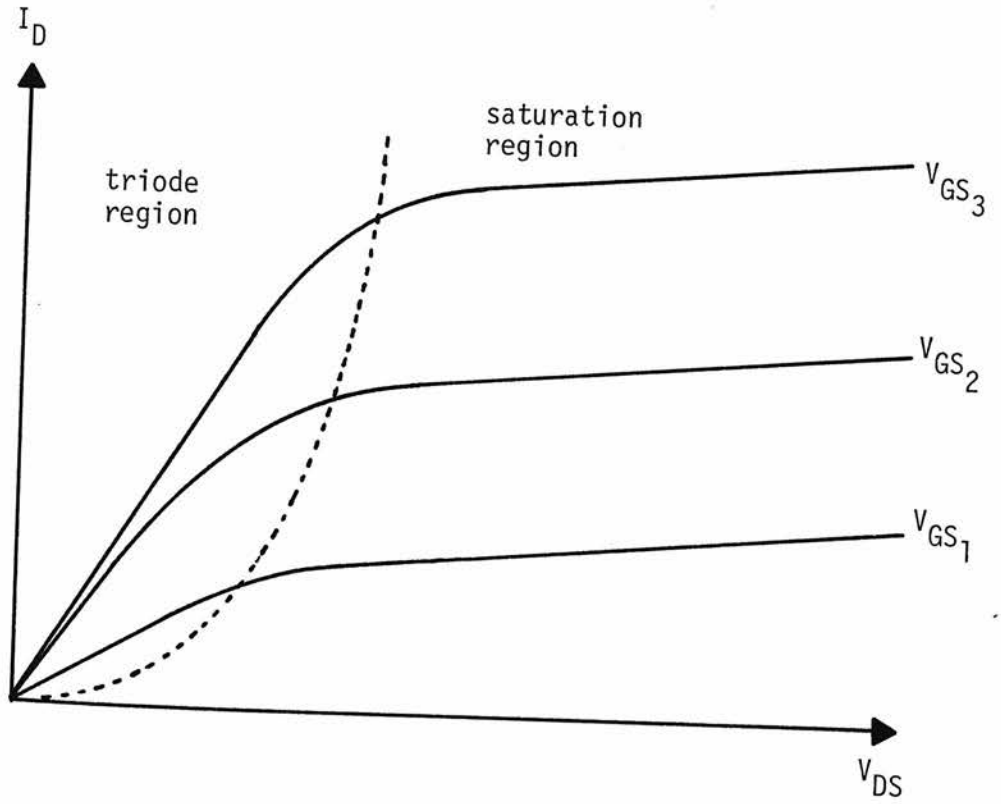

Figure 5.3.3 Typical IGFET electrical characteristics

I_D = drain current

V_{DS}= drain-source voltage

V_{GS}= gate-source voltage

in the saturation region. The 'gain constant', β, and the 'threshold voltage', V_T, are constants of the semiconductor process used to produce the transistor. They are determined by factors such as the thickness and dielectric constant of the gate insulator and the density of electronic trapping states at the semiconductor-insulator interface. The 'aspect ratio', $\frac{W}{L}$, of the transistor on the other hand is determined by the width, W, and length, L, of the channel region of the device. These dimensions are determined at the photolithographic stage of the manufacturing process and may therefore be different for different devices produced on the same silicon substrate. The complete theory of the IGFET is presented in standard texts[88,89] and those aspects necessary for the analysis of the ISFET are reviewed in Appendix 4.

It can be seen from Figure 5.3.2 that the structure of the ISFET is similar to that of the IGFET except that the gate electrode is not present and the gate insulator is replaced by a film of an ion sensitive material. (Two layer structures in which the ion sensitive material is deposited on top of an insulator layer have also been proposed[90]). The device may be fabricated by similar techniques to those described for the IGFET. An important difference however is that the ISFET cannot be completely encapsulated in the conventional way because of the need to expose the ion sensitive area of the device to an aqueous solution. This leads to severe practical difficulties as will be described in subsequent chapters. These problems can be reduced to some extent by making the ISFET chip rather larger than typical IGFETs but a limit is imposed by the well known difficulties of obtaining satisfactory manufacturing yields of large semiconductor devices.

A model for the operation of the ISFET device is developed in Appendix 4. The model assumes that an ion exchange process takes place at the interface between the aqueous solution and the ion sensitive material, as described in Chapter 4 for the glass electrode. An electrical potential difference related to solution ion activities is therefore developed between the solution and a point just inside the ion sensitive layer. It was further assumed, in the original paper of Appendix 4, that no diffusion potential exists in the ion sensitive material for the particular case of single-ion exchange. A recent paper by Isard[43] however has shown that a diffusion potential does exist at each surface of a glass membrane electrode, although the *total* diffusion potential is zero in the *membrane* case (Chapter 4). We note however that the diffusion potential is a constant related to ionic mobilities (Equation 4.29) and will assume that it is developed across a region which is narrow compared with the total thickness of the ion sensitive phase. The original model of a potential step across the interface then remains applicable. (Note that Isard's analysis[43] gives only an expression for the integral of the diffusion potential between the solution and a point deep inside the membrane. It does not describe the spatial distribution of the potential). The phase boundary potential step may be related to conditions at the semiconductor surface by drawing upon the established theory of the IGFET as described in Appendix 4. An important conclusion from this argument is that it is necessary to use a reference electrode in conjunction with the ISFET in order to define the electrical potential of the substrate of the device with respect to the potential of the test solution. This conclusion has since been supported by Janata and Moss[91] and by Buck and Hackleman[92]. It is also shown that a necessary

condition for operation as a field effect device is that the interface between the insulator and the semiconductor is polarisable. This requirement may be contrasted with that for the potentiometric device discussed above. It should be noted that the application of IGFET theory in deducing conditions at the semiconductor surface involves an implicit assumption that the ion sensitive layer may be regarded as an insulator. It is clear however that an ion sensitive material will show a degree of ionic conductivity and the possible consequences in terms of polarisation effects are discussed in Appendix 4.

It follows from the above discussion that we may derive the electrical characteristics of the ISFET from conventional IGFET theory by regarding the potential just inside the ion sensitive material (at the solution interface) as an 'equivalent gate voltage', a concept which has previously been used by Bergveld[93]. The equivalent gate voltage is the sum of the potential differences which would be seen in moving from the semiconductor, via the reference electrode and the test solution, to a point just inside the ion sensitive layer. The equivalent gate voltage therefore includes constant components (due to the reference electrode potential and any work function difference between the reference electrode and the semiconductor) together with an activity dependent component originating at the interface between the ion sensitive material and the solution. For the case of an ion sensitive glass, the latter component is given by Equation 4.30 for the potential difference at a *single* glass-solution interface. The equivalent gate voltage, V_{eq}, may then be written

$$V_{eq} = \text{constant} + \frac{nRT}{F} \ell n \left[(a_A")^{\frac{1}{n}} + (K_{AB}^{pot} \, a_B")^{\frac{1}{n}} \right] \qquad (5.3.3)$$

where the constant includes all of the above mentioned constant components of potential together with the constant terms ψ^o and $\frac{nRT}{F} \ln \frac{u_A'}{u_B'}$ in Equation 4.30. The constant K_{AB}^{pot} has been used in place of $K_{AB} (\frac{u_B'}{u_A'})^n$ for simplicity and the sign preceding the $\frac{nRT}{F}$ term in Equation 4.30 has been changed in order to refer the equivalent gate voltage to the semiconductor substrate. Using Equations 5.3.1 and 5.3.2 we may then write

$$I_D = \beta \frac{W}{L} [(V_{eq} - V_T) V_{DS} - \tfrac{1}{2} V_{DS}^2] \qquad (5.3.4)$$

for an ISFET operating in the triode region and

$$I_D = \frac{\beta}{2} \frac{W}{L} (V_{eq} - V_T)^2 \qquad (5.3.5)$$

in the saturation region

5.4 REFERENCE ELECTRODES

It was noted in Section 2.2 that an 'external' reference electrode is an essential feature of conventional electrode systems for the measurement of activity. The requirement for a reference electrode is equally pertinent to systems in which the ion sensitive element is constructed using microelectronic methods (although the function of the reference electrode may not always be apparent at first sight, as is shown in Appendix 4 for the interesting case of the ISFET device). It is of course perfectly possible to conceive an electrode system

comprising a microelectronic ion sensitive element used in conjunction with a conventional (eg calomel) reference electrode, with or without liquid junction. It is considered however that, in practical terms, many of the potential advantages of the microelectronic device would not be realised in such a system owing to the limitations on performance, reliability, ease of maintenance and cost which would be imposed by the conventional reference electrode. Some benefits may be obtained however in systems in which the reference electrode may be situated remote from the sensing electrode (eg in certain biomedical applications such as the measurement of local oral pH[94]). The limitations imposed by the reference electrode may also be less dominant when the microelectronic transducer incorporates an array of sensors for different ions. (The problem of characterising the performance of such an array with sufficient accuracy to permit meaningful measurements has already been mentioned in Chapter 1). It appears therefore that the full potential of the microelectronic approach will only be realised if a solid state reference element can be incorporated into the device. This could be achieved by using a cell without liquid junction in which an additional ion sensitive element incorporated into the device is used as a reference. The disadvantage of this approach is that the test solution must be controlled with respect to the concentration of the ion to which the reference electrode responds and any interfering ions must be removed. It should be noted however that one of the practical restrictions on the choice of reference electrode in the past has been its electrical impedance,since instrumentation problems are increased when both measurement and reference probes have high impedance[10].

This problem has largely been overcome by fairly recent developments in instrumentation however and would be further reduced by the small size of the microelectronic system and the incorporation of integral pre-amplifiers. There are certain situations in which the nature of the test solution itself suggests the use of a second ion selective electrode as the reference. When measuring small changes in the pH of sea water for instance, a Na^+ sensitive electrode may be used as reference as shown by Wilde and Rodgers[95]. An exactly similar situation has been noted by Riseman and Wall[80] with regard to pH measurement in mammalian blood. Furthermore, as observed by Garrels[96], the potential difference between two ion selective electrodes is related to the *ratio* of the activities of ions to which they are selective.* An interesting example of the direct application of an activity ratio measurement is the diagnosis of incipient mastitis in cattle. It has been shown that the clinical symptoms are preceded by quite significant changes of the ratio of Na^+:K^+ in the milk and the possibility of continuous screening of milk samples by an electrode technique has been suggested[97]. It must be accepted however that in the majority of applications there will be a clear requirement for a reference electrode of 'invariant' potential without pre-treatment of the test solution. This requirement can only be met at present by the use of a 'salt bridge' and it remains for the time being a matter of speculation whether a solid state form of salt bridge could be devised.

* Provided that the ions concerned carry charges of like sign.

CHAPTER 6: DEVICE FABRICATION

6.1 INTRODUCTION

It was shown in the previous chapter that an inherent feature of any 'microelectronic' electrode will be a solid state contact to the ion sensitive material, in place of the conventional filling solution and internal reference electrode. It was also shown that the solid contact may be classified as 'potentiometric' or 'field effect'. Contacts of the field effect variety are employed in devices such as the ISFET which are derived from semiconductor (in practice silicon) technology. The fabrication of an ISFET device is described in Section 6.3. Contacts of the 'potentiometric' variety are appropriate to the fabrication of microelectronic electrodes using thick film hybrid circuit techniques and have also been employed in electrodes constructed by conventional (non-microelectronic) methods.

It is apparent from the published work on 'conventional' solid connected electrodes (reviewed in Chapter 5) that their mechanism of operation is not well understood and that there are large differences between the values of standard potential stability reported by different authors. It was therefore necessary to develop an experimental technique which would permit further investigation of the potentiometric type of solid contact with a view to its subsequent application in microelectronic devices.

It was decided from the outset to employ pH sensitive glass as the ion sensitive material for these studies. The glass electrode has a long history of successful practical application and there exists a large body of literature concerning both the techniques of

its use and its mechanism of operation. Furthermore, there is a wide application area for pH measurement and hence a large potential market for a novel or improved type of electrode.

The 'thick film' microelectronic electrode proposed in Section 5.2 employs a deposited film of ion sensitive material. For the purpose of studying the properties of the potentiometric type of solid connection however,it was thoughtbest initially to use material in bulk form since the process of film deposition is itself likely to cause compositional and structural changes in glass which could affect its pH response.

Most of the published research on glass electrodes has employed devices of the 'blown bulb' or 'flow-through tube' configuration but the curved surfaces of these structures would severely restrict the application of microelectronic techniques for the deposition of the solid contact. It was decided to adopt instead a planar structure in which the pH glass was used in the form of thin discs which were prepared by cutting sections from a solid cast cylinder of the material as described in Section 6.5. The method involved the use of sawing, lapping and polishing techniques which are used in the preparation of silicon and other crystals for microelectronics research and were readily available.

The fabrication of solid connected disc electrodes is described in Sections 6.6 and 6.7. These devices employ metal contacts, deposited by vacuum evaporation,but the disc structure is expected to be equally applicable to the investigation of other forms of solid connection (such as the halide doped glass technique described in Section 5.2), although these have not yet been studied.

An attractive feature of the disc approach (in contrast to the

use of deposited films of the pH sensitive glass) is that the discs can be used to construct membrane electrodes, using conventional aqueous filling solution, to enable a direct comparison with the solid connected devices under investigation. The fabrication of membrane electrodes is described in Sections 6.6 and 6.7. Other advantages of the disc method are that the membrane has a more uniform and accurately known thickness than a blown bulb and its surface condition is probably more reproducible since flame working is not involved and effects such as alkali loss and 'flame annealing' do not occur.

6.2 DEVICE ENCAPSULATION AND ELECTRICAL LEAKAGE

The 'potentiometric' and 'field effect' types of device described in Chapter 5 both incorporate an active area of ion sensitive material which is exposed to the test solution. The rest of the device must be protected from the solution. Inadequate protection can result in errors in the output of the device resulting from the development of electrical leakage conductance. Leakage effects have been found to be the source of severe practical problems and the development of a leakage-free structure comprised a major part of the experimental work which was carried out for this thesis.

The leakage problem is well known in ion selective electrode work and Dole[98] has shown how the leakage resistances can form a 'potential divider' with the membrane resistance (which is usually high) and lead to an apparent reduction in the electrode response. In the case of the conventional glass membrane electrode these problems are avoided by blowing the bulb of pH glass directly on to a tube of

high resistance stem glass. Leakage through the glass-glass seal so formed is negligible and the residual problem of surface leakage along the outside of the electrode stem to the inner contact is minimised by such techniques as surface coating the stem with hydrophobic material and the use of a well fitting cap. This is undoubtedly the most widely used method for the construction of commercial glass electrodes.

The similar problem of the environmental protection of semiconductor devices is familiar in the microelectronics industry. It is commonly resolved by the direct passivation of integrated circuit chips by a thick layer of deposited glass supported by the final encapsulation of the entire device. Hermetic encapsulation using ceramic packs with glass-metal seals and soldered jointing is regarded as desirable for high reliability applications although moulded plastic (non-hermetic) packages are widely used. It has been pointed out[99] that especially severe environmental conditions are encountered by electronic devices used for surgical implantation and much useful research has been carried out by workers in this area[99,100].

Experience in both glass electrode technology and microelectronics clearly indicates that the most reliable sealing methods are those which employ only glass or metal as the water impermeable material. The jointing techniques involved with these materials (eg glass-metal seals) involve high temperatures however and are inconvenient or even impossible to use in many applications, owing to difficulties in matching coefficients of thermal expansion for example.

Many alternative techniques for the construction of glass electrodes have been suggested, especially in connection with microelectrodes for biological applications[33,47], although the devices have

usually been restricted to laboratory use. Adhesives, such as silicone rubbers or epoxy resins, have been used to join the glass membrane to an insulating tube[33,45]; O-ring and compression seal techniques have also been used for this purpose[45]. Another approach has been to construct the entire electrode from ion sensitive glass and subsequently desensitise parts of it by coating with paints, varnishes or waxes[47]. Hinke[33] has noted however that electrodes which involve a join between an ion sensitive glass and another material (with the exception of a glass to glass seal) are very prone to early failure due to the development of electrical leakages. The problem originates largely in the hydrated nature of the surface of ion sensitive glass which makes adhesion to it especially difficult[80].

Organic materials have also been used for the encapsulation of microelectronic devices. A conformal coating of silicone rubber has been advocated by White[101] and by Donaldson[99] (who distinguishes between 'adhesive' and 'non-adhesive' or 'casting'formulations). Mackay[100] has found certain waxes to be useful moisture barriers although they are brittle and prone to cracking. Epoxy resins have generally been found less suitable since they absorb significant amounts of water and swell in the process. Donaldson[99] has described how this can lead to failure of the interfacial bond and the subsequent development of surface leakages. It is important to exercise caution in using published specifications[102] such as water absorption and water vapour permeability to estimate the usefulness of these materials. Epoxy resins for example show weight increases of several per cent when soaked in saline solutions for a few weeks[100]. Silicone rubbers, on the other hand, show no weight increase but they

are nevertheless very permeable to water vapour[100]. The mechanism of moisture protection has been discussed by White[101] who has pointed to the importance of the chemical interaction of the encapsulant with the hydroxyl groups which are almost always present on a hydrophilic surface. This concept explains the effectiveness of a silicone rubber coating in reducing electrical leakage across a ceramic substrate, in spite of the relatively high water vapour permeability of this encapsulant.

The fabrication of experimental electrodes for the investigation of solid contacts involved the assembly of ion sensitive glass discs into suitable electrode structures. The use of organic adhesives for this purpose appeared to be attractive because, in contrast to glass-glass sealing methods, it does not require temperatures high enough to affect the structure of the glass. The performances of several adhesives in sealing to glass surfaces were evaluated as described below. The purpose of this work was to estimate the degree of electrical leakage in structures similar to those which were to be used in the measurements on disc electrodes.

The adhesives studied included: two varieties of silicone rubber, RTV 108 (General Electric Co, USA), Silcoset 153 (ICI Ltd); two epoxy resins, Epotek 731 (Epoxy Technology Inc), Araldite Rapid (Ciba Geigy UK Ltd); and several waxes, Apiezon W40 wax (Shell Chemicals Ltd), 70C Cement (Hugh Courtright and Co), 'Sticky Wax' (Cottrell and Co).

The experimental arrangement is shown in Figure 6.2.1. A Pyrex tube of 7 mm (nominal) inside diameter and approximately 1 mm wall thickness was cut into approximately 4 cm lengths using a precision

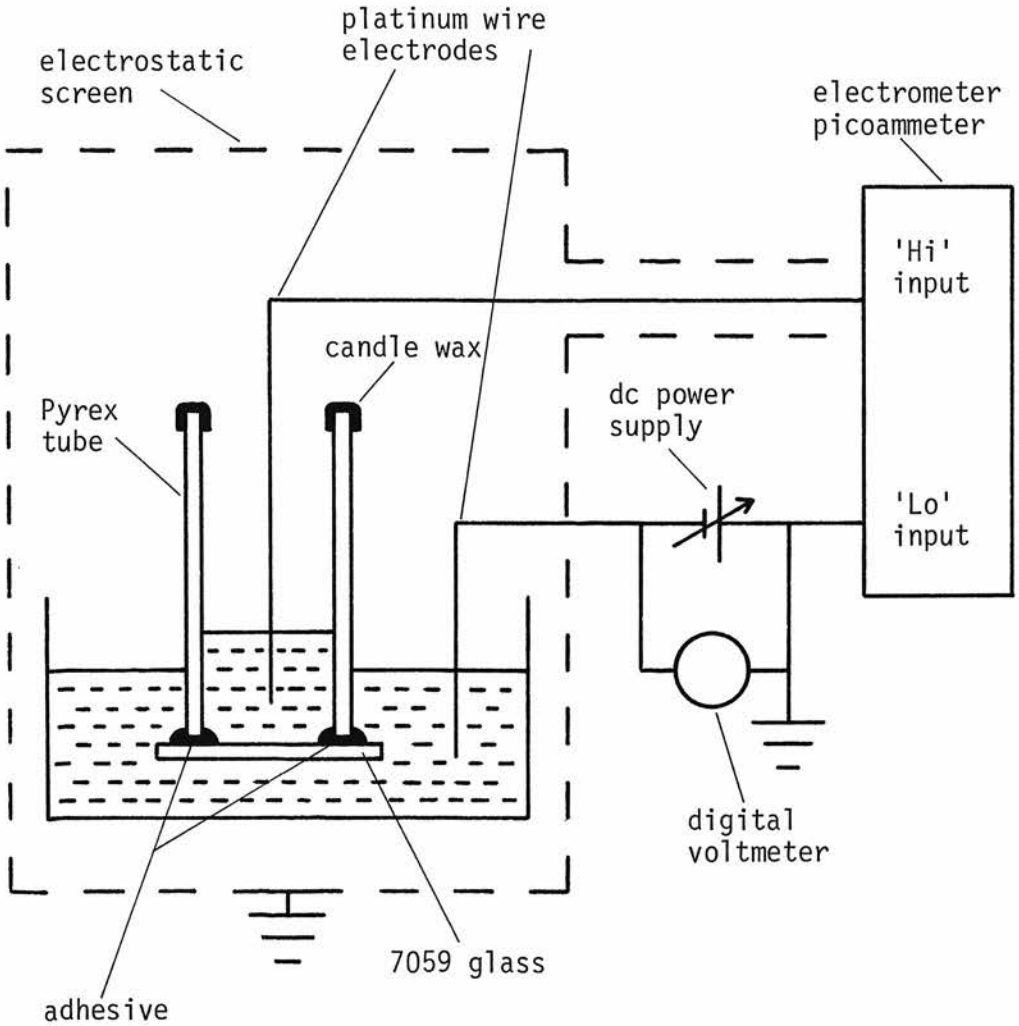

Figure 6.2.1 Estimation of electrical leakage at an adhesive-glass interface

diamond saw to give a flat, chip-free end. Each tube was sealed to a small (approximately 1 cm square) plate of type 7059 glass (Corning Glass Works). The tube and plate were thoroughly degreased beforehand. The silicone and epoxy adhesives were applied in accordance with the manufacturers' instructions and were allowed to cure at room temperature for several days. The waxes were applied by dipping the end of the Pyrex tube into the molten wax and then allowing it to touch the plate and cool. Two or three samples were made for each adhesive. The open ends of the tubes were dipped in candle wax to form a barrier to surface electrical leakage between the inside and the outside of the tube. The tubes were then part filled with tap water and immersed in a beaker of tap water to below the level of the seal. Platinum wire electrodes were placed in the beaker and inside the tube and the current between them was measured at an applied potential of 6 V. The small currents involved were measured using an electrometer picoammeter (Keithley Instruments Inc, Model 610C), the sample being contained in an electrically screened box and the usual precautions being taken to eliminate interference and to maintain insulation levels (see Chapter 8). Current-voltage curves were plotted for several of the samples between 1 V and 6 V to verify that any small difference of electrode potential between the platinum electrodes was in fact negligible.

A control experiment was also made in which the current was measured with the platinum wires lifted out of the water in order to assess the level of leakage current involved in the experimental system and to estimate background currents induced by microphonic effects in cables etc. The background current at an applied voltage of 6 V (with the sample removed) was of the order of 10^{-12} A.

The current values measured on the day of first exposure to water were between 1.0×10^{-12} A and 4.0×10^{-12} A for the silicone rubber and epoxy samples and up to 5.5×10^{-11} A in the case of the wax samples. The current was re-measured at intervals over a period of about one month. At the end of this period, all three samples of Silcoset 153 measured less than 2.0×10^{-12} A (variations over the month between 1.0×10^{-12} A and 3.0×10^{-12} A were observed however). Out of three samples of RTV 108 two had recorded less than 5.0×10^{-12} A throughout the month, the third having increased to 1.0×10^{-9} A after about one week. All of the epoxy samples (Araldite and Epotek) had increased to greater than 10^{-9} A by the end of the month. In the case of the waxes there was considerable variation between samples but the measured current in all cases had increased to at least 5.0×10^{-11} A by the end of the period, many results being much higher than this value. It was concluded that only the silicone rubbers would consistently provide an adequate level of insulation over a reasonable period of time.

The effect of acids and alkalis on the silicone rubbers was investigated by repeating the measurements using 0.1 M solutions of hydrochloric acid and sodium hydroxide instead of tap water. Some increase in the measured current was observed over periods of two and four weeks respectively in each solution, though it did not exceed 1.0×10^{-11} A in any instance.

The above results confirmed the published evidence that the most satisfactory organic adhesives for sealing to glass surfaces are the silicone rubbers. Silcoset 153 performed marginally better than RTV 108. The leakage levels observed were considered just adequate to allow meaningful experimental work to be carried out with membranes

having resistances of the order of 10^9 Ω in the presence of acid, alkaline or neutral solutions for periods up to about a month.

Glass disc pH electrodes, in both metal connected and membrane form, were assembled by direct adhesion of Silcoset 153 to the disc, as described in Section 6.6. Their pH responses were measured over periods of several months (Chapter 9). The results were encouraging but the electrode response invariably declined after a few weeks exposure to the test solutions. The failures appeared to be due to the development of electrical leakages in the electrode structures which were at least an order of magnitude greater than those measured in the tests described above. The most likely reason for this is the greater degree of hydration of the pH glass surface[80] as compared with the 7059 glass used in the tests. It is clear that data concerning adhesion to glass surfaces in general may be misleading when applied to the particular case of ion selective glasses. It was concluded that the constructional advantages of using adhesives were in practice outweighed by the measurement problems caused by leakage effects and the difficulty of distinguishing these from the 'true' electrode response.

It appeared that a lasting solution to the encapsulation problem, especially for a commercial device, would require the use of a fused glass-glass or glass-metal seal in place of the adhesive. In conventional glass bulb electrodes the ion sensitive membrane is fused to a tube of 'stem-glass' by standard glass blowing techniques. For compatibility with microelectronic methods however, a planar structure is required and the fusing should be carried out in a furnace rather than by flame working. The assembly of glass disc pH electrodes using a fusion technique is described in Section 6.7

and it will be shown in Chapter 9 that leakage effects were almost completely eliminated with these devices.

6.3 ISFET DEVICES

The ISFET device described here (which is similar to that due to Bergveld[93]) was studied at an early stage of the work when the difficulties of encapsulation described in the previous section were not fully appreciated. It also preceded the work on disc electrodes which was carried out following a change in the direction of the project from field effect to potentiometric devices, as discussed in Section 7.4.

The device comprises six ISFETs and a conventional metal gate test transistor on a silicon chip approximately 3.5 mm square. A composite drawing of the three mask layout appears in Figure 6.3.1 and a photograph of the actual chip in Figure 6.3.2. The first mask defines the source and drain (diffused) regions of the transistors. The second mask defines the 'contact hole' regions where silicon dioxide is etched away from the surface of the silicon to make contact between the underlying diffusions and the metal contact areas which are themselves defined by the third mask. The device was produced using an n-channel MOS transistor process which was under development in connection with work on charge coupled devices. The active gate material of the ISFETs was therefore the thin film of silicon dioxide used as the gate insulator in the conventional IGFET. The use of silicon dioxide as an'ion sensitive material' (which was also a feature of Bergveld's ISFETs[93]) is further discussed in Section 6.4. The gate area of the device, to be exposed to the

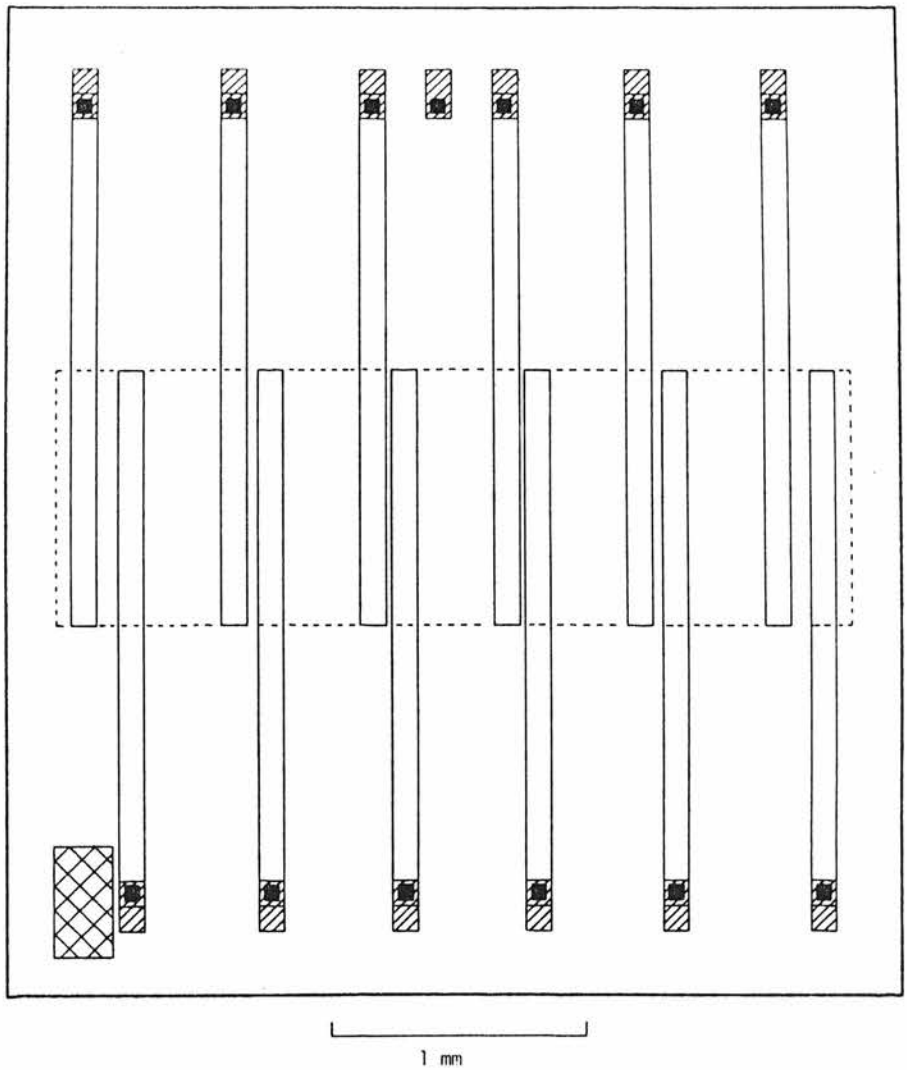

Figure 6.3.1 Composite drawing of ISFET chip

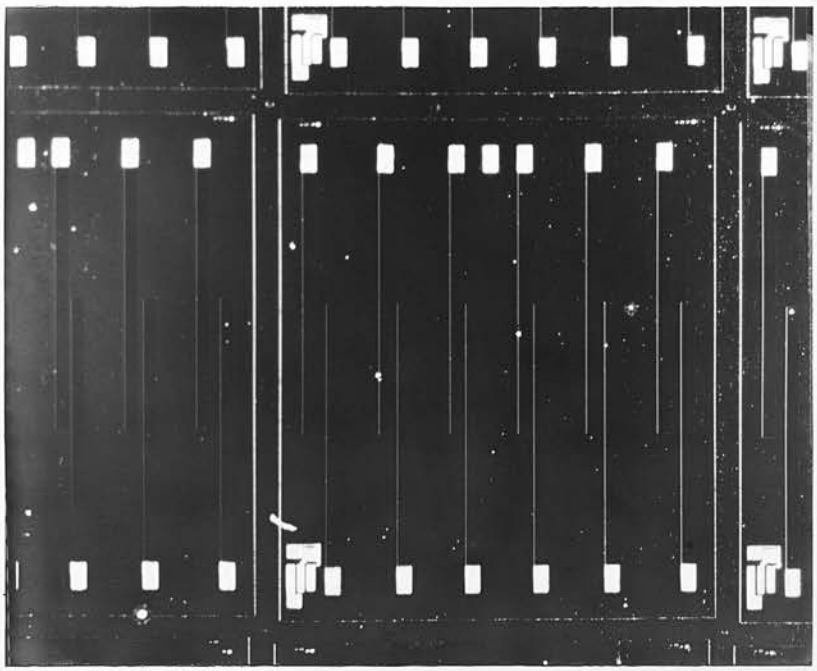

Figure 6.3.2 Photograph of ISFET chip prior to scribing of wafer.

solution, was defined when encapsulating the chip as described later in this section. This involved the manual application of epoxy resin to protect the entire chip apart from the gate area. The definition of the gate area by this method was clearly imprecise but the 'overlapping finger' device design assisted by, to some extent, defining the gate area geometrically. The device dimensions were designed to be large by usual transistor standards (eg diffusions 2.2 mm long and a device channel width of 1 mm) in order to simplify the encapsulation process. Devices having channel lengths of 20 μm, 40 μm and 80 μm were included on the chip. A substrate contact was incorporated so that reliable connection could be made to the substrate without using the 'back contact' on the reverse side of the chip. A conventional metal gate test transistor was also included to allow a simple check of the diffusion and oxidation processes for each chip. The 'drawn' channel dimensions for this device were 200 μm wide by 10 μm long.

The cutting of 'Rubyliths' and preparation of 'first reduction' and 'step and repeat' photomasks was carried out in the usual way by the technical staff of the Microelectronics Unit in this Department, who also carried out the wafer processing. Brief details of the process are given in Appendix 5. In view of the early stage of development of the process an extensive evaluation program was carried out by the author in support of the development of the ISFET devices. This work is described in two departmental reports[103,104] and summarised in Appendix 6. The test chips used for this work were processed simultaneously with the ISFET wafers as a single batch. The processed ISFET wafers were scribed into chips and visually poor devices were discarded. (Owing to an error in the step and

repeat photography the overall yield was poor).

For ease of subsequent handling,the devices were mounted on a specially prepared alumina substrate on to which conductor patterns had been deposited by the standard thick film hybrid circuit technique. Figure 6.3.3 is a photograph of a mounted chip. All edge connections were taken from one side of the substrate for convenience in exposing the device to solutions. The chips were attached to the substrate using 'Permabond' adhesive (Double H International Marketing Ltd), the contact pad on the front of the chip being used to make electrical connection to the silicon substrate. Connections between the chip and the thick film substrate were made by staff of the Poultry Research Centre using ultrasonic wire bonding equipment. In order to simplify the bonding operation, the outermost (80 μm channel length) ISFETs on the chip were not connected and measurements could not therefore be made on them.

Connection to the tracks along the edge of the alumina substrate was made using insulated equipment wire. The entire face of the alumina substrate and silicon chip, except for the ISFET gate area, was then coated with a two-part epoxy resin, Stycast 2850 FT/Catalyst 9 (Emerson and Cuming Inc). It was necessary to use a fairly high proportion of the liquid catalyst in order to achieve a mixture of sufficiently low viscosity to apply to the device without damaging the delicate bond wires. The coating was applied manually using a glass rod and was cured at room temperature according to the manufacturers' instructions. Care was taken to ensure that the entire device was coated, including the ends of the wires soldered to the alumina substrate. A second coat was applied where necessary, after curing the first. Ideally, the resin would have been applied to

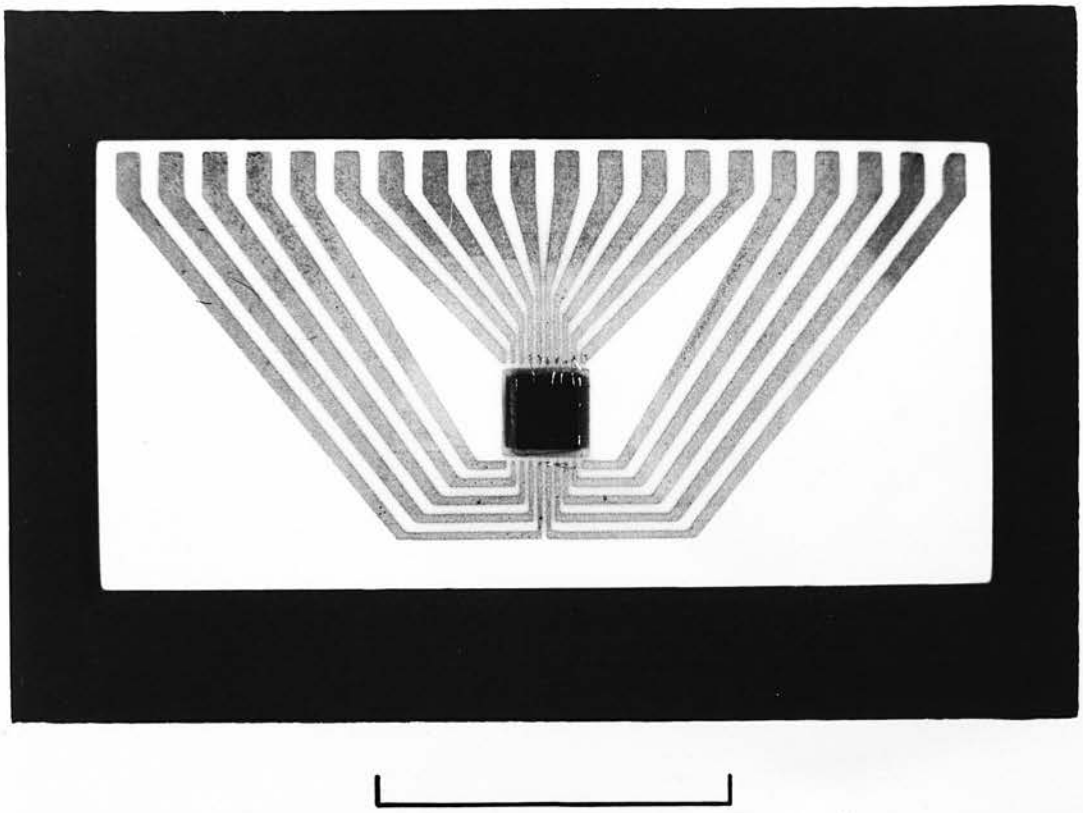

Figure 6.3.3 ISFET chip bonded to alumina substrate, prior to encapsulation

the entire chip except for the gate area defined by the dotted line in Figure 6.3.1. In practice, it was restricted as far as possible to the area outside this line. This does result in a wider gate area but the effect is minimised by the 'overlapping finger' geometry and the considerable (1 mm) length of the designed gate area. It will be clear from the foregoing discussions that accurate prediction of the aspect ratio (W/L) of the ISFET devices was not possible. The gate definition could have been improved by using an additional processing stage to deposit a layer of an inert material, such as silicon nitride, over the chip followed by selective etching to define the gate area. This technique was not employed however, in order to simplify the wafer processing.

6.4 SILICON DIOXIDE DEVICES FOR POTENTIOMETRIC MEASUREMENTS

The extensive work of Eisenman[19] on the ion sensitivity of certain silicate glasses has shown that the selectivity of the response to different ions depends critically on the glass composition. For example, the incorporation of quite small amounts (a few atomic per cent) of aluminium into a pH sensitive alkali silicate glass can introduce a marked cation sensitivity.

The ISFET described in Section 6.3 (like Bergveld's device[93]) uses silicon dioxide as the ion sensitive material. Detailed information on the ion sensitivity of silicon dioxide is not available although there is evidence for the transfer of ions between aqueous solution and thermally oxidised silicon[105]. Sensitivity to both H^+ and Na^+ was reported by Bergveld[93] although the magnitude and selectivity of the response apparently varied greatly between

different devices. The precise structure of 'silicon dioxide', and even its stoichiometry, depends greatly on the method of its growth or deposition, eg by wet or dry oxidation of silicon, evaporation of quartz or chemical vapour deposition[106]. The likely differences in ion sensitivity between films formed by these different techniques are unpredictable. In view of these uncertainties, it was decided to carry out potentiometric measurements of the ion response of oxidised silicon in support of the ISFET work. For this purpose silicon wafers, similar to those used for the ISFETs, were oxidised using the same oxidation and annealing procedures as were employed for the growth of the thin gate oxide of the ISFETs (Appendix 5) except that the time for the wet oxidation stage was varied to obtain different oxide thicknesses. These wafers and the ISFET devices were processed as separate batches.

Four half-wafers were oxidised allowing times of 11 min, 19 min, 27 min and 40 min for the wet stage. The corresponding nominal oxide thicknesses of 0.1 μm, 0.15 μm, 0.2 μm and 0.25 μm were approximately verified by the colours of the oxidised wafers although there was a noticeable variation of thickness across the wafers. The back contact of each wafer was etched and metallised with aluminium by vacuum evaporation. The wafers were scribed to form chips approximately 5 mm square.

For convenience in handling the chips, and for making electrical connection to them, it was necessary to mount the chips on a suitable substrate. Glass substrates, 25 mm by 12.5 mm, metallised with copper-nichrome films (as used for thin film hybrid circuits) were supplied by the Poultry Research Centre. The metal film was completely etched away for a few millimetres around the edge of each

substrate, leaving an approximately rectangular metallised area at the centre (Figure 6.4.1). The chips were attached to this area using a two-part, conducting epoxy resin (Elecolit 325A/325B, Industrial Science Ltd), which was cured by baking for two hours at 60°C. The central conductor of a screened, low-noise coaxial cable was soldered to the end of the copper area on the substrate. The entire assembly was then painted with several coats of 'Lacomit stopping off medium' (W. Canning and Co Ltd) leaving an exposed area approximately 3 mm square at the centre of the chip†. A glass tube was then slid over the connecting cable and attached to the substrate using 'Sticky Wax', the wax being caused to form a thick coating over the solder connection and to seal the end of the tube.

Six devices were assembled in this way, together with a control device prepared using a wafer of unoxidised silicon. The purpose of the control wafer was to identify, by comparison, any of the oxidised samples in which the test solution had come into direct contact with the silicon, as a result of encapsulation failure for example.

6.5 PREPARATION OF GLASS DISCS

It was originally intended to use a modern lithia pH glass for this work. The precise composition and properties of these glasses tend to be subject to commercial secrecy however and it was felt that this could cause difficulties, especially at a later stage when comparison between disc and deposited film electrodes may be required.

†An earlier batch of devices had been made, employing the Stycast 2850FT epoxy resin encapsulant which was used with the ISFET devices. Measurements on this batch indicated some ion-sensitivity but were subject to serious uncertainty due to premature failure of the encapsulation. The work described in this section was carried out prior to the investigation of adhesives discussed in Section 6.2.

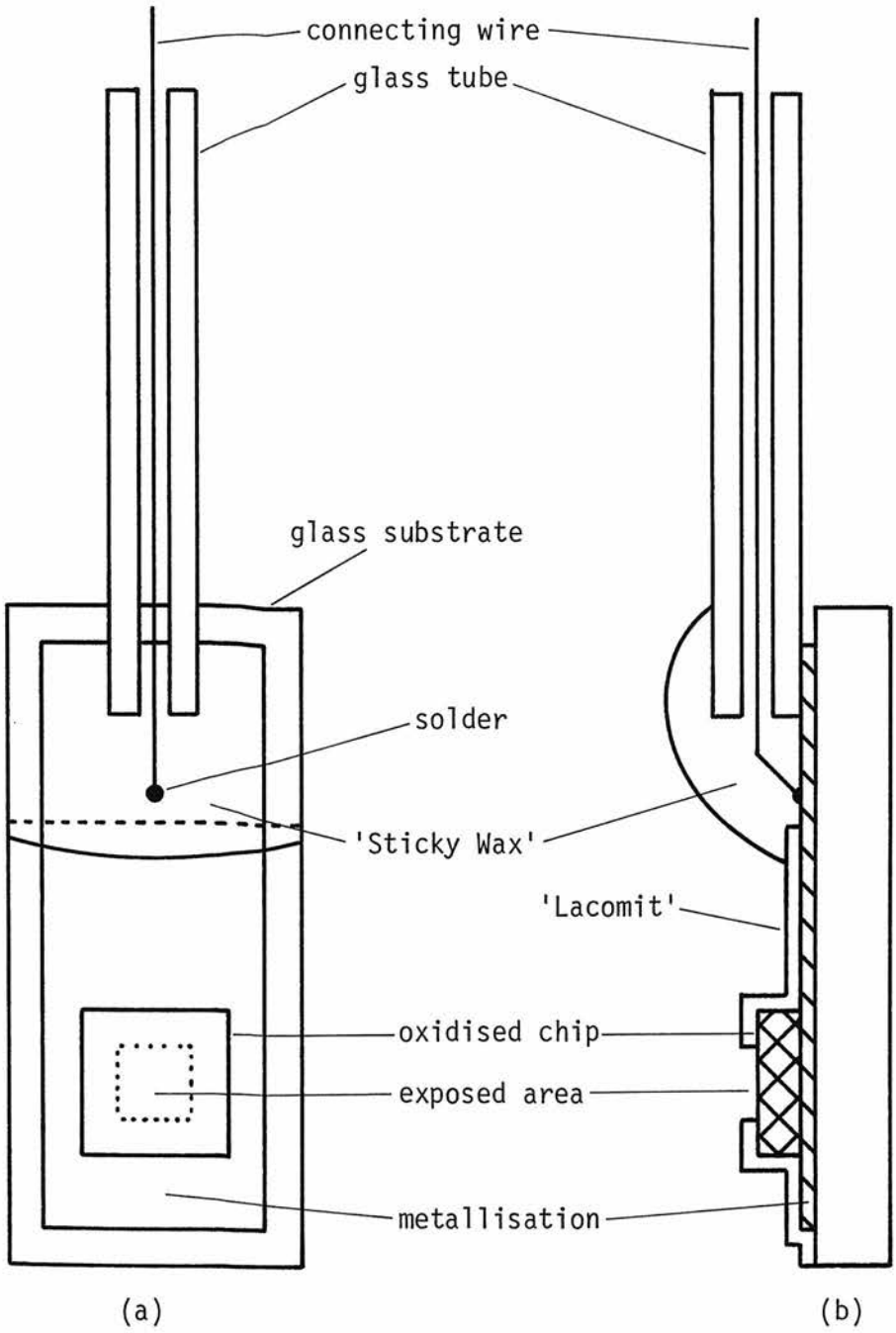

Figure 6.4.1 Mounting of oxidised silicon chips for potentiometric measurements of ion sensitivity.
(a) plan, (b) cross-section

It was therefore decided to use a glass having the composition of the well known 'Corning 015' pH glass. This has a simple chemical composition and low melting point and was available in a suitable form in the UK,although its disadvantages with respect to the modern materials (especially its sensitivity to alkali ions) were recognised. Conclusions about the nature and performance of any method of solid connection would be expected to apply generally to all ion sensitive glasses, although constructional factors depend greatly on the properties of individual materials,such as melting point and expansion coefficient.

The glass, in the form of cylindrical rods approximately 22 mm in diameter, was kindly supplied by Dr J.O. Isard of the Department of Ceramics, Glasses and Polymers at the University of Sheffield. The specified composition was that recommended by MacInnes and Dole[39] for use in pH electrodes ie 72 mole % SiO_2, 22 mole % Na_2O, 6 mole % CaO. Glass of this composition is also marketed by the Corning Glass Works as 'Corning 015' (recently renamed as Corning 0150). The material was prepared by melting a pure grade of sand together with chemically pure sodium carbonate and calcium carbonate. The first batch of material was supplied as rods about 7 cm long and contained a considerable density of occlusions visible to the naked eye. Subsequent batches were cast in much shorter lengths (1 to 2 cm) and were substantially free of such defects. The castings were annealed by cooling at approximately 3 deg C/min to prevent breakages when sawing.

The glass rods were sectioned into discs, nominal diameter 22 mm, using a diamond saw (Capco Model Q35 Mk2, Caplin Engineering Co Ltd) with a 200 μm thick annular blade coated with '300 grit' diamond. The feed rate was approximately 38 cm/hour. The rods were mounted on a

glass plate using 70C cement melted by means of a hot air blower. The melting point of the cement is 150°C. It was found necessary to use three slabs of supporting glass so that the cut disc was attached at three points (Figure 6.5.1). With this technique very few of the discs suffered breakage. After cutting, the discs were removed from the glass support by melting the cement. Surplus cement was removed by dissolving in boiling iso-propanol.

The thicknesses of the cleaned discs were measured using a dial gauge having a resolution of 2 μm (Thomas Mercer and Co Ltd). Measurements were made near the centre of the disc and at four points evenly spaced around the edge. The disc was then turned over and the measurements repeated to eliminate misleading results due to a raised 'lip' noticed at the edge of the disc in some cases.

Using an annular saw as described it was possible to cut discs to a nominal thickness as small as 200 μm. (In the earlier stages of the work a perimeter blade on a different machine was used but it was difficult reliably to obtain discs thinner than 400 to 500 μm). The sawn discs commonly carried crescent shaped markings presumably due to abrasion from the saw blade. In addition they had been unavoidably exposed to cooling oil during sawing. Although there was no evidence that these factors would affect electrode response it was decided as a matter of routine to lap the surfaces of all discs to ensure a reproducible, clean surface condition. In the early stages of the work a precision lapping machine (Logitech Ltd) was used. A disadvantage of this method is the need to adjust the orientation of the specimen with respect to the lap. If this is not done accurately a tapered slice results. Furthermore, the pressure applied to the specimen is controlled by a spring arrangement which

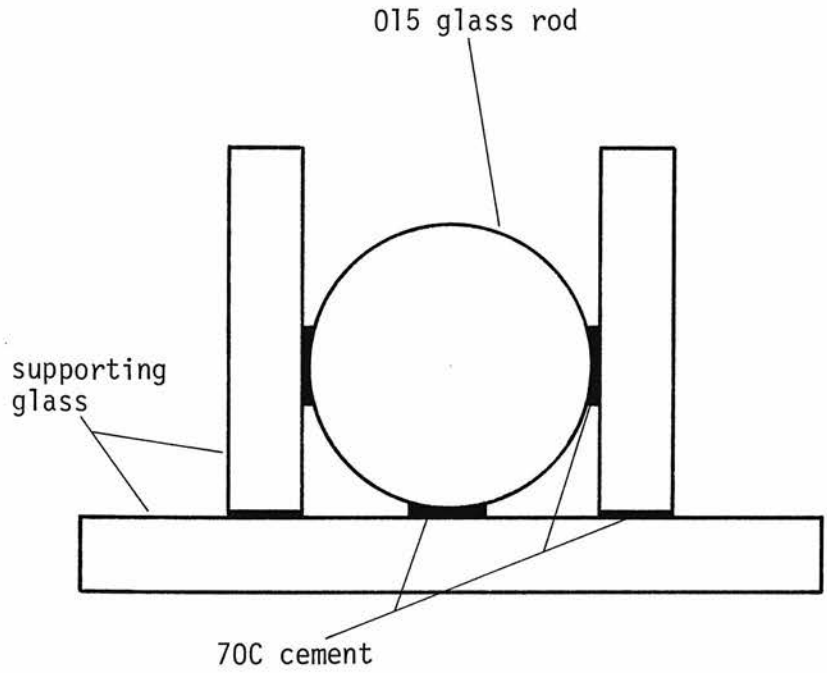

Figure 6.5.1 Cross section of glass rod mounted for sectioning

is not calibrated so that it is difficult to predict the lapping rate in advance. It was concluded that this equipment, although capable of high precision work, was unsuitable for the present purpose, especially since fairly large numbers of specimens were involved. A much simpler, manual lapping technique was therefore adopted. The sawn disc was attached, using 'Sticky Wax', to the end face of a steel cylinder approximately 38 mm long by 34 mm diameter. The cylinder had been previously machined to fit closely inside a steel annulus, 64 mm outside diameter by 30 mm deep. The arrangement was manually moved across the surface of the lap by holding the annular part so that the pressure on the specimen was determined only by the weight of the central cylinder. The clearance between the specimen mount and the annulus minimises tilting of the specimen due to uneven finger pressure. The lap used was simply a piece of window glass, about 25 cm square.

The effect of different abrasives and lapping times was investigated using a mechanical surface measuring instrument (Talysurf 4, Rank Taylor Hobson) to assess the surface roughness of the material after each treatment. It can be seen from Figure 6.5.2 that the surface condition after lapping for five minutes using a water slurry of 400 grade carborundum powder was similar to that of the freshly sawn surface. Further treatment with 600 grade and 800 grade carborundum respectively (using a new lap in each case) resulted in an increased surface smoothness after five minutes lapping with each grade. Similar results were obtained using alumina powder of the corresponding particle size. It was concluded that the material could quickly and simply be lapped to sufficient smoothness to permit subsequent polishing if required.

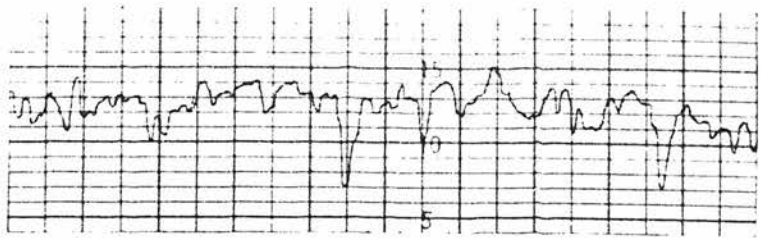

(a)

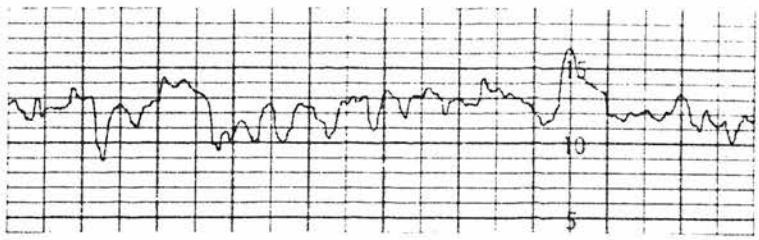

(b)

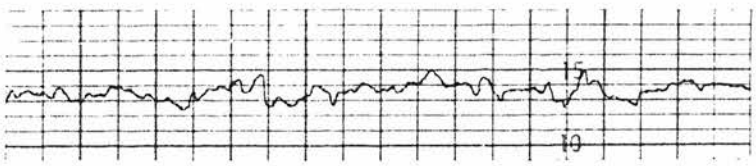

(c)

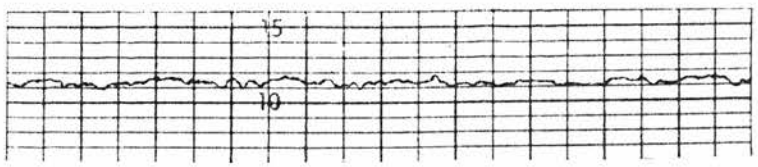

(d)

Figure 6.5.2 Surface roughness of 015 glass disc; (a) as sawn, (b) after lapping with 400 grade carborundum powder, (c) after lapping with 600 grade carborundum, (d) after lapping with 800 grade carborundum.

Vertical scale = 1 μm/division
Horizontal scale = 50 μm/division

Apart from some preliminary work with electrodes using discs of different thicknesses, the following standard technique for the preparation of discs was employed. The discs were sawn to a nominal thickness of 350 μm and, after cleaning in boiling iso-propanol, were lapped for five minutes on each side by the manual method described above using 400 grade carborundum powder in deionised water. The resulting matt finish and relatively rough surface (see Figure 6.5.2(b)) apparently had no adverse effect on electrode response. After removal from the lapping cylinder the disc was cleaned using trichlorethylene to remove surplus wax.

The thicknesses of the resulting specimens were measured using the dial gauge as described above. The variation of readings across a disc was typically 10 to 15 μm and the mean of the readings for discs prepared in this way varied between 250 and 300 μm. This was considered adequate for the work in hand but it should be noted that a more sophisticated lapping technique would be required if improved uniformity and reproducibility of specimen thickness was desired, in order to carry out precise resistivity measurements for example.

In certain cases, the discs underwent additional treatment before being assembled into electrodes. Surface etching was commonly used, with the intention of removing the surface layer of glass which may have been strained in the course of lapping. A two minute exposure to a standard silicon dioxide etchant ('Isoform', Micro Image Technology Ltd) was adopted as standard for this purpose. It was shown (both by weighing and by direct measurement) that this removed approximately 10 μm of material, ie 5 μm from each face of the disc.

A number of discs were polished in order to compare their

electrode performance with that of the matt finished disc described above. A shiny surface finish was obtained by lapping the standard disc for a further ten minutes using 800/1000 grade carborundum in a water slurry, followed by polishing for several hours in a vibratory polisher, using colloidal silica (Syton W30, Monsanto Ltd) as the polishing medium. The etching treatment was not used with these discs.

Several discs were subjected to a careful annealing procedure in order to identify any effect of such heat treatment on electrode performance. Discs having the standard matt finish were etched as described above. They were annealed by heating to 600^{o}C for 10 min and then cooling to room temperature at 0.34 deg C/min. A programmable furnace (Stanton Redcroft Model LVP-C) was used for this purpose, the disc being laid on a flat slab of polished vitreous carbon to which it showed no tendency to adhere.

Instances where the above mentioned additional treatments were employed will be specifically noted in subsequent chapters.

6.6 DISC ELECTRODE ASSEMBLY USING ADHESIVES

Glass discs were prepared as described in the previous section. The fabrication of metal connected electrodes began with the vacuum evaporation of a circular contact at the centre of one face of the disc. At the same time, an additional annular contact was deposited around the periphery of the disc (Figure 6.6.1) for use in connection with the method described in Section 8.5 for the assessment of electrical leakage effects. It was decided to avoid the use of conventional photolithographic techniques for defining the metallisation pattern in case the pH response of the device was affected by

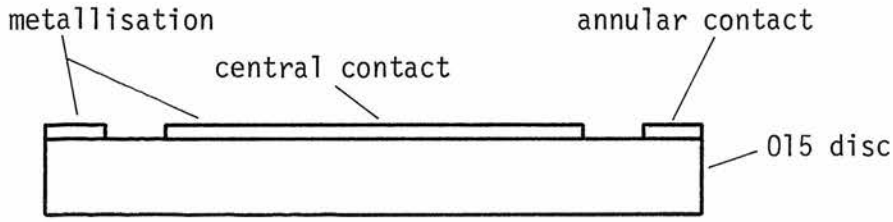

(a)

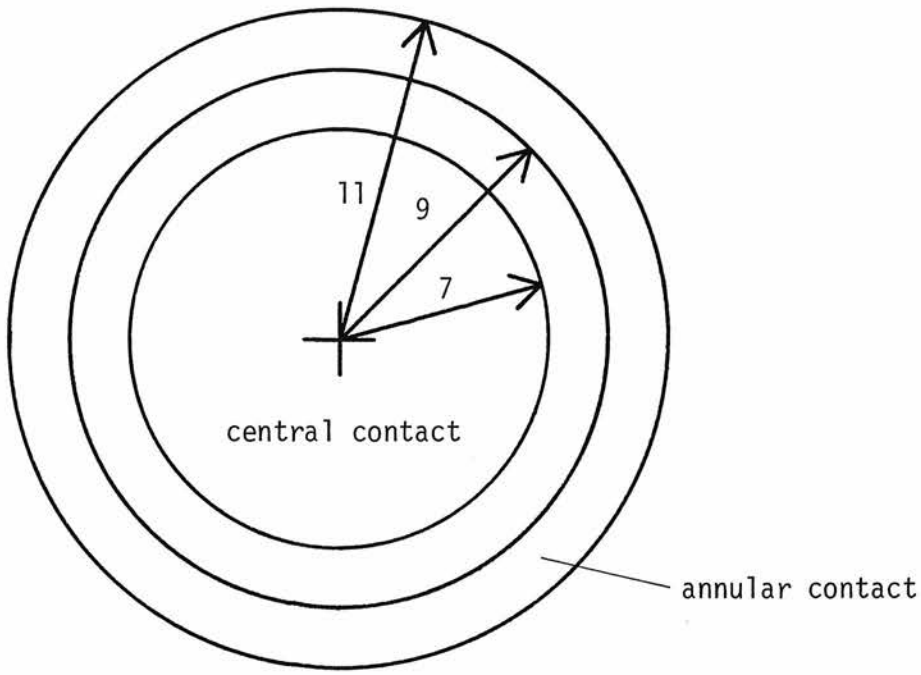

(b)

Figure 6.6.1 Metallisation of glass discs
(a) cross-section, (b) plan

(Dimensions in mm)

the chemicals involved. The simple masking technique of Figure 6.6.2 was used instead. This allowed adequate definition for the purpose and also prevented any deposition of metal on to the opposite face of the disc.

Deposition was carried out using an electron beam evaporator (Model T300-RG2, Birvac Ltd). Source materials were high purity metals (Johnson Matthey and Co Ltd) contained in molybdenum crucibles. Gold-nichrome metallisation (as used in thin film circuits) was employed initially. With this method, the very thin (typically 10 nm) layer of nichrome promotes adhesion between the glass and the thicker (typically 0.5 μm) gold layer, to which ohmic contacts can be reliably made. In later work single layer films of gold, silver and copper were used in order to investigate the effect on electrode performance of contacts of different electrochemical activity.

Radiant energy from the evaporation source commonly causes the substrate temperature to rise above 100^{o}C in the Birvac system but this effect was minimised (to avoid possible effects of heat treatment on the pH response) by carrying out the evaporation in several short stages. Temperature sensitive papers stuck on to the disc indicated that the maximum reached during evaporation was between 80^{o}C and 100^{o}C.

It should be noted that the thickness of the deposited metal film was small compared with the surface roughness of the glass disc. (see Figure 6.5.2(b)) and accurate measurement of film thickness was not possible. Extensive previous experience with the equipment concerned however,suggests that a mean film thickness of about 0.5 μm would result from the evaporation time and beam current used.

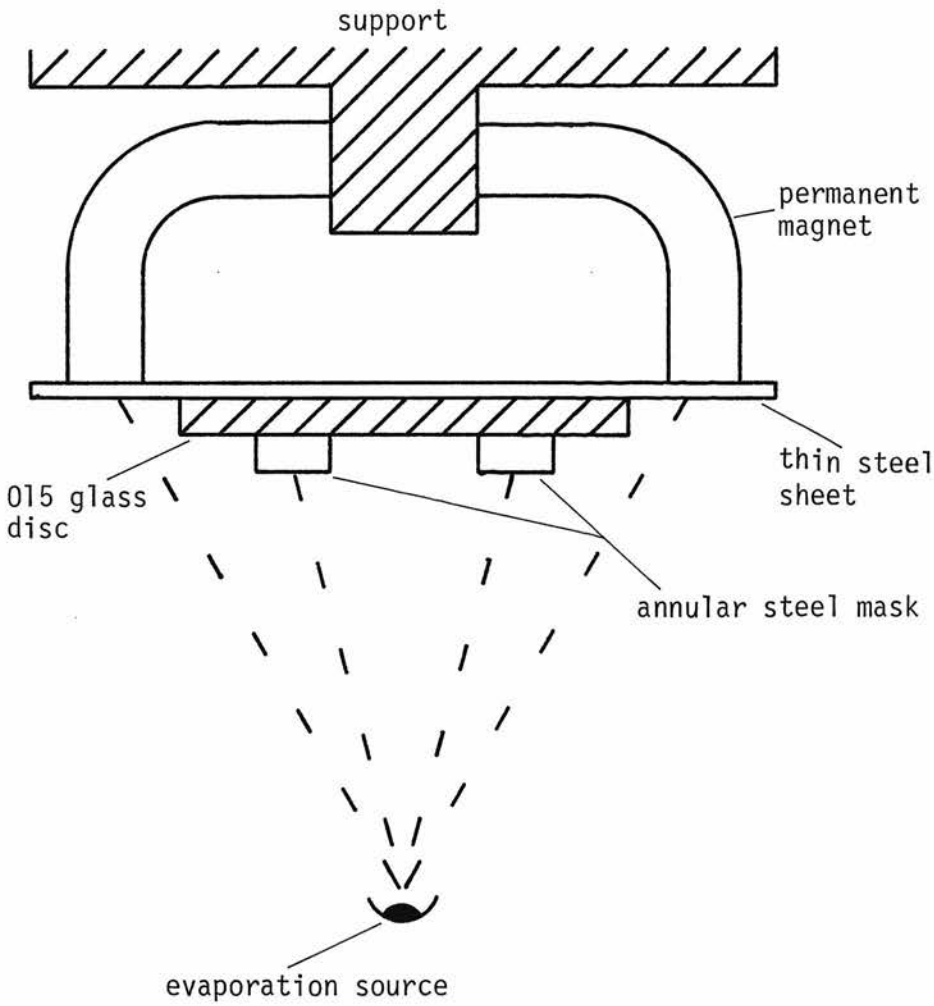

Figure 6.6.2 Masking technique used for the evaporation of metal contacts on to glass discs

Pyrex tubes of 1 mm nominal wall thickness and inside diameter slightly larger than the central metal contact were cut to length using a precision diamond saw to give a smooth, flat, end cross-section. A tube was attached to each side of the glass disc using Silcoset 153 silicone rubber, as shown in Figure 6.6.3. On the advice of the manufacturers, the Silcoset was allowed to cure for three days in a high humidity environment. The open ends of the Pyrex tubes were dipped in molten candle wax to minimise electrical surface leakage across them.

In this arrangement, the central metal contact on the glass disc was aligned as nearly as possible with an area on the opposite face of the disc defined by the silicone rubber attaching the Pyrex tube. These areas formed the opposite faces of a metal connected electrode membrane, the test solution being contained inside the electrode in contact with the non-metallised side of the disc while the metal contact served as the reference side of the membrane. The annular contact was separated from both sides of the electrode by the Pyrex tubes. The requirement for the Pyrex tube on the metallised face of the disc was clearly indicated by preliminary measurements which revealed very high leakage conductance between metal contacts deposited on an 015 glass disc. Leakage was greatly reduced by the presence of the tube and silicone rubber adhesive separating the metal contacts.

Electrical connection to the metallised areas was made by attaching short strips of thin copper foil using 'Elecolit' conducting epoxy resin. Connecting wires were then attached to the foil using crocodile clips.

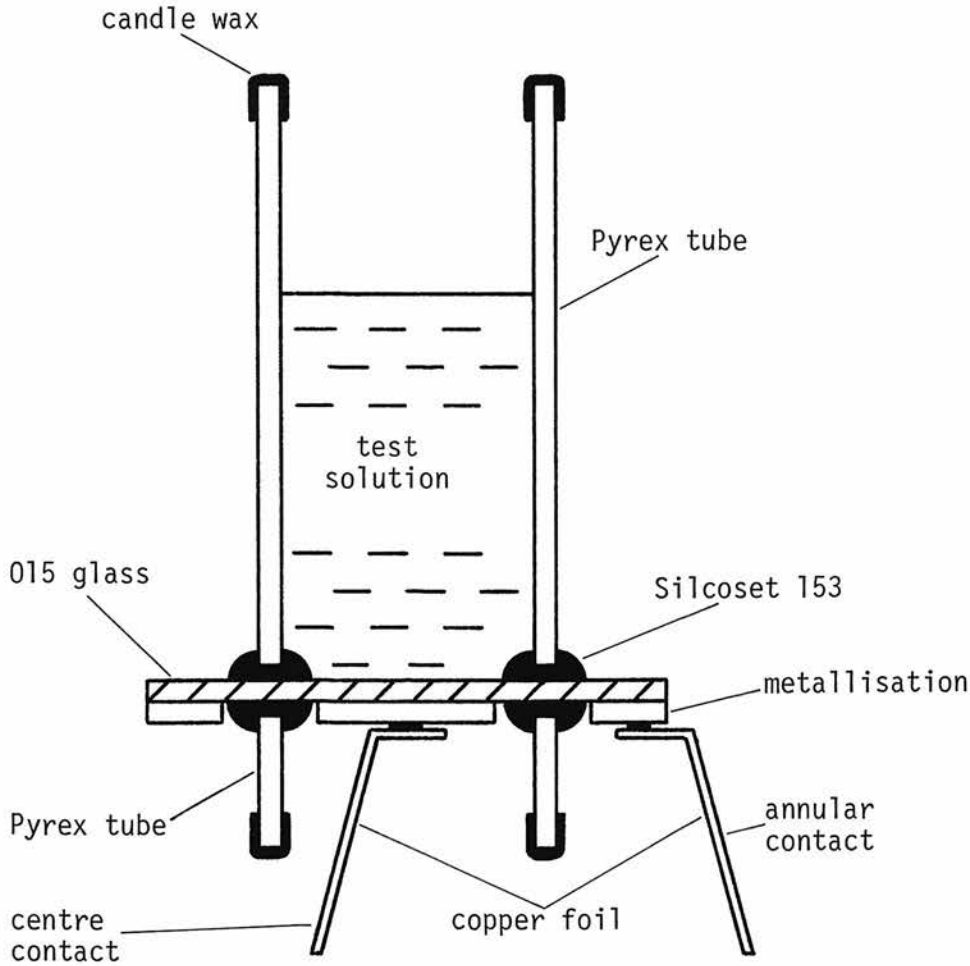

Figure 6.6.3 Assembly of metal connected disc electrode using silicone rubber adhesive

Membrane electrodes were also made for comparison with the metal connected devices. Early samples were constructed by attaching a glass disc to the end of a short length of Pyrex tube using Silcoset 153, as shown in Figure 6.6.4. At a later stage in the work it was required to use the method of Section 8.5 to estimate the degree of electrical leakage across the membrane. For this purpose the arrangement of Figure 6.6.5 was used in which Pyrex tubes, previously worked to the required shape, were sealed to opposite faces of the disc. Filling solutions were placed in each tube to make contact to both sides of the membrane. A gold-nichrome contact was deposited around the periphery of one face of the disc, prior to assembly, using the evaporation and masking techniques described above.

See Figure 6.6.6 for a photograph of the devices described in this section.

6.7 FUSED DISC ELECTRODES

It was noted in Section 6.2 that unacceptable electrical leakages were found to develop in devices which relied upon the direct adhesion of silicone rubber to a pH glass surface. The direct seal was eliminated by using the arrangement of Figure 6.7.1 in which the pH sensitive disc is fused to a sheet of a suitable carrier material through which a hole has previously been bored. The main requirements for the carrier material, as for the stem glass in a conventional glass electrode, are that it must have a high bulk resistivity and be compatible with the ion sensitive glass with regard to softening point and expansion coefficient.

Fusing of a number of materials to 015 glass was investigated using a 32 mm diameter horizontal tube furnace fitted with a programmable temperature controller (Model LVP-C, Stanton Redcroft

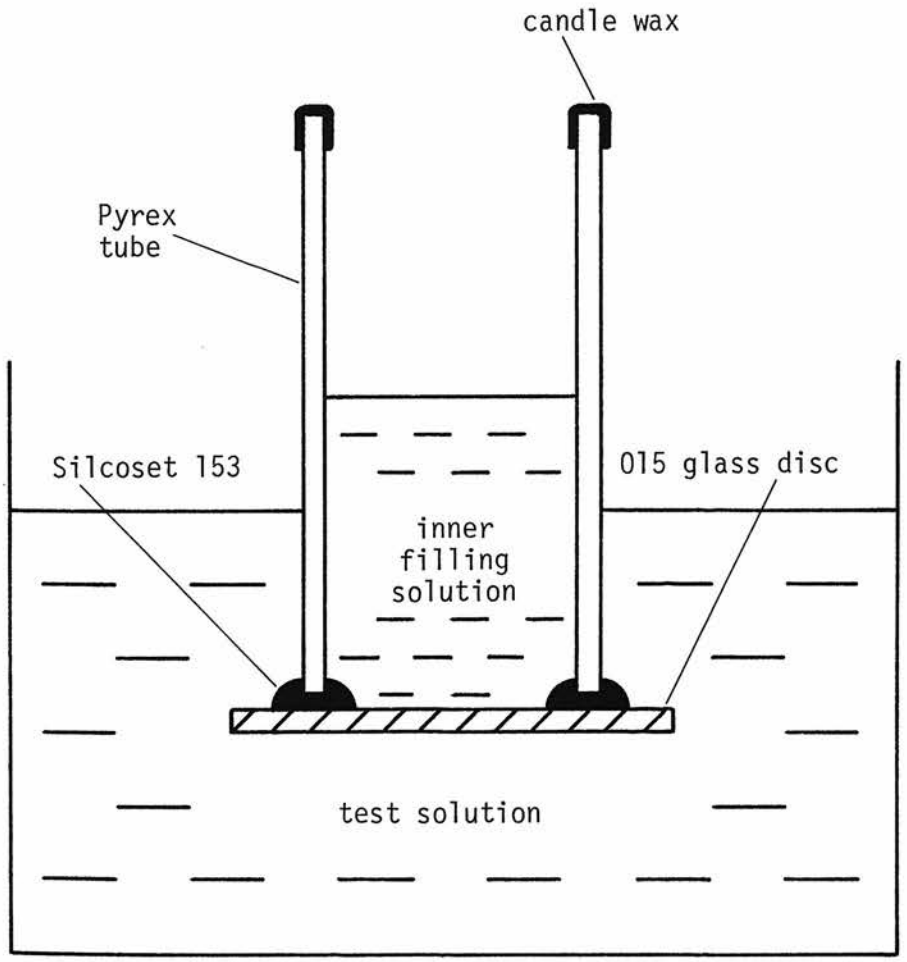

Figure 6.6.4 Assembly of glass disc membrane electrode using silicone rubber adhesive

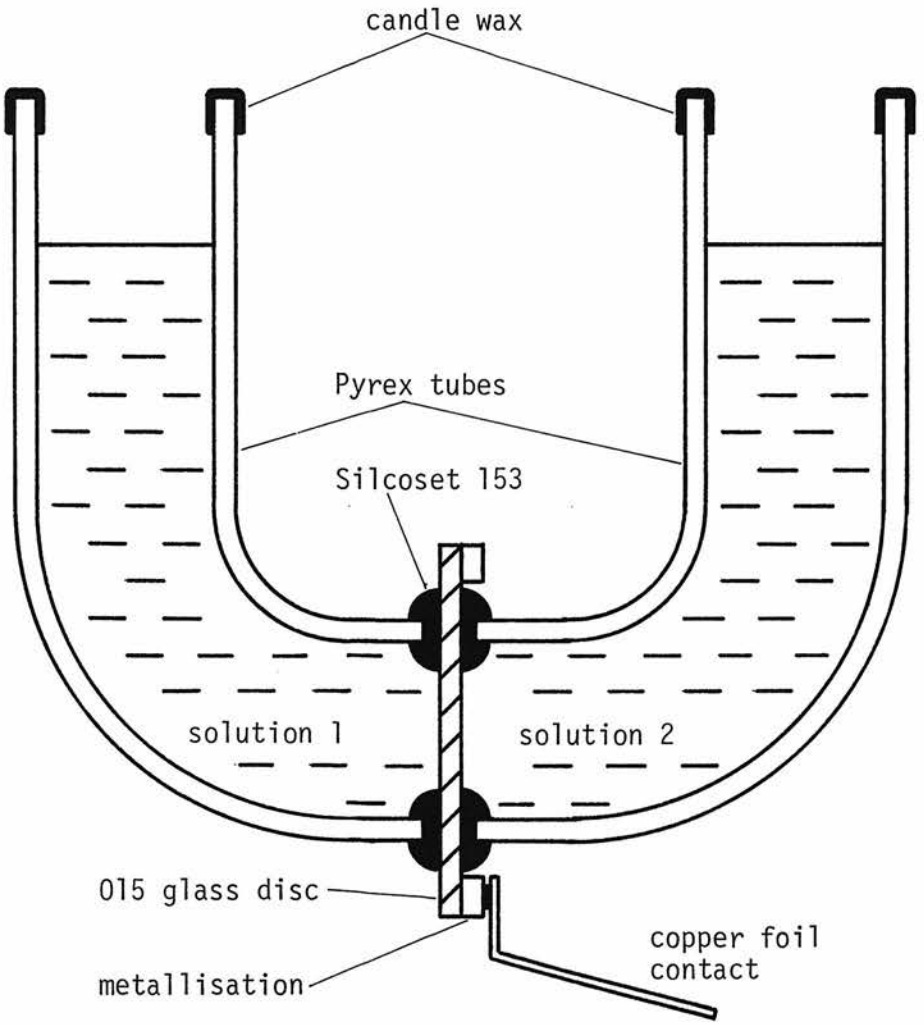

Figure 6.6.5 Disc membrane electrode incorporating annular contact for electrical leakage measurements

Figure 6.6.6 Photograph of glass disc membrane electrode (left) and metal connected electrode (right), assembled by the 'direct adhesion' method described in Section 6.6.

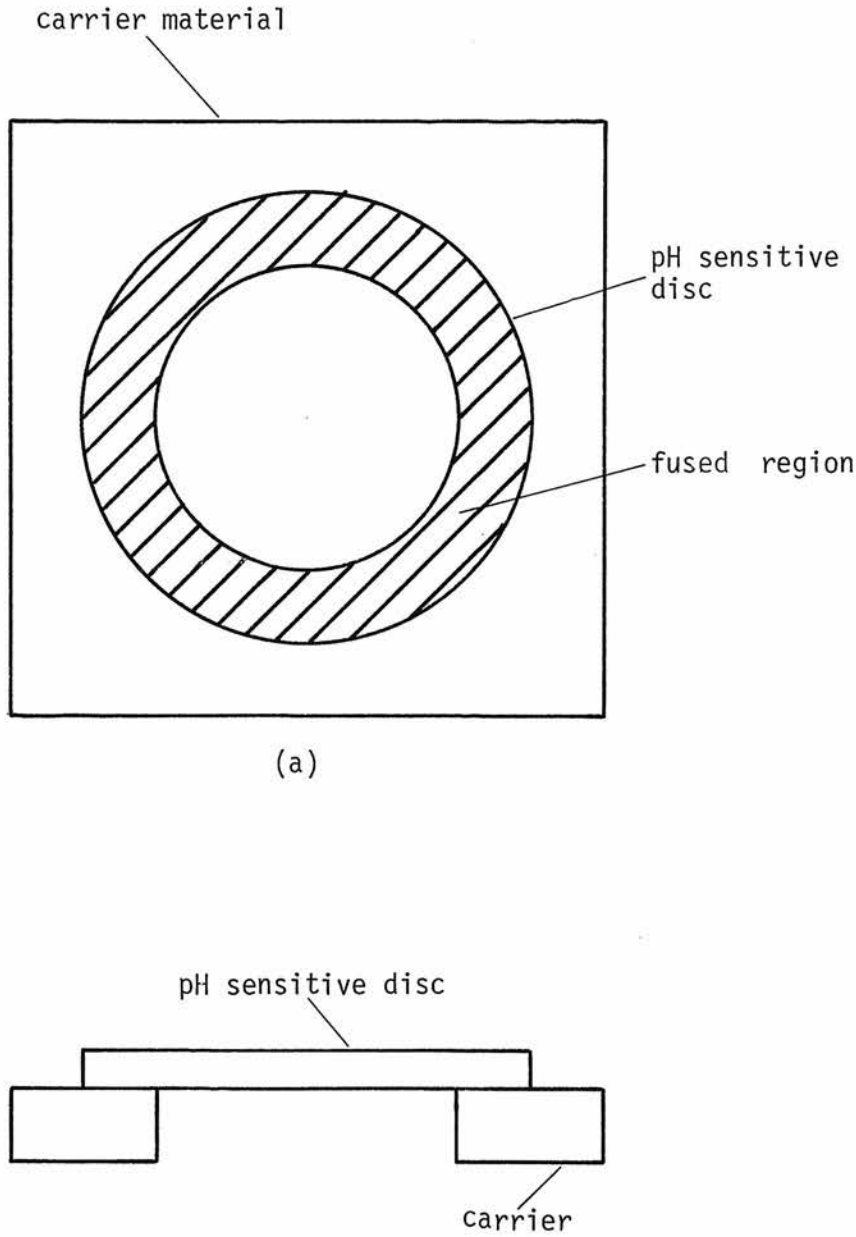

Figure 6.7.1 Fusion of pH sensitive disc to an inert carrier. (a) plan, (b) cross-section

Ltd). A 300 μm thick, 22 mm diameter disc of 015 glass,prepared by the method of Section 6.5, was placed on top of a one to two millimetre thick sheet of the carrier material which was laid on a flat piece of quartz and introduced into the controlled zone of the furnace. The quartz was preheated to minimise the quenching effect when it was introduced into the hot zone. Some preliminary work was done to determine suitable firing conditions by fusing together two pieces of 015 glass. It was found that 600^{o}C was the lowest temperature at which a strong bond was obtained and it was necessary to maintain this temperature for one hour, after which time the matt surface of the lapped material had assumed a fairly shiny appearance. Firing at higher temperatures tended to cause deformation of the disc. Note that Corning Glass Works quote the softening point of 015 glass as 656^{o}C[107].

For use with membranes of 015 glass (which has a large expansion coefficient of 110 x 10^{-7} per deg C),a lead glass sold as Corning 0120 is commonly used as the stem material. It was not possible to obtain this material in sheet form but a lead glass known as'L92' having a similar expansion coefficient (90 x 10^{-7} per deg C) was kindly supplied by Glass Tubes and Components Ltd. This glass is used mainly in the manufacture of cathode ray tube screens, in which form it was supplied and subsequently cut into suitably sized pieces. This material fused satisfactorily to 015 glass after firing for 1 hour at 600^{o}C but it was necessary to cool the fused structure slowly (0.3 deg C/min) to prevent cracking. Unfortunately, as a result of the similar softening temperatures of the two materials, considerable deformation took place.

It was clear that a substrate material having a softening

temperature much higher than that of the 015 glass was required. Some ceramics meet this requirement and the use of alumina, which was readily available in the form of substrates for thick film hybrid circuits, was investigated. Unfortunately its expansion coefficient is of the order of 70 x 10^{-7} per deg C (in the range 40°C to 500°C) which is much less than that of 015 glass and, although these materials were found to fuse strongly together, the 015 glass fractured on cooling even at rates of less than 0.3 deg C/min. Another class of ceramics, the steatites, have rather larger expansion coefficients than alumina. An example is Frequentite (Steatite and Procelain Products Ltd) which has a coefficient of 86 x 10^{-7} per deg C in the range 20°C to 600°C. Satisfactory results were usually obtained when fusing Frequentite to 015 glass by firing for 1 hour at 600°C and cooling at 0.3 deg C/min. Fractures did sometimes occur however and the resulting materials were presumably highly stressed†.

The most promising materials for this application however are the glass-ceramics, one example of which, known as EE1087, was obtained from GEC Power Engineering Ltd in the form of discs 114 mm diameter by 12 mm thick. This particular composition was readily available and has a nominal expansion coefficient of 114 x 10^{-7} per deg C (20°C to 700°C) which is close to that of 015 glass. It has been found that this material can be fused strongly to 015 glass by firing for 1 hour at 600°C. No visible damage is observed even when the fused materials are air quenched from 600°C to room temperature. An important property of the glass-ceramics is that they can be

†Since carrying out this work, two further ceramics having larger expansion coefficients have been noted and it would be interesting to investigate their suitability for fusing to 015 glass. They are Forsterite (Semitek Agents, Birmingham, Ltd) and PF2 (Steatite and Procelain Products Ltd).

designed to have expansion coefficients over a wide range. This feature may be valuable in future work using glasses other than 015.

Electrodes were constructed as follows. Square pieces of glass-ceramic EE1087 (28 mm x 28 mm x 2 mm) were cut from the slabs supplied, using a diamond saw. A hole (diameter 9.5 mm) was bored in the centre of each square, using a diamond trepanning drill. The part was then thoroughly cleaned ultrasonically using trichlorethylene followed by Decon 90. It was then laid on a flat piece of quartz (which had been pre-heated to 600^{o}C) and a 300 μm thick disc of 015 glass, prepared as described in Section 6.5, was placed on top of the glass-ceramic as near centrally as possible over the hole. The boat was introduced into the hot zone of the furnace (at 600^{o}C) for 1 hour. It was then pulled to the end of the furnace tube and allowed to cool for about 10 min before being removed completely from the furnace. A strong and visually good bond between the materials was observed and deformation of the 015 glass disc was slight, the sag at the centre of the hole being less than 0.5 mm. Fabrication of a membrane electrode was completed by attaching a Pyrex tube (20 mm outside diameter, 1.5 mm wall thickness) to the glass-ceramic, using Silcoset 153 as shown in Figure 6.7.2. Metal connected electrodes were constructed, as shown in Figure 6.7.3, by using the method of Section 6.6 to evaporate a metal film over the whole of one face of the disc/carrier structure, prior to attaching the Pyrex tube. The annular ring contact described in Section 6.6 was omitted from these devices and masking was not required. See Figure 6.7.4 for a photograph of these electrodes. The reduction in leakage effects which was obtained with these devices (see Chapter 9) shows that effective adhesion was obtained between the silicone rubber and the glass-ceramic and is further indirect evidence that the difficulties experienced in sealing directly to ion sensitive glass are rather exceptional.

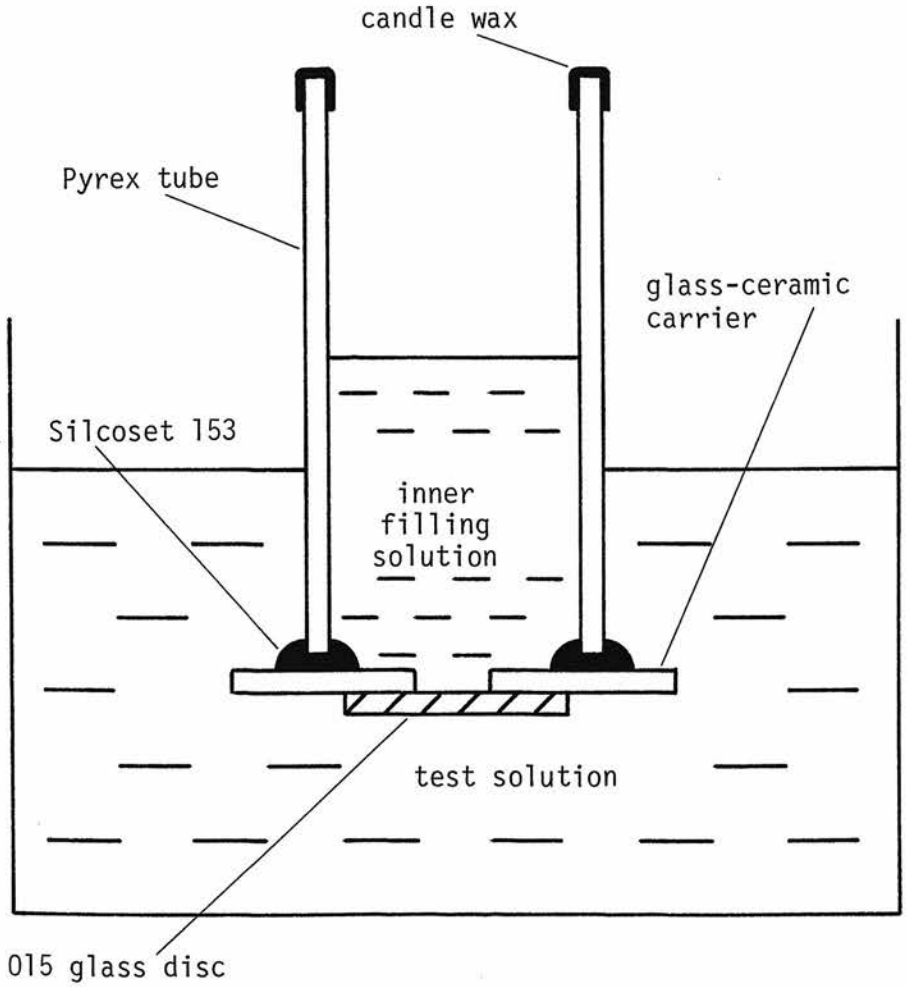

Figure 6.7.2 Fused disc membrane electrode

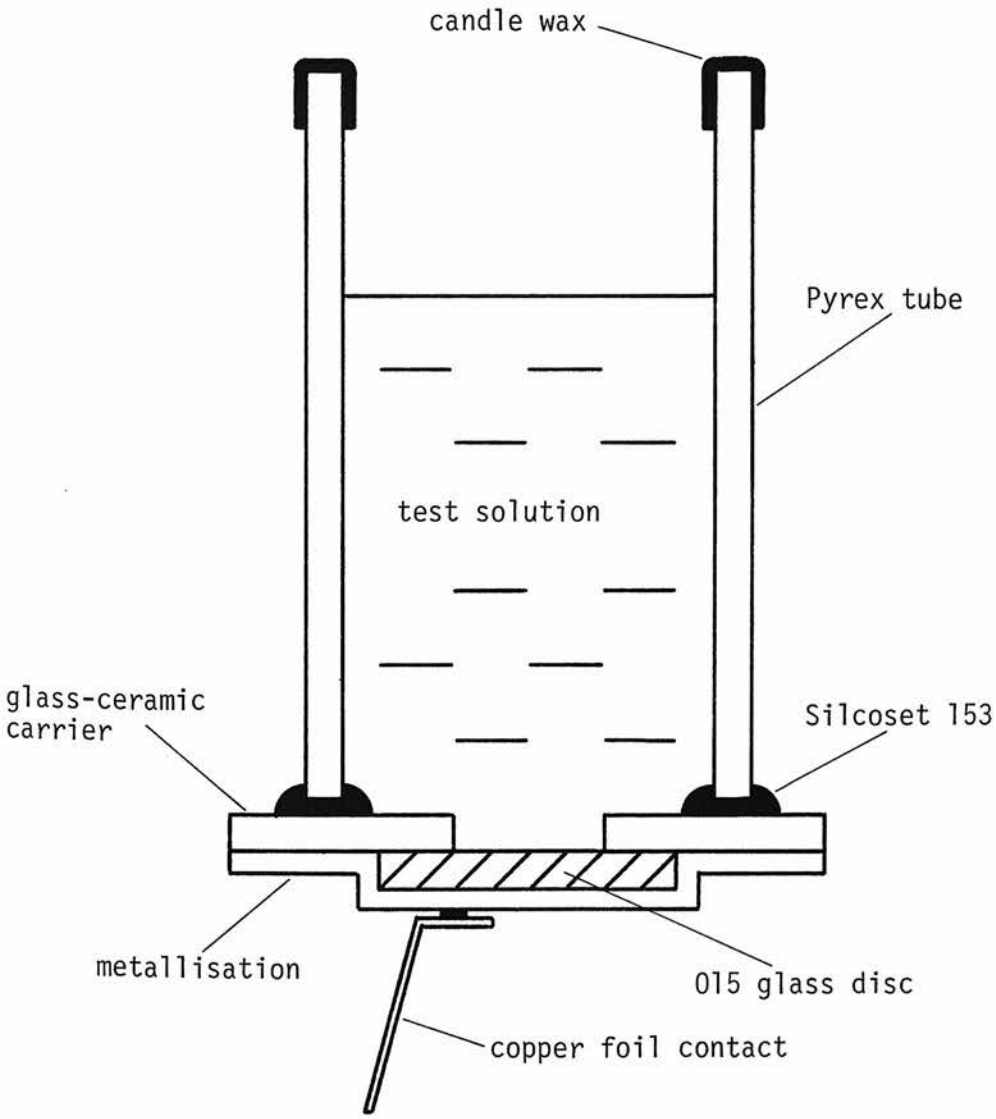

Figure 6.7.3 Fused disc metal connected electrode

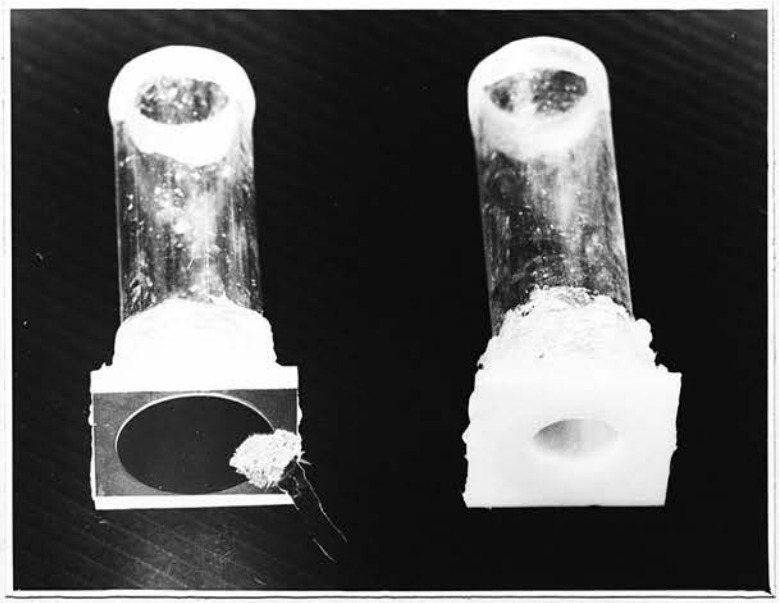

Figure 6.7.4 Photograph of metal connected glass disc electrode (left) and membrane electrode (right), assembled by the 'fusion' method described in Section 6.7.

CHAPTER 7: ISFET DEVICES

7.1 PRELIMINARY ELECTRICAL MEASUREMENTS

The following measurements were carried out on the four ISFET devices and the test transistor on each of four chips assembled according to Section 6.3 in order to assess the quality of the silicon processing and to reveal any damage (to the bond wires for example) caused by the encapsulation. The measurements were carried out using a transistor curve tracer (Model CT71, Telequipment Ltd).

First, the forward and reverse current-voltage characteristics of each source and drain diffusion diode were measured in order to identify any breakdown effects in these large area diodes and also to reveal open circuits resulting from damaged bond wires. Apart from some obviously faulty devices, the curves were typical of p-n junction diodes (Figure 7.1.1), the forward currents being similar for all devices and the reverse breakdown voltages generally comparing well with measurements on the test chip summarised in Appendix 6. A summary of data taken from the curve tracer display is presented in Table 7.1.1.

The transistor characteristics of the ISFET devices were then measured. Since ISFETs do not have a gate electrode the characteristics comprise a single drain current - drain-source voltage curve. (The silicon substrate was connected to the device source for these measurements). Clearly the effective gate voltage of these devices is determined by electrical leakage conductances and/or static charge accumulated on the gate oxide. (Care was taken at all times

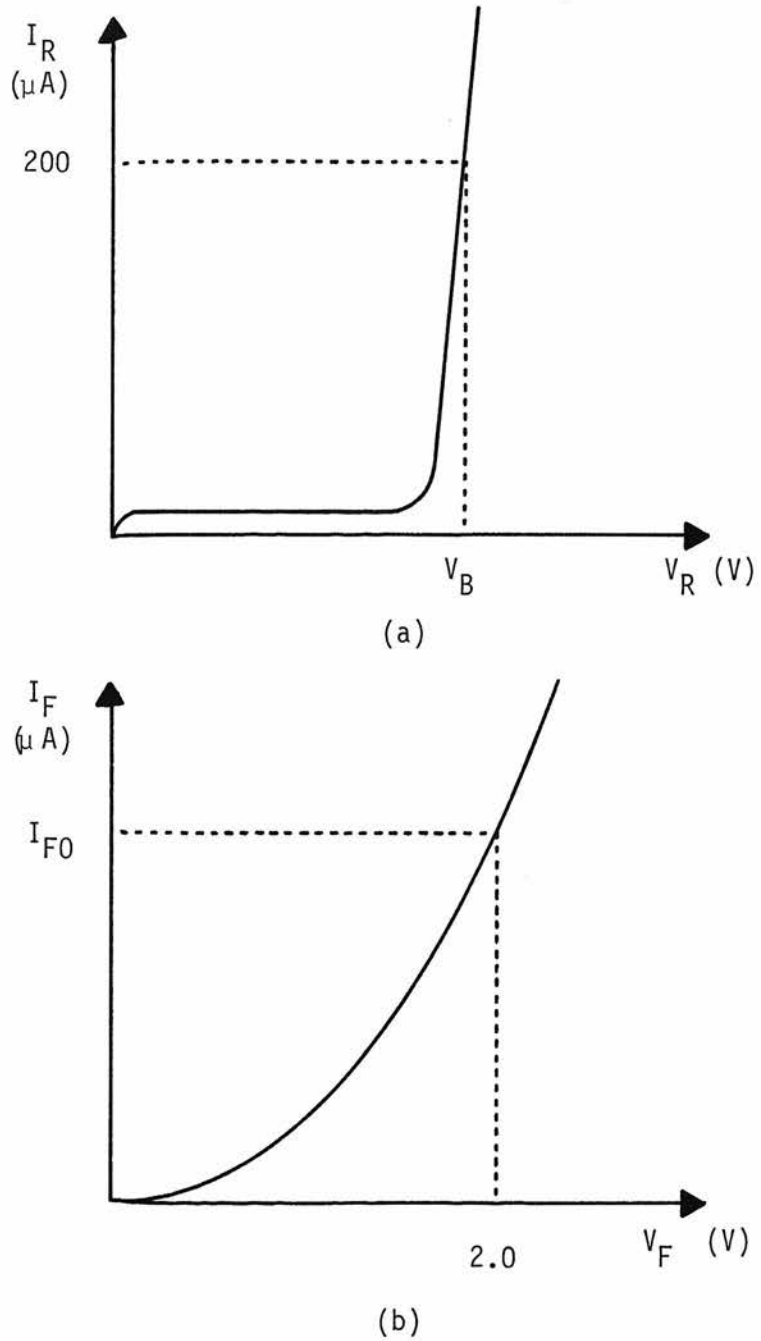

Figure 7.1.1 Typical form of current-voltage characteristics for p-n junction diodes, (a) reverse bias, (b) forward bias, showing the specifications of breakdown voltage (V_B) and forward current (I_{FO}) referred to in Table 7.1.1.

chip no	device no	I_{FO} (μA)		V_B (V)	
		source	drain	source	drain
1	1	700	680	100	104
	2	710	700	100	100
	3	720	680	98	98
	4	680	630	100	67*
2	1	500	500	100	100
	2	570	520	97†	100
	3	550	520	95*	96†
	4	500	480	100	98
3	1	660	640	58*†	54*†
	2	740	690	56*†	56*†
	3	730	700	58*†	48*†
	4	660	650	58*†	56*†
4	1	510	530	102	88†
	2	600	570	100	74*
	3	590	-	100	-
	4	520	-	98	-

Table 7.1.1 Forward current, I_{FO}, and reverse breakdown voltage, V_B, (defined as shown in Figure 7.1.1) for the source and drain diffusion diodes of ISFET devices.

* *reverse breakdown characteristic not very sharp*

† *breakdown voltage varied slightly during period of observation*

to avoid touching the exposed oxide in order to minimise electrical and mechanical damage). In spite of these uncertainties, the observed curves had the typical shape of MOS transistor drain characteristics shown in Figure 5.3.3. Furthermore the saturation region output impedance was generally higher for the devices with 40 μm channel lengths than those with 20 μm channels, as would be expected from the phenomenon of 'channel length modulation' in IGFETs[108]. Typical curves are sketched in Figure 7.1.2. The saturation region drain current measured for a drain-source voltage of 10 V is given in Table 7.1.2. It can be seen that for each chip the currents for the shorter channel devices (numbers 2 and 3) are approximately double those for the longer channel devices (1 and 4), as expected. The considerable differences between the currents for different chips is probably due partly to variations in the transistor gain and threshold voltage across the wafer (see Appendix 6) and partly to different effective gate voltages.

Measurements on the fully encapsulated metal gate test transistors indicated grossly faulty devices on two chips. Typical transistor curves were obtained from the devices on the other two chips although their threshold voltages were somewhat different (Table 7.1.3).

7.2 ION SENSITIVITY OF ISFET DEVICES

The choice of test solutions for the measurement of the ion sensitivity of the devices described in this and the following section was complicated by the unknown sensitivity and selectivity of silicon dioxide to different ions. The use of conventional pH

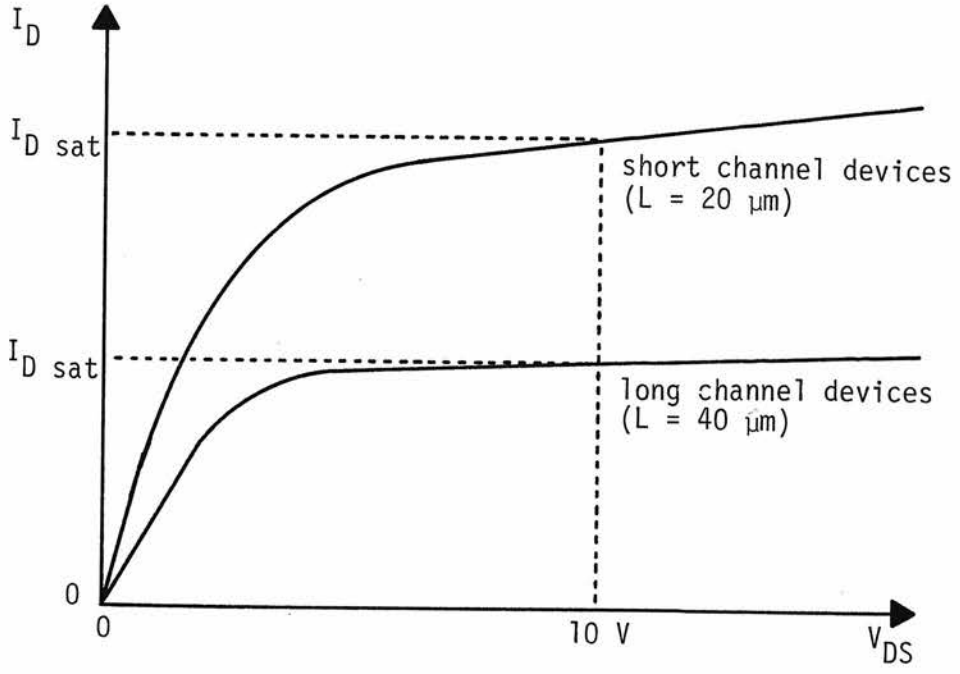

Figure 7.1.2 Typical form of ISFET drain-source characteristics, prior to exposure to solutions. (See also Table 7.1.2).

chip no	$I_{D\ sat}$ (μA)			
	device no			
	1	2	3	4
1	48	130	105	50
2	36	100	130	44
3	*	*	*	*
4	155	400	†	†

Table 7.1.2 Saturation region current, $I_{D\ sat}$, (defined as shown in Figure 7.1.2) for ISFET devices, prior to exposure to solutions.

* *not measurable due to low value of drain-source breakdown voltage*

† *not measurable due to failure of drain diode*

chip no	V_T (V)
1	-
2	-
3	-6
4	-4

Table 7.1.3 Threshold voltage, V_T, of metal gate test transistor included on each ISFET chip.

buffers was avoided on the grounds that they contain different activities of alkali metals to which the devices could well be sensitive. For the measurement of the pH sensitivity of the ISFET devices a range of solutions of different pH was made up using mixtures of 0.1 M sodium hydroxide and concentrated hydrochloric acid, sodium chloride being added to adjust the Na^+ concentration to 0.1 M in all cases. The nominal pH values of the solutions were 2.0, 4.0, 7.0, 10.0, 11.0 and 12.0.

Preliminary measurements to establish the existence of ion sensitivity were carried out by directly displaying the drain-source characteristics of the ISFET using a Telequipment CT71 Curve Tracer connected as shown in Figure 7.2.1. The source and substrate of the ISFET were electrically referenced to the test solution using a calomel reference electrode incorporating a liquid junction (Pye-Ingold). All unused connections to the chip were 'floating'. After being allowed to hydrate for 48 hours in deionised water, the ISFET and reference electrode were introduced to a beaker of each test solution in turn, in order of decreasing pH. Several minutes settling time were allowed before making measurements and the device was rinsed using deionised water when transferring between solutions. The device was then exposed to the pH 2 solution for one hour before being measured in each solution again, this time in order of increasing pH. Care was taken to avoid immersing the device to above the level of the epoxy encapsulation.

The measured drain-source characteristics had the usual IGFET form, Figure 7.2.2 being a typical example. The saturation region drain current was estimated from the curve tracer display at a drain-source voltage of 8 V. The values for each solution are given

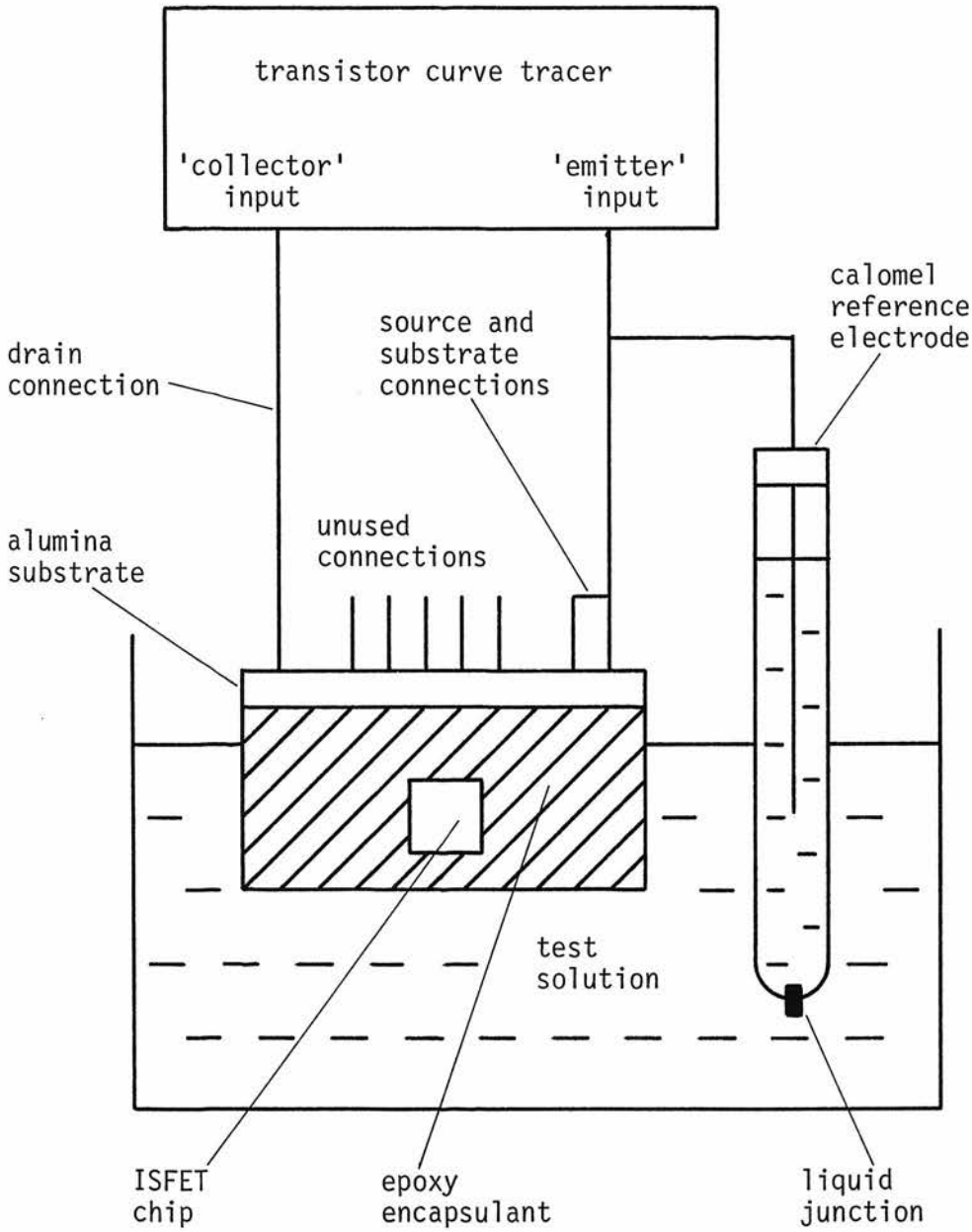

Figure 7.2.1 Measurement of ISFET ion sensitivity using a standard transistor curve tracer.

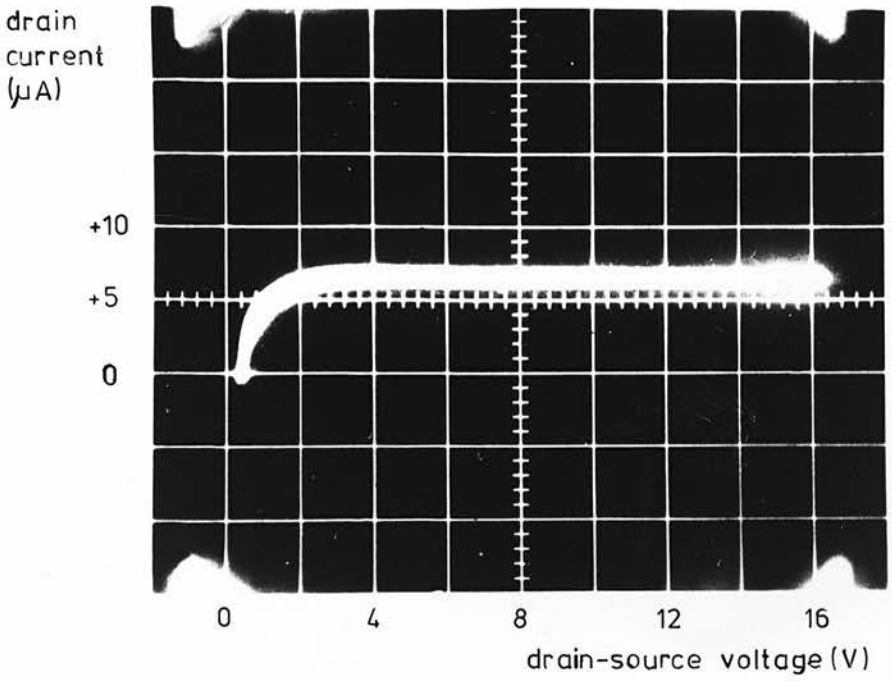

Figure 7.2.2 Transistor curve tracer display of the drain-source characteristics of an ISFET device exposed to a pH 12 solution. (Chip no 1, device no 1).

in Table 7.2.1 which shows an approximately reversible dependence on pH, although a noticeable drift took place during the one hour exposure to the pH2 solution.

Frequent checks, using a commercial pH meter, revealed a noticeable drift in the pH values of the unbuffered test solutions in the course of the above measurements, presumably due to dilution and carbon dioxide absorption. It was also noticed that the ISFET drain current was somewhat sensitive to ambient light levels which could possibly have affected the results. The experimental arrangement was therefore modified slightly to take account of these effects and to obtain better reading accuracy than was obtainable with the curve tracer.

The circuit of Figure 7.2.3 was used, in which the drain-source voltage was manually varied, current and voltage values being read from a multimeter (Type 8, Mk III, Avo Ltd) and an electrometer voltmeter (Model 610C, Keithley Instruments Inc) respectively. The input impedance of the electrometer was sufficiently high that its presence would not introduce appreciable error into the current measurement. In view of the previously noted drifts of the test solutions the pH was continuously monitored using a commercial combination pH/reference electrode incorporating a liquid junction (Pye-Ingold) and a pH meter (Model 291, Mk 2, Pye-Unicam Ltd). The reference element of the combination electrode also served as the reference for the ISFET measurement circuit. The apparatus was covered with a heavy black cloth to eliminate light. In all other respects the technique was as described previously.

Measurements were carried out using the same ISFET device as in the previous work, the chip having been exposed to deionised

pH (nominal)	Series I*		Series II†	
	pH (measured)	$I_{D\ sat}$ (μA)	pH (measured)	$I_{D\ sat}$ (μA)
2	2.0	25	2.0	27
4	4.0	21	4.0	25
7	6.4	18	6.2	20
10	9.7	13	9.0	13
11	10.9	8	10.5	6
12	12.0	7	11.8	4

Table 7.2.1 ISFET saturation region drain current, $I_{D\ sat}$, (measured at a source-drain voltage of 8 V) as a function of solution pH. (Chip no 1, device no 1).

** Series I measurements were made in order of decreasing pH (commencing at pH 12).*

† Series II measurements were made in order of increasing pH (commencing at pH 2).

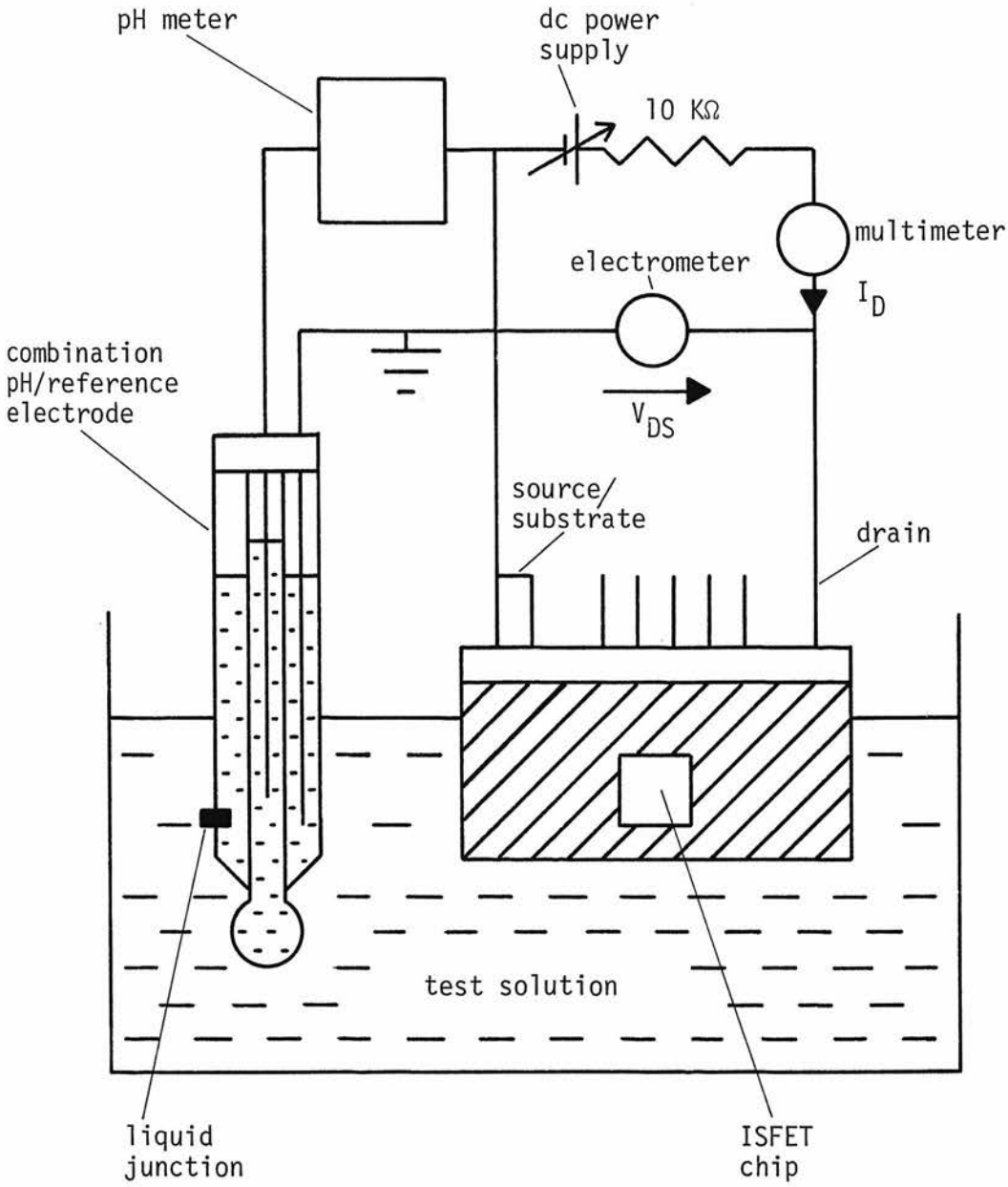

Figure 7.2.3 Improved circuit for the measurement of ISFET ion sensitivity.

water for about 24 hours in the meantime. Transistor-like characteristics were again obtained but the sensitivity of the drain current to pH was much smaller than previously. The measurements were repeated after a further 24 hours but the drain currents of all the ISFETs on the chip were very unsteady and it was suspected that this was due to penetration of the device encapsulation by the solution and the development of electrical leakage paths.

The measurements were then carried out on several ISFETs on the other three chips which had by then been hydrating in deionised water for three days. In the cases of two of these chips the readings were again unsteady. The following results were obtained from the third chip, using an ISFET having the same channel length as the device reported above. A drift of the measured current (typically 0.5 μA over 10 min) was noticed but did not seem to decrease with time after changing the solution pH. It was concluded that this represented a long term drift, rather than a response to pH change, and readings were therefore taken as quickly as possible after changing solutions. As before the device was exposed to a full cycle of pH changes, first in the direction of increasing pH then decreasing.

Transistor-like curves were again obtained (Figure 7.2.4). The saturation region drain current varied with pH over a similar range of values to that previously measured but the reproducibility was poor between the two values of the drain current measured in each solution (Table 7.2.2).

The device was then left exposed to the final solution of the measurement series (pH2, nominal) for two days in an attempt to

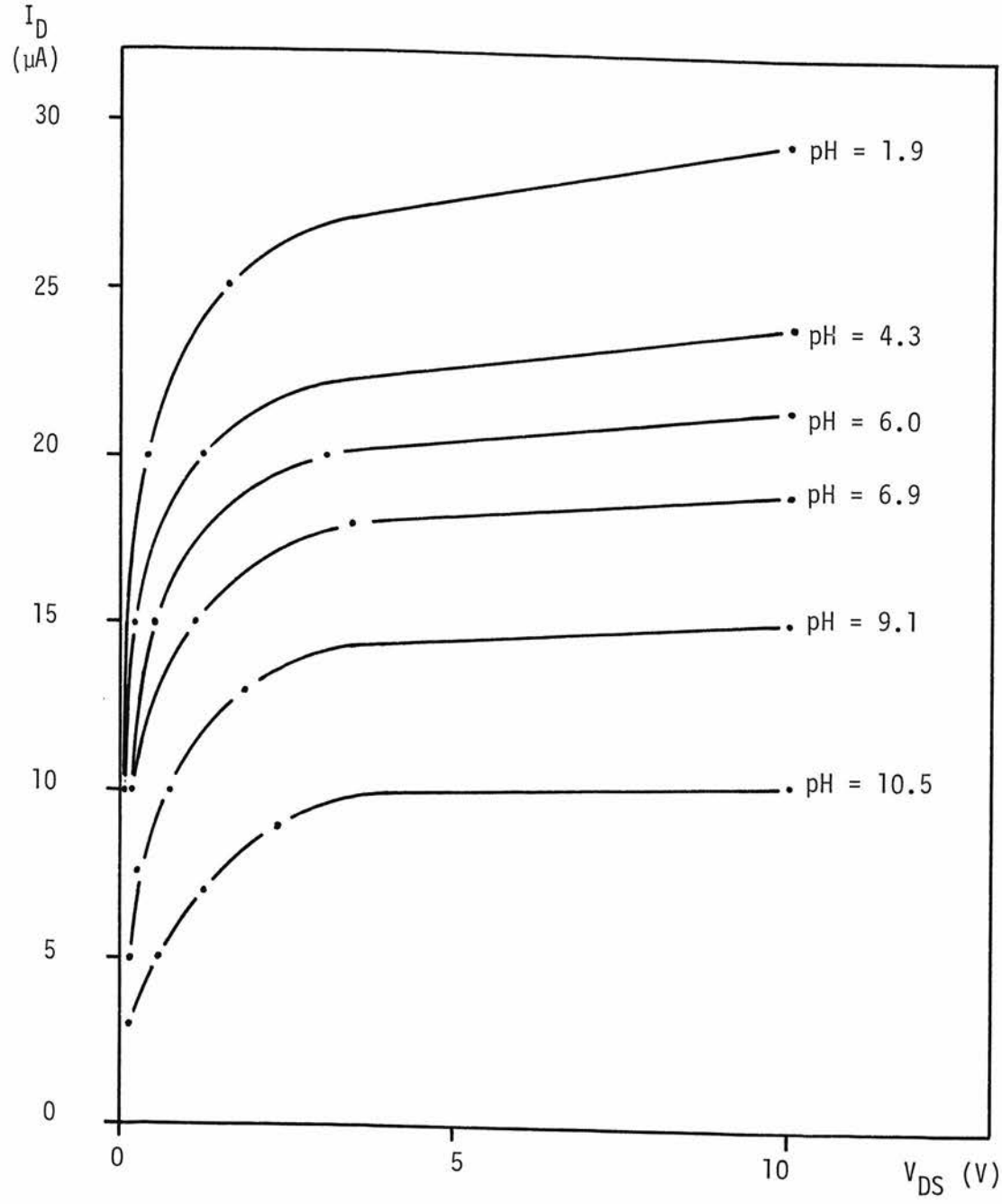

Figure 7.2.4 ISFET drain-source characteristics as a function of pH, obtained using the circuit of Figure 7.2.3. (Chip no 2, device no 1). See also Table 7.2.2, Series I.

Series I*		Series II†	
pH (measured)	$I_{D\ sat}$ (μA)	pH (measured)	$I_{D\ sat}$ (μA)
1.9	29.5	2.0	24.8
4.3	24.0	4.3	15.6
6.0	21.5	6.1	13.3
6.9	19.0	7.0	12.4
9.1	15.2	9.0	11.5
10.5	10.4	-	-

Table 7.2.2 ISFET saturation region drain current, $I_{D\ sat}$, (measured at a source-drain voltage of 10 V) as a function of solution pH. (Chip no 2, device no 1).

Series I measurements were made in order of increasing pH. (See also Figure 7.2.4).

†*Series II measurements were made in order of decreasing pH, immediately following Series I. The result for pH 10.5 is common to both Series.*

measure the long term drift. Unfortunately when measurements were again attempted it was found that the drain currents of all the transistors had fallen drastically and the characteristic curve was not obtained.

The 'failed' devices were left exposed to water for a further two weeks and were then examined under a low power (x20) optical microscope. It was observed that there existed, between the epoxy resin and the silicon dioxide surface, a sufficiently wide gap to introduce a narrow slip of thin paper. When one of the coated alumina substrates was broken in half however, the epoxy resin appeared to be quite hard and well preserved (although a slight whitening of the outer surface was noted). Adhesion to the alumina was apparently still good. It appeared that the device failures were due to penetration of solution at the interface between the resin and the silicon dioxide, as a result of poor adhesion of the organic material to the hydrated silica surface. It is interesting to note in this connection that a completely encapsulated ISFET chip (in which epoxy resin had been inadvertently allowed to cover the entire face of the chip) continued to show transistor characteristics, even after several weeks exposure to solutions.

In the course of the above work, one or two measurements of ISFET characteristics were made without using a reference electrode. Although stable characteristics were observed, the reproducibility of readings during exposure to a series of solutions was poor and no clear relationship with pH could be established.

7.3 ION SENSITIVITY OF SILICON DIOXIDE

Potentiometric measurements of ion sensitivity were made on the batch of seven devices described in Section 6.4. The nominal oxide thicknesses of the devices are listed in Table 7.3.1. Optical microscopic examination (x20) revealed surface scratches on two of the chips.

For ease of handling, the devices were fitted to a sheet of Perspex which could be placed across the mouth of a wide glass vessel containing the test solution, as shown in Figure 7.3.1. In this way the time spent in changing solutions was reduced since several devices could be handled simultaneously. When changing solutions, the devices and the vessel were rinsed, first with deionised water and then with the appropriate buffer solution.

A serious limitation of the test solutions described in the previous section was the presence of a high background concentration of Na^+. It follows from Equation 2.3.2 that the sensitivity of an electrode to pH changes is reduced to less than the Nernstian value by the presence of a sufficiently large concentration of another ion to which the electrode is sensitive. The H^+ selectivity of silicon dioxide is not known and the high background concentration of Na^+ might well have had such an effect on the measurements of the previous section. The technique was improved by the adoption of a range of buffer solutions which have been proposed by Filomena et al[109] specifically for the testing of pH electrodes. These solutions employ organic compounds to achieve high pH values without the use of alkali metals. They may be used for measuring pH response in the absence of alkali metals or (by the addition of

device no	nominal oxide thickness (nm)
2	150
3	control sample (no oxide)
4*	100
5	250
7	200
9*	200
11	150

Table 7.3.1 Devices used for the potentiometric measurements of the ion sensitivity of silicon dioxide.

* *surface scratches observed under low power optical microscopic examination*

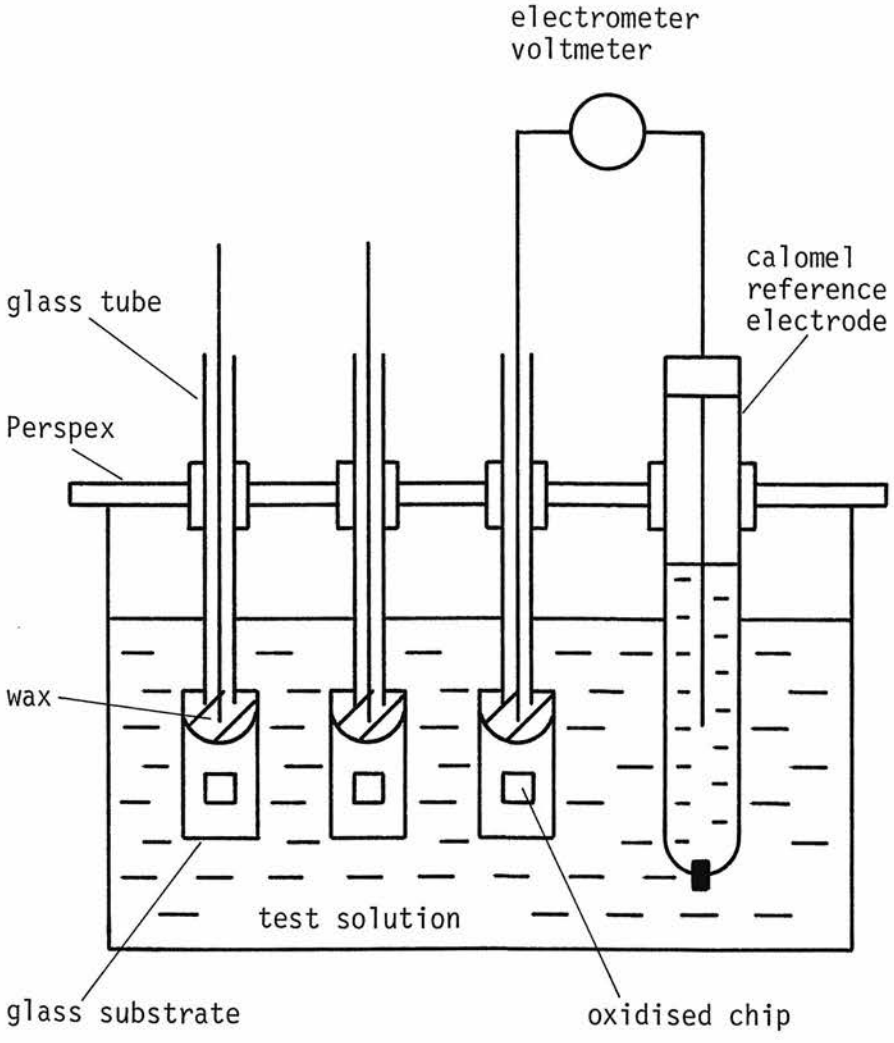

Figure 7.3.1 Experimental arrangement for carrying out potentiometric measurements of ion sensitivity.

The devices are connected in turn to the electrometer

a sodium salt) for measuring Na^+ response at a constant high value of pH. They are however rather prone to drifts of their pH values due to carbon dioxide absorption (Section 8.7).

The sensitivity of the silicon dioxide devices to Na^+ was measured by repeated exposure of the devices to solutions B3NO, B3N1 and B3N2 (Table 7.3.2) using a calomel reference electrode (Pye-Ingold) and electrometer voltmeter (Model 610C, Keithley Instruments) for the direct measurement of electrode potential. The results of this series of measurements, which were made over a period of three days, are presented in Figure 7.3.2. The stability of the potential is indicated by the several readings taken at intervals of between a few minutes and an hour in each solution. Figure 7.3.2 shows a clear correlation between the Na^+ ion concentration and the potential for three of the devices (numbered 5, 7 and 11), although noticeable drifts of the potential took place. The magnitude of the response was generally greater for device number 7 than for the others although it was much less than the Nernstian value in all cases. None of the other devices (including the control device of unoxidised silicon) showed any response.

The sensitivity to pH was then measured, using the sodium free pH buffer, B4, and 0.1 M and 0.01 M solutions of HCl. None of the devices showed any response. An attempt was then made to repeat the measurements of Na^+ sensitivity but no response was obtained. It was concluded that a device failure (probably of the encapsulation) had taken place and the apparent lack of pH response cannot be regarded as significant.

After several more weeks exposure to aqueous solutions obvious

solution	pH at 25°C	Na^+ concentration (M)
B3N0	9.385	1.0
B3N1	9.385	0.1
B3N2	9.385	0.01
B4	11.336	0

Table 7.3.2 Test solutions employed in potentiometric measurements of the Na^+ and H^+ sensitivity of silicon dioxide.

After Filomena et al[109].

Figure 7.3.2 Electrode potentials (mV vs calomel reference electrode) of oxidised silicon devices measured in solutions of different sodium ion concentration (see Table 7.3.2) over a three day period.

Time intervals are referred to the commencement of exposure of the devices to each solution and are approximate only, owing to the finite time required to take readings. All devices were exposed to de-ionised water during the two overnight periods in the course of this measurement series.

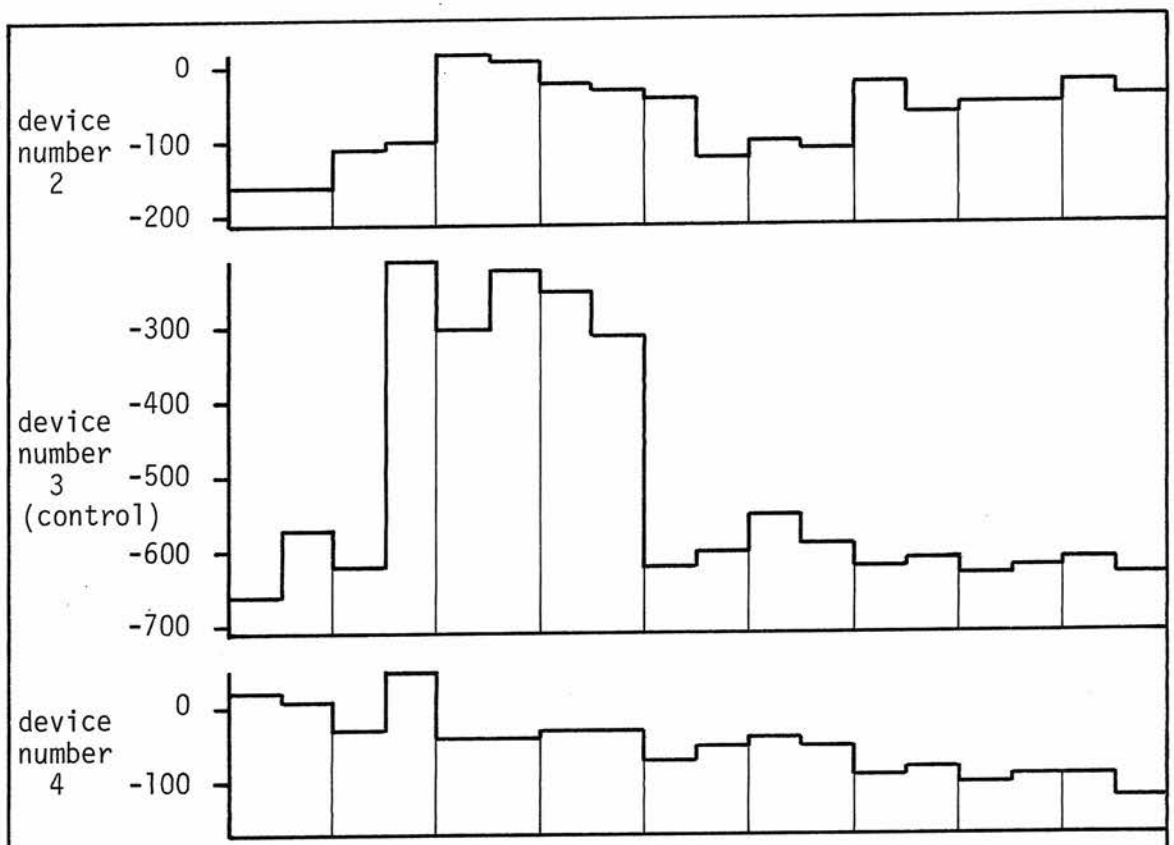

time (min)	0	10	0	30	0	10	0	20	0	30	0	30	0	10	0	10	0	60
solution	B3N2		B3N0		B3N2		B3N0		B3N2		B3N0		B3N2		B3N1		B3N0	
day	1				2				3									

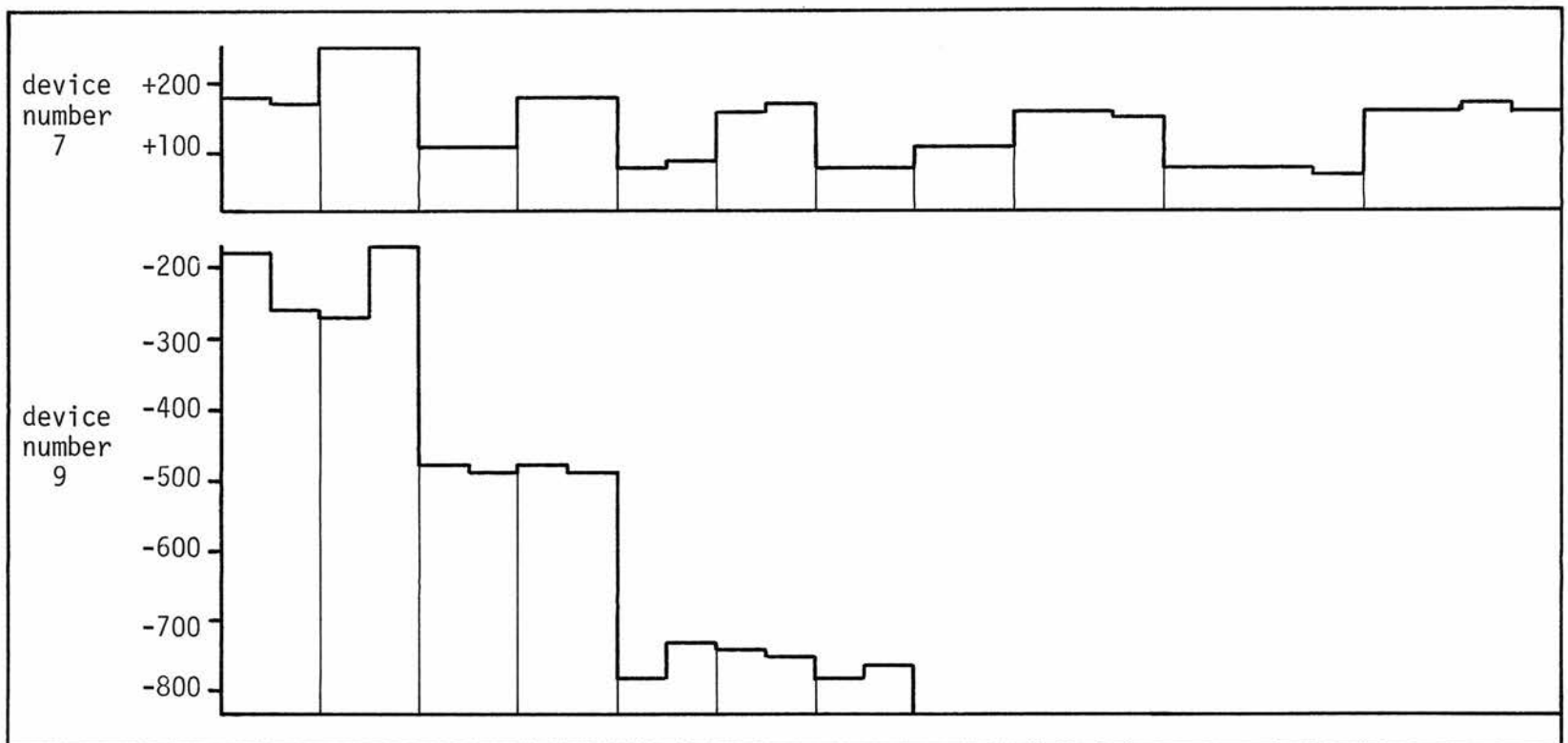

time (min)	0	10	0	30	0	10	0	20	0	30	0	30	0	10	0	10	0	60	70	0	15	30	45	0	15	30	45
solution	B3N2		B3N0		B3N2		B3N0		B3N2		B3N0		B3N2		B3N1		B3N0			B3N2				B3N0			
day	1				2				3																		

Figure 7.3.2 (continued)

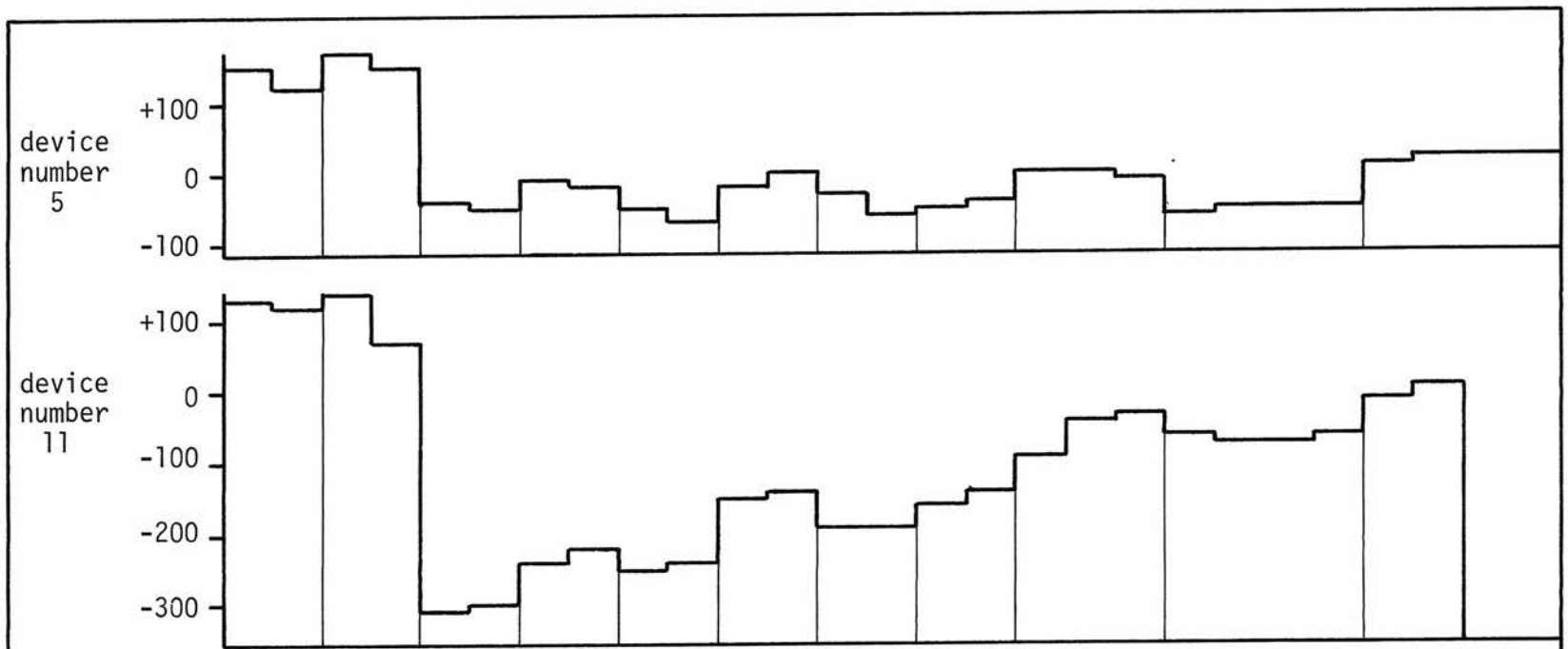

time (min)	0	10	0	30	0	10	0	20	0	30	0	30	0	10	0	10	0	60	70	0	15	30	45	0	15	30	45
solution	B3N2		B3N0		B3N2		B3N0		B3N2		B3N0		B3N2		B3N1		B3N0			B3N2				B3N0			
day	1				2				3																		

Figure 7.3.2 (continued)

deterioration of the encapsulation was observed, flakes of the 'Lacomit' film having become detached from the device surface.

7.4 DISCUSSION

Ion sensitivity measurements on both the ISFET and the silicon dioxide devices were subject to drift and poor reproducibility. In view of the gross degradation of the encapsulation which was generally observed after only a few days or weeks exposure to solution, it appears most likely that electrical leakage effects were responsible for the unstable performance. The device failures are not surprising in the light of the studies of leakage effects and adhesive performance which were carried out (subsequent to the work of this chapter) in connection with the investigation of disc electrodes (Section 6.2 and Chapter 9).

Some of the silicon dioxide devices showed a clear, although less than Nernstian, response to Na^+. It must be remembered however that leakage effects could result in the measurement of spurious electrochemical emfs due, for example, to diffusion potentials or to redox potentials at the metallised parts of the chip. Special caution is therefore required in explaining responses which are significantly sub-Nernstian and subject to drift. The pH sensitivity of silicon dioxide remains uncertain owing to the premature failure of the devices. It is interesting to note here that Bergveld[93] observed very different selectivities between ISFET devices which had nominally similar gate oxides. The number of 'working' devices was not sufficient to draw conclusions about the effect of oxide thickness. (The oxide thicknesses of the three working devices were 150 nm, 200 nm and 250 nm respectively, the greatest response

being obtained from the 200 nm device).

The feasibility of making ISFET devices was confirmed by the measurements of Section 7.1 which were carried out on the encapsulated chips before they had been exposed to water. Breakdown voltages were satisfactory in a reasonable proportion of the large area source and drain diffusions for example and the application of the epoxy resin encapsulant had not caused extensive damage to the bond wires. The metal gate test transistor continued to function correctly in at least two of the four chips, despite the handling which they had undergone. The ISFETs continued to exhibit typical source-drain characteristics when exposed to the test solutions. The saturation region drain current showed a clear *qualitative* relationship to solution pH over a full cycle of increasing and decreasing values, although drift was again observed.

The saturation region drain current of the ISFET can be related to solution ionic activity by Equations 5.3.3 and 5.3.5. If the gate material of the device is highly selective to pH it follows from Equation 5.3.3 that the equivalent gate voltage is linearly dependent on pH. Equation 5.3.5 then shows that a linear relationship exists between pH and the square root of the drain current. If the gate material shows significant sensitivity to an interfering ion however, the relationship between the equivalent gate voltage and pH is non-linear. This corresponds to the non-linear region of mixed response in Figure 2.3.1 and implies a non-linear dependence of $I_{Dsat}^{\frac{1}{2}}$ on pH. Non-linear behaviour would be expected in connection with the ISFETs described in the previous section in view of the observed sodium sensitivity of silicon dioxide and the high

background concentration of Na^+ in the test solutions which were used for the pH response measurements.

Graphs of $I_{Dsat}^{\frac{1}{2}}$ against pH for the ISFETs described in Section 7.2 are plotted in Figures 7.4.1 and 7.4.2. It is clear from the irreproducibility of the two curves for the same device that the 'true' nature of the variation is obscured by drift in the measurements and it is not possible to establish a rigorous relationship between the data and the theoretical equations. We may however carry out a very approximate calculation to relate the order of magnitude changes in drain current and pH. It can be seen from Figure 7.4.2 that a change in $I_{Dsat}^{\frac{1}{2}}$ of about 2.0 $\mu A^{\frac{1}{2}}$ was associated with a change in solution pH from 2.0 pH to 10.5 pH. The corresponding change in the equivalent gate voltage may be calculated using Equation 5.3.5. The typical value of the gain constant, β, was measured as 7 $\mu A/volt^2$ for IGFET devices which had been processed as part of the ISFET batch (Appendix 6). The value of the aspect ratio , W/L, is imprecisely defined for the reasons discussed in Section 6.3 but the dimensions of the overlapping finger geometry indicate a value of 25 for the 40 μm channel device. Using these figures, the observed change in drain current corresponds to a change of about 214 mV in the equivalent gate voltage and this corresponds, by Equation 5.3.3, to an approximately half Nernstian response to pH. There are of course large uncertainties in the values of β and W/L as well as in the use of the first order transistor model itself but the above result is in agreement with expectations on an order of magnitude basis.

It was clear from the above work that further studies of ISFETs

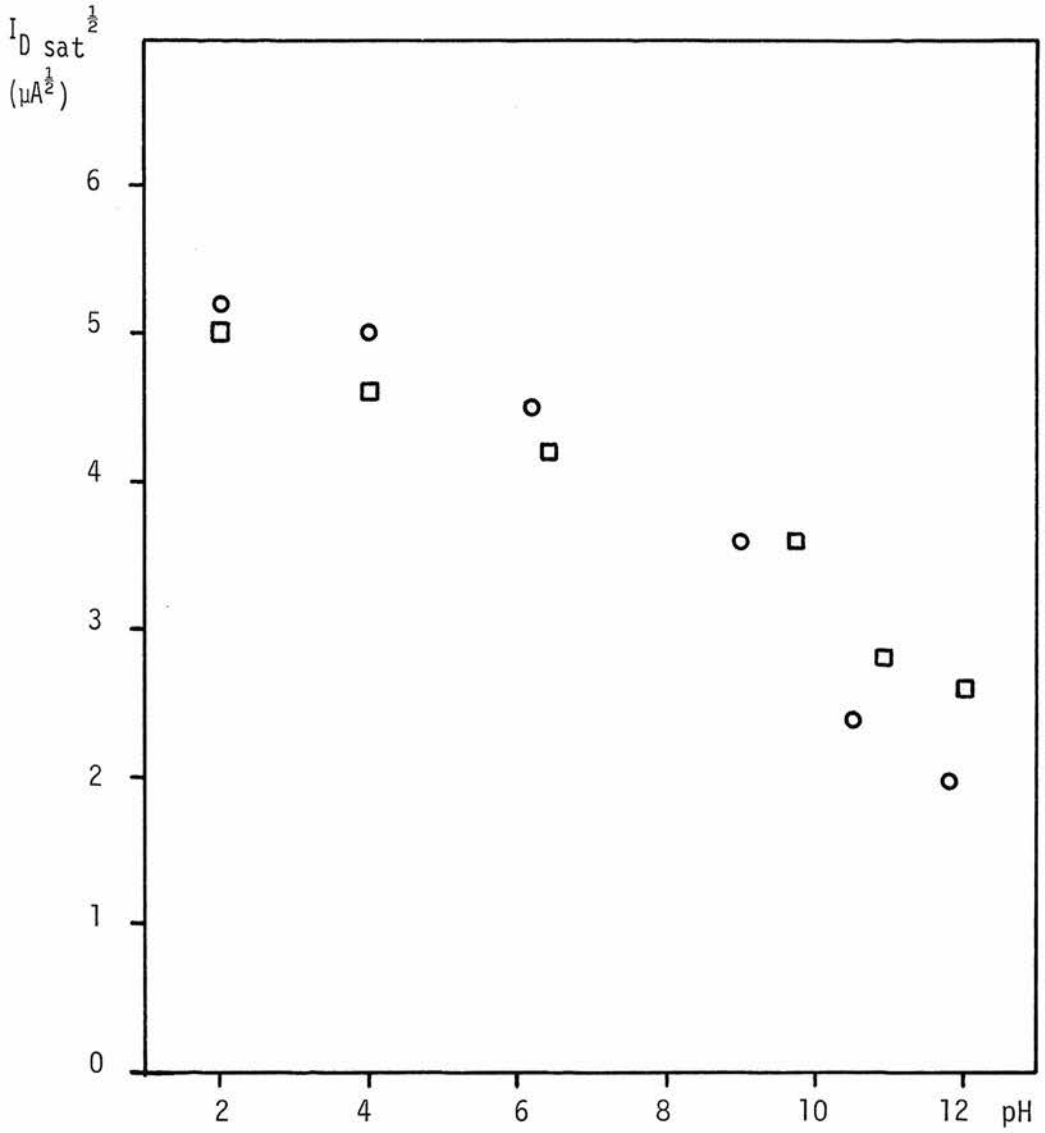

Figure 7.4.1 Variation of $I_{D\ sat}^{\frac{1}{2}}$ with pH for the ISFET device of Table 7.2.1. (Chip no 1, device no 1).

□ Series I measurements (decreasing pH)

○ Series II measurements (increasing pH)

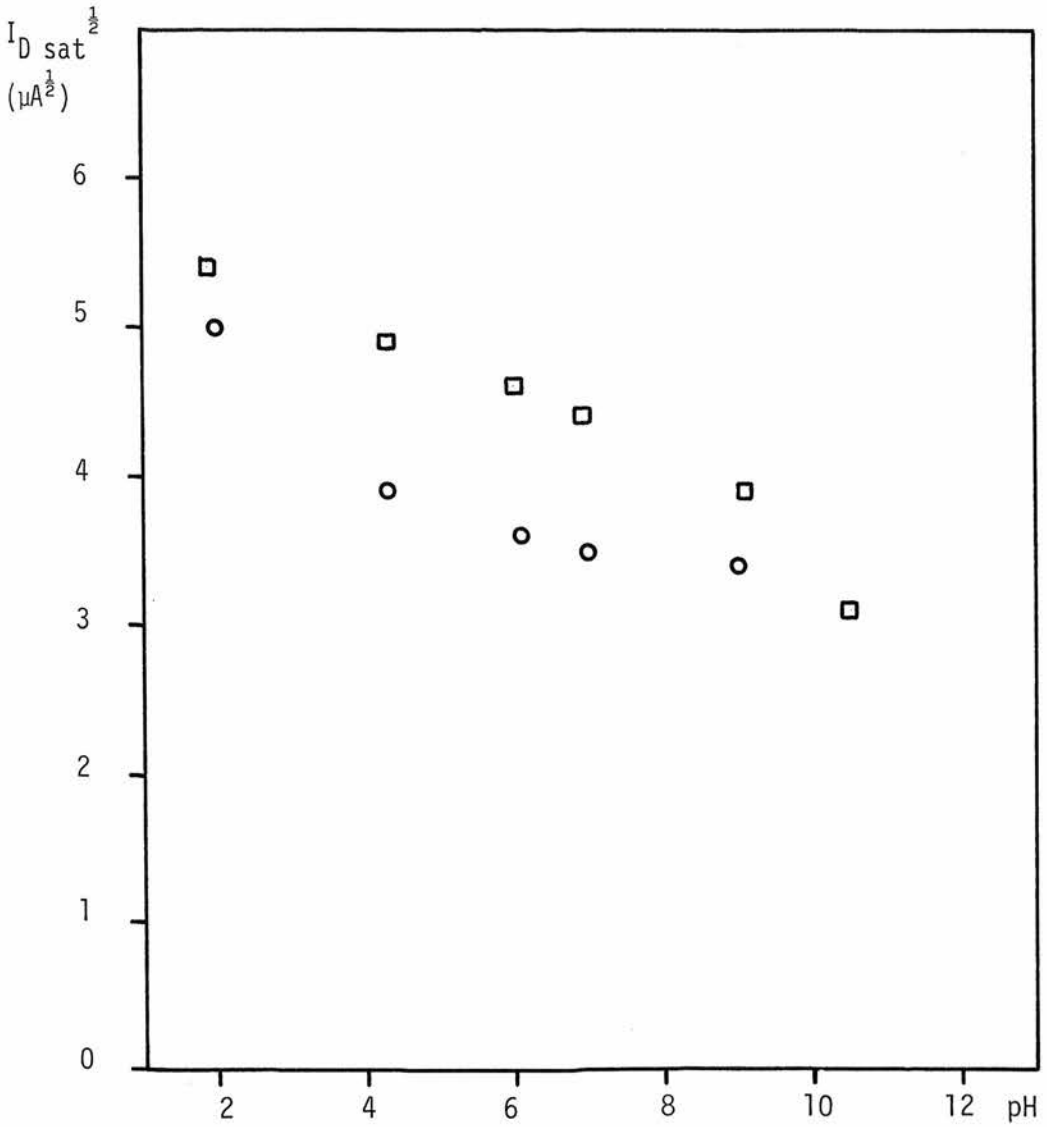

Figure 7.4.2 Variation of $I_{D\ sat}^{\frac{1}{2}}$ with pH for the ISFET device of Table 7.2.2. (Chip no 2, device no 1).

□ Series I measurements (increasing pH)

o Series II measurements (decreasing pH)

would require greatly improved methods of encapsulation so that ion sensitivity measurements could be carried out over an extended period. The encapsulation problem is especially severe with ISFET devices because of the unavoidable presence of delicate bond wires on the face of the chip, close to the area which must be exposed to solution. It is difficult to see how a fusion technique (as described in Section 6.7 for example) could be used with the ISFET. It is possible however that the adhesion of an organic encapsulant might be improved by the deposition of a layer of silicon nitride over the chip. With this method, the underlying ion sensitive material would have to be exposed in the gate area by selective etching to remove the nitride.

The continued use of silicon dioxide as an ion sensitive material would require further work to establish its sensitivity and selectivity and their dependence on processing factors. It would be interesting in this connection to compare the performances of oxide films deposited or grown by alternative methods such as rf sputtering, evaporation or chemical vapour deposition. It may well be however that a more promising route to a practical device would be by investigating the deposition of films of conventional ion selective materials on to an ISFET structure, an approach which has already been followed by Moss et al[90].

It was decided however to suspend work on the ISFET in favour of the alternative approach of developing a potentiometric sensor using hybrid microcircuit techniques, as discussed in Section 5.2. The principal reason for this decision was the formidable problem of encapsulating the ISFET, both in the laboratory and in any future production environment. The severity of this problem has been

noted by other workers[90] in the ISFET field and has been confirmed by its persistence into subsequent work with the larger and less complex disc electrodes described in Chapter 9. It was also recognised that a practical ISFET would almost certainly require the deposition of a film of an ion selective material (glass or otherwise) on to the silicon substrate. Any materials and deposition techniques used for this purpose would have to be compatible with the small size and nature of the silicon device and might require, for example, the development of suitable selective etchants. The 'yield' of working ISFET devices is limited by the usual factors associated with silicon wafer processing, together with further losses at the encapsulation stage. From an experimental point of view, this makes it necessary to process, assemble and test fairly large batches of devices in order to obtain sufficiently large samples to obtain representative measurements.

In addition to these practical difficulties in fabricating ISFET devices, there are serious doubts about their advantages for many applications. Early work by Bergveld[93] suggested that ISFET measurements had the very attractive feature of not requiring a reference electrode. The reasoning of Appendix 4 however shows that a reference electrode is in fact required for stable operation. A further conclusion from Appendix 4 is that ISFETs may be prone to instability resulting from polarisation effects in the ion sensitive material. It must be noted however that stable devices have been reported by Moss et al[90] and this matter must remain unresolved until more experimental evidence is available. Although the active area of an ISFET may be as small as a few micrometres square, the requirements of handling, bonding and encapsulating the device imply a

minimum chip size of one or two millimetres square and a final encapsulated device which is even larger. For applications such as water quality monitoring and industrial process measurement, the small active area is not necessary and will be very prone to fouling by solid matter. For applications where a small sensor is required however, the ISFET may be inappropriate because of its overall size and essentially planar structure. Microelectrodes for insertion into biological material for example are usually spear shaped with tip diameters as small as 1 μm[47].

It was felt that the benefits of using microelectronic methods, in terms of the physical structure, reliability etc of the device, could be equally well achieved by means of the hybrid microcircuit approach discussed in Section 5.2. The manufacturing methods are less sophisticated than those required for ISFET fabrication and are likely to be more easily adaptable to the particular requirements of ion sensors, especially with regard to encapsulation. The requirement for a reference electrode applies equally to both approaches and its implications for the utility of the overall measurement system were discussed in Section 5.4. The main requirement for the hybrid circuit approach is the development of a stable, solid state potentiometric connection and the work described in the following chapters was directed to this objective.

CHAPTER 8: MEASUREMENT TECHNIQUES FOR GLASS DISC ELECTRODES

8.1 INTRODUCTION

The techniques described in this chapter were used for making potentiometric measurements of the pH sensitivity and long term stability of glass disc electrodes in both membrane and metal connected form.

The resistances of the glass discs were typically $2 \times 10^9\ \Omega$ so that the resistance associated with parallel leakage paths in the electrode and associated instrumentation had to be greater than $10^{11}\ \Omega$ for reasonably accurate measurement. It is well known, from experience with conventional glass electrodes for example, that effects such as surface conduction across insulators must be reckoned with when attempting to achieve this level of insulation. Electrostatic screening is also required because high impedance instrumentation is very susceptible to electrical interference resulting from electromagnetic radiation and 'body capacitance' effects. It is interesting to note that these effects were not encountered in the work described in Chapter 7, presumably because the very thin ion sensitive films employed had a relatively low resistance. In the case of the ISFET measurements, a degree of screening is also provided by the test solution which completely surrounds the device and is connected to earth through a reference electrode of fairly low impedance (see Figure 7.2.1 for example). This arrangement is analogous to conventional combined pH/reference electrodes in which the reference electrode filling solution is contained in an annular space surrounding the internal filling solution of the pH electrode

itself.

The difficulty of eliminating leakage effects from the electrode structure itself has already been noted in Chapter 6. A measurement technique for distinguishing leakage effects from the 'true' electrode response is discussed in Section 8.5 below.

An important aspect of work on solid connected electrodes is the measurement of the stability of the standard potential, E_o, over an extended period of time. This data is required both as a performance specification for practical purposes and also as an indication of the reversibility or otherwise of the process taking place at the solid phase contact. It is necessary for this purpose to distinguish the long term stability of the electrode itself from other factors such as reference electrode drift, temperature induced effects, etc. The demands which this makes on the measurement system are more severe than those which arise in conventional laboratory electrode measurements in which the electrode is frequently calibrated against standard buffer solutions and drift effects are cancelled by adjustment of an offset control on the pH meter.

8.2 SOURCES OF UNCERTAINTY

Possible sources of uncertainty in the measurement of pH sensitivity and electrode stability were identified as follows:

- resolution of voltage measurement.
- errors due to leakage conductances and the finite input impedance of the electrometer.
- emfs induced in cables both electrically, by capacitative or inductive coupling, and mechanically, by microphonic effects.

- temperature effects on the test electrode or on reference electrodes.
- drift of the pH value of buffer solutions as a result of temperature changes, contamination or dilution.
- instability of reference electrodes and associated liquid junctions.
- electrokinetic effects and the influence of stirring on electrode potentials.

In the case of measurements of electrode *resistance*, temperature effects are even more significant as a consequence of the exponential dependence of glass resistivity on temperature (Section 2.3). Polarisation effects[28], in both the glass and reference electrodes, have also to be reckoned with in measurement situations which involve significant current flow.

8.3 INSTRUMENT ACCURACIES

An electrometer voltmeter (Model 610C, Keithley Instruments Inc) was used for all measurements of electrode potential. The rated input resistance of this instrument is greater than 10^{14} Ω and its effect on measurements of glass disc electrodes having resistances of the order of 2×10^{9} Ω was considered negligible. The manufacturers claim an accuracy for this instrument of ±1% of full scale, exclusive of noise and drift[110]. (The results of calibration checks carried out by the author are presented below). For measurements of cell potentials up to 100 mV, the electrometer voltage resolution corresponds to ±0.02 pH (assuming approximately Nernstian response) which was considered sufficient for the present purpose. In practice

however, cell potentials in excess of 500 mV were encountered and direct measurement using the 1 volt scale of the electrometer introduced uncertainties of ±10 mV. Direct measurement was used in obtaining some early results presented in Section 9.1 but in later stages of the work a dc signal generator (Type 123, G & E Bradley Ltd) was used to partially 'back off' the cell potential as shown in Figure 8.3.1. For stability and response time measurements a chart recorder (Model PR2, Farnell Instruments Ltd) was driven from the chart recorder output of the electrometer.

The electrometer, dc voltage source and chart recorder were calibrated as follows at intervals of about six months throughout the experimental work. A 5½ digit digital voltmeter (Model 8300A, John Fluke Manufacturing Co Ltd) was used as the voltage standard for this work. This instrument is maintained as a departmental voltage reference and is calibrated at approximately yearly intervals against a source traceable to the National Physical Laboratory. The Bradley dc source was set up to a suitable nominal voltage which was measured using the Fluke dvm. The electrometer was then zeroed and substituted for the dvm. The electrometer meter reading was noted and the voltage at its chart recorder output was measured, using a digital multimeter (Model 160, Keithley Instruments Inc). The latter instrument had previously been calibrated against the Fluke dvm and shown to be accurate to three significant figures. Finally, the Bradley output voltage was again measured using the dvm to verify that no significant drift had taken place. The calibration was carried out using each electrometer range between 30 mV and 10 V full scale, several voltages being used in each case to cover the range 0.1 x full scale to 1.0 x full scale. It was found that the chart recorder output of the electrometer was in all cases accurate to

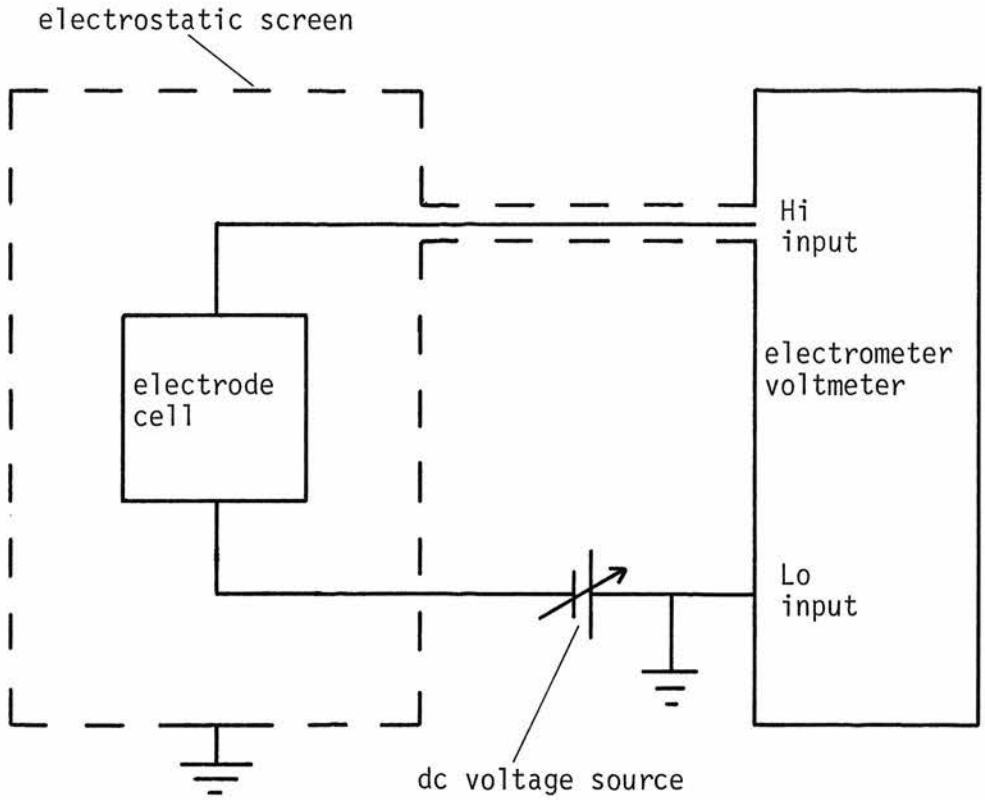

Figure 8.3.1 Circuit for the measurement of cell potentials

±1% of full scale. In one or two cases, the meter reading was not quite as accurate but was always within ±2% of full scale.

The accuracy of the Bradley dc source was also checked against the Fluke dvm. A number of output voltages in the range zero to 500 mV were used, employing both x1 and x10 control settings and positive and negative outputs. Zero error was found to vary between ±4 mV over a period of several days. When zero error was allowed for however, accuracies of within ±1 mV were consistently obtained. Using the x1 range, the error appeared to be a fairly constant scale error of about 0.2% of reading. On the x10 ranges however the readings were more scattered but always within ±0.25 mV of the nominal value.

Electrode response measurements were made using the circuit of Figure 8.3.1, the Bradley dc source being set to voltages of 0, ±100 mV, ±200 mV, ±300 mV, ±400 mV (using x10 range) as necessary to allow the electrometer always to be used on a 100 mV range. In this way, a measurement accuracy of ±2 mV was expected, provided the instruments were zeroed and readings corrected as necessary.

The accuracy of the Farnell chart recorder was estimated by setting up a voltage using a stabilised power supply and a ten turn potentiometer and comparing the chart recorder deflection with the voltage value measured using a $3\frac{1}{2}$ digit multimeter which was known to be accurate to three significant figures. Both channels of the recorder were checked using the two input modules available. The main sources of error were mechanical backlash and variation in gain between different ranges. An overall accuracy of ±2% of full scale was obtainable, improving to ±1% if zero and gain adjustments were

made whenever the range was changed.

The zero drifts of the instruments were also checked because of their influence on long term measurements of electrode potential. The typical observed overnight zero drift of the electrometer was ±1.5 mV which is consistent with the manufacturer's specification[110] of 1 mV per 24 hours and 150 μV/deg C. In the case of the Bradley dc source the typical overnight drift was ±1.0 mV, although variations of up to ±4 mV were observed over a period of several days. The overnight zero stability of the Farnell chart recorder was surprisingly good, being well within ±1% of full scale. It was concluded that an instrument drift of ±4 mV could be expected when making overnight measurements of electrode potential using the circuit of Figure 8.3.1 and the chart recorder.

8.4 ELECTRICAL INTERFERENCE

An electrostatically screened enclosure, approximately 25 cm x 25 cm x 25 cm was constructed from light aluminium sheet. The electrode under test, together with associated buffer solution etc, was supported by a retort stand and clamps, the entire assembly being placed inside the screened box (Figure 8.4.1). Connection between the screened enclosure and external instruments was by short (approximately 50 cm) lengths of cable. PTFE insulated screened cable and connectors were used for connections at high impedance levels,equipment wire and 4 mm plugs and sockets elsewhere. No significant electrostatic pick-up effects were observed with this arrangement. A significant microphonic emf was caused by touching the screened electrometer input cable, but the time constant was only

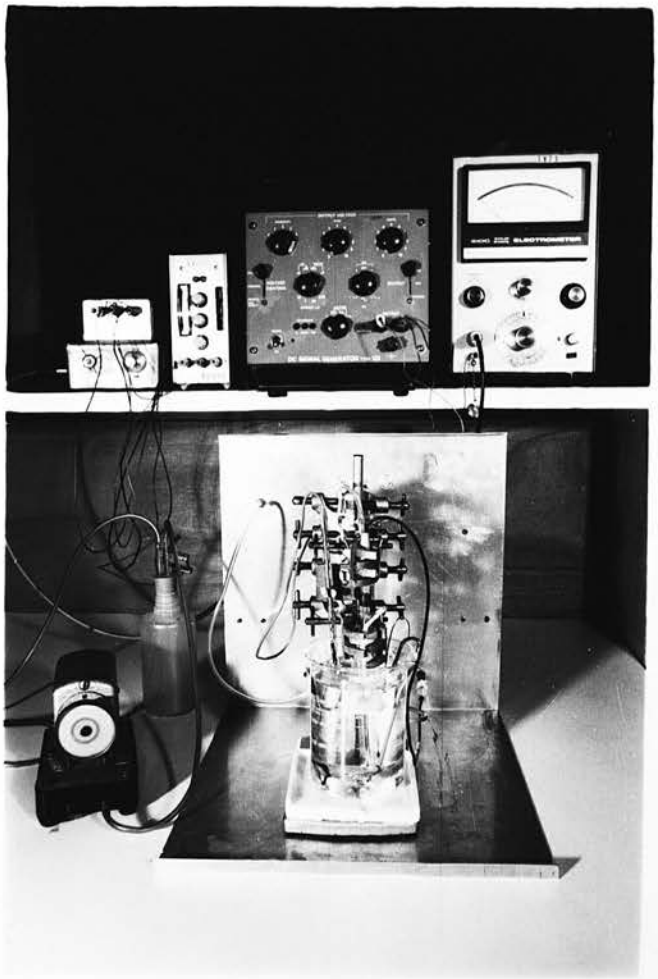

Figure 8.4.1 Apparatus for pH sensitivity measurements on glass disc electrodes

The electrode assembly is shown in position inside the electrostatic screen. (Prior to making measurements, the screened enclosure was completed by means of a lid which has been removed in the photograph). The electrometer and dc voltage source which were used for the measurement of electrode potentials are seen at the top right of the photograph. The electrode is immersed in a beaker containing oil at a controlled temperature, as described in Section 8.6. The temperature control unit is at the top left of the photograph and the pump for the associated bubble stirrer is to the left of the screened box.

about one second and the effect was not troublesome. Occasional difficulties were also experienced as a result of vibrations set up by extractor fans, mechanical X-Y recorder etc. These were easily eliminated however and normal vibration due to movement of personnel caused no significant effect. An oscilloscope connected to the chart recorder output of the electrometer was used to confirm the absence of pick-up at higher frequencies (eg 50 Hz) since this could result in a dc offset due to rectification in the measuring circuit.

8.5 ELECTRICAL LEAKAGE EFFECTS

The problem of minimising electrical leakage effects in the electrode structure was discussed in Section 6.2. For measurement purposes, the situation may be modelled by the equivalent circuit of Figure 8.5.1. The potential of the glass electrode cell is represented by a pH dependent potential, E_g, in series with a constant potential, E_{og}, due to reference electrode and glass asymmetry potentials. The internal resistance of the cell,which is mainly due to the glass membrane resistance, is represented by R_g. An electrical leakage path is modelled generally by a resistance, R_ℓ, a constant potential, $E_{o\ell}$, and a pH dependent potential, E_ℓ. The cell potential actually measured at the terminals AA' is V_m while the measured resistance of the cell is referred to as R_m. The potential, $E_\ell + E_{o\ell}$, which arises from electrochemical emfs in the leakage path, may well be ill-defined and unstable. Using simple circuit theory, it can be shown that

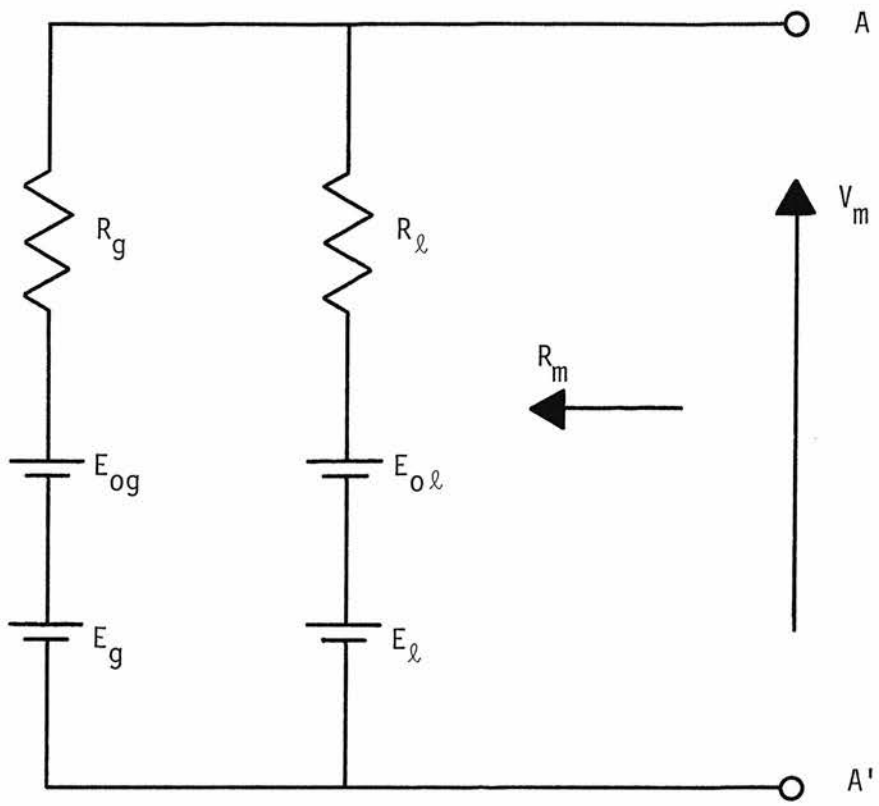

Figure 8.5.1 Equivalent circuit showing the effect of an electrical leakage path on the measurement of the glass electrode cell potential.

$$V_m = E_{o\ell} + E_\ell + \frac{R_\ell}{R_\ell + R_g}(E_g + E_{og} - E_\ell - E_{o\ell}) \qquad (8.5.1)$$

and $$R_m = \frac{R_g \; R_\ell}{R_g + R_\ell} \qquad (8.5.2)$$

By differentiation of Equation 8.5.1 with respect to pH (remembering that E_{og} and $E_{o\ell}$ are independent of pH) and substitution of Equation 8.5.2, it can be shown that

$$\frac{dE_g}{d(pH)} = \frac{R_g}{R_m}\frac{dV_m}{d(pH)} + \left(\frac{R_m - R_g}{R_m}\right)\frac{dE_\ell}{d(pH)} \qquad (8.5.3)$$

Equation 8.5.3 expresses the 'true' pH sensitivity of the glass, $\frac{dE_g}{d(pH)}$, in terms of the measured pH sensitivity, $\frac{dV_m}{d(pH)}$, of the cell and the measured cell resistance, R_m.

It was noticed at an early stage in the experimental work (Section 9.1) that the measured pH sensitivities of many of the disc electrodes declined over a period of, typically, a few weeks exposure to the test solutions. The measured cell resistances also decreased over the same period. An increasing leakage conductance is the obvious explanation for such observations but it can be seen from Equation 8.5.3 that the calculation of the 'true' glass sensitivity from the measured data requires additional information about the pH sensitivity of the leakage path. Furthermore, it is difficult to make accurate resistance measurements on glass membranes because of the marked temperature dependence of the glass resistivity and the problems of interpretation resulting from dielectric polarisation effects[28]. The observed decrease in pH sensitivity was of the order

of 20% over several weeks. If this was entirely due to leakage effects, a similar decrease in the cell resistance would be expected (neglecting the effect of $\frac{dE_\ell}{d(pH)}$). It is doubtful however that the reproducibility of the resistance measurements over a prolonged period was adequate to detect a change of this order. As a consequence of the uncertainties in the measured values of R_m and in the estimation of $\frac{dE_\ell}{d(pH)}$, it was difficult to distinguish between the effect of an increasing leakage conductance and a decline in the 'true' electrode sensitivity. Further insight into the role of leakage in the deterioration of electrode response was sought using the following technique which allows a more direct measurement of leakage conductances.

Consider the glass disc membrane electrode of Figure 8.5.2, in which an annular metal contact is deposited around the periphery of one face of the disc. The pH sensitivity of this device may be measured using the reference electrodes designated A and B in the figure. If an electrical leakage path exists at the interface between the disc and the electrode body, then it must cross the annular contact (designated C in Figure 8.5.2) in order to make connection between the solutions at each side of the membrane. The degree of leakage may be assessed by measuring the resistances, R_{AC} and R_{BC}, between the annular contact and each of the reference electrodes. The technique may also be used with metal connected electrodes as shown in Figure 6.6.3.

In the case of a well made device, in which leakage effects are small, the values of R_{AC} and R_{BC} would be expected to be much greater than R_{AB}, the resistance measured between the opposite sides of the membrane. In practice however, the maximum value of leakage

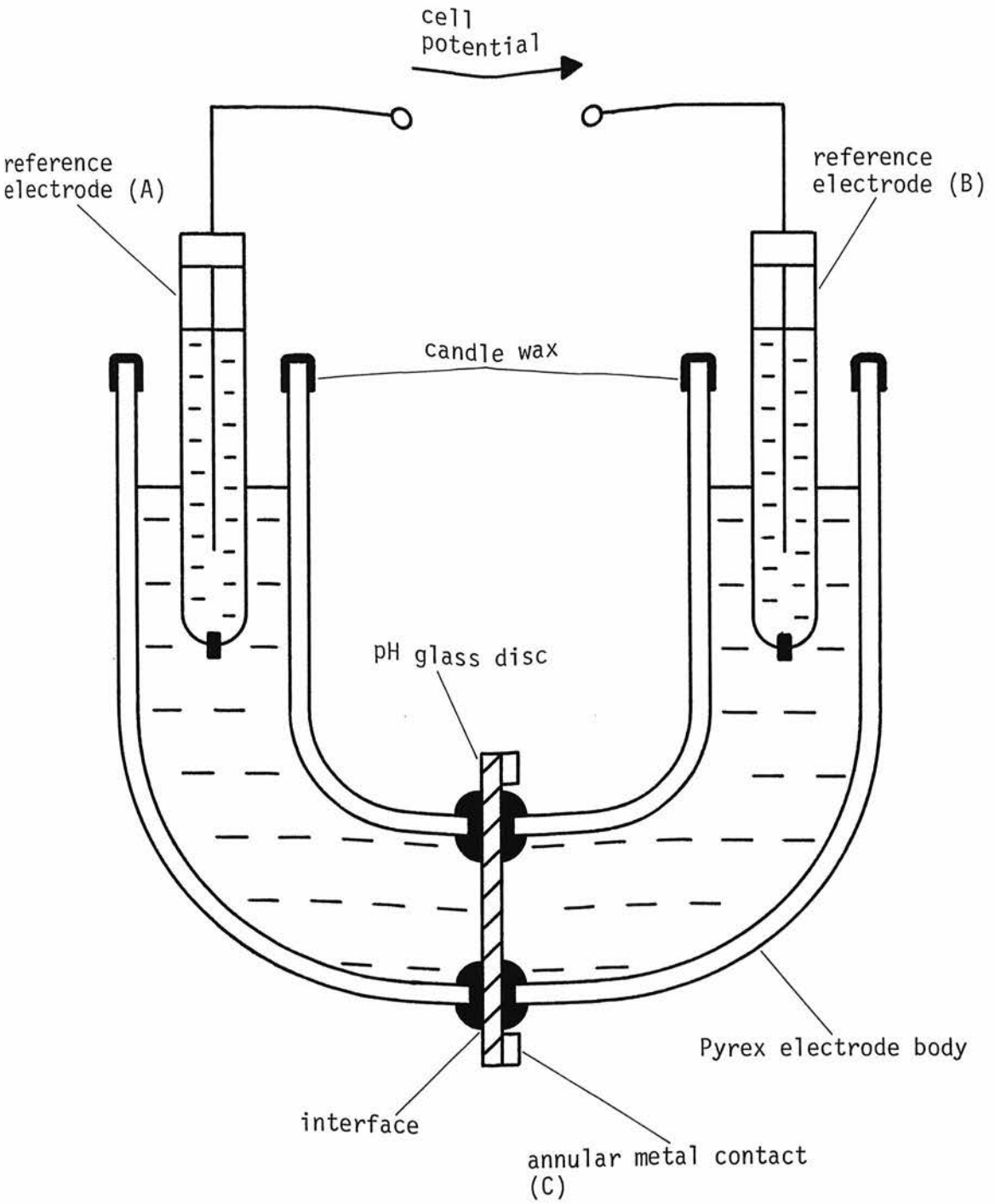

Figure 8.5.2 Method for estimation of electrical leakage effects in glass disc electrode cells.

The leakage effects are assumed to be associated with the interfaces between the pH sensitive disc and the electrode body.

resistance which can be detected is limited by transverse conduction through the glass disc and depends on the geometry of the arrangement (Figure 8.5.3).

The resistance, R_o, between the contact areas A and B on opposite faces of a thin glass disc is given by

$$R_o = \frac{\rho d}{\pi r_o^2} \tag{8.5.4}$$

where ρ is the resistivity of the glass and r_o and d are dimensions defined in Figure 8.5.3. The resistance between the annular contact area, C†, and the areas A or B is determined by the resistivity of the glass and the distribution of current over the cross section of the disc. A precise calculation would be tedious but we note that the minimum value of this transverse resistance, R_t, is determined by the cross section PQRS in Figure 8.5.3. This minimum value may be calculated by considering an annular element, Δr wide, at radius r from the centre of the disc. The resistance, ΔR_t, of this element is given by

$$\Delta R_t = \frac{\rho \, \Delta r}{2\pi r d} \tag{8.5.5}$$

By integration of Equation 8.5.5 from $r = r_o$ to $r = r_o + t$, we obtain

$$R_t = \frac{\rho}{2\pi d} \ln \frac{r_o + t}{r_o} \tag{8.5.6}$$

---

† Contact C is shown on both sides of the disc in Figure 8.5.3 for the sake of symmetry. In practice the annulus was deposited on one face of the disc but surface leakage across the glass surface was sufficient to make an effective contact with the opposite face.

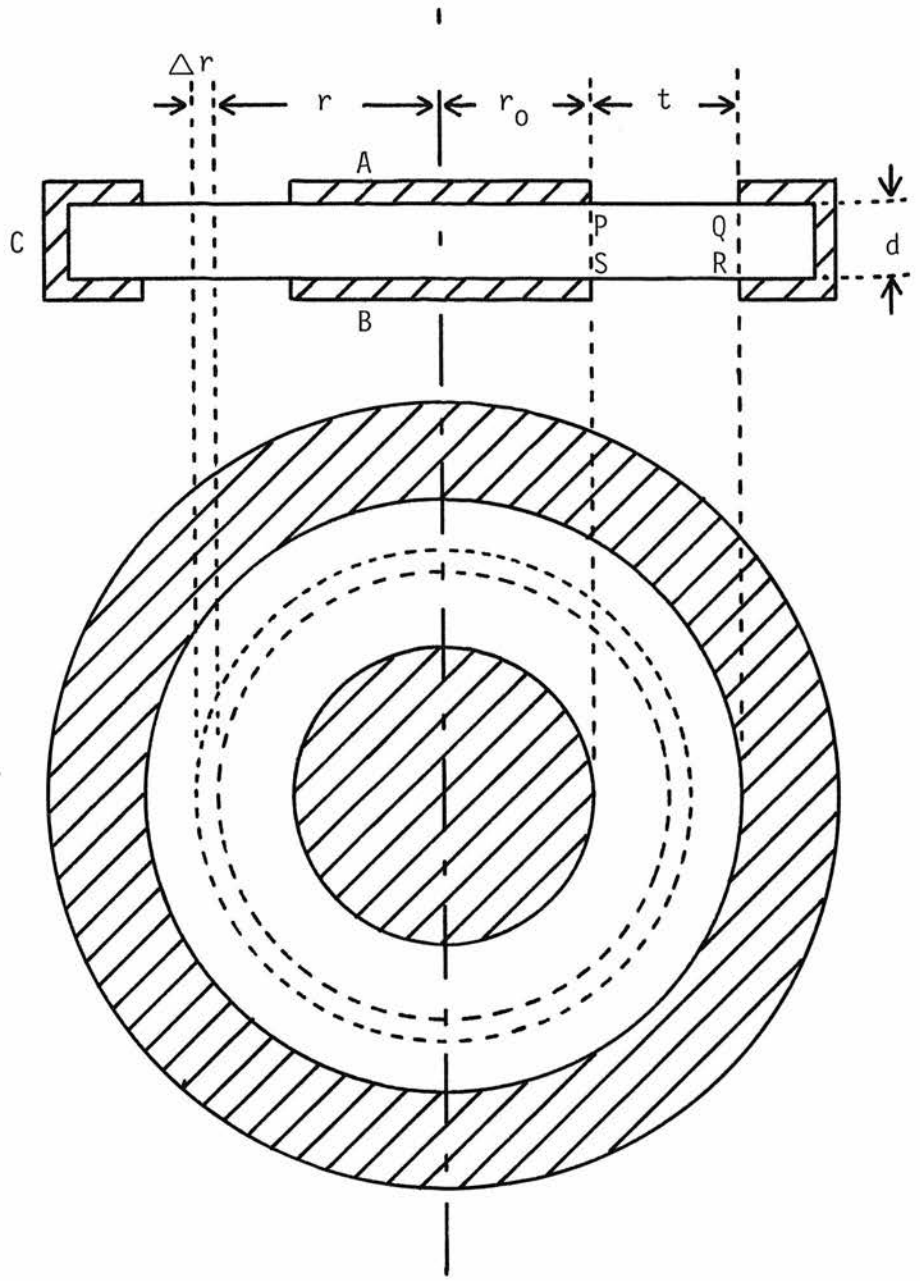

Figure 8.5.3 Cross-section (upper) and plan (lower) of a pH sensitive disc incorporating a metal annular contact (C) for the estimation of electrical leakage effects.

Areas A and B denote the metal or aqueous centre contacts to each face of the disc.

Combining Equations 8.5.4 and 8.5.6, the ratio of the transverse resistance, R_t, and the membrane resistance, R_o, is given by

$$\frac{R_t}{R_o} = \frac{r_o^2}{2d^2} \ln \left(\frac{r_o + t}{r_o}\right) \qquad (8.5.7)$$

It is a function only of the geometry of the device and is independent of the resisitivity of the glass and therefore of temperature.

Any leakage resistances associated with the seal between the glass disc and the electrode body will appear in parallel with R_t and it is therefore necessary for the ratio $\frac{R_t}{R_o}$ to be large in order to detect large values of leakage resistance. It can be shown that the maximum value of $\frac{R_t}{R_o}$ (for a given size of annulus) occurs when the radius of the central contact, r_o, is approximately 0.6 times the inside radius, $r_o + t$, of the annulus. The value of $\frac{R_t}{R_o}$ is not very sensitive to the dimensions however and other practical factors may be considered in choosing them.

The equivalent circuit of Figure 8.5.4 represents an electrode in which there are leakage paths between the annular contact, C, and the contacts, A and B, to each side of the glass disc. Sources of emf have been omitted from the diagram since they have no bearing on the following reasoning which is concerned only with resistance measurements. The resistances R_{AB}, R_{AC} and R_{BC} which are accessible to measurement comprise a series/parallel combination of the membrane resistance, R_o, the transverse glass resistance, R_t, and the leakage resistances $R_{\ell 1}$ and $R_{\ell 2}$. For an ideal electrode which has no leakages, $R_{\ell 1}$ and $R_{\ell 2}$ are infinitely large. The measured value of R_{AB} is then equal to the membrane resistance, R_o, and the measured

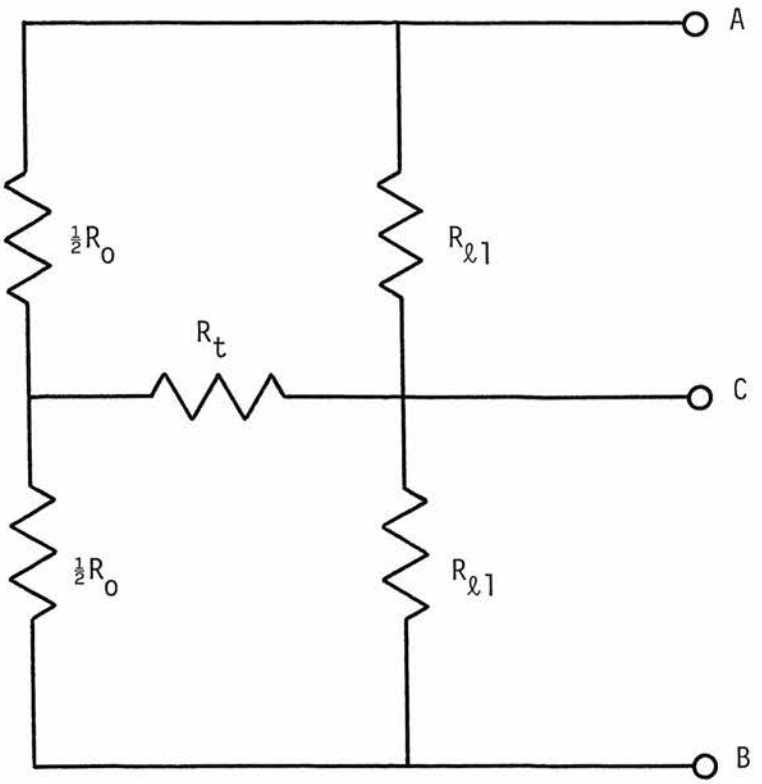

Figure 8.5.4 Lumped component equivalent circuit for the disc electrode of Figure 8.5.2.

R_o and R_t denote respectively the membrane resistance and the transverse resistance of the glass disc. $R_{\ell 1}$ and $R_{\ell 2}$ represent leakage paths.

values of R_{AC} and R_{BC} are approximately equal to the transverse resistance, R_t, (assuming $R_t >> R_o$). In this case, the ratios $\frac{R_{AC}}{R_{AB}}$ and $\frac{R_{BC}}{R_{AB}}$ approach the limiting value of $\frac{R_t}{R_o}$ given by Equation 8.5.7. If, on the other hand, the values of $R_{\ell 1}$ and $R_{\ell 2}$ are comparable with R_t then the measured values of R_{AC} and R_{AB} are less than R_t and the ratios $\frac{R_{AC}}{R_{AB}}$ and $\frac{R_{BC}}{R_{AB}}$ are less than $\frac{R_t}{R_o}$. Consider now the case where only one of the leakage resistances ($R_{\ell 1}$ say) is significant and the other ($R_{\ell 2}$) is large. The value of R_{AC} is then influenced by $R_{\ell 1}$ and the ratio $\frac{R_{AC}}{R_{AB}}$ is again reduced. In this case however, the measured value of R_{BC} is *not* related to the leakage resistance $R_{\ell 2}$ because the latter, high, resistance appears in parallel with a relatively low resistance due to the series combination of R_o and $R_{\ell 1}$. The ratio $\frac{R_{BC}}{R_{AB}}$ is therefore also reduced. It is thus possible, by comparing the ratios $\frac{R_{AC}}{R_{AB}}$ and $\frac{R_{BC}}{R_{AB}}$ with the calculated ratio $\frac{R_t}{R_o}$, to identify positively the case where both $R_{\ell 1}$ and $R_{\ell 2}$ are large. It is not possible however to identify the case where only one of $R_{\ell 1}$ or $R_{\ell 2}$ is large. For the purposes of measuring pH sensitivity however, the leakage resistance of interest is that between A and B, with node C not connected, ie $R_{\ell 1} + R_{\ell 2}$. An electrode which appears to have a serious leakage could therefore still function satisfactorily from the point of view of pH response.

The fabrication of both membrane and metal connected electrodes incorporating annular contacts was described in Section 6.6. The ratio, $\frac{R_t}{R_o}$, for these devices is a function of dimensions which are defined largely by the area of glass which is covered by a manually applied coating of silicone rubber adhesive. It was difficult to measure $\frac{R_t}{R_o}$ precisely because of the irregular shape of the adhesive coating, but its value was estimated as between 50 and 100. Resistance

measurements on the devices were made using current-voltage plots as described in Section 8.9 and the results are discussed in Chapter 9.

The annular contact technique was devised specifically to detect leakages originating in the seal between the glass disc and the electrode body. Leakages can also occur at any other part of the measurement system which is connected to the 'high' input terminal of the electrometer, if insulation is inadequate. Examples are surface conductances across the open ends of the Pyrex tubes attached to the glass disc or via the structures used to support the pH electrode or the associated reference electrodes. These effects were estimated by preliminary measurements as follows.

Leakage across Pyrex surfaces was investigated using the arrangement of Figure 8.5.5 in which a small Pyrex beaker containing water was placed inside a larger Pyrex basin, also containing water. Connection to the water was made by platinum wires suspended from ptfe insulators. A current-voltage plot was made by varying the power supply voltage and using the electrometer as an ammeter to measure the leakage current into the inner beaker. When used in the ammeter mode, the electrometer indicates the voltage across its terminals with a standard resistor connected internally[110]. The voltage between the platinum electrodes in Figure 8.5.5 is thus the algebraic sum of the power supply voltage, V_b, and the electrometer voltage, V_k. A fairly linear current-voltage plot was obtained and corresponded to a resistance of 5×10^9 Ω. The experiment was repeated after melting a little candle wax round the rim of the inner beaker. An increased resistance of 10^{11} Ω was then recorded. The beakers were then removed and the measurement was repeated with the

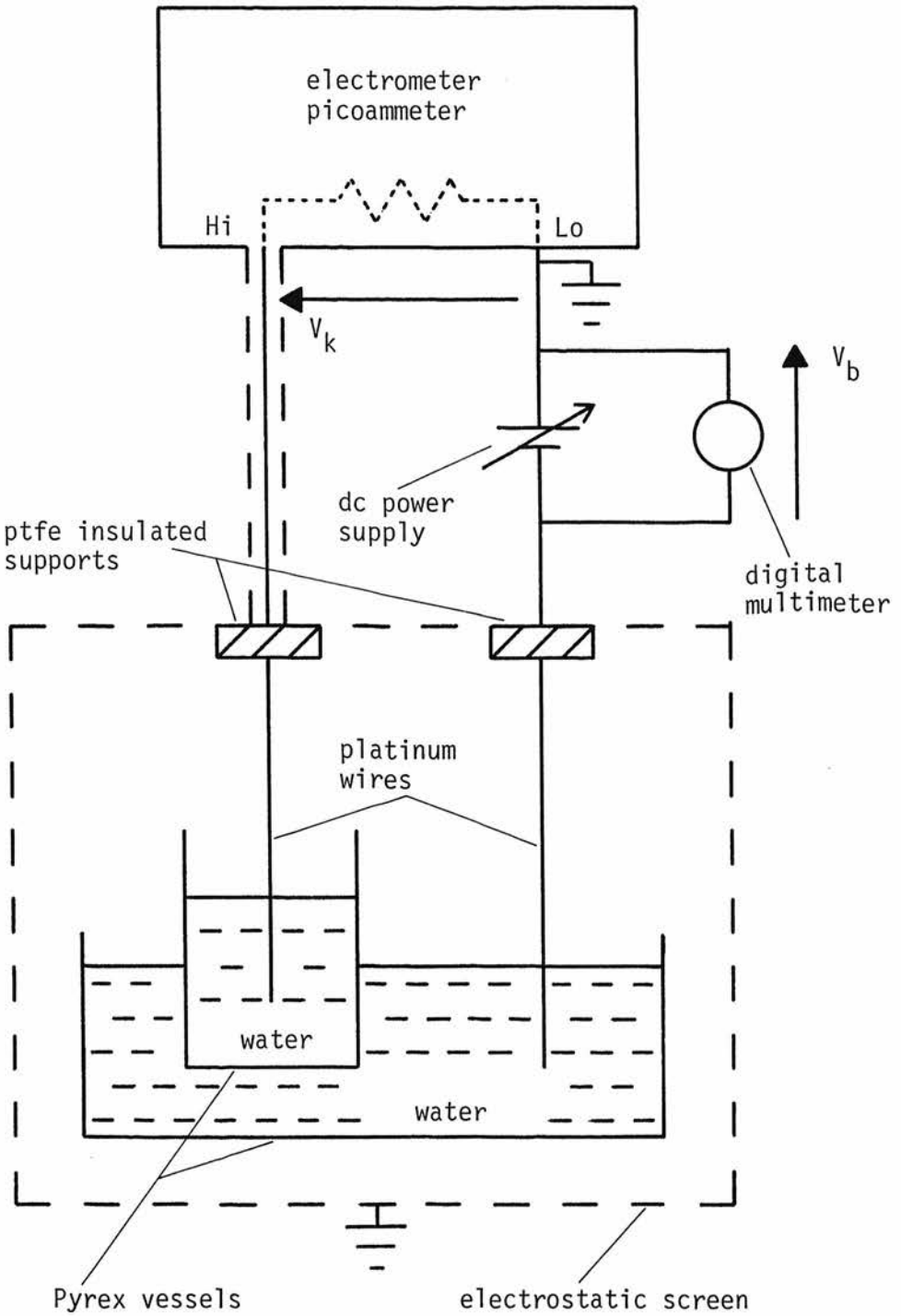

Figure 8.5.5 Estimation of leakage conductance across Pyrex surfaces.

platinum wires suspended as before. A background resistance of the order of 10^{13} Ω was recorded but the readings were subject to considerable drift. It was concluded that the application of candle wax to a Pyrex surface reduced surface conductance sufficiently to make measurements on membranes having a resistance of around 10^{9}Ω.

Another possible source of leakage is associated with the reference electrode used to make contact with the 'high' side of the glass membrane. For the measurements on membrane electrodes, the reference was a conventional calomel electrode supported by a retort stand which was in contact with the earthed screened enclosure. The arrangement was rather more simple in the case of metal connected electrodes since all that was required was a short length of light wire connecting the metal contact to the insulated centre conductor of a bnc connector in the side of the screened box. This wire did not need to contact any other part of the apparatus. Leakages introduced in this way were examined as follows. Four high-value resistors (Keithley Instruments Inc) of 10^{8} Ω, 10^{9} Ω, 10^{10} Ω and 10^{11} Ω were mounted in a small metal case using ptfe insulators. This resistor box was placed inside the screened enclosure and connections were made to it using short lengths of light wire also supported by ptfe insulators. Current-voltage measurements were made using the circuit of Figure 8.5.6 and the resistor values were confirmed to within $\pm$5%, which could be explained by instrument errors and the resistor tolerances. The insulation resistance of a typical electrode measurement was then modelled by means of a calomel reference electrode, supported by a retort stand, which was connected to the 'high' side of the standard resistor. The effect was not very reproducible but certainly introduced significant errors when

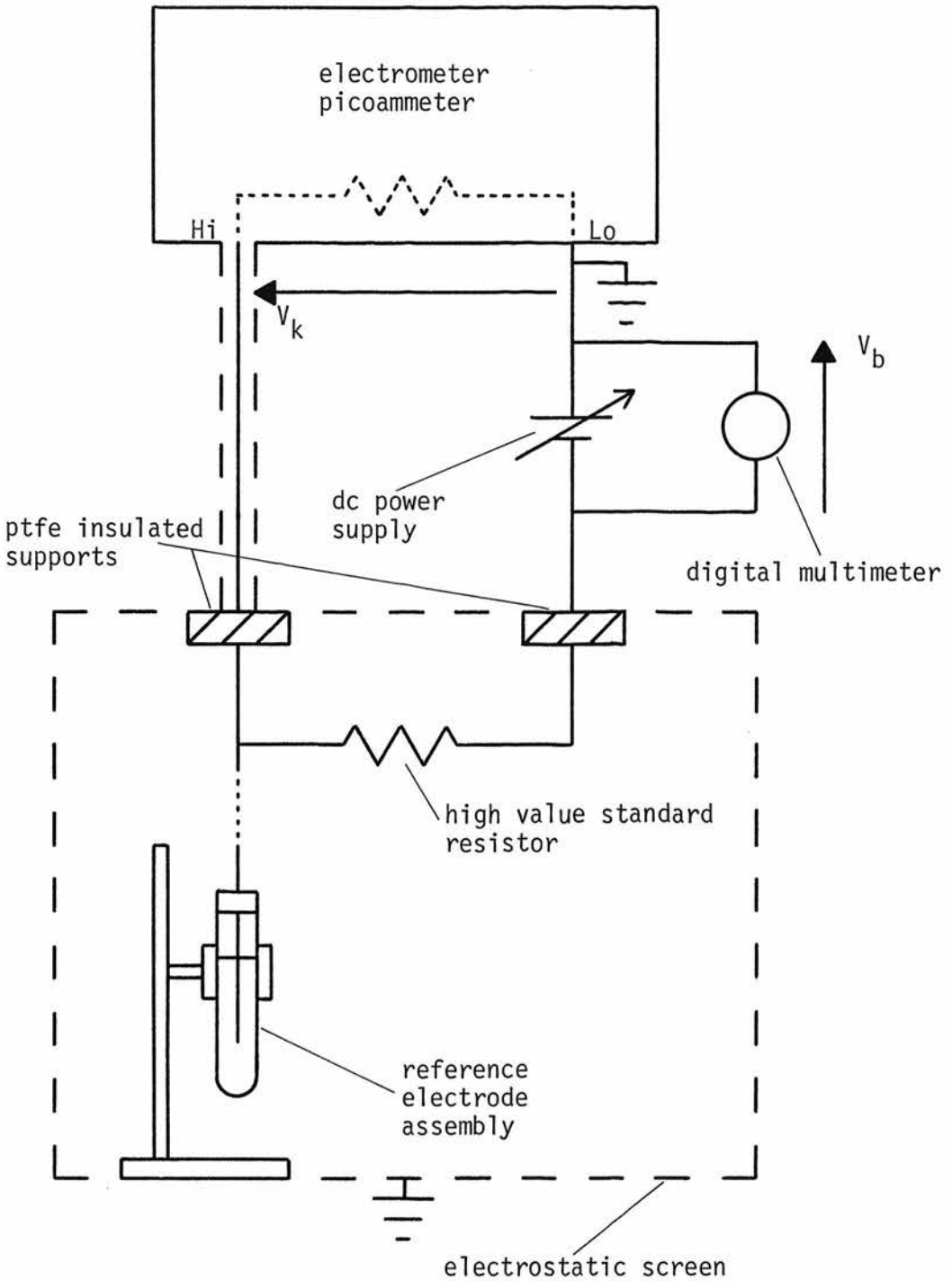

Figure 8.5.6 Estimation of electrical leakage effects associated with the experimental arrangement.

Comparative measurements of the value of the standard resistor were carried out with and without the connection (shown dotted) to the reference electrode.

measuring 10^{11} Ω. It was quite insignificant when measuring 10^{9} Ω however.

8.6 TEMPERATURE CONTROL

Temperature variations can affect electrode measurements in several ways. The effect on the 'Nernst slope' is given by the RT/F term in the Nernst equation and usually amounts to a variation of only a few per cent for ambient temperature changes in a typical laboratory environment (Section 2.2). The E_o values of reference electrodes are also temperature dependent however and the total cell potential can be significantly temperature sensitive when inner and outer reference electrodes are of different kinds[111]. Particular care is needed with metal connected electrodes in which the metal contact constitutes one of the references and its mechanism and temperature sensitivity are not known. It must also be remembered that 'hysteresis' effects encountered with calomel reference electrodes can result in temperature-induced time-dependent drifts in potential (Section 8.8). Measurements of membrane resistance are also highly temperature sensitive, the resistivity of typical glasses being known to double for a 7 deg C decrease in temperature[28].

Some preliminary work was carried out in ambient conditions (Section 9.1) but the room temperature was found to be subject to very wide variations in the particular laboratory which was used. Even measurements made during the day were subject to considerable uncertainty as a result, and overnight measurements of stability were meaningless. The ideal solution would have been to temperature-control the air inside the screened enclosure. This approach was

rejected on grounds of cost and complexity however and a simple thermostatic oil bath was used instead.

In order to obtain good thermal contact between the glass disc and the temperature controlled oil it was decided to immerse the electrode structures of Figures 6.6.3 and 6.6.5 directly in the oil. The metal connections to the devices were therefore in contact with the oil which was required to have a resistivity commensurate with the rest of the experimental arrangement. The relative resistivities of several oils were estimated as follows.

Conductive films, 10 mm square, were printed on to alumina substrates, 50 mm by 13 mm, using a thick film circuit process. A small piece of ptfe was used to space a pair of substrates a few millimetres apart with the conductor areas facing one another. The resistance between them was measured by plotting a current-voltage curve as described in the previous section. A resistance of the order of 10^{13} Ω was observed when the device was suspended in air but this reduced to about 10^{12} Ω when it was placed in a proprietary heating bath oil (BDH Ltd). Immersion in silicone fluid (Type F4, Edwards High Vacuum) reduced the resistance to as little as 10^{9} Ω. When the device was placed in Liquid Paraffin BP (Boots Ltd) however a resistance of the order of 10^{14} Ω was observed and it was concluded that the latter medium would support leakage conductances no greater (and possibly slightly smaller) than the ambient atmosphere.

The oil bath and its associated heating element were to be placed inside the electrostatic screen and it was necessary to ensure that no electrical interference was created by the heater. A proportional band controller, using dc heater current, was therefore

preferred to the simple 'on-off' type of thermostat which might introduce switching transients. An oil bath capacity of 500 mℓ was required and a temperature of 30°C was chosen as standard for the work, this being a little higher than maximum summer temperatures in the room in question. The capability to vary the temperature over a small range was also required for temperature coefficient measurements. No commercial system fulfilling these requirements was readily available so a controller circuit was designed and built. Two 100 Ω, 10 W wire wound resistors connected in parallel served as a heater (directly immersed in the liquid paraffin) and a thermistor temperature sensor was used. Power was derived from standard laboratory power supplies. Set point temperature was adjustable between 25°C and 39°C and a variable gain control was included. Details of the controller circuit are given in Appendix 7.

It was necessary to stir the oil to eliminate temperature gradients within the bath. The mechanical paddle wheel type of stirrer was avoided for the present purpose because of the inconvenience of introducing the drive shaft into the electrostatically screened enclosure. A magnetic stirrer (A Gallenkamp and Co Ltd) was found to be very efficient, reducing temperature variations across the bath to less than 0.1 deg C. Unfortunately it was found that this stirrer introduced a significant amount of interference at the electrometer output when it was placed beneath the screened box. The interference comprised ac signals of several millivolts at both 50 Hz and at the rotation frequency of the stirrer. It appeared to be caused by mechanical vibration as well as by inductive coupling to the measurement circuit (which was completed by a short length of wire short-circuiting the electrometer input

inside the screened enclosure). The stirring method which was finally adopted employed a simple air bubbler. A small pump was used to blow a slow stream of bubbles down a Perspex tube with its mouth close to the heating element which was placed at the bottom of a 500 mℓ beaker containing liquid paraffin. The minimum inside diameter of the tube for effective stirring was about 7 mm and the optimum bubbling rate was about 3 per second. (Slower rates caused inefficient mixing while higher rates caused severe vibration and microphonic effects). The temperature profile across the oil bath, both horizontally and vertically, was measured and a maximum deviation of $\pm$0.3 deg C from nominal was noted. This occurred only in the corners of the bath however, a constancy of $\pm$0.1 deg C being achieved over most of its volume.

The overall performance of the temperature control system was investigated as follows. The thermistor temperature sensor was placed near the centre of the bath and the gain of the controller was adjusted by trial and error to give a reasonable compromise between response time and overshoot of the oil temperature. The temperature was then increased in steps, the oil temperature being measured using a mercury thermometer with a resolution of 0.5 deg C. A calibration curve of the controller dial setting against oil temperature was plotted over the range 24^{o}C to 39^{o}C and was found to be nearly linear. The overnight stability of the oil temperature was also monitored, the oil temperature being measured by means of a platinum resistance thermometer (Sangamo Weston Ltd) in conjunction with a chart recorder (Model PR2, Farnell Instruments Ltd) which incorporated a temperature input module. (This system was found to be in agreement with the mercury thermometer to within $\pm$0.5 deg C

over the range 24.5 to 28.5°C). The oil bath temperature was found to remain between 38.5°C and 39°C throughout an overnight period during which the room temperature varied between approximately 15°C and 24°C. It was concluded that the oil temperature could be expected to remain constant to within 0.5 deg C at temperatures as much as 25 deg C above ambient.

A photograph of the complete apparatus for electrode sensitivity measurement appears in Figure 8.4.1 and close-ups of the thermostat arrangement in Figure 8.6.1.

8.7 TEST SOLUTIONS

Many of the pH sensitivity measurements reported in the following chapter were carried out using the four test solutions of Table 8.7.1. These solutions are part of a range of buffers proposed by Filomena et al[109] for the testing of pH electrodes. They are free of alkali metal ions and were used to eliminate the possibility of non-linearities in the pH response resulting from the alkali metal sensitivity of 015 glass. (Other solutions from this range were used for testing the silicon dioxide devices described in Section 7.3). The solutions are described primarily in terms of the voltage difference to be expected when an 'ideal' pH electrode is transferred between them, using a silver-silver chloride reference electrode in a cell without liquid junction. The nominal pH of each buffer was also given in the original paper[109] however and these values were employed in the present work, using a calomel reference electrode with liquid junction. A disadvantage of these solutions is that their pH values tend to drift, probably as a result of carbon dioxide absorption. The problem was particularly serious in the present experimental arrangement in which the measurement of E_o stability required the test solution to remain in the electrode

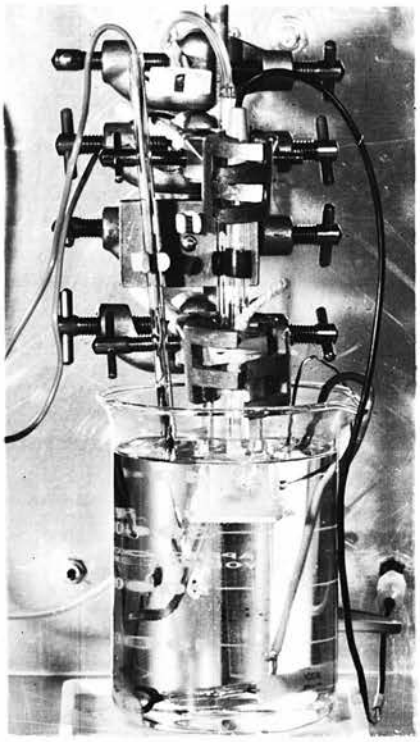

(a)

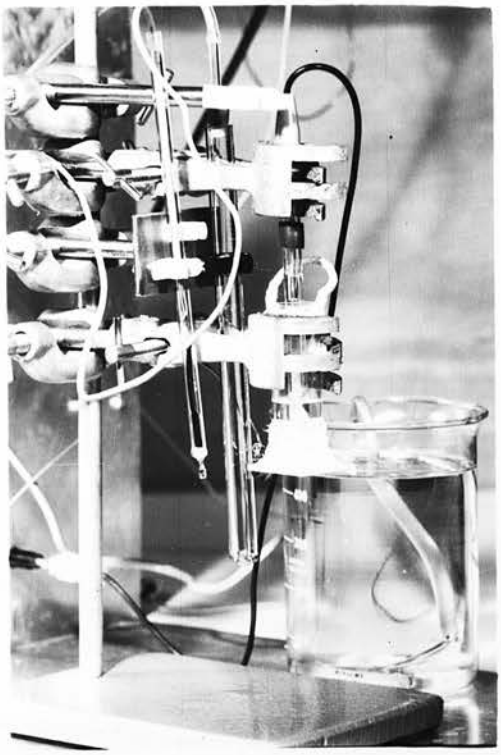

(b)

Figure 8.6.1 Thermostatic oil bath arrangement, (a) assembled, showing 100 Ω resistance heaters at the bottom of the beaker, (b) with beaker removed to show the thermistor probe (left), air bubbler tube (centre) and metal connected electrode (right), with calomel inner reference electrode.

solution	pH at 25°C
0.020 M Ethanolamine + 0.030 M Ethanolamine Hydrochloride	9.385*
0.020 M Bis-Tris + 0.020 M Bis-Tris Hydrochloride	6.540*
0.02 M Succinic Acid + 0.02 M tetramethylammonium hydrogen succinate	4.216†
0.1 M HCl	1.09†

Table 8.7.1 Alkali-metal-free test solutions

**after Filomena et al[109].*

†details kindly supplied by Dr A K Covington (personal communication)

for several days at 30°C and exposed to the atmosphere. Measurements to indicate the extent of the drift were made on the solutions of pH 6.540 and pH 9.385. A commercial glass electrode (Pye-Ingold) and calomel reference electrode were transferred between these solutions and the change in electrode potential was measured. The solutions were then allowed to stand in open vessels for three days and the measurement was repeated. The two results differed by 32 mV.

Alternative test solutions, having pH values of 4.0, 7.0 and 9.2, were made up using pH buffer tablets (BDH Ltd) which are commonly used for calibrating conventional pH electrodes. The buffer solutions were used in conjunction with a solution of 0.1 M hydrochloric acid (Table 8.7.1) to extend the measurement range. This range of solutions was used in the preliminary work described in Section 9.1 but was replaced by the solutions of Table 8.7.1 for much of the subsequent work, with the object of eliminating'alkaline errors'as a possible source of non-linearity in the pH response curves. As a consequence of the drift problems experienced with these solutions however, the solutions prepared from the BDH buffer tablets were readopted for the final stages of the experimental work, using metal connected fused disc electrodes (Section 9.3). The linearity of the resulting graphs of electrode potential against pH indicates that alkaline error is in fact negligible with 015 glass electrodes in the pH range 1 to 9. Stability measurements were greatly simplified by the constancy of the pH values of these buffers over periods of several weeks at 30°C.

The electrode system was thoroughly flushed when changing test solutions,to ensure the removal of any traces of the previous solution from the membrane.

It has been shown[112,113] that glass electrode measurements can be subject to errors resulting from the dissolution of the glass membrane itself. The products of the dissolution alter the composition of the boundary layer of solution adjacent to the membrane. The effect is significant in low-level measurements on unbuffered solutions and can be eliminated by vigorous agitation of the test solution†. Stirring was not employed in the present work however, since all test solutions were buffered and the effect of glass dissolution was not expected to be significant.

8.8 REFERENCE ELECTRODES

The buffer solutions of Table 8.7.1 were designed for accurate measurements using silver-silver choride electrodes in a cell without liquid junction[109]. Chlorided silver wires, prepared by the thermal technique[115], were obtained from Electronic Instruments Ltd but measurements on a number of them indicated large bias potential differences of several millivolts. The alternative, bi-electrolytic, type of electrode[115] could not be obtained commercially and early attempts at making them resulted in devices which exhibited considerable drift of potential. (These difficulties were later shown to be due to a faulty glass-metal seal where the silver wire entered the electrode body). It was also felt that the very thin plated layer of silver chloride in the bi-electrolytic type of electrode would be particularly liable to damage due to current flow, either accidental or in the course of resistance measurements.

---

† It has been noted however that the use of stirred or flowing solutions for this purpose can itself introduce errors due to effects such as flow induced pressure head variations at the reference electrode[114], transport of ions from the salt bridge to the measuring electrode[114] and streaming potentials[113].

The use of silver-silver chloride electrodes also restricts the choice of test solutions to those with defined chloride concentrations and introduces the possibility of errors due to changes in the (unbuffered) chloride ion activity of the solution, which might result from dilution or evaporation.

In order to avoid difficulties with the availability and use of silver-silver chloride electrodes, it was decided to employ commercially available calomel reference electrodes throughout the experimental work. It was recognised however that the accuracy of the buffer system of Table 8.7.1 was prejudiced by the liquid junction which is incorporated in these reference systems. Most of the commercially available electrodes had a body diameter of about 12 mm which was too large for use with the glass disc electrodes. A range of electrodes having 6 mm diameter bodies is available however (Simac Instrumentation Ltd). The model R110C/1 which was chosen is a refillable single junction calomel type with ceramic plug salt bridge and 3.8 M potassium chloride filling solution. These electrodes were used in much of the work described in the following chapter although some difficulties with bias potential drift were experienced at a late stage in the work. An alternative electrode (Type K401, Radiometer A/S) was used for the measurements on fused disc electrodes (Section 9.3).It is similar to the Simac model described previously but has a slightly wider (7.5 mm) body and uses saturated potassium chloride filling solution.

The performance of reference electrode systems has been extensively reviewed[21,24,116] but it remains difficult to determine the overall uncertainty introduced into a particular measurement situation by the reference electrode. Hills and Ives[117] have

identified several factors which can cause irreversibility and instability in calomel electrodes. Many of these effects are influenced by the procedures used to construct the electrode and are clearly outwith the direct control of the user of commercially available devices. (It appears however that electrodes obtained from different suppliers might differ significantly in performance). The reference systems used in the present work incorporated a liquid junction so that the reference electrode itself was in contact with a solution of invariant composition. Mattock and Band[118] have noted that the requirements of the reference electrode in this situation are less stringent than in the case of a cell without liquid junction because factors such as the response time of the electrode to the ion with which it is in equilibrium are of no consequence. The main sources of instability in the reference electrode itself are then due to thermal effects and Mattock[119] has claimed that 'well-prepared calomel electrodes are stable to within 0.1 mV over periods of several weeks or even months if stored in a thermostat.' It is necessary at this point to note a deficiency of the oil bath thermostat described in the previous section. In the Simac and Radiometer electrodes which were used, the calomel element itself is situated a few centimetres from the tip of the electrode body. It was therefore above the level of the filling solution in the metal connected disc electrode of Figure 6.6.3 and also above the level of the temperature controlled fluid in the oil bath. It consequently experienced temperature variations not much less than those of the ambient atmosphere. The temperature sensitivity of the calomel half-cell (using saturated KCℓ) has been reviewed by Mattock[119] who has noted that the differential temperature coefficient

is 0.2 mV/deg C. This is the value which is measured in a cell comprising two calomel electrodes with a temperature gradient between them and is less than the commonly quoted value for the calomel cell measured against a standard hydrogen electrode. The differential figure is appropriate to the present work because the half-cell comprising the metal contact was thermostatted and only the calomel half-cell was subject to temperature changes. (The effect was probably less pronounced in the case of the membrane electrodes of Figure 6.6.5 in which the two calomel elements are similarly situated). Assuming an overnight ambient temperature variation of about 10 deg C, a drift in cell potential of the order of 2 mV would be expected. A further complication is the so-called 'temperature hysteresis' effect[119] in calomel electrodes in which the potential shows a slow drift for many hours following a temperature change.

The potential of the reference electrode system is subject to an additional uncertainty due to the liquid junction. It is well known[21,24] that the liquid junction potential cannot be calculated from purely thermodynamic data. Less rigorous calculations have been made however using methods such as the Henderson approximation[24]. They indicate that an absolute potential of a few millivolts arises at the junction between a highly concentrated, or saturated, solution of potassium chloride and a wide range of buffer or salt solutions. Factors which affect the liquid junction potential have been reviewed by Mattock[21] and by Mattock and Band[24]. An important example is the effect of extreme values of pH (outside the range 2 to 10) which can cause potentials in excess of 10 mV at a junction with saturated

potassium chloride, as a consequence of the high mobilities of the H^+ and OH^- ions. Variations in the ionic strengths of test solutions can also cause an uncertainty of about $\pm$0.02 pH in the measurement and a temperature change between 25°C and 38°C has been observed to cause a variation of 0.55 mV in the liquid junction potential[24]. The performance of the ceramic plug liquid junction (the type used in the present work) has been summarised by Mattock[21] who claims a reproducibility of $\pm$0.2 mV in the potential at a junction between 3.8 M KCℓ and buffer solutions of intermediate pH. At a junction between 3.8 M KCℓ and 1.0 M HCℓ however, the reproducibility is only $\pm$0.8 mV.

8.9 RESISTANCE MEASUREMENTS

Resistance measurements were made in connection with the technique described in Section 8.5 for the detection of electrical leakage. They were carried out by plotting current-voltage curves over the range 0 to 5 V in order to eliminate the effect of electrochemical potentials. The circuit of Figure 8.9.1 was used. The electrometer was used as a picoammeter in the 'FAST' mode in which the electrometer 'high' terminal is a virtual earth due to the action of feedback within the instrument[110]. The total voltage across the sample is then very nearly equal to the power supply voltage and the current through the sample is measured directly by the electrometer. The current-voltage curve was plotted directly using an X-Y recorder (Type 25000, Bryans Southern Instruments Ltd) as shown, the power supply voltage being varied manually.

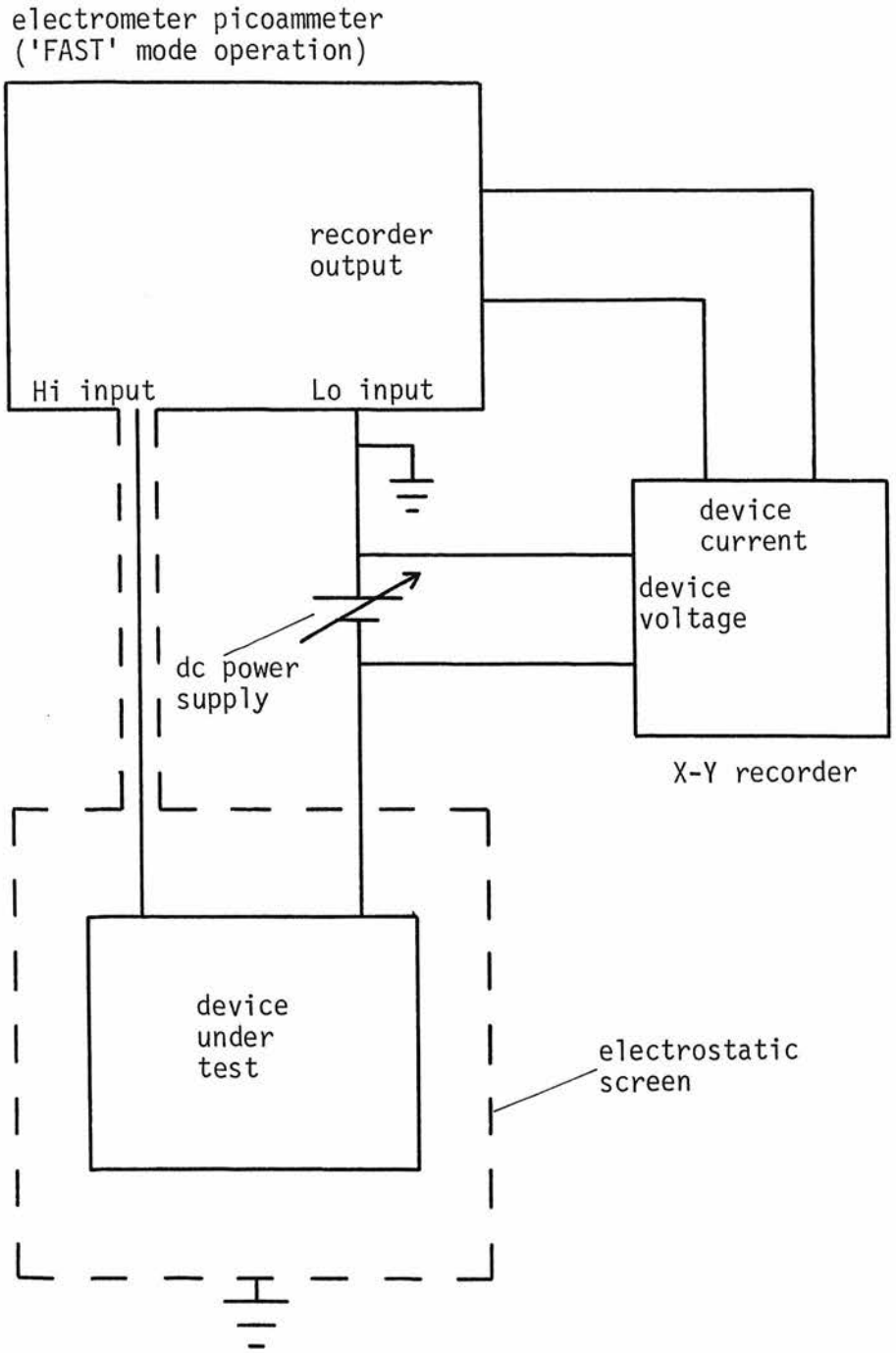

Figure 8.9.1 Circuit for directly plotting the current-voltage characteristic of a device.

The 'Hi' input terminal of the electrometer is a 'virtual earth' when the 'FAST' mode of operation is used.

Calomel electrodes were used when connection to aqueous phases was required. In other cases direct metal connection to the glass membrane was used. These measurements are clearly influenced by polarisation effects and must be interpreted only with the utmost caution. Experience showed however that the results were sufficiently repeatable to give useful information on an 'order of magnitude' basis concerning electrical leakage effects.

8.10 OVERALL EXPERIMENTAL UNCERTAINTY

Many of the measurements of electrode sensitivity to be described in Chapter 9 were made within a period of a few hours, using the circuit of Figure 8.3.1. Assuming an uncertainty of ± 2 mV in the potential measurement itself and a further ± 1 mV due to pH and ionic strength effects on the liquid junction, a scatter of at least ± 3 mV in the measured data was expected. This figure does not take account of inaccuracies in the nominal pH values of buffer solutions. For measurements over a longer period however, the effect of temperature variation on the (inadequately thermostatted) calomel reference element contributed a further uncertainty of the order of ± 1 mV and data derived from chart recorder measurements was subject to an additional error of ± 2 mV. The overall accuracy of long term measurements was therefore ± 4 mV for 'spot' measurements and ± 6 mV for recorder data. The instruments were frequently corrected for zero drift which is not included in the above figures. In the case of data obtained from recorder traces taken over prolonged periods however, an additional zero error of at least ± 4 mV must be reckoned with.

CHAPTER 9: PERFORMANCE OF GLASS DISC ELECTRODES

9.1 PRELIMINARY MEASUREMENTS

The preliminary work described in this section was carried out in order to establish that significant pH responses could be obtained using glass disc electrodes in both membrane and metal connected form.

Electrode potentials were measured directly, using an electrometer voltmeter (Figure 9.1.1) and the measurements were made at room temperature. Experimental uncertainties associated with these techniques were noted and led to the development of the improved measurement methods described in the previous chapter. The effects on pH sensitivity of disc thickness and of surface etching treatment were investigated at this stage and standard procedures were adopted for use in subsequent work.

A batch of seven membrane electrodes were constructed by sealing discs of 015 glass to Pyrex tubes using silicone rubber adhesive as shown in Figure 6.6.4. The discs were prepared by the method of Section 6.5. The final surface treatment comprised a five minute lapping using 400 grade carborundum. (Surface etching was not employed with these discs). The nominal thicknesses of the discs were 80 μm, 300 μm and 450 μm (two samples of each thickness) and 200 μm (one sample).

The pH sensitivities of the electrodes were measured using test solutions of pH 4.0, 7.0 and 9.2, prepared using buffer tablets, together with a solution of 0.1 M hydrochloric acid (Section 8.7).

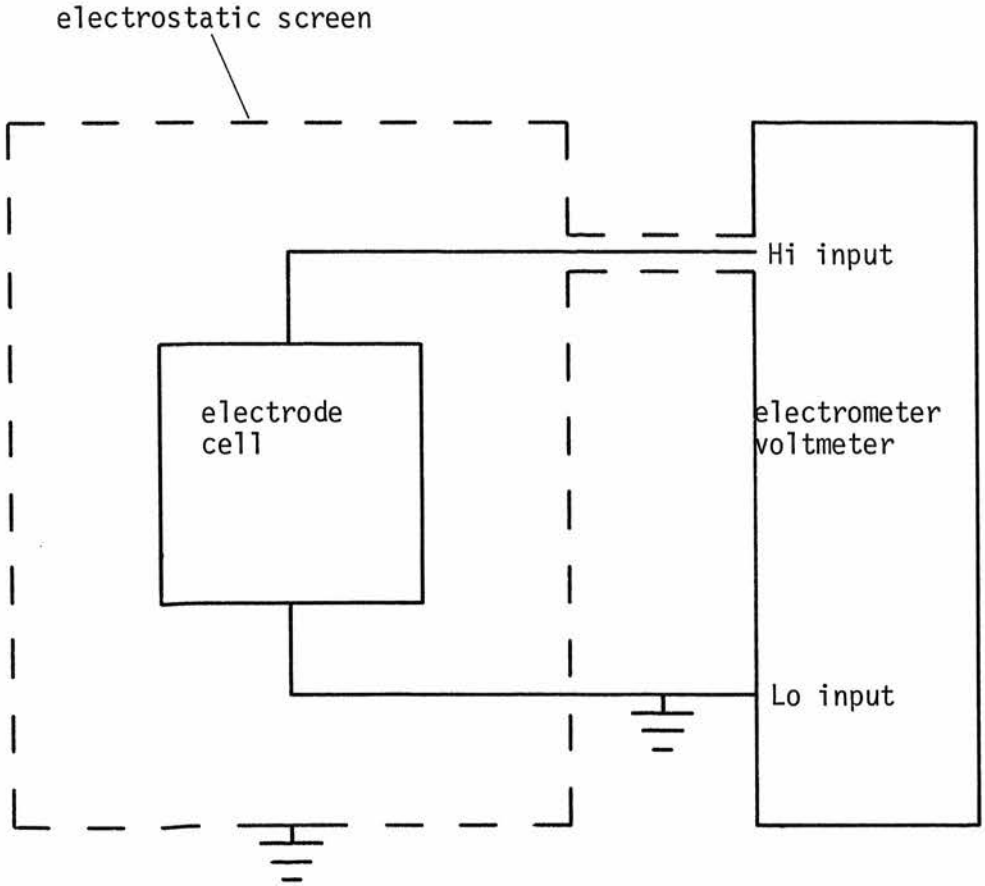

Figure 9.1.1 Direct measurement of glass electrode cell potential, using an electrometer voltmeter

An internal filling solution of pH7 was used throughout. Simac calomel electrodes were used as the internal and external references (Section 8.8).

With one exception, the electrodes all showed fairly linear responses of between 45 and 55 mV/pH, after a few hours hydration in a pH7 solution. The asymmetry potential, measured in a pH7 solution, was large (typically 100 mV) in all cases. Electrode resistances were measured by the method of Section 8.9 and the values for each device on the first day of exposure to solution are given in Table 9.1.1. The correlation with membrane thickness is only very approximate but the discrepancies can probably be explained by variations in room temperature. The measurements of pH sensitivity and electrode resistance were repeated over a period of several weeks. The responses of four of the electrodes declined to about 10 mV/pH by the end of this period and the membrane resistance of each of these devices also fell progressively to about a quarter of its initial value. The responses and asymmetry potentials of the other electrodes remained fairly constant over this period and their membrane resistances showed random variations over a range of about 2:1, which could be explained by temperature variations and uncertainties in the resistance measurement. Typical data for devices displaying each kind of behaviour are given in Figures 9.1.2 and 9.1.3 and Tables 9.1.2 and 9.1.3.

These measurements indicated that significant pH sensitivities can be obtained with glass disc electrodes and that the performance of the electrodes is not noticeably dependent on membrane thickness in the range 80 μm to 450 μm. It was decided to adopt a standard nominal thickness of 300 μm for further work. Discs of this thickness could be easily handled with very few breakages and had a

electrode number	nominal thickness (μm)	resistance (MΩ)
31	80	*
33	80	330
30	200	820
35	300	1300
36	300	1300
34	450	1200
26	450	1300

Table 9.1.1 Resistances of glass disc membrane electrodes, measured during their first day of exposure to aqueous solution.

* *resistance varied in the course of measurement*

The measurements were made at room temperature

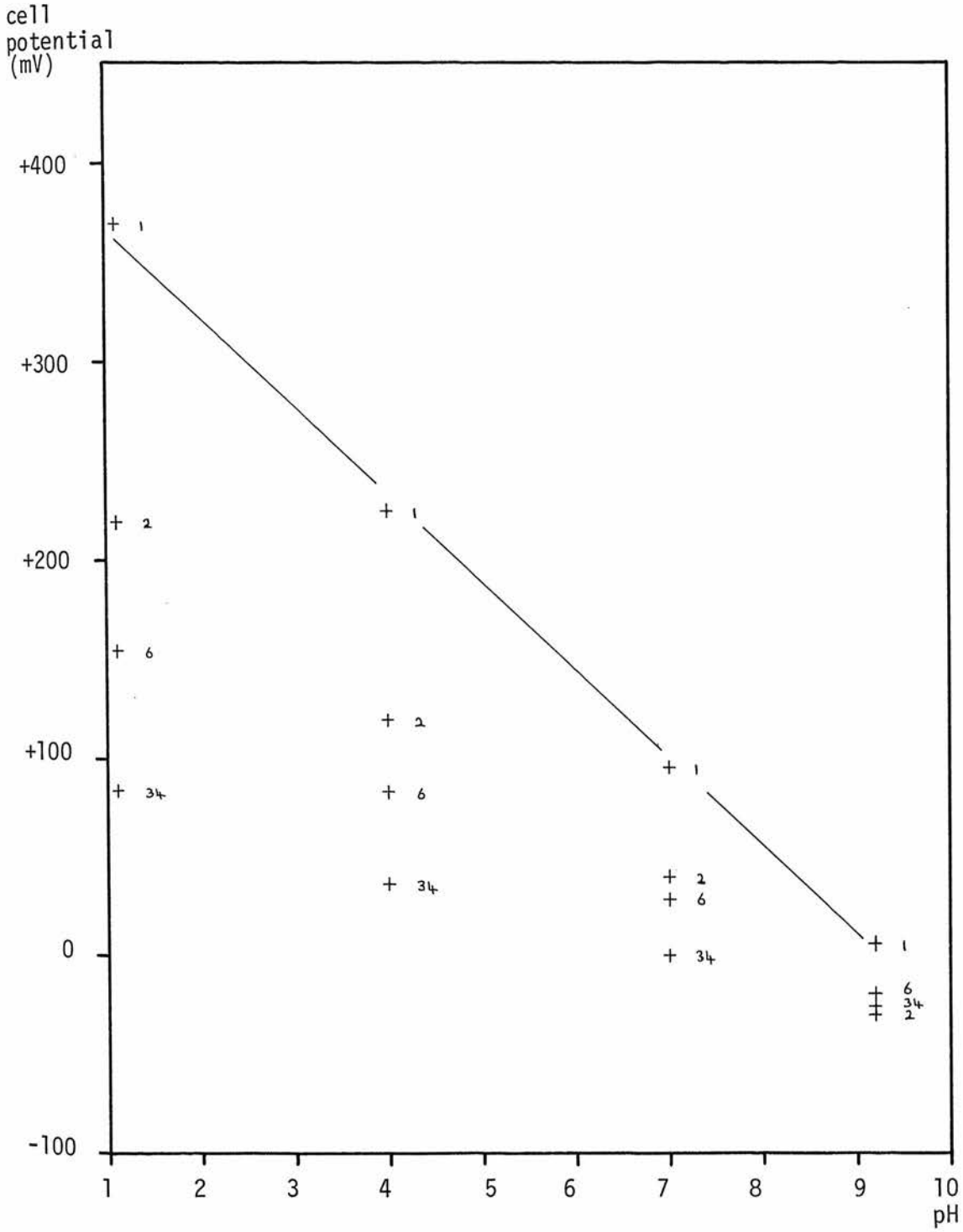

Figure 9.1.2 pH response of a glass disc membrane electrode showing a fall in sensitivity after exposure to test solutions (Electrode no 33, see also Table 9.1.2).

Sensitivity measurements were made at room temperature after 1, 2, 6 and 34 days exposure to solution. For clarity, a visually estimated 'best straight line' is shown for the day 1 data only.

time (day)	pH sensitivity (mV/pH)	resistance (MΩ)
1	45	330
2	30	140
6	22	110
34	14	82

Table 9.1.2 Time variation of membrane resistance for the case of an electrode which exhibited a declining pH sensitivity during exposure to solutions (Electrode no 33, see also Figure 9.1.2).

The measurements were made at room temperature

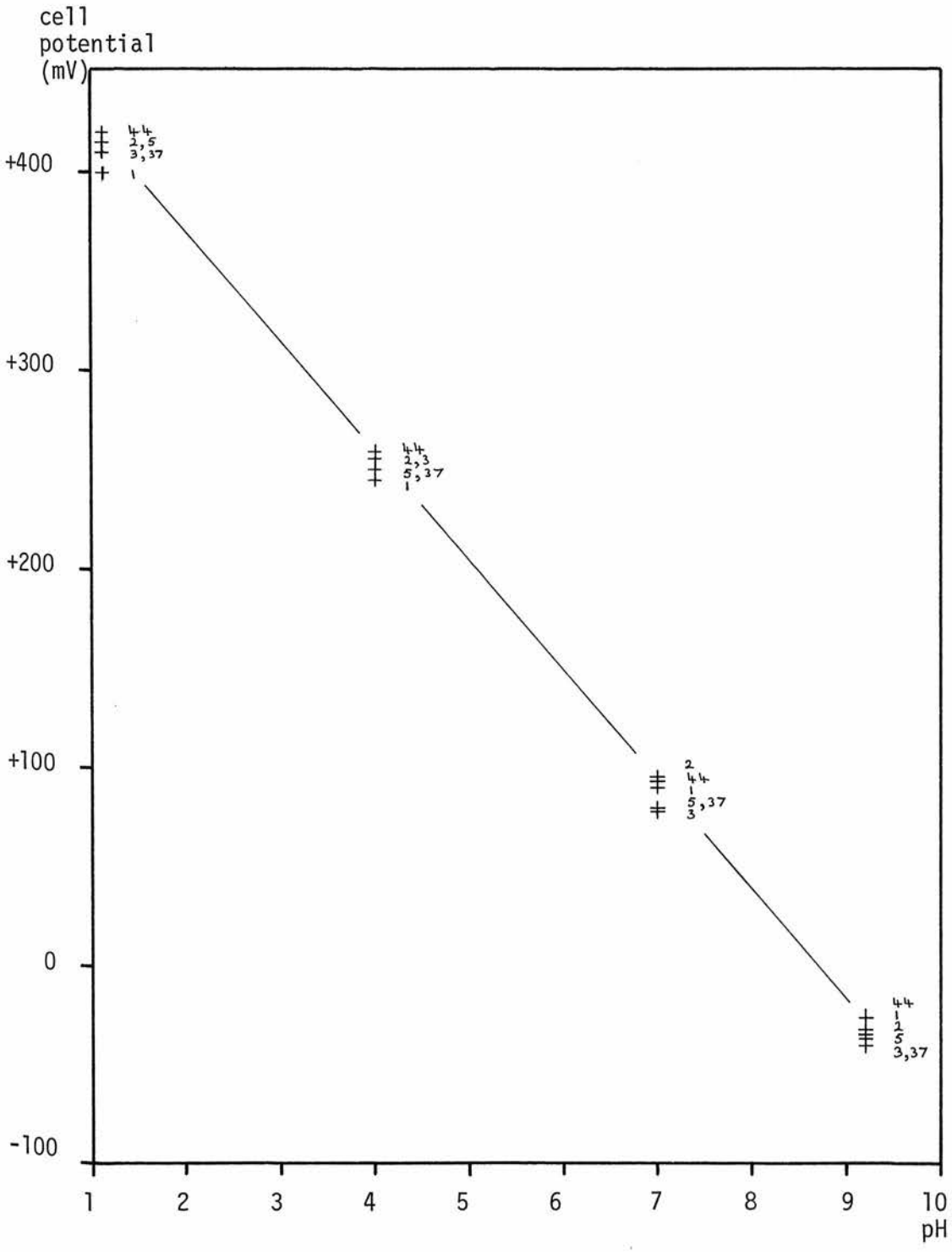

Figure 9.1.3 pH response of a glass disc membrane electrode showing fairly constant sensitivity over a period of several weeks (Electrode no 36, see also Table 9.1.3).

For clarity, a visually estimated 'best straight line' is shown for the day 44 data only. Scatter of the data points is greater for certain of the other days. The measurements were made at room temperature.

time (day)	pH sensitivity (mV/pH)	resistance (MΩ)
1	54	1300
2	56	1300
3	57	1500
5	56	890
37	56	1200
44	56	830

Table 9.1.3 Time variation of membrane resistance for the case of an electrode which exhibited a substantially constant pH sensitivity during exposure to solutions (Electrode no 36, see also Figure 9.1.3).

The measurements were made at room temperature

resistance of the order of 10^9 Ω. The declining pH response and resistance observed in four of the electrodes could obviously be explained in terms of an increasing electrical leakage conductance. In view of the problem of interpretation discussed in Section 8.5 however, a further batch of membrane electrodes was fabricated to allow measurements using the 'annular contact' method.

Glass discs, 300 μm thick, were prepared as before, except that in this case the etching treatment described in Section 6.5 was employed. (It was thought that electrode performance might be affected by surface damage resulting from the lapping process). A nichrome-gold annulus was evaporated on to one face of each disc and three electrodes were assembled using silicone rubber adhesive as shown in Figure 6.6.5. One side of the electrode was arbitrarily chosen to be the reference and contained a filling solution of pH7. Simac calomel electrodes were again used to make contact with the solutions on each side of the membrane. The bias potential between these electrodes was measured, in a pH7 buffer solution, and was found to be less than 1 mV.

The pH sensitivities of the disc electrodes were measured, using the same test solutions as before, and results for one of the electrodes, over a period of 40 days, are presented in Figure 9.1.4 and Table 9.1.4. The resistance R_{AB} in the table denotes that measured between the calomel electrodes while R_{AC} and R_{BC} are the resistance measured between each calomel electrode (denoted by A and B respectively) and the annular metal contact (denoted by C). The pH response was nearly Nernstian during the first week or so of operation but it subsequently declined considerably. The asymmetry potential (in contrast to the earlier devices) remained less than

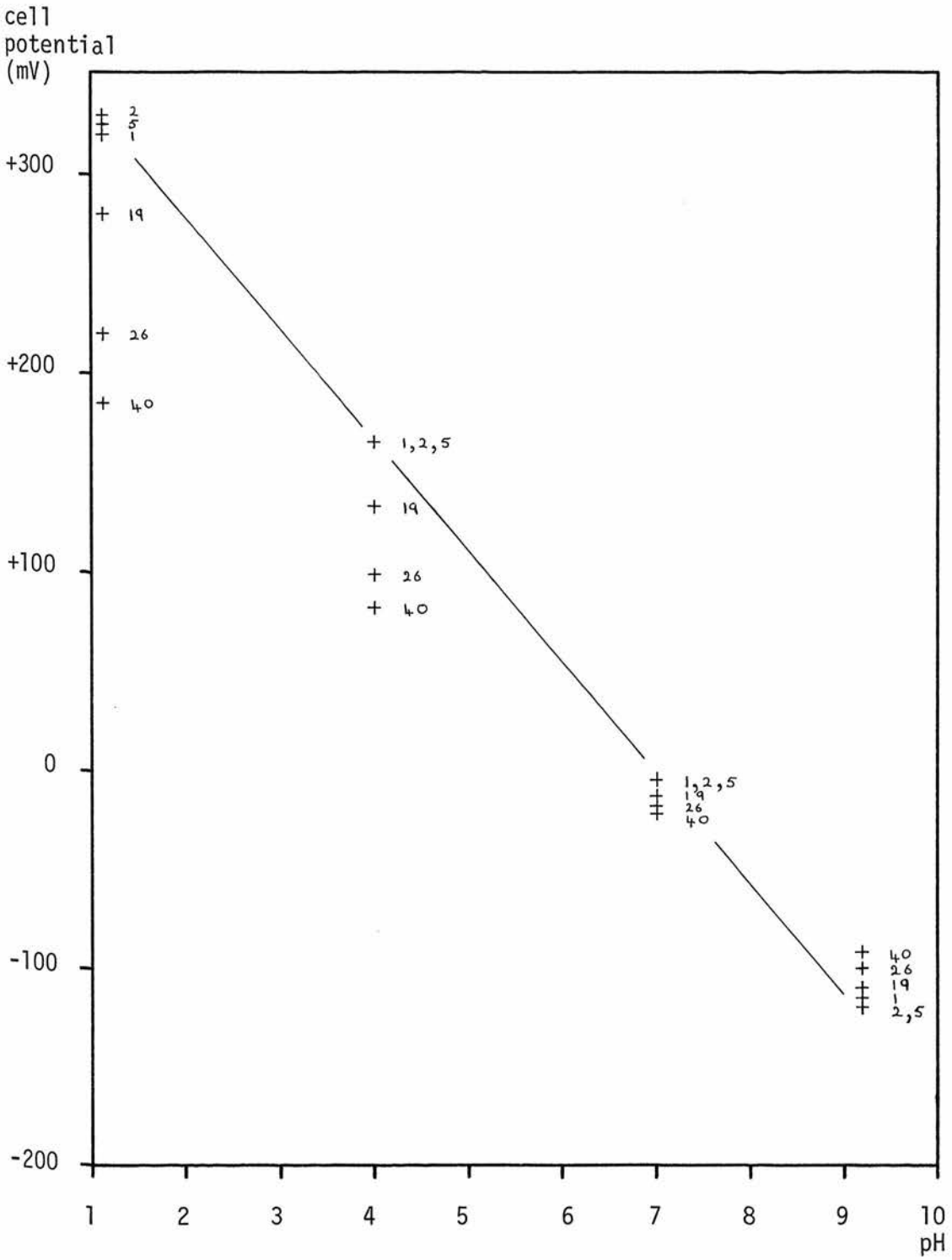

Figure 9.1.4 pH response of a glass disc membrane electrode measured over a period of 40 days. (Electrode no UR2, see also Table 9.1.4).

For clarity, a visually estimated 'best straight line' is shown for the day 2 data only. Scatter of the data points is greater for certain of the other days. The measurements were made at room temperature.

time (day)	room temperature (^{o}C)	R_{AB} (GΩ)	R_{AC} (GΩ)	R_{BC} (GΩ)	$\frac{R_{AC}}{R_{AB}}$	$\frac{R_{BC}}{R_{AB}}$	pH sensitivity (mV/pH)
1	21.5	2.1	150	150	72	72	55
2	21.0	2.0	170	170	85	85	56
5	25.2	1.4	130	120	93	86	56
19	23.5	1.5	110	110	73	73	49
26	23.0	1.3	110	110	85	85	40
40	22.0	1.2	110	110	92	92	34

Table 9.1.4 Time variation of pH sensitivity and resistance data for a glass disc membrane electrode (Electrode no UR 2, see also Figure 9.1.4).

$\pm$5 mV during the initial period although it increased somewhat as the response declined. The most interesting feature of these results is the resistance values of Table 9.1.4. The reasoning of Section 8.5 shows that, in the absence of electrical leakage effects, the values of the ratios $\frac{R_{AC}}{R_{AB}}$ and $\frac{R_{BC}}{R_{AB}}$ should be approximately 50 to 100 (independent of temperature). The data of Table 9.1.4 lie within this range, implying that leakage conductances were insufficient to explain the observed decline in pH response. The pH response of another of the electrodes of this batch varied in a very similar manner to that of Table 9.1.4. The sensitivity of the third device was initially smaller (47 mV/pH) and it also declined (to 32 mV/pH) over 40 days. The values of the resistance ratios were rather smaller (between 30 and 50) in the case of the latter two electrodes however, and again varied randomly from day to day.

Metal connected electrodes were also investigated during this initial phase of the work. A batch of six glass discs, of 300 μm nominal thickness, were again prepared by the standard method of Section 6.5. The surface etching treatment was used with three of the discs but omitted in the case of others. Electrodes incorporating an evaporated gold-nichrome back contact and an annular contact were assembled, using silicone rubber adhesive, as described in Section 6.6. Test solutions prepared from buffer tablets, together with an 0.1 M solution of hydrochloric acid, were again used for the measurement of pH sensitivity. The test solution was placed inside the electrode and connection to it was made using a Simac calomel electrode. The metal back contact comprised the 'reference' side of the membrane in this case and was connected to the 'high' terminal of the electrometer.

Similar results were obtained for each of the three electrodes employing discs which had not been etched. Results for one of these devices are given in Figure 9.1.5 and Table 9.1.5. The subscripts A and B in the table denote the test solution and the metal contact respectively and C denotes the annular contact as before. The pH sensitivities of these electrodes were significantly sub-Nernstian and varied randomly over a period of twelve weeks. The cell potential measured at pH7 also varied randomly during this period, over a range of about 60 mV. This figure includes a component due to the difference in potential between the calomel electrode and the (unspecified) half cell at the back contact and it cannot be compared with the simple asymmetry potential values of the membrane electrodes described previously. Furthermore, the iso-potential pH value of the metal connected electrode cell is not known and the potential measured at pH7 is likely to be more temperature sensitive than the true asymmetry potential measured in the case of the symmetrical membrane electrodes. The values of the resistance ratios, $\frac{R_{AC}}{R_{AB}}$ and $\frac{R_{BC}}{R_{AB}}$, in Table 9.1.5 are significantly smaller than the 'ideal' value of 50 to 100 and this suggests the presence of leakage conductances. The large day to day variations in the ratios correlated only approximately with the variations in pH sensitivity however. The variations in the measured resistance, R_{AB}, can be attributed to the temperature sensitivity of the glass membrane resistance.

Results for one of the etched, metal connected electrodes are given in Figure 9.1.6 and Table 9.1.6 and are typical of the performances of all three etched devices. The pH sensitivities of these devices were initially rather larger than those of the

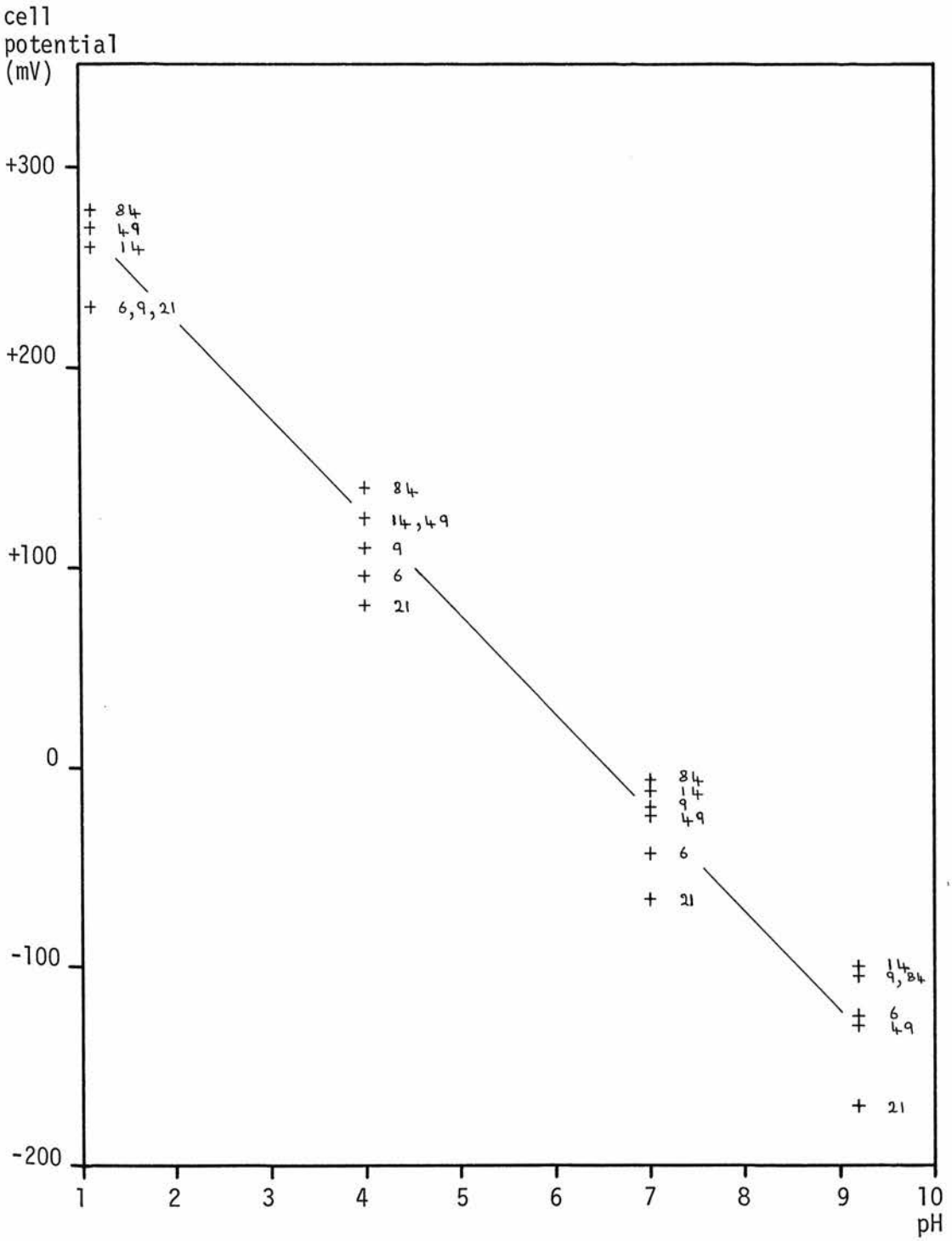

Figure 9.1.5 pH response of a metal connected glass disc electrode (not etched), measured over a period of 84 days. (Electrode no 37, see also Table 9.1.5).

For clarity, a visually estimated 'best straight line' is shown for the day 49 data only. Scatter of the data points is greater for certain of the other days. The measurements were made at room temperature.

time (day)	room temperature (^{o}C)	R_{AB} (GΩ)	R_{AC} (GΩ)	R_{BC} (GΩ)	$\frac{R_{AC}}{R_{AB}}$	$\frac{R_{BC}}{R_{AB}}$	pH sensitivity (mV/pH)
6	20.0	1.7	28	28	17	17	44
9	17.5	2.0	10	8.7	5	4	42
14	21.0	1.5	14	13	9	9	44
21	31.5	0.63	21	20	33	32	49
49	24.7	1.1	45	43	41	39	49
84	21.0	1.4	38	42	27	30	48

Table 9.1.5 Time variation of pH sensitivity and resistance data for a metal connected glass disc electrode which had not been subjected to etching treatment (Electrode no 37, see also Figure 9.1.5).

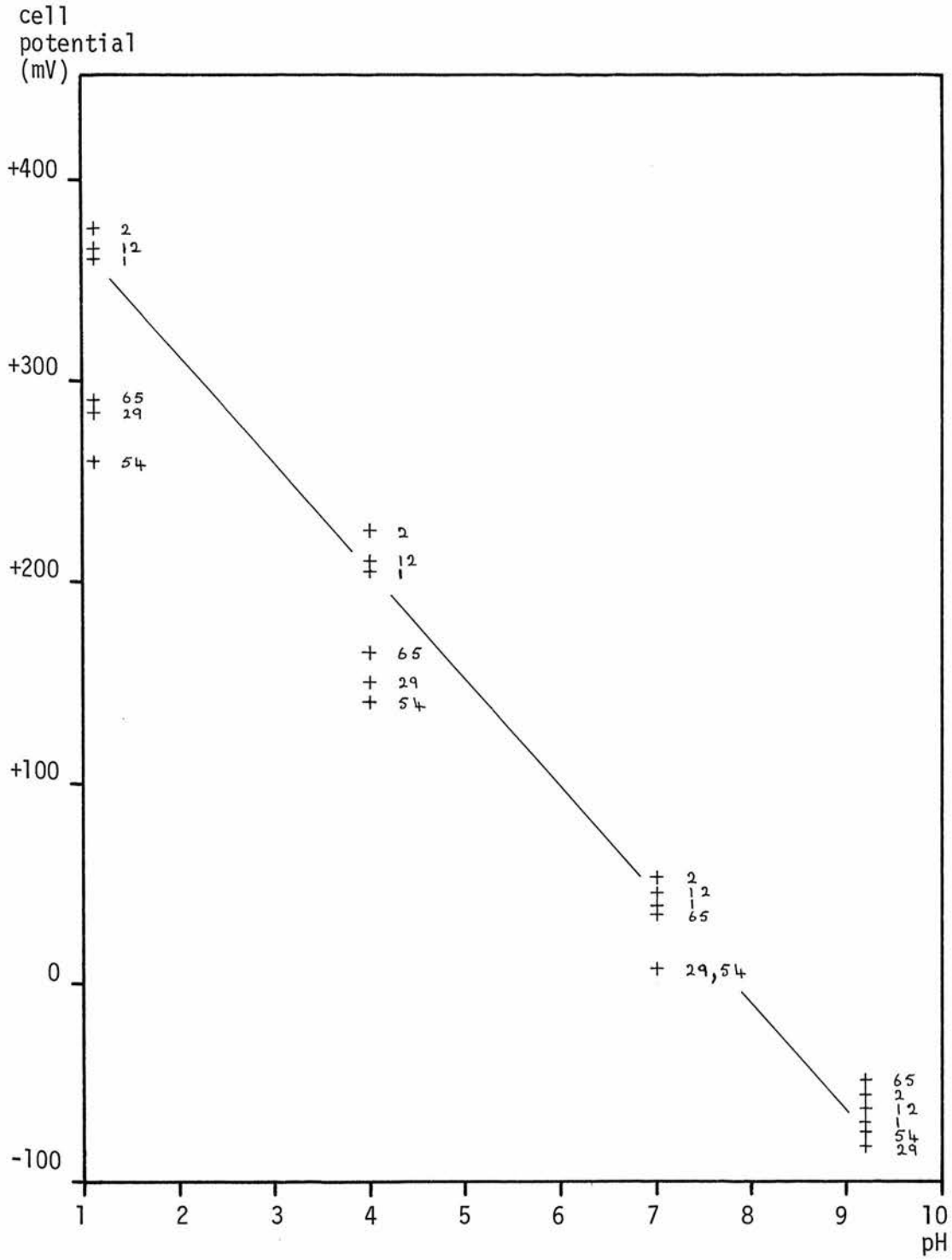

Figure 9.1.6 pH responses of a metal connected glass disc electrode (etched), measured over a period of 65 days (Electrode no E1, see also Table 9.1.6).

For clarity, a visually estimated 'best straight line' is shown for the day 1 data only. Scatter of the data points is greater for certain of the other days. The measurements were made at room temperature.

time (day)	room temperature (^{o}C)	R_{AB} (GΩ)	R_{AC} (GΩ)	R_{BC} (GΩ)	$\frac{R_{AC}}{R_{AB}}$	$\frac{R_{BC}}{R_{AB}}$	pH sensitivity (mV/pH)
1	29.5	0.97	80	77	83	80	54
2	26.5	1.2	110	100	92	83	54
12	24.0	1.6	130	120	81	75	54
29	24.0	1.3	120	120	92	92	46
54	24.0	1.3	120	120	92	92	42
65	21.0	1.6	150	150	94	94	42

Table 9.1.6 Time variation of pH sensitivity and resistance data for an etched, metal connected glass disc electrode (Electrode no E1, see also Figure 9.1.6).

electrodes which were not etched although they declined to a similar value during the measurement period. The resistance measurements show a marked difference however, the ratios in the case of the etched devices remaining greater than 75 throughout, which suggests that leakage effects were not sufficient to explain the observed decline in pH sensitivity.

It was clear from these results that significant pH responses could be obtained from both metal connected and membrane glass disc electrodes. The sensitivities were generally sub-Nernstian however and declined further during a period of several weeks exposure to the test solutions. Resistance ratio measurements, using the annular contact method of Section 8.5, indicated that leakage conductances were insufficient to explain the loss of sensitivity in some of the electrodes, although leakage effects were present in other cases. Surface etching of the disc did not appear to affect its pH sensitivity but there was some evidence that leakage conductances were smaller in the case of the etched devices, possibly due to better adhesion between silicone rubber and a freshly etched surface. (Compare the resistance ratio data for the etched devices of Tables 9.1.4 and 9.1.6 with the values for the electrodes of Table 9.1.5, which were not etched). It was decided to adopt the etching treatment as standard in subsequent work and to use a nominal disc thickness of 300 μm. It was clear from this work that thermostatting was required in order to eliminate the effect of temperature variations on the resistance of the glass discs and on the potential at the metal contact. The poor precision of the direct method of potential measurement of Figure 9.1.1 was also noted and the improved measurement methods described in Chapter 8 were introduced in the work described in the following sections.

9.2 MEMBRANE ELECTRODES

Five glass discs, of nominal thickness 300 μm, were prepared by the standard method of Section 6.5. Three of the discs were subsequently polished and the other two were annealed, also using the techniques described in Section 6.5. Membrane electrodes were assembled as illustrated in Figure 6.6.5, exactly as previously. Measurements on these devices were carried out at 30°C using the thermostat described in Section 8.6. Potential measurements were made with the circuit of Figure 8.3.1 in which a dc voltage generator is used to partially offset the cell potential. The test solutions used for this work were those of Table 8.7.1. One side of each electrode was arbitrarily defined as the reference and always contained a solution of pH 6.54. A settling time of several minutes was allowed, after changing the test solution, before recording the value of the cell potential. Simac calomel electrodes were again used to make contact with the solutions on each side of the membrane. The bias potential between these electrodes was typically one or two millivolts, measured in a solution of pH 6.54.

Graphs of cell potential against pH were plotted as before. Most of the measured data were found to lie within ±6 mV of the visually determined 'best straight line', although greater deviations were sometimes observed. This scatter is rather greater than that predicted in Section 8.10 for 'short term' response measurements. It is now considered most likely that it was caused by thermal effects associated with the introduction of different filling solutions into the electrode, as discussed in Section 9.3. The results may also have been influenced by the drift in test solution pH values noted

in Section 8.7. The pH sensitivity and the asymmetry potential (measured at pH 6.54) were read from each graph and are summarised over a period of 44 days in Figures 9.2.1 and 9.2.2. The pH sensitivities of these electrodes, like many of those of the previous section, declined from, typically, 55 mV/pH initially to about 40 mV/pH at the end of the period. It appears that the polishing and annealing treatments had no significant effect on either the sensitivity or the longevity of the devices. The asymmetry potentials of these electrodes varied from day to day and values of 50 mV or more were observed on many occasions. A surprising feature of the results is that the general trend of the variation is similar for both of the annealed electrodes. The measurements on these two devices were made on the same days within an hour or so of each other, using the same pair of reference electrodes. Similarly, there is clearly some correlation between the asymmetry potentials of the three polished electrodes which were also measured as a batch at substantially the same times. Furthermore, the long term drift for all five devices was in the same (negative) direction although the electrode structures were symmetrical. These observations suggest that the drift may have to some extent originated in the measurement system rather than in the properties of the individual glass discs. On the other hand, there were many occasions when the magnitudes of the day to day changes differed widely between devices, which eliminates factors such as drift of reference electrode bias potentials as the sole cause of the observed behaviour. Nor can the results be explained entirely by drifts of buffer solution pH since high asymmetry potentials were recorded for several electrodes on day one, when fresh solutions were used. The solutions were also

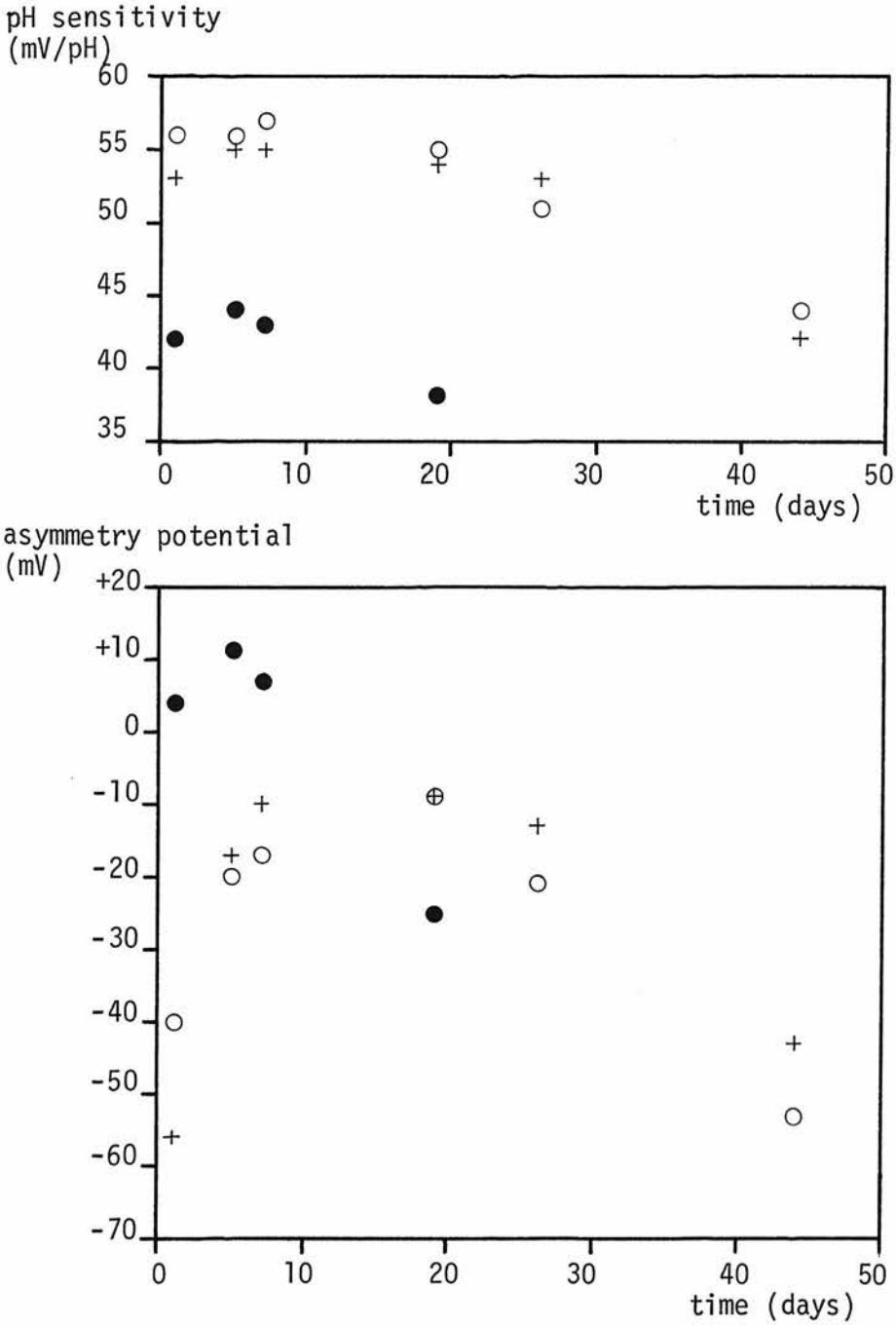

Figure 9.2.1 Time variation of the pH sensitivity and asymmetry potential of polished glass disc membrane electrodes. (See also Table 9.2.1).

+ Electrode no P1
● Electrode no P2
○ Electrode no P3

Temperature ≒ 30°C

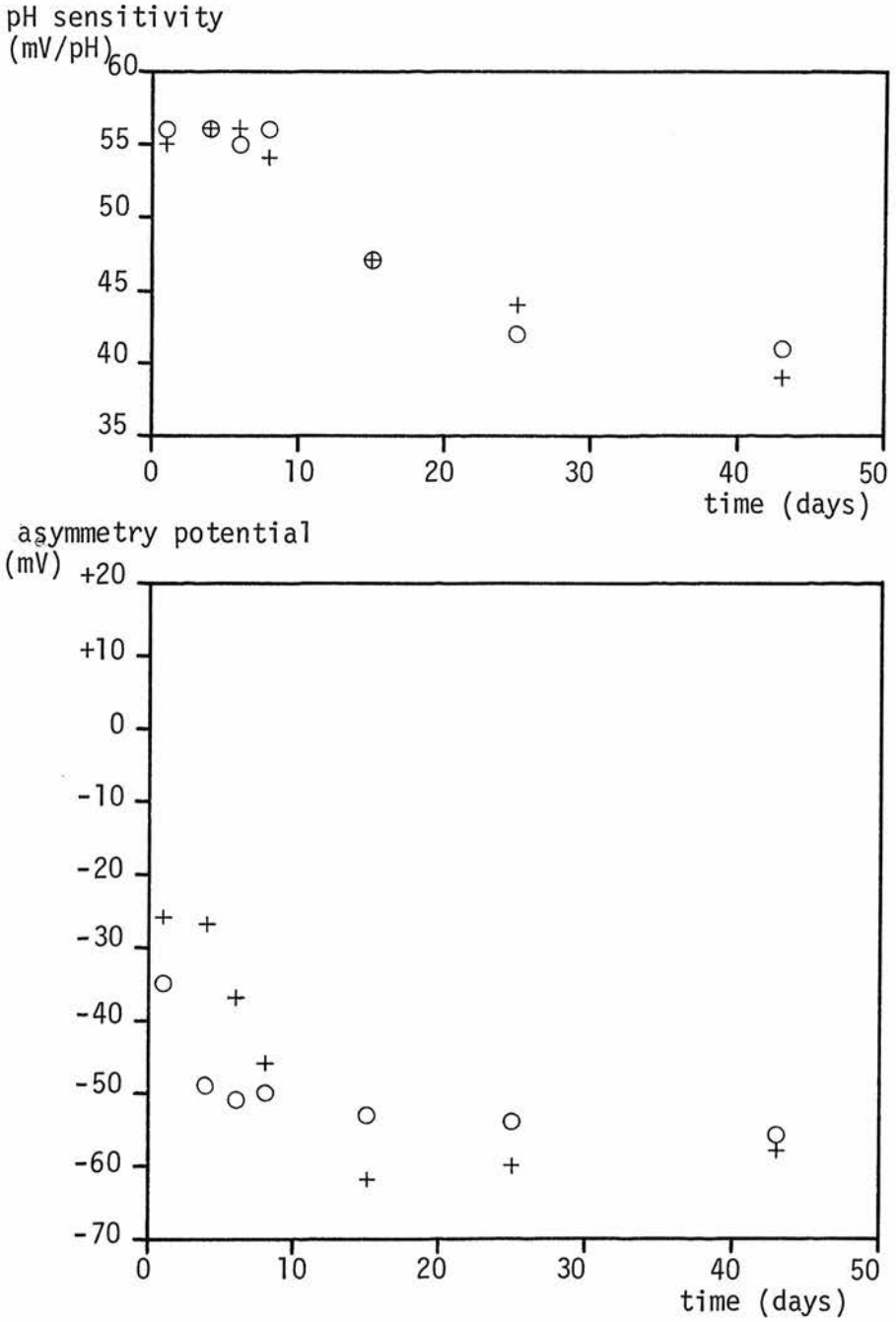

Figure 9.2.2 Time variation of the pH sensitivity and asymmetry potential of annealed glass disc membrane electrodes. (See also Table 9.2.2).

+ Electrode no A1
○ Electrode no A2

Temperature = $30^{o}C$

replaced at intervals during the measurements as a standard practice. Although no conclusive explanation can be offered for this aspect of performance, it does indicate the importance of carrying out control experiments with membrane electrodes before drawing conclusions concerning the stability, or otherwise, of metal connected devices.

The resistance values, R_{AB}, for the three polished electrodes are given in Table 9.2.1. They are in agreement with those values in Section 9.1 which were measured at a comparable temperature (ie $30^{o}C$). The measured values of R_{AC} and R_{BC} for each of these devices were of the same order as R_{AB}, indicating poor insulation between at least one side of the membrane and the annular contact, as discussed in Section 8.5. The results of resistance measurements on the two annealed electrodes are presented in Table 9.2.2. The values of R_{AB} for both of these devices are significantly larger than those for the polished electrodes. This would be expected as a consequence of the more ordered structure of the annealed material, and shows that the annealing process was in fact effective. The ratios, $\frac{R_{AC}}{R_{AB}}$, were initially fairly large (although somewhat less than predicted by calculation) but they subsequently declined, suggesting a deterioration in the insulation level. This correlates qualitatively with the fall in pH sensitivity. There are some anomalies in the data however, especially the large fall in sensitivity of the device of Table 9.2.2(b) between days 8 and 15, which was not accompanied by a change in the ratio $\frac{R_{AC}}{R_{AB}}$.

The above results showed that leakage effects were significant in many of the disc electrodes, in spite of the earlier instances of apparently leakage-free devices noted in Section 9.1. Correlation

time (day)	Electrode no P1		Electrode no P2		Electrode no P3	
	R_{AB} (GΩ)	pH sensitivity (mV/pH)	R_{AB} (GΩ)	pH sensitivity (mV/pH)	R_{AB} (GΩ)	pH sensitivity (mV/pH
1	0.73	53	0.54	42	0.79	56
5	-	55	-	44	-	56
7	-	55	-	43	-	57
19	-	54	-	38	-	55
26	0.73	53	-	-	0.65	51
44	0.59	42	-	-	0.48	44

Table 9.2.1 Time variation of pH sensitivity and resistance data for polished glass disc membrane electrodes (see also Figure 9.2.1)

Temperature = $30^{o}C$

time (day)	R_{AB} (GΩ)	R_{AC} (GΩ)	$\frac{R_{AC}}{R_{AB}}$	pH sensitivity (mV/pH)
1	1.3	53	41	55
4	1.2	27	23	56
6	1.3	21	16	56
8	1.2	14	12	54
15	0.81	3.6	4.4	47
25	0.89	1.2	1.3	44
43	0.79	0.42	0.53	39

(a)

time (day)	R_{AB} (GΩ)	R_{AC} (GΩ)	$\frac{R_{AC}}{R_{AB}}$	pH sensitivity (mV/pH)
1	1.2	45	38	56
4	1.2	22	18	56
6	1.2	21	18	55
8	1.1	18	16	56
15	0.96	15	16	47
25	0.88	8.2	9.3	42
43	0.87	0.047	0.05	41

(b)

Table 9.2.2 Time variation of pH sensitivity and resistance data for annealed glass disc membrane electrodes; (a) Electrode no A1, (b) Electrode no A2. (See also Figure 9.2.2).

Temperature = $30^{o}C$

between the pH sensitivity and resistance ratio measurements was by no means exact but it was nevertheless felt that there was significant evidence that the results were influenced by leakage effects. The 'fused disc' construction method was therefore developed and measurements on membrane electrodes constructed by this technique will now be described.

The electrodes were prepared by fusing 300 μm thick discs of 015 glass to substrates of type EE 1087 glass-ceramic, as described in Section 6.7. The annular contact was omitted from these devices because the use of the resistance ratio technique involves the additional complexity of a seal to each side of the glass membrane (as in the structure of Figure 6.6.5 for example). The simpler electrode configuration of Figure 6.7.2 was employed instead. Measurements of pH sensitivity were made on a batch of four devices, using the test solutions of Table 8.7.1. The solution of pH 6.54 was again used as the inner filling solution. Simac calomel electrodes were used as the inner and outer reference elements, the inner one being connected to the 'high' terminal of the electrometer. The requirement for a vessel containing the outer solution made it impractical to use the thermostat arrangement of Section 8.6 and the measurements were therefore carried out at room temperature.

Cell potentials were again measured using a 'backing off' voltage, as described in Section 8.3, and graphs of cell potential against pH were plotted. The scatter of the data was again rather larger than predicted by the uncertainty calculations of Section 8.10, the experimental points being found always to lie within ± 6 mV of the visually determined 'best straight line'. Furthermore, it was noticed that the

scatter of the measured points was usually similar for different devices measured on the same day, suggesting that it originated in the measurement system rather than in the disc electrodes themselves. The values of pH sensitivity and asymmetry potential obtained from these graphs are summarised in Table 9.2.3. (Measurements on the two electrodes in part (a) of the table were carried out on the same days. Similarly for the pair of devices of part (b)). The electrode responses were substantially Nernstian throughout the measurement period with no indication of the decline in sensitivity which occurred in the previous work. The asymmetry potentials of these membrane electrodes (measured with both sides of the glass disc in contact with the solutions of pH 6.54) were never greater than 20 mV which is somewhat smaller than those of some of the earlier devices. Day to day variations for each electrode were typically 20 mV but correlation was again observed between the data for devices measured on the same day and this suggests that the results may have been influenced by factors other than variations in the asymmetry potential of the glass membrane itself.

The performance of the fused electrodes was clearly superior to that of the earlier devices which employed direct adhesive seals to the pH glass. In particular, their pH sensitivities were substantially Nernstian and remained so for several weeks. The improvements were almost certainly a consequence of reduced electrical leakage effects in these devices.

time (day)	Electrode no 01		Electrode no 02	
	pH sensitivity (mV/pH)	asymmetry potential (mV)	pH sensitivity (mV/pH)	asymmetry potential (mV)
1	58	+17	57	+16
2	-	+ 9	-	+12
4	58	+ 9	58	+11
10	58	+ 8	57	+11
18	-	+13	-	+10
58	57	- 3	57	- 2

(a)

time (day)	Electrode no 03		Electrode no 04	
	pH sensitivity (mV/pH)	asymmetry potential (mV)	pH sensitivity (mV/pH)	asymmetry potential (mV)
1	58	+12	56	+15
2	-	-	57	+15
4	-	-	58	+19
16	58	- 6	57	- 6

(b)

Table 9.2.3 Time variation of the pH sensitivity and asymmetry potential of glass disc membrane electrodes of the 'fused' type.

The measurements on Electrodes 01 and 02, in part (a) of the table, were carried out on the same days.

The measurements on Electrodes 03 and 04, in part (b), were carried out on the same days (but separately from those of part (a)).

The measurements were made at room temperature.

9.3 METAL CONNECTED ELECTRODES

The results to be presented in the first part of this section were obtained using electrodes which had been fabricated by the direct adhesion of silicone rubber to pH glass discs. The fused construction technique of Section 6.7 was subsequently adopted however and the improved performance of metal connected electrodes made by this method will be described later in the section. It should be noted that the evolution of construction methods for the metal connected devices took place in parallel with the corresponding development of membrane electrodes which was described in Section 9.2.

Glass discs, of nominal thickness 300 μm, were again prepared by the standard method of Section 6.5, the surface etching treatment being included. A metal centre contact and annular ring was evaporated on to each disc as described in Section 6.6. Gold, silver and copper contacts were employed, three samples being made with each metal. Single layer gold metallisation was used, the underlying nichrome layer being omitted to give an electrochemically simpler interface. The metals were chosen to compare the performance of a noble metal, gold, with that of the electrochemically active metals, silver and copper. Electrodes were assembled by sealing Pyrex tubes to the discs using silicone rubber adhesive as shown in Figure 6.6.3. Measurements of pH sensitivity were carried out using the test solutions of Table 8.7.1 in conjunction with a Simac calomel reference electrode. A settling period of several minutes was allowed, after changing the test solution, before reading the value of cell potential. The circuit of Figure 8.3.1 was again employed, the 'high' terminal of the electrometer input being connected to the metal back

contact of the electrode. The measurements were carried out at 30°C using the thermostat described in Section 8.6. The pH responses of the electrodes were measured over periods of up to 130 days, in the course of which extensive use was made of continuous chart recorder measurements of the cell potential in order to assess its stability. The effects on the potential of temperature variations and of passing current through the cell were also studied. Resistance ratio measurements are unfortunately not available for these devices, as a result of difficulties with the connection of wires to the annular contact.

Electrode pH responses were determined by plotting graphs of cell potential against solution pH as before. The scatter of the experimental data was such that most points again lay with $\pm$6 mV of the visually determined best straight line. Values of electrode pH sensitivity obtained from these graphs are summarised in Figures 9.3.1, 9.3.2 and 9.3.3. They declined from initial values of between 50 and 55 mV/pH to around 40 mV/pH (with day to day variations) after two or three weeks. The actual values of cell potential, measured using the pH 6.54 solution, are also shown in the figures, as an indication of long term stability.

The short term stability of one of the gold connected electrodes was monitored by continuously recording the cell potential (using a chart recorder) for periods of a few days on several different occasions. The magnitude and direction of the drift was found to be quite random, its rate being typically between 0.5 and 1.0 mV/hour, although faster changes sometimes occurred over a few hours. There was some evidence for a cyclic component overnight, possibly

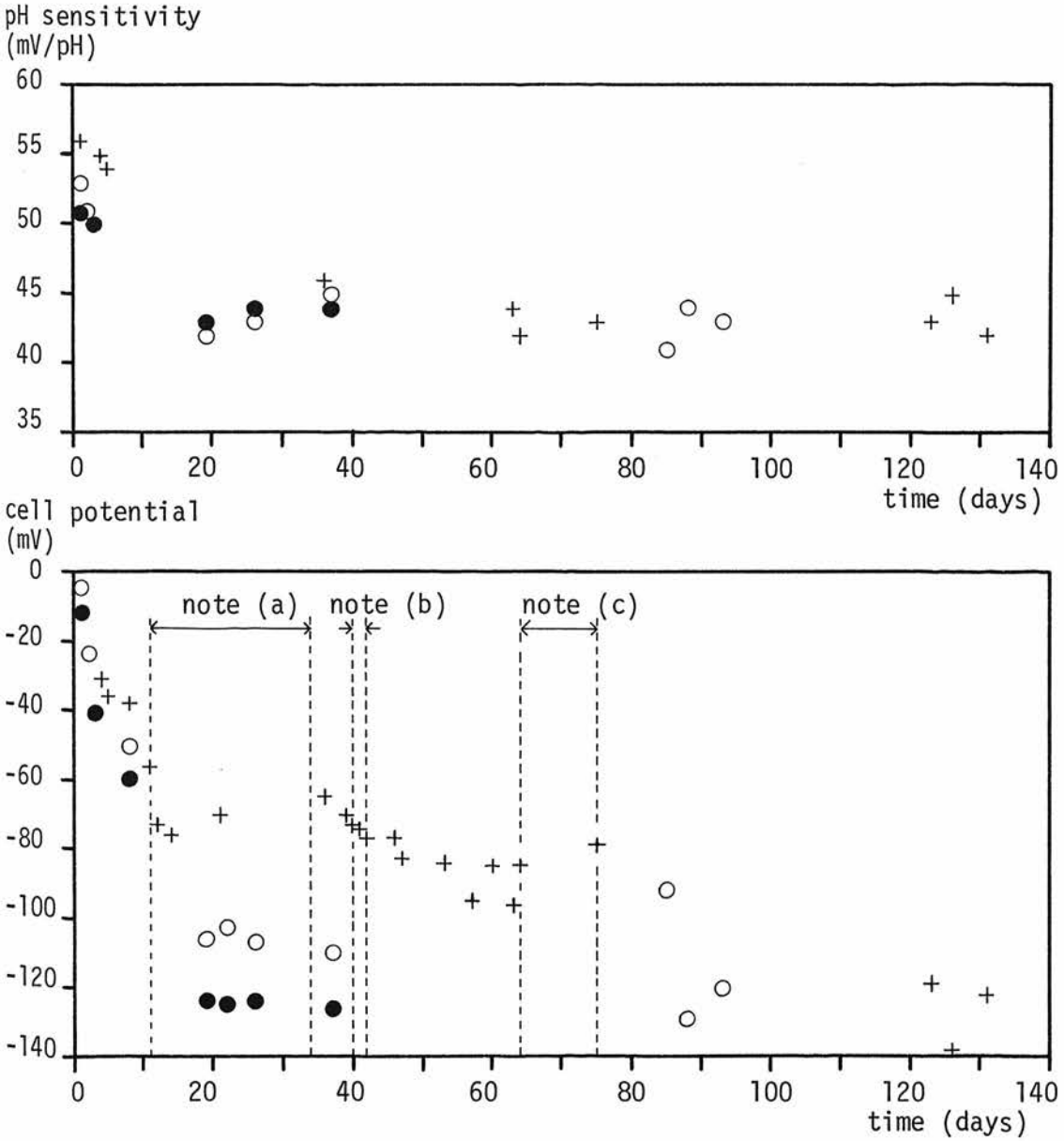

Figure 9.3.1 Time variation of the pH sensitivity and cell potential (at pH 6.54) of gold connected glass disc electrodes.

○ Electrode no Au 1
+ Electrode no Au 2
● Electrode no Au 3

Note (a): Temperature sensitivity measurements were carried out between day 11 and day 34, using Electrode no Au 2 (see text p 169). All other measurements were made at 30°C.

Note (b): Current polarisation tests were carried out between day 40 and day 42, using Electrode no Au 2 (see text p 170).

Note (c): See Table 9.3.1.

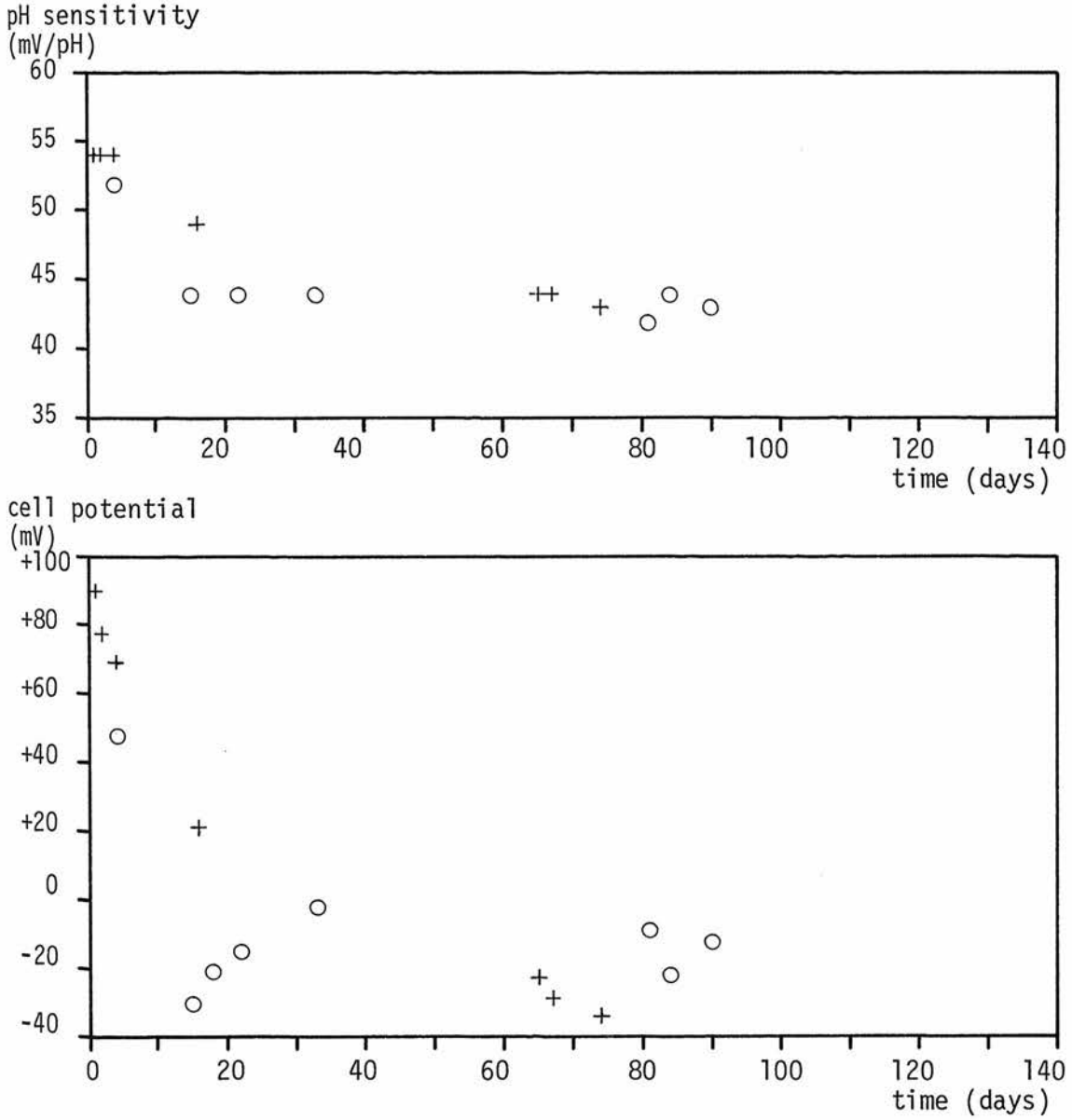

Figure 9.3.2 Time variation of the pH sensitivity and cell potential (at pH 6.54) of silver connected glass disc electrodes.

○ Electrode no Ag 1
+ Electrode no Ag 2

Temperature = $30^{o}C$

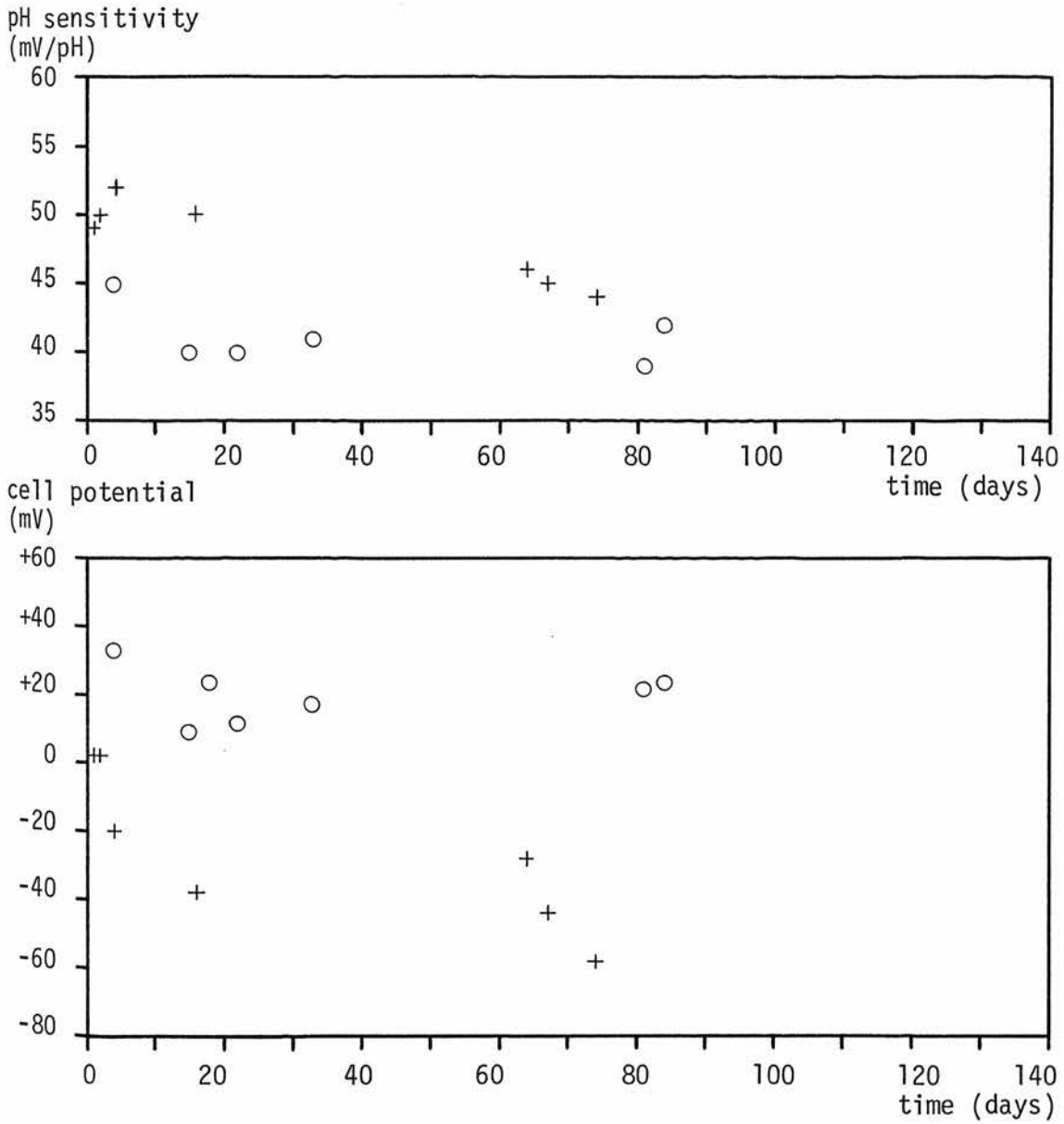

Figure 9.3.3 Time variation of the pH sensitivity and cell potential (at pH 6.54) of copper connected glass disc electrodes

○ Electrode no Cu 1
+ Electrode no Cu 2

Temperature = $30^{o}C$

resulting from temperature variations of the calomel reference element as discussed in Section 8.8. The data obtained from one of these periods of continuous measurement is summarised in Table 9.3.1. The cell potential in the pH 1.09 solution was recorded for a period of 54 hours and its value at six hourly intervals is given in the table. The solution was then changed to pH 4.216 and the cell potential was measured as soon as possible (ie within one or two minutes). Its values at intervals over the succeeding 70 hours were obtained from the chart recorder trace and are also tabulated. The procedure was repeated for each of the remaining solutions, finally returning to pH 1.09. The potential values (apart from that recorded immediately after changing the solution) were constant to within the limits of uncertainty for chart recorder measurements, discussed in Chapter 8. The poorest stability occurred in the sequence of readings in pH 4.216, with a maximum variation of 11 mV over an interval of 18 hours. The range of potentials measured in the pH 1.09 solution was similar at the beginning and the end of the twelve day period over which the data was obtained. It can be seen from Figure 9.3.1 however, that the data of Table 9.3.1 pertain to a period when the stability of the device was greatest and different results would probably have been obtained at other times. The relatively large changes in cell potential which were observed during the 30 minutes subsequent to a change of solution were probably due to temperature effects which will be discussed in Section 9.4. The experimental arrangement used here is not suitable for the investigation of electrode response time because of the time delays and temperature changes which are inevitably associated with a change in test solution pH.

time (hr)	first solution pH 1.09	second solution pH 4.216	third solution pH 6.540	fourth solution pH 9.385	fifth solution pH 1.09
0	-	+32	-78	-192	+150
½	-	+26	-83	-196	+160
1	-	+25	-83	-196	+160
4	-	+24	-84	-194	+159
10	+156	+24	-86	-192	+157
16	+155	+23	-85	-191	+159
22	+155	+22	-86	-192	+158
28	+156	+21	-	-192	-
34	+157	+24	-	-192	-
40	+157	+29	-	-191	-
46	+158	+32	-	-191	-
52	+158	+26	-	-192	-
58	+159	+27	-	-192	-
64	+159	+26	-	-191	-
70	-	+26	-	-192	-

Table 9.3.1 Stability and reproducibility of the potential of a gold connected glass disc electrode (Electrode no Au 2).

The above data were derived from continuous recordings of cell potential, obtained using a chart recorder. The electrode was exposed to each test solution in turn in the sequence shown, starting and finishing with pH 1.09. The entire series of measurements was completed within a period of 12 days (see Figure 9.3.1, Note (c)). The times in the table are referred to the first exposure of the device to each solution. All measurements were carried out at 30°C.

The reproducibility of the cell potential under conditions of changing temperature was also investigated, as a further indication of the stability of the metal contact. The gold connected electrode which was used in the previous work was again employed (see Figure 9.3.1, Note(a)). The temperature was varied repeatedly between ambient and 40°C, the cell potential being measured using a test solution of pH 6.54 and a Simac calomel reference electrode. The oil bath temperature was found to stabilise in less than ten minutes when heating and one hour when cooling. Changes in the cell potential were clearly initiated by the temperature changes but they persisted for, typically, 10 to 20 hours. The reversibility of the effect is indicated by the following sequence of data which were obtained over a period of 24 days. The cell potential was first measured at 30°C and was found to remain between -71 mV and -76 mV for a period of 36 hours. The thermostat was then switched off and the cell was allowed to cool to room temperature for 6 days during which period the potential changed to -12 mV. It was then heated to 30°C again and potentials between -64 mV and -70 mV were subsequently observed for a continuous period of 44 hours. The procedure was then repeated. The potential on this occasion changed to 0 mV at room temperature. When the temperature was increased to 30°C however, the potential was observed to remain between -67 mV and -73 mV for a period of 54 hours. The effects of temperature changes were therefore reversible to within the limits of experimental uncertainty. The temperature coefficient of the cell potential in this case was of the order of -3 mV/deg C but it must be remembered that the filling solution which was used did not necessarily correspond to the iso-potential pH of the cell and different temperature

sensitivities would presumably be observed at other pH values.

The effect of passing current through a metal connected electrode was also studied, again using the same gold connected device (see Figure 9.3.1, Note(b)). The cell potential was first measured for a period of 78 hours (using a pH 6.54 solution at $30^{o}C$) during which it remained between -67 mV and -73 mV. A power supply was then connected between the cell and the 'low' terminal of the electrometer. The electrometer was used in a current measuring mode, as described in Section 8.9 in connection with resistance measurements. The calomel electrode was replaced by a platinum wire to avoid polarising the reference element. The power supply voltage was then adjusted manually to maintain a steady current of 10^{-8} A through the cell for 200 seconds. When the circuit was reconnected for potential measurement (using the calomel reference) it was found that the cell potential was 80 mV more positive than its original value, towards which it was rapidly changing. The cell potential after a further 18 hours was -74 mV and it varied between this value and -77 mV over the following 24 hour period.

The measurements on these electrodes confirmed that significant pH sensitivities could be obtained from glass electrodes employing metal connection. The nature of the contact metal had no bearing on the pH response. The potentials of different devices using the same contact material were different however and the cell potentials varied considerably in the course of the prolonged measurement period of Figures 9.3.1, 9.3.2 and 9.3.3. These results suggest the existence of a non-equilibrium process at the metal contact, as might be expected. It must be remembered however that large and varying asymmetry potentials were also observed in many of the membrane

electrodes of Section 9.2 and the instability cannot therefore be firmly attributed to the metal connection. Furthermore, the gold connected electrode of Table 9.3.1 was substantially stable for a period of 12 days and the same device showed almost complete reproducibility of its potential following temperature changes and current polarisation. The pH sensitivities of these devices declined in the course of several weeks use and the development of electrical leakages must be suspected as a likely cause. The long term stability of the electrodes could well have been influenced by electrochemical emfs associated with the leakage path.

Another batch of metal connected electrodes was prepared, this time using the fused disc construction method of Section 6.7. Discs of 015 glass, 300 μm nominal thickness, were prepared by the standard method of Section 6.5 and subsequently fused to substrates of type EE 1087 glass-ceramic. Contacts of gold, silver and copper were deposited by vacuum evaporation, two samples using each metal being made. The annular contact was omitted from these devices, as was the case with the fused membrane electrodes described in Section 9.2. Electrodes were assembled by attaching a Pyrex tube to the ceramic, using Silcoset 153 silicone rubber adhesive, as shown in Figure 6.7.3. Measurements of pH sensitivity were carried out at 30^{o}C using the thermostat described in Section 8.6. The circuit of Figure 8.3.1 was again employed, the metal back contact of the electrode being connected to the 'high' input terminal of the electrometer. The test solutions derived from BDH buffer tablets were readopted at this stage of the work, in order to reduce the drift of solution pH values which was discussed in Section 8.7. Solutions of pH 4.0, 7.0 and 9.2 were used, together with an 0.1 M solution of hydrochloric acid (pH 1.09). A Simac calomel reference electrode

was again used to make contact with the test solution contained inside the electrode. Readings of cell potential were taken when the meter reading had become steady (by visual estimation), typically 15 to 30 minutes after changing the test solution.

Graphs of cell potential against pH were plotted and, with one exception, were found to be linear with Nernstian slopes of between 59 and 60 mV/pH. The exception was one of the silver connected electrodes for which the potential readings were subject to drift and the response curve was non-linear and sub-Nernstian. For three of these electrodes (one using each of the contact metals) the measurements were repeated several times over a period of 20 weeks. The observed pH sensitivities in all cases lay between 57 and 61 mV/pH. Day to day variations between these limits were random, with no consistent tendency to decline. With very few exceptions, the experimental points lay within $\pm$6 mV of the visually estimated 'best straight line' and in many cases even smaller scatter was noted. (The expected scatter for short term measurements was $\pm$3 mV). Typical curves obtained for each of the three electrodes at the beginning and end of the measurement period are given in Figures 9.3.4, 9.3.5 and 9.3.6. These results contrast markedly with those for the metal connected devices described previously, in respect of both the magnitude of the initial pH response and its maintenance over a prolonged period. As in the case of the membrane electrodes of Section 9.2, the improvements probably resulted from a reduction in electrical leakages obtained by using the fused construction technique.

Cell potentials were also monitored continuously, using the chart recorder. It was found that the potential drifted by as much

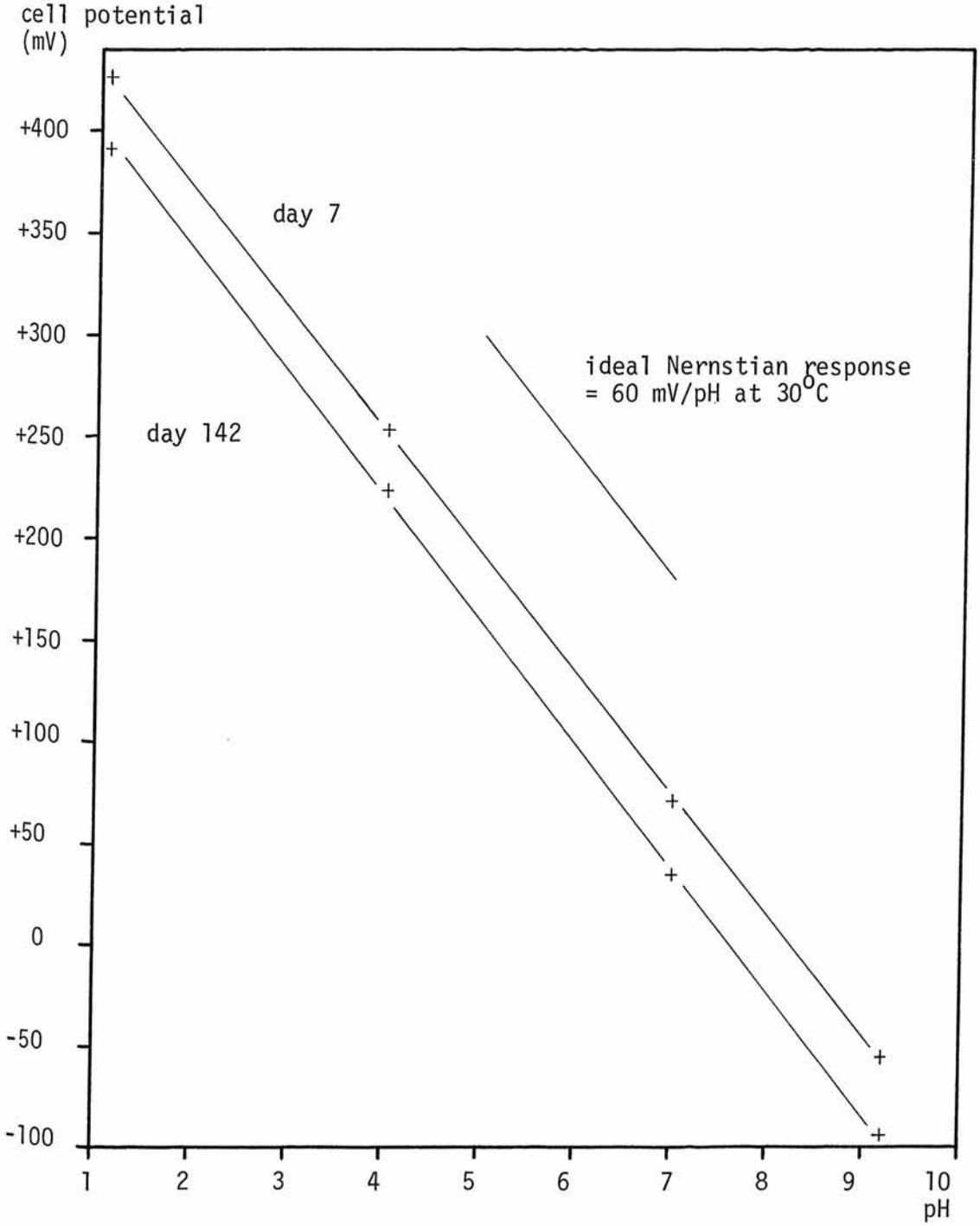

Figure 9.3.4 pH response of a silver connected glass disc electrode of the 'fused' type (Electrode no Ag 5) after 7 days and 142 days exposure to solution.

Temperature = 30°C
The stability *of the cell potential should not be inferred from these graphs owing to uncertainties concerning reference electrode potentials (see text p 174). For stability data, see Table 9.3.3.*

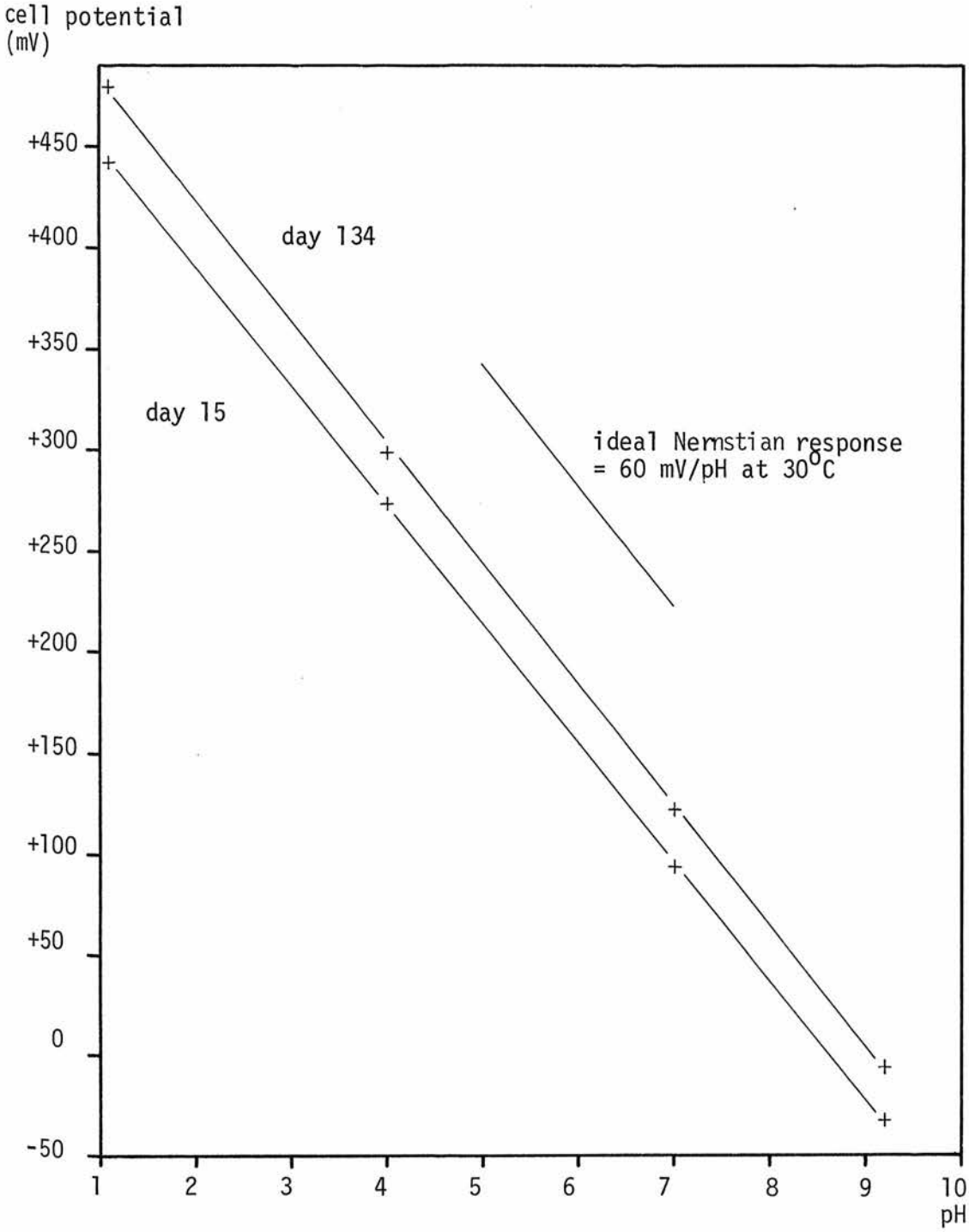

Figure 9.3.5 pH response of a copper connected glass disc electrode of the 'fused' type (Electrode no Cu 7) after 15 days and 134 days exposure to solution

Temperature = 30°C
The stability *of the cell potential should not be inferred from these graphs owing to uncertainties concerning reference electrode potentials (see text p 174). For stability data, see Table 9.3.3.*

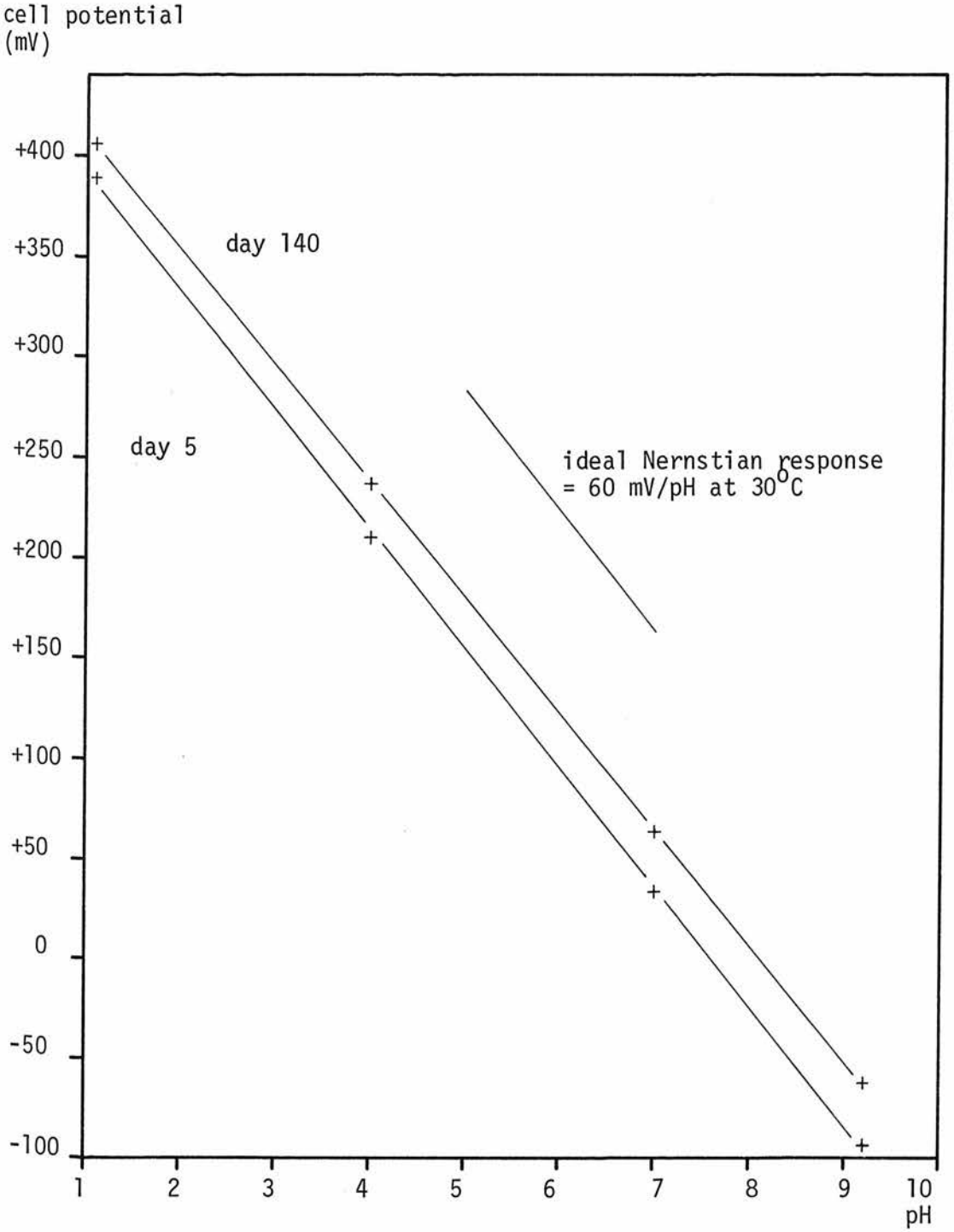

Figure 9.3.6 pH response of a gold connected glass disc electrode of the 'fused' type (Electrode no Au 8) after 5 days and 140 days exposure to solution.

Temperature = 30°C
The stability *of the cell potential should not be inferred from these graphs owing to uncertainties concerning reference electrode potentials (see text p 174). For stability data, see Table 9.3.3.*

as 10 or 15 mV during the hour or so following a change of the test solution. On many (but not all) occasions a reversal then took place in the direction of the drift, a somewhat smaller rate of change in the opposite direction being observed for several more hours. Subsequently, the potential usually remained constant to within ± 2 mV for periods of 10 hours or more (and up to 40 hours on one occasion), which is well within the limits of experimental uncertainty. In one exceptional case however a drift of about 0.5 mV/hour persisted for as long as 15 hours. In the light of earlier work on the response times of glass electrodes[41], it does not seem likely that the change in cell potential was due to the 'true' response time of the glass membrane to solution pH. A more probable explanation is that it was caused by temperature effects associated with the introduction of fresh solution (at room temperature) into the electrode which was thermostatted at 30°C. Table 9.3.2 gives values of cell potential which were measured when the initial drift had become negligible (usually within one to six hours of changing the test solution). The data pertain to one of the copper connected electrodes which was exposed to the four test solutions in turn in each of two series of measurements (in the pH sequence 1.09, 4.0, 7.0, 9.2, 1.09, 4.0, 7.0, 9.2), all of the results in the table being obtained within a period of seven days. These results confirm that the relatively high rates of drift which were sometimes observed over short periods did not persist in the same direction for more than a few hours. The cumulative drift over several days was only a few millivolts and therefore was not significant in terms of the experimental uncertainties. A graph of cell potential against pH, using the data of Table 9.3.2, is plotted in Figure 9.3.7.

pH	cell potential (mV)	
	Series I	Series II
1.09	+457	+460
4.0	+296	+294
7.0	+112	+108
9.2	- 19	- 21

Table 9.3.2 Cell potentials of a copper connected glass disc electrode of the 'fused' type (Electrode no Cu 7, see also Figure 9.3.7).

The above data were derived from continuous (chart recorder) measurements of cell potential at 30°C. They refer to the values of the potential which were observed several hours subsequent to changes in solution pH, when drift had become negligible. The data were obtained over a period of 7 days, the electrode being exposed to the four test solutions in two series of measurements, in order of increasing pH in each case.

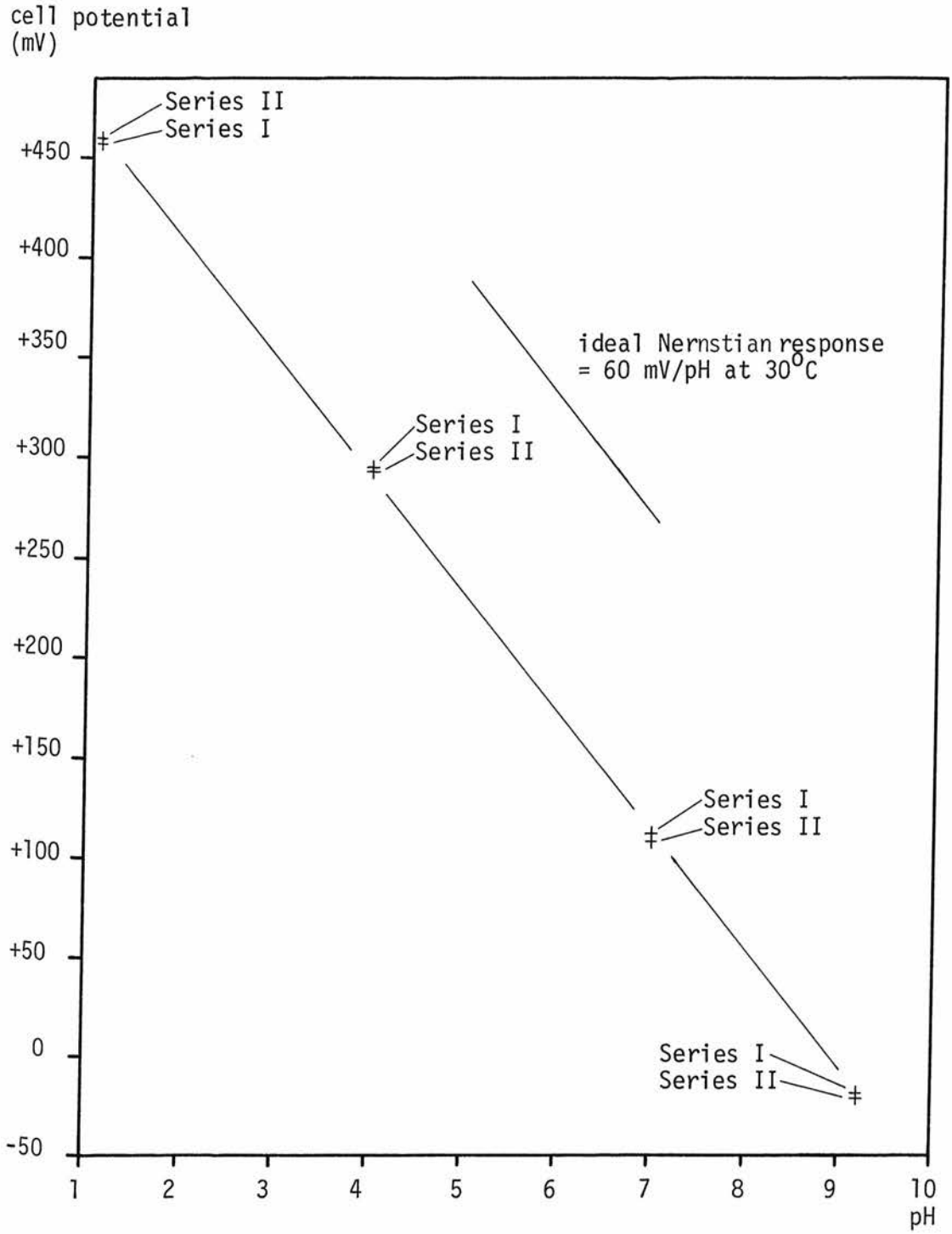

Figure 9.3.7 pH response of a copper connected glass disc electrode of the 'fused' type (Electrode no Cu 7), derived from the data of Table 9.3.2.

Temperature = $30^{o}C$

It was discovered, in the course of making the measurements on the fused metal connected electrodes, that serious drifts had developed between the bias potentials of a certain batch of the Simac calomel reference electrodes. It is unfortunately not clear exactly when the trouble first developed, although electrodes of this type had been used throughout the experimental work and previous occasional checks on bias potentials had given acceptable results. An alternative type of calomel electrode (Type K401, Radiometer A/S) was used for the following measurements of the 'long-term' stability of the cell potential. Two of these calomel electrodes were used as controls. They were stored in a solution of saturated potassium chloride at laboratory temperature. Their bias potentials were measured daily, for a period of several weeks, by placing them in a pH 7 solution which was also at room temperature in order to avoid the rapid temperature changes involved with the use of a thermostat. The readings were taken about one hour after the electrodes were placed in the buffer solution and the maximum observed bias potential was 0.2 mV. The third electrode was used as the working reference for measurements on the experimental devices. It was also stored in a saturated KCl solution and was calibrated before use against the control electrodes in a pH 7 solution as described above. Its bias potential against the control electrodes was never greater than 0.7 mV. Doubts about the long term stability of the reference electrodes were thus substantially removed. Cell potential measurements were carried out using one of the copper connected fused electrodes which was stored in the thermostat at a constant temperature of $30^{o}C$ throughout the measurement period. The device was exposed to a pH 7 buffer solution throughout to avoid any transient effects associated with equilibration at the solution-glass interface. The buffer solution was renewed frequently

to minimise the effect of any drift in its pH value. The solution changes were made immediately *after* each measurement in order to allow ample time (several days) for the cell potential to stabilise before taking the next reading. A drift of the measured potential of, typically, 2 or 3 mV was usually noticed during the hour or so following the introduction of the working reference electrode into the experimental cell. This was presumably due to the temperature change experienced by the calomel element. Readings were taken after one hour when the drift had become negligible. These measurements commenced when the electrode had already been in use for 76 days and they continued over a further period of 35 days. The results are given in Table 9.3.3 from which it can be seen that the total range of the measured values of cell potential was 11 mV. The greatest variation took place at the beginning of the measurement series however and much smaller changes were observed for a considerable time. The drift was clearly not cumulative over the full period. The uncertainty in these measurements (due mainly to the electrometer and to temperature changes affecting the calomel reference element) was probably less than $\pm$3 mV however, so the observed drift must be regarded as significant.

It was clear from the foregoing work that the greatest variations in cell potential occurred during the hours following a change of the test solution. The probable effects of temperature changes on both the glass and reference electrodes have been noted. It was recognised that these effects could have contributed to the scatter of the previously reported electrode response graphs because readings of cell potential were usually taken within 15 to 30 minutes of the change of test solution. The following measurements of electrode response were carried out at room temperature in order to eliminate possible thermal effects. Cell potentials were measured in each of

time (day)	cell potential at pH 7.0 (mV)
76	139
80	128
84	134
93	136
106	132
111	137

Table 9.3.3 Stability of the cell potential of a copper connected glass disc electrode of the 'fused' type (Electrode no Cu 7).

Temperature = $30^{o}C$

the four test solutions as before except that the thermostat was switched off 24 hours before the commencement of the work. The series of measurements was completed within a period of two or three hours during which time the room temperature varied by less than 1 deg C. The electrode potential was monitored, using the chart recorder, for 30 minutes following each change of solution, the record commencing within two or three minutes of the actual change. The experiment was carried out using one electrode with each of the three contact metals and a typical set of results (for a gold connected device) is given in Table 9.3.4. Similar results were obtained with the other electrodes, the variation in cell potential during the 30 minute period being not greater than 2 mV on any occasion. Response graphs were plotted for each electrode (Figure 9.3.8 is a typical example) and the data in each case were found to lie within ± 3 mV of the visually estimated 'best straight line'. This scatter is consistent with the uncertainty estimates of Section 8.10 and is smaller than that which was sometimes observed in measurements made at 30°C, offering further evidence that drifts in the cell potential were caused by thermal effects which accompanied changes in the test solution.

9.4 DISCUSSION AND CONCLUSIONS

Glass disc electrodes were constructed, in both membrane and metal connected form, and significant sensitivities to pH were observed in all but a very few cases.

The discs were simply prepared by cutting 300 μm thick sections from a 22 mm diameter cylinder of 015 glass and subsequently lapping their surfaces to a matt finish, using 400 grade carborundum powder. The effects of annealing the discs and of surface etching and

time (min)	cell potential (mV)			
	pH 1.09	pH 4.0	pH 7.0	pH 9.2
5	+308	+139	-38	-171
10	+308	+139	-39	-171
15	+308	+139	-39	-171
30	+309	+139	-39	-171

Table 9.3.4 Cell potential of a gold connected glass disc electrode of the 'fused' type (Electrode no Au 6) during the 30 minutes following exposure to each test solution at room temperature ($25 \pm 0.5^{o}C$). See also Figure 9.3.8.

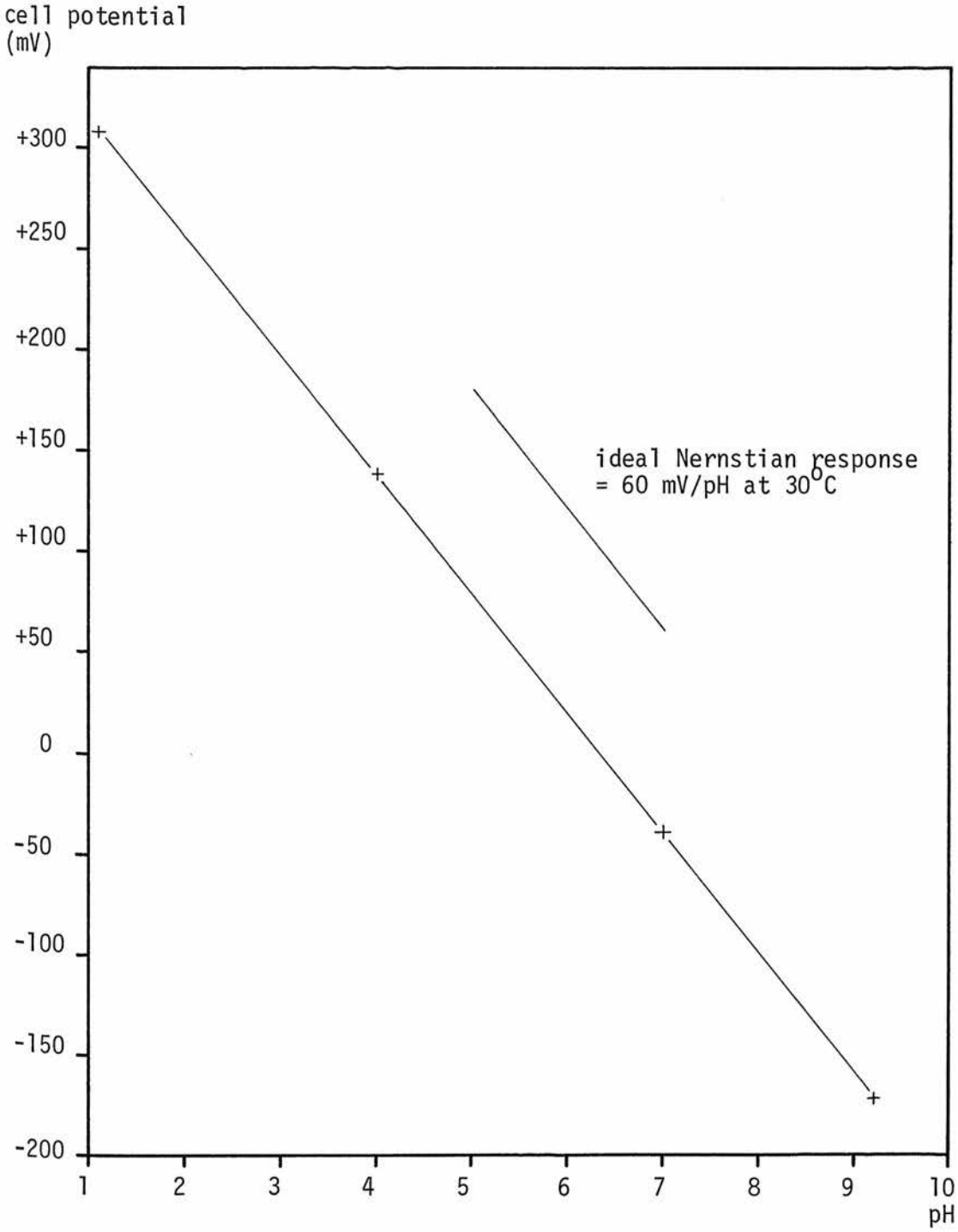

Figure 9.3.8 pH response of a gold connected glass disc electrode of the 'fused' type (Electrode no Au 6).

Cell potentials were measured at room temperature (25°C) after the device had been exposed to each test solution for 30 minutes (see Table 9.3.4).

polishing treatments were also studied but were found to have no influence on pH sensitivity. It seems likely that similar sensitivities would be obtained using 'as sawn' discs although this has not yet been investigated and the surface lapping treatment was employed in all cases.

Many of the electrodes were constructed by sealing the glass disc to a Pyrex tube, using silicone rubber adhesive. The pH sensitivities of these devices were invariably sub-Nernstian and usually declined further after a few weeks exposure to test solutions. An alternative method of construction involved fusing the glass disc (at 600^{o}C) to a suitably pre-formed glass-ceramic substrate. Most of the devices made by this technique had substantially Nernstian pH sensitivities which were maintained during several months exposure to test solutions. The most likely explanation for the failure of the former devices is the development of electrical leakage conductances associated with the direct seal between the adhesive and the glass surface. These difficulties were anticipated, in view of preliminary work on the insulation resistances of similar structures (Section 6.2), although the leakage conductances appeared to be much higher than had been expected. Measurements using the 'annular contact' technique, described in Section 8.5, confirmed that significant leakage effects were present in many of the electrodes. In others however the method implied that insulation levels were much too high to explain the observed decline in pH response and this aspect of the results remains unexplained. It would be interesting, for comparison, to apply the annular contact technique to electrodes constructed by the fusion method. From a practical point of view however, the maintenance of Nernstian responses for prolonged periods provides ample indirect

evidence that leakages were minimal in these devices.

Metal connected electrodes were fabricated using silver, copper, gold and nichrome-gold contacts. Their pH sensitivities were similar to those of the membrane electrodes and were independent of the nature of the contact metal.

Electrode sensitivities were obtained by plotting graphs of cell potential against pH. The scatter of the experimental data was generally rather greater than would be expected from the experimental uncertainties deduced in Chapter 8. This was probably a consequence of temperature changes caused by the introduction of test solutions (at room temperature) into electrodes which were maintained at 30^{o}C in a thermostat. Metal connected electrodes comprise asymmetrical cells for which the iso-potential pH is not known and large temperature coefficients of potential were observed. Furthermore, the response time of the cell potential to temperature changes was protracted and temperature induced drifts persisted for several hours. The electrode sensitivity data were usually obtained over a much shorter period and were therefore subject to drift as a result of the thermal effects associated with changing the test solutions. The scatter is smaller in the case of Figure 9.3.8, which is derived from data obtained at room temperature. It must also be remembered that many of the electrodes were affected by electrical leakage which may well have contributed to the scatter of the data.

Two possible sources of error, additional to those discussed in Chapter 8, were identified in the course of carrying out the experimental work. They involved drifts in the bias potentials of calomel reference electrodes and in the pH values of certain test

solutions. The former problem was associated with a certain batch of 'Simac' calomel electrodes and is thought to be the result of a manufacturing fault. For the purposes of future work, it is strongly recommended that two or more electrodes should be used as control devices, their bias potentials being monitored daily. The working reference should then be compared against the controls before every measurement, as described in the previous section. The second difficulty concerned the drift in the pH values of the test solutions of Table 8.7.1. A brief investigation of this matter, described in Section 8.7, indicated a drift of 32 mV over three days[†]. It is unlikely that the reference electrode drift was sufficiently fast to contribute to the scatter of the response graphs, for which the values of the cell potential in all of the test solutions were obtained within a short period of time, using the same reference electrode. Solution pH drift however might well have contributed to the scatter in some of the results.

The long term *stabilities* of disc electrodes of the membrane type were measured, for comparison with the metal connected devices. The potentials of these symmetrical cells were surprisingly large in many cases and showed greater day to day variations than many of the metal connected electrodes. It was noticed that there was some correlation between the day to day variations for different devices however and this suggests that the effect may have partly originated in the measurement system. (It should be borne in mind that the measurements on membrane electrodes of the *fused* type were made at

---

[†]The method involved the measurement of the *difference* in potential of a commercial glass electrode when transferred between two of the solutions. It should not therefore have been affected by any drift of reference electrode potential which might have taken place during the three day period.

room temperature, whereas much of the other data was obtained at 30°C). The previously noted drifts in reference electrode potentials and test solution pH values could have contributed to the apparent instability of these cells. It was shown in Section 9.2 however that the observed drifts in cell potential could not always be attributed entirely to these effects. Furthermore, it is not clear why the observed stability in many cases (eg Table 9.3.1) was actually much better than would be expected in view of the extent of the solution pH drift noted above.

In the case of metal connected electrodes, the stability of the electrode potential is of interest, both as a practical performance specification and as an indication of the thermodynamic reversibility of the process taking place at the metal contact. The potential of a copper connected electrode cell (of fused construction) was measured several times, at constant temperature, over a period of 35 days. The total range of the measured values was 11 mV which is larger than would be expected from the estimated experimental uncertainties. (The drifts in reference electrode potential and solution pH had been recognised when these measurements were made and precautions were taken to eliminate their effects). In view of the unexplained drifts noted in connection with the 'control' measurements on membrane electrodes however, the above data cannot be regarded as conclusive evidence of instability due to the metal contact. Furthermore, it is well known that the asymmetry potentials of conventional membrane electrodes can drift by several millivolts from day to day. Measurements over a 12 day period on a gold connected electrode (fabricated by the direct adhesion method) gave similar results to those obtained using the copper connected device described above.

The potential of the gold connected electrode varied more widely over a longer period but it must be noted that leakage effects could have influenced these results. The same gold connected electrode was employed in studies of the effect on cell potential of temperature changes and current polarisation. Potential changes of between 60 and 80 mV were induced by varying the temperature of the cell or by passing current through it. When the initial conditions were restored, it was found that the potential continued to drift for, typically, 10 to 20 hours. The range of potentials observed over a subsequent period of several hours lay within 12 mV of the values measured prior to the experiment. This data was derived from extensive chart recorder measurements, for which the expected uncertainty limits were only slightly less than the range of measured values. The results might also have been affected by the previously noted drifts in reference electrode potentials and test solution pH values, as well as by leakage effects.

Despite the large uncertainties in some of these measurements, they nevertheless indicate a degree of stability in the potential of metal connected electrodes which is comparable with that of conventional glass membrane electrodes. This stability, especially under conditions of varying temperature and current polarisation, suggests the existence of a fairly well defined process at the metal contact.

The deficiencies of the simple oil-bath thermostat described in Section 8.6 have already been noted. The temperature of the calomel reference electrode was not adequately controlled using this system and the glass disc electrode itself was subject to temperature changes as a consequence of the introduction of cold test solutions into the electrode at $30^{o}C$. These effects were probably largely responsible

for the drifts in cell potential which took place following changes of the test solution. The maximum possible heating and cooling rates of the oil bath were too slow to be regarded as step changes in temperature, for the purpose of temperature response measurements. The response time of the change in cell potential was too long to be attributed purely to thermal mass effects however and the magnitude of the potential change was much greater than would be expected as a consequence of the temperature coefficient of the calomel electrode (Section 8.8). It follows that the change in cell potential was largely due to the effect of temperature on the metal contact to the glass disc. The protracted response to temperature changes requires further investigation and could be a serious drawback in a practical electrode.

The potential drifts of the metal connected electrode cells (see Figures 9.3.1 to 9.3.3) were of the same order as the published data for similar devices (reviewed in Section 5.2). The long term drift of Thompson's electrode[74] for example was of the order of 75 mV over 250 days and the devices reported by Guignard and Friedman[78] drifted by about 100 mV over ten months. The drift of the latter devices was alternatively quoted as 0.2 mV/hour which again compares with the results of the present work. In Thompson's work[74] however, the effect of current polarisation appeared to be irreversible. The stability of the metal connected electrodes in the present work was at least equal to that of the more complicated metal-metal halide connected devices described in a patent filed by Beckman Instruments Inc[81]. The best stability claimed in the latter work corresponded to a variation in cell potential of 12 mV over a three day period during which the temperature was varied between 25°C and 40°C. The

performances of some of the electrodes quoted were even poorer.

The fused method of device fabrication should clearly be used in further studies of the performance of metal connected electrodes. More detailed investigation of the temperature dependence of cell potential is especially necessary, in order to distinguish between temperature induced drift and 'random', long term effects. The iso-potential points of metal connected cells should also be established by carrying out response measurements over a range of temperatures. An improved type of thermostat will be required for this purpose. It should control the temperature of the entire cell (including reference electrodes) and be adjustable over a wider temperature range with more rapid response time. Means should also be provided for changing test solutions without causing temperature changes. The use of a small air conditioned room would offer the ideal solution.

Continuous monitoring of reference electrode bias potentials and test solution pH values should be routine in future work. The use of silver-silver chloride reference electrodes (without liquid junctions) would eliminate one source of experimental uncertainty. This would involve the use of the test solutions of Table 8.7.1 and precautions would be required to prevent errors in long term measurements resulting from drifts in solution pH. The use of a cell without liquid junction would also simplify the thermostat since the reference electrode would be in direct contact with the filling solution.

Another important objective of future work will be the comparison of the standard cell potentials of different electrodes

using the same contact metal. The effect of different metals on the standard potential should also be studied. These measurements will require a degree of stability which was not obtained in much of the work described in this chapter. It should be achievable however, by using electrodes of the fused type in conjunction with the suggested improvements in the experimental techniques.

It is strongly recommended that future work on metal connected electrodes should again be supported by control measurements on membrane electrodes, as a means of revealing drifts which might originate in the measurement system itself. For this purpose, the thermostat should be designed to accommodate membrane (as well as metal connected) electrodes to permit measurements on both types of device under similar conditions. It is particularly important to establish whether the large asymmetry potential drifts which were noted in Section 9.2 can be reduced by the suggested improvements in experimental technique.

CHAPTER 10: CONCLUSION

The application of microelectronic techniques to the construction of ion sensitive devices is expected to offer certain advantages, especially in respect of mechanical durability and reliability.

It has been shown that the use of microelectronic methods will lead to a planar device incorporating solid state connection to the ion sensitive material. Two classes of solid state contact have been identified, namely the 'field effect' and 'potentiometric' types. The mechanism of operation of each class of device has been discussed from a theoretical standpoint, with particular reference to the ion sensitive field effect transistor (ISFET) as an example of the former type. It is clear that both types of device would be expected to be sensitive to changes in ion activity but their long term stability and reproducibility is less certain.

An important conclusion from the theoretical arguments is that it is necessary to use a suitable reference electrode in conjunction with sensors employing either type of contact. This conclusion has been supported by other workers in the field[91,92], although it is at variance with the opinion expressed in certain previously published work[93] concerning the ISFET. It is believed that the requirement for a reference electrode places serious limitations on the benefits which may be realised by means of the microelectronic approach because experience with conventional electrode systems suggests that their deficiencies are often associated with the reference electrode rather than with the ion sensitive device itself. The relevance of the microelectronic approach to a particular application can clearly be judged only with full regard to the requirements of the overall system

of sensing and reference elements. Examples of appropriate applications (activity ratio measurement, for example) were noted in Section 5.4.

It has been shown that severe practical difficulties are involved in the encapsulation of microelectronic ion sensors. The 'active' area of the device is exposed to aqueous solution but a high level of electrical insulation of neighbouring parts must be maintained. The problem is especially severe with field effect devices, such as the ISFET, which involve wire bond connections to the face of a silicon chip, in close proximity to the active area. Devices which rely upon the direct adhesion of organic materials (eg silicone rubber) to glass surfaces have generally been found to fail after a few weeks use, presumably as a consequence of electrical leakage effects. It has been noticed in this connection that it is especially difficult to obtain good adhesion to ion-sensitive glass, although acceptable performance has been observed in devices involving adhesion to Pyrex and glass-ceramic surfaces. Certain improvements to the techniques described in this thesis could be investigated. They include refinements to the method of application of silicone rubber or epoxy encapsulants, which have been described by Donaldson[99], and the use of suitable primers in conjunction with these materials[102]. It is considered unlikely that adequate performance will be obtained by direct adhesion to glass surfaces however and it is strongly recommended that the alternative 'fused' method of construction is employed in future work. Its application to ISFET devices would not be straightforward however.

One consequence of the development of electrical leakage is that the apparent ion sensitivity of a potentiometric device is reduced to

less than the Nernstian value. The converse is not necessarily true however and a decline in sensitivity could result from causes other than poor insulation. The annular contact technique described in Section 8.5 allows a more direct measurement of leakage conductances and it confirmed their presence in many of the electrodes which were studied. Several anomalies were noticed in the results of measurements using this method however and they show the difficulty of obtaining satisfactory data from devices in which significant leakage is present.

Ion sensitivity measurements have been carried out on both field effect (ISFET) devices and on potentiometric electrodes employing direct metal contacts to pH sensitive 015 glass. The pH sensitivity of both types of device was confirmed but the stability and reproducibility of the ISFETs was poor, probably as a result of electrical leakages. The interpretation of the ISFET results was further complicated by the unknown selectivity of the silicon dioxide film which acted as the ion sensitive material in these devices.

It is felt that the attractiveness of the ISFET is severely prejudiced by the now widely recognised requirement for a reference electrode and by the difficulties of encapsulation. The alternative 'hybrid circuit' approach (described in Chapter 5) appears to be more promising, provided that sufficiently stable potentiometric contacts can be implemented.

The properties of potentiometric contacts have been studied using metal connected glass disc electrodes. Devices of this type which were fabricated by direct adhesion of silicone rubber to glass were again prone to early failure. Greatly improved performance was obtained using electrodes in which the glass disc was fused to a

pre-formed, glass-ceramic substrate. The pH sensitivities of metal connected electrodes constructed in this way remained Nernstian for several months. The stability of these devices was similar to published data for metal connected electrodes. The electrode potential drifted for many hours following a temperature change however and this could be a serious disadvantage in a practical measurement system. Further work is necessary to distinguish the temperature induced drift from other possible sources of long term instability.

It is expected that the fused disc electrode structure will be applicable to further studies of the performance and mechanism of solid connected electrodes of the potentiometric type. The reproducibility of the standard potential of metal connected electrodes must be investigated by measurements on several devices using the same contact metal. Differences in standard potential between devices using dissimilar metals should also be studied. As noted in Section 5.2, it might be possible to obtain information about the nature of the electrode process which takes place at the metal contact by means of an investigation of the effect on the cell potential of the partial pressures of gases in the atmosphere. The properties of two-layer metal-metal halide contacts (described in Section 5.2) should also be studied, for comparison with the simple metal connected type. The fused disc structure could again be used. A film of halide doped glass could be printed on to the reverse side of an 015 glass disc, using the thick film circuit process. The film would be fired at the same time as the disc is fused to the glass-ceramic substrate. Deposition of the metal contact (on top of the halide doped layer) would be as before. Possible difficulties associated with the deposition

of the ion sensitive glass in film form would thus be avoided and a direct comparison with the metal connected devices would be possible. It is appropriate to recall at this point that the stability of the single layer metal connected electrodes reported in Chapter 9 was equal to that of metal-metal halide devices which have been described in the literature and reviewed in Chapter 5.

The fused disc technique was originally developed as an experimental vehicle for investigating solid state potentiometric contacts, prior to the fabrication of 'microelectronic' electrodes by the deposition of films of ion sensitive material. It is now considered however, that the fused disc structure itself may have direct practical application. The use of a glass-ceramic tube, instead of the usual 'stem glass', would enable glass membrane electrodes to be fabricated by fusion in a furnace, instead of by conventional 'flame-working' methods. The fusion technique seems more appropriate to large scale production and improved performance may be obtained as a result of greater reproducibility and uniformity of the thickness and surface condition of the glass membrane. It must be understood however that a commercial device would employ an ion sensitive glass of more modern composition than 015 and a glass-ceramic of appropriate thermal expansion coefficient would be required. The fused disc electrode also suggests an alternative form of the 'thick film' electrode proposed in Section 5.2. A device similar to that shown in Figure 5.2.4 could be fabricated by depositing the back contact materials (single or multi-layer) on to an inert substrate and subsequently fusing on a thin ion sensitive glass membrane, as an alternative to depositing a film of the glass. This method could be used if the film deposition process is found to have an adverse effect on

the properties of the ion sensitive glass or if greater thicknesses than can be achieved with printed films are required. It is clear that devices of this type (or those incorporating a deposited film) would require a substrate which has an expansion coefficient similar to that of the ion sensitive glass which is employed. The required properties of the substrate material (eg expansion coefficient, softening temperature, electrical resistivity and adhesion to the ion sensitive glass) are similar to those of the 'carrier' or 'substrate' in the fused disc structure described in Section 6.7 and it is expected that the glass-ceramics would again be suitable.

Ion selective glass was chosen as the sensor material for the work described in this thesis because the mechanism of the glass electrode has been extensively studied and because a large market exists for glass pH electrodes. Certain of the other ion sensitive materials which were briefly reviewed in Section 2.4 may be more appropriate to the microelectronic approach however. The constructional difficulties associated with achieving adequate adhesion to glass surfaces would not arise and, in the case of metal-metal salt electrodes, a mechanism has been proposed for the process which takes place at the solid contact.

It is clear that the application of microelectronic production methods will allow many interesting developments in the technology of ion sensitive electrodes. It must be recognised however that the advantages of the microelectronic device may not be fully realised in measurement systems in which a conventional reference electrode must be employed. In the case of devices using ion sensitive glass, further work is required to establish the stability and operating mechanism of the solid state contact.

APPENDIX 1: THE LIQUID JUNCTION POTENTIAL

The liquid junction may be regarded as the simplest case of a boundary between two electrolytes since no limitation is imposed on the transport of any ion across the junction[120]. Each ion diffuses freely across the junction and a diffusion potential arises as a consequence of the different mobilities of the several ions involved. The potential between the electrically neutral bulk solution phases is known as the 'liquid junction potential'. It should be noted that the diffusion processes involved are of an essentially non-equilibrium nature and are associated with a continuing transference of ions between the electrolytes on either side of the junction.

For a system in which the concentrations etc vary only in the x-direction, the flux of species k is given by the Nernst-Planck equation (Equation 3.2.5), in which unity activity coefficients are assumed.

$$J_k = -RT\, u_k \frac{dc_k}{dx} - u_k\, c_k\, z_k\, F \frac{d\psi}{dx} \qquad (3.2.5)$$

The zero current condition is expressed by

$$\Sigma\, z_k\, F\, J_k = 0$$

By solving the above equations for $\frac{d\psi}{dx}$, it can be shown that

$$\frac{d\psi}{dx} = -\frac{RT}{F} \Sigma \frac{t_k}{z_k} \frac{d}{dx} \ln c_k$$

where t_k is the 'transport number' of species k, given by

$$t_k = \frac{z_k^2 u_k c_k}{\Sigma z_k^2 u_k c_k}$$

The liquid junction potential is then given by the commonly used equation[24,120]

$$E_j = \psi'' - \psi' = - \frac{RT}{F} \sum \int_{c_k'}^{c_k''} \frac{t_k}{z_k} d \ln c_k \qquad (A1.1)$$

where the single and double primes denote the solutions at each side of the junction.

For the special case in which a *single* electrolyte is present at different concentrations on each side of the junction, it follows from a consideration of charge neutrality in the interphase region that the transport numbers, t_+ and t_-, of the positive and negative ions are constant (independent of x). Equation A1.1 can then be integrated[120] to give

$$E_j = - \frac{RT}{F} \left(\frac{t_+}{z_+} + \frac{t_-}{z_-}\right) \ln \frac{c''}{c'}$$

where c' and c" represent the concentrations of the electrolyte in the bulk solutions on each side of the junction. If all the ions involved are monovalent, the previous equation further reduces to

$$E_j = - \frac{RT}{F} \left(\frac{u_+ - u_-}{u_+ + u_-}\right) \ln \frac{c''}{c'}$$

where u_+ and u_- are the mobilities of the positive and negative ions.

Integration of Equation A1.1 is more difficult in the general case in which there are several electrolytes in the solutions. A simplification which is commonly employed is the so-called 'Henderson approximation', in which the concentration of each species is assumed to vary linearly with distance through the junction, the boundary values being the concentrations in the bulk solutions. Integration of Equation A1.1 then gives[120]

$$E_j = - \frac{RT}{F} \frac{\Sigma z_k u_k (c_k'' - c_k')}{\Sigma z_k^2 u_k (c_k'' - c_k')} \ln \frac{\Sigma z_k^2 u_k c_k''}{\Sigma z_k^2 u_k c_k'}$$

The Nernst-Planck equations can be integrated without the use of the simplifying Henderson approximation but an explicit expression for the liquid junction potential cannot be obtained. The mathematical procedure has been reviewed by Koryta[120], for the case of an electrolyte comprising only monovalent ions under steady state, zero current conditions. The value of the liquid junction potential is obtainable from Equations 2.2.23 and 2.2.32 of the above mentioned review[120], which may be written in the present notation as

$$E_j = \frac{RT}{F} \ln \xi$$

$$\text{and} \quad \frac{\xi U'' - U'}{V'' - \xi V'} = \frac{\xi c'' - c'}{c'' - \xi c'} \frac{\ln \frac{c''}{c'} - \ln \xi}{\ln \frac{c''}{c'} + \ln \xi} \qquad \text{(A1.2)}$$

where $U'' = \Sigma u_i c_i''$

$V'' = \Sigma u_j c_j''$

$U' = \Sigma u_i c_i'$

$V' = \Sigma u_j c_j'$

$$c' = \Sigma\, c_i' = \Sigma\, c_j'$$
$$c'' = \Sigma\, c_i'' = \Sigma\, c_j''$$

and the single and double primes denote the solutions on each side of the junction.

The liquid junction may also be regarded as a limiting case of the fixed charged membrane for which the membrane charge, c_S', tends to zero. The total membrane potential in this case is obtainable from Equations 3.4.5 and 3.4.26. The latter equation is expressed entirely in terms of solution concentrations and may be re-written in the notation employed above by using single and double primes respectively to denote the solutions adjacent to the membrane surfaces at x = 0 and x = d. Putting

$$U'' = \Sigma\, c_{id}''\, u_i'$$
$$V'' = \Sigma\, c_{jd}''\, u_j'$$
$$U' = \Sigma\, c_{io}''\, u_i'$$
$$V' = \Sigma\, c_{jo}''\, u_j'$$
$$c'' = c_d''$$
$$c' = c_o''$$

the equation becomes

$$\frac{\xi' U'' - U'}{V'' - \xi' V'} = \frac{\xi' c'' - c'}{c'' - \xi' c'} \quad \frac{\ell n \frac{c''}{c'} - \ell n\, \xi'}{\ell n \frac{c''}{c'} + \ell n\, \xi'} \qquad \text{(A1.3)}$$

which has the same form as Equation A1.2.

APPENDIX 2: MASS TRANSFER THROUGH MEMBRANES

Consider the Donnan equilibrium described in Section 3.3 in which the monovalent ions, A^+ and B^-, are permeable through the membrane and an impermeable singly charged species, S^-, is present at concentration $c_S^{-'}$ on one side of the membrane only. Suppose the *initial* concentrations of these species are

$$c_A^{+'} = c_S^{-'} = c_o$$

and $$c_B^{-'} = 0$$

in the solution on the (') side of the membrane and

$$c_A^{+''} = c_B^{-''} = \tfrac{1}{2} c_o$$

and $$c_S^{-''} = 0$$

on the (") side. We note that these conditions satisfy the requirements of charge neutrality in each solution and that there are concentration gradients of each species across the membrane. Diffusion of the permeable species will therefore take place and, when thermodynamic equilibrium is reached, the *equilibrium* concentrations must satisfy the Donnan relationship of Equation 3.3.5. That is, assuming unity activity coefficients,

$$c_A^{+'} \, c_B^{-'} = c_A^{+''} \, c_B^{-''}$$

The conditions for charge neutrality in each solution are expressed by the equations

$$c_A^{+'} = c_B^{-'} + c_S^{-'}$$

and $$c_A^{+''} = c_B^{-''}$$

The total amounts of A^+ and B^- in the system must be the same at equilibrium as they were initially. Hence, assuming for simplicity that we have unit volumes of solution on each side of the membrane, we may write for the equilibrium concentrations

$$c_A^{+'} + c_A^{+''} = \frac{3}{2} c_o$$

and $$c_B^{-'} + c_B^{-''} = \frac{1}{2} c_o$$

By solving the above set of five equations it can be shown that the *equilibrium* concentrations are given by

$$c_A^{+'} = \frac{9}{8} c_o$$
$$c_B^{-'} = \frac{1}{8} c_o$$
$$c_A^{+''} = \frac{3}{8} c_o$$
$$c_B^{-''} = \frac{3}{8} c_o$$

It can be seen that, in this particular case, a large (25%) change has taken place in the concentration of solution (") and, furthermore, that species A^+ has been transported *against* the 2:1 concentration gradient which was initially present.

APPENDIX 3: THE SPACE CHARGE NEUTRALITY ASSUMPTION

One of the assumptions which is commonly employed in the analysis of membranes is that of 'macroscopic space charge neutrality'. It is used for example in the analysis of the liquid junction potential[120], in the TMS theory of Section 3.4 and in the glass electrode theory of Chapter 4.

Poisson's equation (from electrostatics) states that, for the one dimensional case,

$$\frac{d^2\psi}{dx^2} = \frac{q(x)}{\varepsilon}$$

where $q(x)$ is the charge density and ε is the dielectric constant of the medium. If $q(x) = 0$, the space charge neutrality condition, it follows directly that $\frac{d\psi}{dx}$ is a constant and that the electrical potential varies linearly with distance through the membrane. Analyses which use the space charge neutrality condition however sometimes predict non-linear potential profiles. An example is the derivation of the liquid junction potential presented by Koryta[120]. Integration of Equation 2.2.21 of that analysis yields a logarithmic dependence of potential on distance. In other cases however a linear potential profile does in fact arise. A case in point is the analysis by Karreman and Eisenman[67] of the glass electrode potential under steady state, zero-current conditions.

Several authors have noted this inconsistency and offered alternative methods of analysis. Hafemann[121] carried out a computer

simulation of a simple liquid junction case without assuming electroneutrality. The results indicated that the electroneutrality condition is approximately valid for the usual experimental time scales (ie after several tens of nanoseconds from the formation of the junction) and also showed that the potential is substantially constant after such an interval. MacGillivray[122] employed 'perturbation theory' to solve the Nernst-Planck equations and Poisson's equation for a fixed charge membrane. He concluded that the electroneutrality condition emerges as a limiting case and furthermore that the existence of a Donnan equilibrium at the phase boundaries is a consequence of the Nernst-Planck-Poisson system of equations. This may be regarded as an analytical justification of the model employed in the TMS theory. On the other hand, Okongwu et al[123] have suggested that the inconsistency may be resolved by including the effects of polarisation charges, associated with instantaneous diffusion configurations, which generate the correct diffusion potential. Cooper[124] has presented an analytical solution to the flux equations and Poisson's equation for the limits $t \to 0$ and $t \to \infty$. For the long time limit, the Nernst-Planck equations result.

It must be noted that in spite of the apparent inconsistency in the assumptions, results derived using the space charge neutrality condition have been frequently verified by experiment over many years.

APPENDIX 4: PUBLISHED WORK

Electrochimica Acta, 1977, Vol. 22, pp. 1–8. Pergamon Press. Printed in Great Britain

MICROELECTRONIC APPROACHES TO SOLID STATE ION SELECTIVE ELECTRODES*

R. G. KELLY

Wolfson Microelectronics Liaison Unit, Department of Electrical Engineering, University of Edinburgh, Edinburgh, Scotland

(*Received* 5 *April* 1976)

Abstract—The application of microcircuit production techniques to the construction of ion-sensitive devices is discussed. A qualitative model for the operation of the Ion Sensitive Field Effect Transistor (ISFET) is presented. Alternative devices to the ISFET, also based on microelectronic methods, are proposed.

1. INTRODUCTION

Many novel ion-sensitive materials have been developed in recent years for electrode use. New glass compositions have led to improvements in the well-known glass pH electrode and have allowed the development of Na^+ sensitive and cation sensitive glass electrodes[1]. Liquid membrane electrodes showing selectivity to various anions and cations, including NO_3^-, ClO_4^- and Ca^{2+} have been reported[2]. New types of 'solid state' membrane have been discovered. These include the F^- electrode, which comprises a thin section of crystalline lanthanum fluoride doped with europinum[2], and membranes prepared from mixtures of the sulphides and halides of silver and other metals (such as Pb, Cu and Cd) which have been shown to respond to ions including CN^-, Cu^{2+}, Pb^{2+} and Cd^{2+}[2]. 'Heterogeneous' solid membranes have also been developed, in which the ion sensitive material is embedded in an inert binder such as PVC[3]. Responses to cations and anions, including K^+ Ca^+ and NO_3^-, have been reported[4]. The field has been extensively reviewed by Koryta[5] and Buck[6].

In addition to analytical laboratory applications, electrode measurements are useful in a wide variety of field situations. An important example is the monitoring of pollutants (*eg* F^-, NO_3^-, S^-, Pb^{2+}, Cd^{2+}) in public water supplies and industrial effluents. Industrial applications include measurement of hardness (Ca^{2+}) in boiler feed waters and on-line analysis of industrial processes such as electroplating (F^-,CN^-), photographic processing (halides) and the manufacture of foodstuffs (Pb^{2+}, CN^-). Biomedical applications include the measurement of ions such as Na^+ and Ca^{2+} in blood and chloride levels in sweat for rapid screening for cystic fibrosis. These and many other applications are cited in Refs [7] and [8] and in the further references therein.

For use in field applications, however, improvements in the sensitivity and selectivity of the electrodes must be accompanied by the development of improved mechanical structures. Techniques well known in the production of microelectronic circuits may offer the means of achieving such improvements. In this paper, the methods used in microcircuit production will be briefly summarized and their application to electrode construction will be indicated.

One example of the microelectronic approach is the Ion Sensitive Field Effect Transistor (ISFET) which was first reported by Bergveld [9]. The ISFET is an ion sensitive sensor based on the well known Field Effect Transistor (FET) and is described in Section 3, below. Bergveld's device employed a thin (2000 Å) layer of thermally grown silicon dioxide as the ion sensitive material. The device responded to the concentration of H^+ and Na^+ in solution, although the magnitude of response and selectivity varied considerably between samples. The measured output quantity of an ISFET is the drain current (see Section 3, below) but Berveld calculated that the equivalent potential response was between 10 mV and 100 mV per decade of Na^+ over the range 0.001 M to 1.0 M NaCl. A similar device, due to Leistiko[10], responded to H^+ over the range pH 1–pH 9, the calculated equivalent potential response varying between devices from the Nernstian value to approximately one half of that magnitude. A nearly equal response to K^+ and smaller responses to Na^+ and Ca^+ were also noted. At least two time constants were identified, the slower being of several minutes. Furthermore, results were found to be dependent on device history. 'Doping' the silicon dioxide with boron and phosphorus was found to have no significant effect on the chemical response. Another ISFET described by Matsuo and Wise[11] employed a layer of silicon nitride deposited on top of the 'gate oxide' of the FET structure and in contact with the solution. A nearly linear response to H^+ over the range pH 1 to pH 10 was reported, the calculated equivalent value being nearly Nernstian. The observed response to K^+ and Na^+ was very small. A significant feature of the ISFET due to Moss, Janata and Johnson[12] was the use of a material which is known to be ion sensitive, deposited on top of the conventional FET gate dielectrics. The chemically sensitive material chosen was valinomycin/plasticizer/PVC which is selectively sensitive to K^+ ion[13]. Following an initial preconditioning period of up to 100 hours, the devices were observed to respond to K^+ concentration, the equivalent Nernstian response being calculated between 50 and 60 mV/

* This work has been supported by a grant from the Water Research Centre, Stevenage, Hertfordshire.

decade of K^+. Selectivity over Na^+ was given by $-\log K_{K,Na} \doteq 3$. Decreasing stability and device failure occurred after 380 to 415 h.

A model for the operation of the ISFET devices will be presented in this paper. Alternative structures to the ISFET, also based on microelectronic methods, will be proposed.

2. MICROELECTRONICS TECHNIQUES

The term 'microcircuits' embraces a wide range of circuit types which may be classified for the present purpose into (a) monolithic silicon integrated circuits[14] and (b) hybrid film circuits[15, 16] ('thick-film' and 'thin-film' types). The monolithic circuit is manufactured by the diffusion, growth or deposition of various materials on to a wafer of the semiconductor starting material (usually silicon). The entire circuit (conductors, resistors, capacitors and transistors) is thus embodied in a single, solid material phase as a 'chip', typically 5 mm square. The chip is then 'packaged' for mechanical and environmental protection, connection to the chip within the package being by fine (typically 5 μm dia) wire bonds. In the 'hybrid' microcircuit, the conductors, resistors and sometimes dielectrics are deposited as patterns of material on an inert substrate, transistors and other active devices then being attached to the substrate by the wire bonding method. The thin film technology employs films of materials deposited, usually by vacuum evaporation, in layers typically 1 μm thick. In the thick film process, the materials are dispersed in a colloidal solution to form an ink and the circuit patterns are formed directly by a screen printing process, subsequent heat treatment being used to drive off solvents and fire the materials into homogenous films, typically 15–20 μm thick.

Processes involved in these technologies include:

(a) bulk materials preparation methods including high precision crystal cutting and polishing (*eg* of silicon wafers),

(b) film preparation methods including high vacuum techniques such as evaporation and sputtering and high temperature processing such as diffusion, oxidation and firing (of thick films),

(c) photolithographic and selective etching techniques for high precision definition of patterns in the film.

These processes exist in the highly developed form which is required to manufacture reliable circuits reproducibly on a commercial scale. In particular, methods of ultra-clean working allow excellent control of chemical purity, controllable doping levels of 1 per 10^7 atoms being obtainable for instance. The processes are characteristically capital intensive, allowing low unit costs in large scale production.

The application of microelectronic techniques to the fabrication of ion selective electrodes will lead to an essentially planar structure involving a film or wafer of the ion sensitive meaterial to which electrical contact is made through a contacting layer in an all solid state structure. The various materials may be deposited as films on to an inert (or semiconducting) substrate or, alternatively, the ion selective material itself may serve as substrate where it exists in a suitable physical form (*eg* a wafer of ion sensitive glass).

The small size and weight of such a sensor, and its all solid state construction will offer the high degree of mechanical robustness which is characteristic of microcircuits. The absence of a filling solution will offer further advantages, especially for operation at high temperatures and pressures. The inherent small size of the device (and hence small stray capacitance) will be valuable in biomedical and other applications involving wide bandwidth measurement[11]. The microelectronic approach will enable other useful developments such as the provision of preamplifier circuitry in close proximity to the active material to reduce electrical noise pick up and offer a low impedance output. Furthermore, it will be possible to provide compensation for temperature drift by the incorporation of a temperature sensor in close thermal contact with the ion sensitive material, a technique well known in microcircuit design[17]. In the longer term, it will be possible to incorporate several different ion selective elements into a single small structure, as suggested by Moss *et al*[12]. This would lead to a reduction in the size and cost of the pipework, filters, *etc* associated with the electrode system in applications such as water quality monitoring.

3. ION SENSITIVE FIELD EFFECT TRANSISTORS

One type of microelectronic ion sensitive device which has been described by several workers[9–12] is the ion sensitive field effect transistor ('ISFET' or 'CHEMFET'). It is well known that variations in the threshold voltage (V_T) of Insulated Gate Field Effect Transistors (IGFET) can be attributed (partly) to ionic species incorporated in the device during manufacture[18]. The principle of the ISFET is to employ this effect in a reproducible and reversible form to measure the activity of an ionic species in an aqueous solution to which the gate insulator is exposed.

Certain aspects of the accepted theory of conventional IGFET devices will now be summarised and will then be used to develop a qualitative model for the operation of the ISFET. An important deduction from this model will be that the time response and stability of the ISFET will depend on the mobilities of ions in the bulk ion-sensitive phase.

3.1 *Summary of IGFET theory*

Figure 1(a) is a cross section of a conventional *n*-channel IGFET. The input variable is the gate-substrate voltage (V_{GS}). When this is made sufficiently large, in the positive sense, then the potential energies of electrons and 'holes' at the semiconductor surface, just beneath the insulator, are modified in such a way that the electron concentration increases and the 'hole' concentration decreases with respect to the thermal equilibrium values. An 'inversion layer' of electrons is created and the semiconductor surface region takes on the character of an *n*-type semiconductor. Electrical conduction is then possible between the *n*-type source and drain regions, the extent of conduction depending on the concentration of free electrons in the channel region, which in turn depends on V_{GS}. The output quantity of the device is the drain-source current (I_{DS}). This is a function of V_{GS} and also of the drain-source voltage (V_{DS}), as shown in

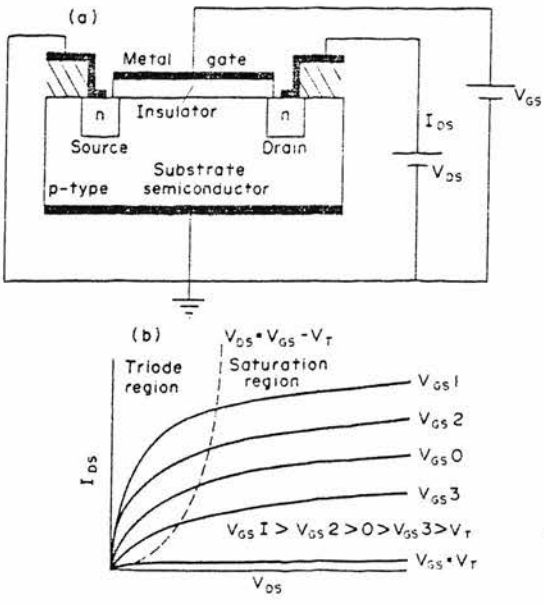

Fig. 1. Conventional IGFET. (a) Structure. (b) Output characteristics.

the typical 'output characteristics' of Fig. 1(b). The threshold voltage (V_T) is the value of V_{GS} for which I_{DS} is reduced to zero.

The non-linear dependence of I_{DS} on V_{DS} is a consequence of the potential gradient (due to V_{DS}) which exists between the source and drain regions (*ie* parallel to the semiconductor surface). This modifies the potential difference across the insulator which is therefore not constant throughout the gate area. A detailed analysis of the output characteristics in both the 'triode region' and the 'saturation region' will be found in text books on solid state devices[19]. All that is required to develop a model for the ISFET, however, is to understand that, for any given value of V_{DS}, I_{DS} depends on the concentration of free electrons in the channel and is thus directly relatable to V_{GS}. We will therefore restrict the analysis to the simpler triode region case ($V_{DS} \ll V_{GS}$) for which the potential throughout the source, drain and channel regions may be taken as that of the bulk semiconductor.

In the 'ideal' metal–insulator–semiconductor (MIS) structure of Fig. 2 it is assumed that there are no electronic surface states at the semiconductor–insulator interface and no electronic states or tapped charge in the insulator, which is assumed to be a perfect insulator. Furthermore, the work functions of metal and semiconductor are assumed to be equal. Figure 2(b) shows an electron energy band diagram for this device under the condition $V_{GS} = 0$ (zero gate-substrate voltage). The Fermi levels in the metal and semiconductor are the same and the conduction and valence bands are level throughout the semiconductor. Hence the electron and hole densities at the semiconductor surface are identical to their bulk values and no conduction is possible between source and drain owing to reverse bias of the p–n junction between the drain and the channel. We now suppose the gate is made positive with respect to the substrate ($V_{GS} > 0$) by means of a suitable external emf (Fig. 2c). The Fermi level in the metal is thus displaced by an amount eV_{GS} below the value in the semiconductor. The system acts somewhat like a capacitor with electrostatic charges being established in the metal (positive charge) and semiconductor (negative charge) phases. The charge in the metal may be regarded as a surface 'sheet' charge but the distribution in the semiconductor is more complex owing to the relatively low density of charge carriers in this material and consequently large Debye length. (Analogous to the complex distribution of charge in a dilute solution, adjacent to a charged electrode). The charge distribution is analysed in standard text books on semiconductor devices[19] and will not be repeated in detail here. It is usual to distinguish two distinct regions, a 'depletion region' and an 'inversion layer', approximated by the square sided distributions Q_d and Q_i in Fig. 2(d). The relatively broad depletion region comprises ionised 'acceptor' atoms which are not mobile. The much narrower inversion layer consists of mobile electrons which contribute to channel conductivity. It can furthermore be shown[19] that, once the depletion charge is established, further increases in V_{GS} have little effect on the depletion region, the change in Q_m being matched by an almost equal change in Q_i. The gate voltage required to establish the depletion region (which does not contribute to channel conductivity) is known as the threshold voltage (V_T) and is a constant of the device.

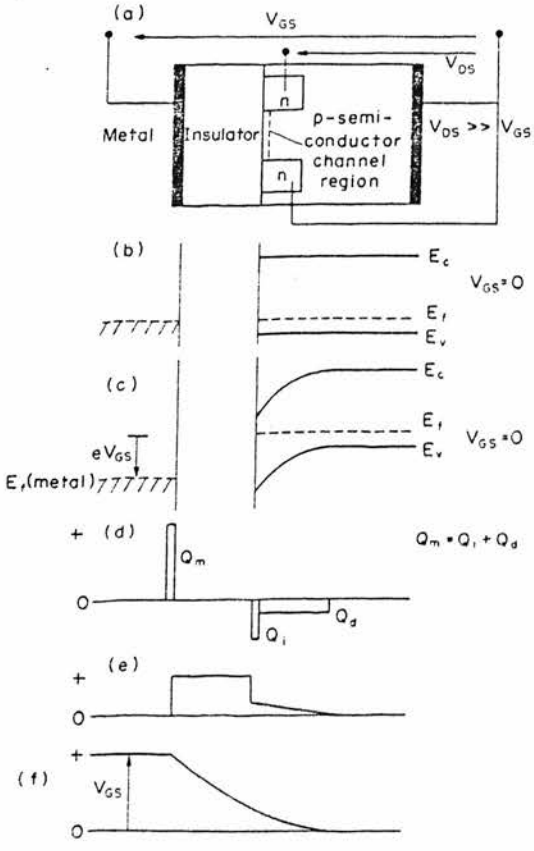

Fig. 2. Ideal MIS device. (a) Structure. (b), (c) Band diagrams. (d) Charge distribution. (e) Electric field. (f) Electric potential. After Sze[19].

The electric field and potential distributions associated with this charge distribution are shown in Figs 2(e) and 2(f), the existence of a potential gradient inside the semiconductor being related to the 'band bending' shown in Fig. 2(c). The creation of the inversion layer results in the semiconductor surface becoming effectively n-type in the channel region and allows conduction to take place between the source and drain regions to an extent determined by the magnitude of V_{GS}.

Practical MIS devices usually exhibit various non-ideal features including metal-semiconductor work function difference, electronic surface states at the semiconductor–insulator interface and the presence of ionic charge in the insulator. These effects contribute to the semiconductor surface charge and are usually described as additional components of the 'threshold voltage' by considering the change in gate-substrate voltage which would cause an opposing effect sufficient to restore the condition of Fig. 2(b), in which the electron energies at the conduction and valence band edges are constant throughout the semiconductor phase. The case of an MIS device having ionic charge in the insulator has obvious similarities with that of an ISFET in which transfer of ionic species between the solution and insulator is involved. There are also significant differences, however, as will be shown below. The standard analysis of insulator charge for the straightforward MIS case, first proposed by Snow *et al*[20], will now be outlined.

The analysis assumes that a layer of positive charge (*eg* Na^+ ions) has been incorporated in the insulator during manufacture. For the purposes of the analysis this charge is assumed to be fixed and is not considered to be in equilibrium with any other material phase. The potential of the metal gate is assumed to be referred to that of the semiconductor through an external electrical connection, the case of a short circuit ($V_{GS} = 0$) being used for simplicity (Fig. 3(a)). Since the insulator charge is fixed and the insulator is perfect, the interaction between the insulator charge and the semiconductor is purely electrostatic in nature and may be deduced by considering the image charges induced in the metal and the semiconductor. For a given value of insulator charge (Q_o) and using the boundary condition $V_{GS} = 0$, the charge, field and potential diagrams are, to a first approximation, as shown in Figs 3(b), (c) and (d). The effect on the semiconductor surface charge depends on the magnitude of the lamina Q_0 and its position with respect to the metal and semiconductor interfaces. The effect of a diffuse distribution may of course be found by straightforward integration). The presence of an inversion layer when $V_{GS} = 0$ contributes to the threshold voltage (V_T) of the MIS device. In practice, the 'fixed' insulator charges may have some degree of mobility in the insulator (usually small at room temperature but more rapid under conditions of 'voltage bias/temperature stress')[20]. This explains the drift of threshold voltage which is sometimes observed.

3.2 *A model for the ISFET device*

Figure 4(a) shows an ISFET device. It may be regarded as an IGFET in which the metal gate is absent and the gate insulator is an appropriate ion-sensitive material. The device is encapsulated in such a way that only the material above the channel is exposed to aqueous solution, electrical leakage paths to the source, drain or substrate regions being prevented. Devices of this type, employing various materials as the chemically sensitive layer, have been reported by several workers[9–12] and have been made in our own laboratory. Drain-source characteristics similar to those of the IGFET have been observed, the parameter in this case being the solution activity of the ion to which the device is sensitive (Fig. 4b).

For the purposes of analysis it will be assumed that the ion-sensitive material does not support electronic conduction and that an ion exchange reaction takes place at its surface when in contact with an ionic solution. A glass of the type used in the conventional ion selective glass electrode would, of course, fit this description. It is now generally accepted, following the work of Eisenman and others[1], that the potential (V_M) of the glass membrane electrode originates in ion exchange reactions at the glass–solution interfaces which give rise to phase boundary potentials (V_{PB1}, V_{PB2}) as shown in Fig. 5(a). In the two-ion exchange case, such as a Na^+ electrode which is also sensitive to H^+, a diffusion potential (V_D) also occurs, in the bulk glass phase[21] (Fig. 5b).

Figure 6(a) represents an ISFET device exposed to an aqueous solution. The electrical potential of the solution with respect to the semiconductor is defined by means of a suitable reference electrode and an external electric circuit, represented generally by the parallel combination of resistance (R_{EXT}) and capacitance (C_{EXT}). We will consider first the extreme case in which the impedance of the external circuit is infinite, ie $R_{EXT} \rightarrow \infty$, $C_{EXT} \rightarrow 0$. The distribution of

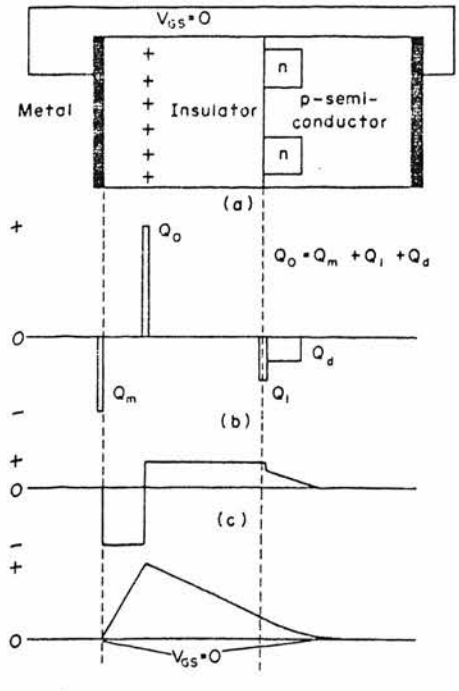

Fig. 3. MIS device with insulator charge. (a) Structure. (b) Charge distribution. (c) Electric field. (d) Electric potential.

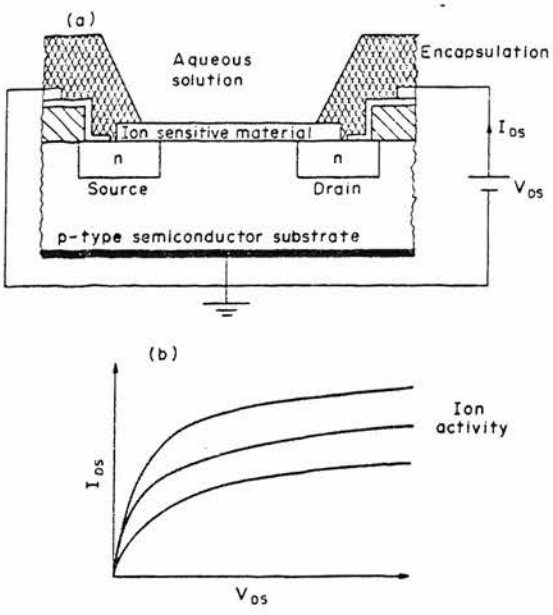

Fig. 4. ISFET (or CHEMFET). (a) Structure. (b) Characteristics.

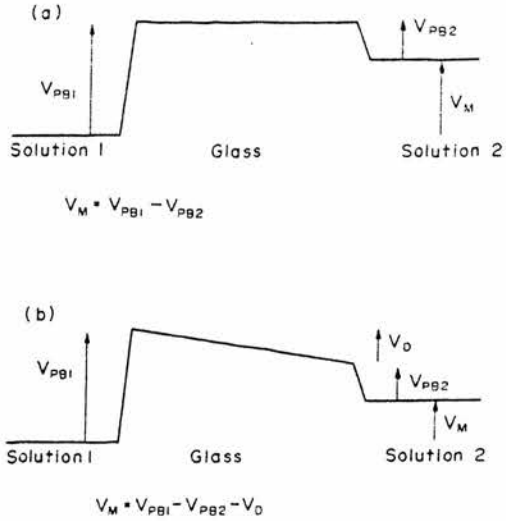

Fig. 5. Glass membrane electrode electric potential distributions. (a) Single-ion exchange. (b) Two-ion exchange.

electrical potential for this case is suggested in Fig. 6(b). The reference electrode potential, V_{REF}, is the *pd* between the bulk solution phase and the external circuit and is assumed to be constant. V_{PB} is the phase boundary potential due to ion exchange. This is a thermodynamically defined potential which is a function of the solution ionic activity and may be calculated by exactly the same method as used by Karreman and Eisenman[22] for each surface of a membrane electrode. (Note however that constants, such as the standard chemical potential of ions in the glass phase and the concentration of ion exchange sites, are explicit in the expression obtained. In the membrane case they cancel out of the expression for the total potential, as a result of the symmetry of the two interfaces). We note that the existence of a constant *potential* here constitutes a significantly different situation from that in the analysis of the IGFET, where a fixed *charge* in the insulator is assumed. The form of the potential distribution in the phase boundary region is not determinable by thermodynamic reasoning but we will assume that the extent of this region is small compared with the thickness of the ion sensitive layer. If, for simplicity, we consider the case of single ion exchange (similar to Fig. 5a) then there will be no diffusion potential in the bulk ion sensitive material.

We must now assume that there is no potential determining mechanism (*ie* no transference of any charged species, ionic or electronic) at the insulator-semiconductor interface. The interaction between the phase boundary process and the semiconductor is therefore purely electrostatic in nature, as in the case of the IGFET.* For the case where the impedance of the external circuit is effectively infinite the entire *pd* due to the phase boundary and reference electrode potentials is developed across the (infinite) external impedance as shown in Fig. 6(b). The development of a *pd* between the semiconductor 'contact' on one face of the ion sensitive membrane and a reference electrode in the test solution is analogous to the development of a *pd* between the inner and outer reference electrodes in a membrane electrode, under open circuit conditions. Notice, however, that the constancy of electric potential through the insulator semiconductor interface (Fig. 6b) implies that there is no field or excess charge at the semiconductor surface due to the effect of V_{PB} and hence no dependence of channel conductivity on solution ionic activity. It must be mentioned at this point that use of an ISFET without a reference electrode (as suggested by Bergveld[9]) is equivalent to the case of infinite external impedance, provided there are no electrical leakage paths or stray capacitances between the semiconductor and the solution. In practice, the condition of infinite external impedance is difficult to achieve, es-

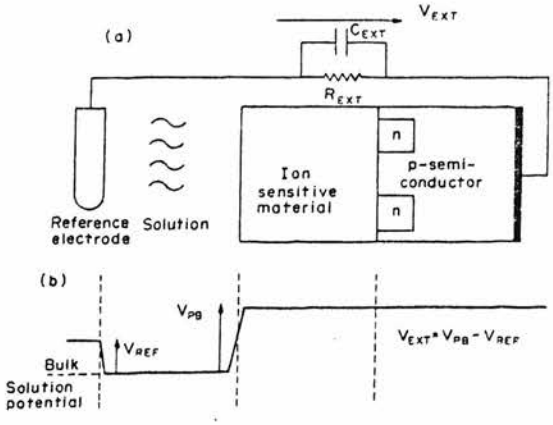

Fig. 6. ISFET operation, open circuit conditions. (a) Structure. (b) Electric potential distribution.

* It is important to realise that if any such mechanism for charge transfer were present, then the device would not be operating in any sense by a 'field effect' but would rather be functioning as a rather complicated type of electrode with undefined mechanism.

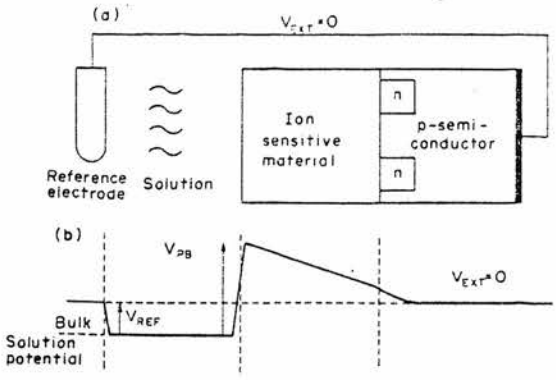

Fig. 7. ISFET operation, short circuit conditions. (a) Structure (b) Electric potential (transient).

pecially in respect of 'stray' capacitance. If we suppose C_{EXT} (Fig. 6a) to have a finite value of the same order as the capacitance of the bulk insulator and semiconductor surface, then charges will appear on the external capacitor and the semiconductor surface and the device will show a response. The magnitude of such response will clearly depend on the values of the external circuit components (V_{REF} and C_{EXT}) and would be stable only when these are properly defined, and not parasitic components. It is interesting that Bergveld *et al.*, in a recent paper[23], introduced the concept of capacitive coupling between the device and solution.

We will now consider the case (Fig. 7a) where the external electrical connection comprises a short circuit between the semiconductor and the reference electrode ($R_{EXT} = 0$). The electrical potential diagram appears in Fig. 7(b). The phase boundary and reference electrode potentials are the same as previously but, due to the constraint imposed by the external connection, the sum of these potentials is now developed across the insulator and the semiconductor surface (the bulk semiconductor must be field free under zero current conditions). Clearly, the channel conductivity is dependent on V_{PB} and hence the device will respond to changes in solution ionic activity.

We see from Fig. 7(b) that a fundamental characteristic of ISFET (and IGFET) operation is the existence of an electric field in the insulator. This field will exert a force on any charged (ionic) species present. In the case of the IGFET, such species are eliminated by careful manufacturing methods. The ion selective materials used in the ISFET however may well contain such species as an essential feature of their structure (*eg* silicate pH glasses). Provided the ionic mobility in the insulator is not negligible, drift of the ions will take place with the development of space charge and a diffusion potential in the bulk insulator. A similar effect is, of course, observed in glass membrane electrodes under short circuit conditions. Equilibrium will only be reached when the electrochemical potential of the ionic species is constant throughout the solution and glass phases. Hence the equilibrium value of channel conductivity will differ from the transient value and the response time of the device will depend on ionic mobility in the insulator. If this is low, as in silicon dioxide and most silicate glasses, then a slow drift of the output would be expected. Leistiko[10] has in fact observed an initial transient followed by a slow response and has also shown that the output may be dependent on the device history. Similar results have been obtained in our own laboratory. We must note, however, that experimental results in this field must be interpreted cautiously as observed time constants could well be associated with effects associated with phase boundary process itself. This is especially relevant when the ion sensitive material is one whose properties, even in membrane form, are not well known (*eg* thermally grown silicon dioxide, as used by Bergveld[9], Leistiko[10] and ourselves). The effects of even low levels of electrical leakage or stray capacitance can also be significant but difficult to identify. Further experimental work is therefore required.

Threshold voltage drift due to ion migration in MIS devices can be greatly reduced by including in the device structure an additional layer of material as an ion barrier. The use of silicon nitride for this purpose is now standard practice in semiconductor work[24]. The ISFET devices reported by Matsuo and Wise[11] (Fig. 8a) and by Moss, Janata and Johnson[12] (Fig. 8b) employed a nitride layer. Matsuo and Wise[11] reported a stable Nernstian response to pH (and much smaller sensitivity to Na^+ and K^+), the sensing mechanism presumably being associated with the nitride–solution interface. The stability may be explained by the low mobility of ions in silicon nitride.

The situation is more complex when the ion-sensitive material is deposited as an additional layer on top of the nitride. If this layer is sufficiently thick that there is a substantial depth of bulk material beneath the region associated with the phase boundary process, then polarisation effects would be expected to take place due to the electric field present

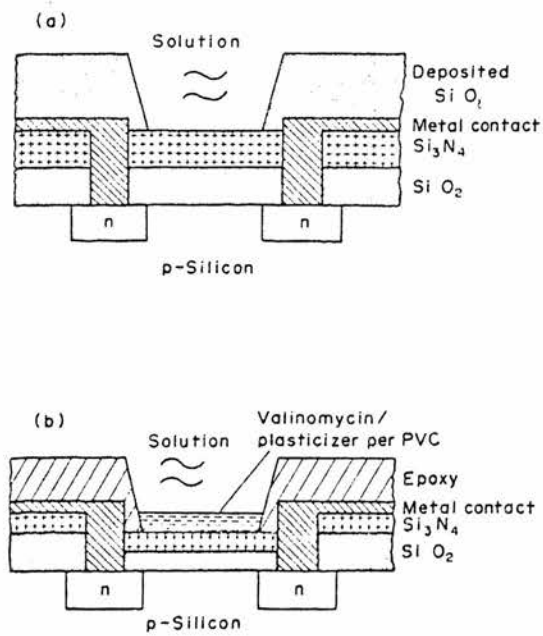

Fig. 8. ISFETs employing silicon nitride. (a) pH sensitive device (after Matsuo and Wise[11]). (b) K^+ sensitive device (after Moss, Janata and Johnson[12]).

in that region, in a similar manner to that described above. The time constants involved would depend on the ionic mobilities in the bulk ion sensitive material. The device due to Moss, Janata and Johnson[12], was of this type, employing a K^+ sensitive layer of valinomycin–plasticizer–PVC deposited on top of a nitride layer. It is interesting that these workers reported a good stability of response during a substantial period of approx 200 h following an initial hydration period. After this an increase in response time was observed, followed by device failure. The explanation of these results will require more detailed study of the transport processes in this type of ion sensitive material.

We will now summarise the important deductions about ISFET operation which follow from this model. Firstly, a properly defined reference electrode will be required for stable operation. Secondly, no process for charge transfer between the insulator and semiconductor phases has been assumed. (The existence of any such process would permit conduction through the device, which would no longer operate in a field-effect mode). Electrical continuity between the phase boundary process and the semiconductor surface is by a purely electrostatic (field effect) mechanism. The existence of this field within the insulator implies that the ionic species are not in thermodynamic equilibrium throughout the device. The response time and/or stability of the device will therefore be dependent on the rates of transport processes in the insulator. These may be modified by the inclusion of an ion barrier layer such as silicon nitride but if a layer of ion sensitive material is deposited on top of the barrier then the rates of polarisation effects in this material must also be considered with regard to their effect on response time and stability.

4. ALTERNATIVE MICROELECTRONIC APPROACHES

Provided it can be shown to be stable throughout a practical working lifetime, the ISFET offers one solution to the problem of solid state connection. The field effect mechanism is equivalent to an extremely high impedance amplifier placed in intimate contact with the potential determining material. ISFET production however requires the use of full silicon processing facilities. This leads to an essentially very small device to which connection must be made by the fine wire bonding techniques used in integrated circuit manufacture. There are severe problems in encapsulating such devices to effectively eliminate electrical leakage and chemical attack after long exposure to aqueous solutions.

It is probable that the solid state connection required for a microelectronic electrode can be implemented by techniques alternative to the ISFET. We recall that solid connection has been employed with several electrode types including glass[25, 26], liquid ion exchange/PVC[27] and metal–salt[28] varieties. Such electrodes are similar to the membrane type in that they form potential sensing systems in which a voltmeter of sufficiently high input impedance is used to measure the total potential due to the series combination of the electrode–solution interface, solid state back contact and external reference electrode. They may be regarded as membrane electrodes in which the functions of the internal membrane–solution interface and the internal reference electrode are both provided by the solid state connection.

For use in field or industrial applications the device must provide a reasonably stable output (*ie* constant E_0 value) over an extended period. This requires the back contact to be a thermodynamically definable 'half-cell' able to supply a small but continuous input current to the amplifier. Buck and Shepard[28] and Koebel[29] have considered the thermodynamics of the solid connection for metal salt and mixed metal sulphide electrodes respectively. Smith, Genshaw and Greyson[30] have also indicated the requirement for a thermodynamically defined connection in the context of coated wire electrodes. They have further suggested that, using very high input impedance amplifiers, a measurable electrode response may be obtained even when the connection is not well defined, although long term drift of E_0 would be expected in such cases. Glass electrodes employing metal connection have also been reported by several workers [25, 26] and the problem of long term drift of E_0 has been demonstrated by Guignard and Friedman[26]. Exactly similar conclusions will obtain in any situation where the potential determining mechanism involves an interfacial reaction at the surface of a medium which is not electronically conducting. In such cases, ion-electron interaction must take place at the back contact which interfaces the ionically conducting phase to an electronic conductor and hence to the external circuit.

The development of a stable solid state contact is therefore essential for a microelectronic electrode based on the potential sensing (as opposed to field effect) method. This problem is currently under investigation for the case of glass electrodes.

5. CONCLUSION

It has been shown that techniques developed for the manufacture of microcircuits may be employed in the development of new forms of ion sensitive electrode, which may offer improvements especially in respect of physical size and durability.

A necessary feature of these devices will be the use of a completely solid state connection to the sensitive material instead of the conventional inner filling solution. This could be achieved either by a 'field effect' connection, as in ISFET type devices, or by the provision of a suitable thermodynamically defined solid phase contact.

A model has been described for the ISFET device and leads to the important conclusion that the response and stability of the device will depend on the mobility of charged species in the ion sensitive material.

The requirements for a thermodynamically defined solid phase contact are now under investigation in this laboratory with the objective of developing an all solid state transducer, using the film deposition methods of hybrid microcircuits.

Acknowledgements—The author wishes to thank his colleagues, Dr A. E. Owen and Dr J. R. Jordan, for many hours of invaluable discussion.

This paper was presented at the *Winter Meeting of the Electrochemical Group of the Chemical Society*, held at the University of Newcastle upon Tyne, 7th–9th January 1976.

REFERENCES

1. G. Eisenman (ed.), *Glass Electrodes for Hydrogen and Other Cations*. Marcel Dekker, New York (1967).
2. J. W. Ross, Jr, Solid state and liquid membrane ion selective electrodes. In *Ion Selective Electrodes*. (R. A. Durst, ed.). N.B.S. Special Pub. 314.
3. A. K. Covington, Heterogeneous membrane electrodes. *op. cit.*
4. G. J. Moody and J. D. R. Thomas, Response time behaviour of liquid ion exchanger and PVC matrix membrane ion selective electrodes. *Lab. Pract.* 475–480 Sept. (1974).
5. J. Koryta, Theory and applications of ion selective electrodes. *Anal. Chim. Acta* **61**, 329–411 (1972).
6. R. P. Buck, Ion selective electrodes, potentiometry and potentiometric titrations. *Analyt. Chem.* **46** (5), 28R–51R (1974).
7. R. A. Durst, Analytical techniques and applications of ion selective electrodes. In *Ion Selective Electrodes* (R. A. Durst, ed).. N.B.S Special Pub. 314.
8. *Orion Research Analytical Methods Guide*, 7th edn. May 1975.
9. P. Bergveld, Development, operation and application of the ion sensitive field effect transistor as a tool for electrophysiology. *IEEE Trans. Biomed. Engng*, **BME-19** (5), 342–351 (1972).
10. O. Leistiko, Jr., Progress with ion sensitive field effect transistors. *Tech. Univ. Lyngby, Res. Report* (1975).
11. T. Matsuo and K. D. Wise, An integrated field-effect electrode for biopotential recording. *IEEE Trans. Biomed. Engng* 485–487 (1974).
12. S. D. Moss, J. Janata and C. C. Johnson, Potassium ion sensitive field effect transistor. *Analyt. Chem.* **47** (13), 2238–2243 (1975).
13. G. J. Moody and J. D. R. Thomas, *Selective Ion Sensitive Electrodes*. Merrow Ltd, Watford (1971).
14. J. R. A. Beale, E. T. Emms and R. A. Hilbourne, *Microelectronics*. Taylor & Francis Ltd, London (1971).
15. M. L. Topfer, *Thick Film Microelectronics*. Van Nostrand & Reinhold Co., New York (1971).
16. L. Stern, *Fundamentals of Integrated Circuits*. Pitman, Bath (1968).
17. *Non-Linear Circuits Handbook*, pp. 179–185. Analog Devices Inc., (1972).
18. J. Mavor (ed.), *M.O.S.T. Integrated Circuit Engineering*. Peter Peregrinus Ltd, Stevenage (1973).
19. S. M. Sze, *Physics of Semiconductor Devices*. Wiley, New York (1969).
20. E. H. Snow, A. S. Grove, B. E. Deal and C. T. Sah, Ion transport phenomena in insulating films. *J. appl. Phys.* **36**, (5), 1664–1673 (1965).
21. R. H. Doremus, *Diffusion Potentials in Glass*. Ref. 1, Ch. 4.
22. G. Karreman and G. Eisenman, Electrical potentials and ionic fluxes in ion exchangers. *Bull. math. Biophys.* **24**, 413–427 (1962).
23. P. Bergveld, J. Wiersma and H. Meertens, Extracellular potential recordings by means of a field effect transistor without gate metal, called OSFET. *IEEE Trans. Biomed. Engng* **BME-23** (2), 136–144 (1976).
24. W. J. Kmeta and J. S. Nadan, Theory and practice of MOS processing techniques—1973. *IEEE Trans. Mnfr. Tech.*, **MFT-2** (2), 37–49 (1973).
25. M. R. Thompson, A metal connected glass electrode *Bur. Stds. J. Res.* **9**, 833–853 (1932).
26. J. P. Guignard and S. M. Friedman, Construction of ion-selective glass electrodes by vacuum deposition of metals *J. appl. Physiol.*, **29** (2), 254–257 (1970).
27. H. James, G. Carmack and H. Freiser, Coated wire ion-selective electrodes. *Analyt. Chem.* **44** (4), 856–857 (1972).
28. R. P. Buck and V. Rogers Shepard, Jr., Reversible metal-salt interfaces and the relation of second kind and 'All Solid-State Membrane Electrodes' *Analyt. Chem.* **46** (14), 2097–2103 (1974).
29. M. Koebel, Standard potentials of solid-state metal ion-selective electrodes. *Analyt. Chem.* **46** (11), 1559–1563 (1974).
30. M. D. Smith, M. A. Genshaw and J. Greyson, Miniature solid state potassium electrode for serum analysis. *Analyt. Chem.* **45** (9), 1782–1784 (1973).

APPENDIX 5: SUMMARY OF PROCESSING STAGES USED IN THE PRODUCTION OF ISFET DEVICES

1. Starting material

silicon wafers, 10-21 Ωcm, <111>, p-type

2. Clean wafer

degrease, 6 parts H_2O/2 parts H_2O_2/1 part NH_4OH (0.9 sg), 85°C, 20 min
wash, DI H_2O, 5 min
remove oxide, 5% HF, 10 sec
wash, DI H_2O, 5 min
oxidise, Analar HNO_3, 110°C, 15 min

3. Grow masking oxide

950°C, gas flows as set
dry O_2, 15 min
wet O_2, 80 min
dry O_2, 10 min

4. Photolithography, mask 1 (phosphorus diffusion)

photo-resist, Micro-image, 40 cps
spin on, 5000 rpm, 30 sec
air dry, 10 min
pre-bake, 80°C, 20 min
expose using polarising filter
develop, Micro-image developer, 45 sec
rinse, Micro-image rinse, 1 min
post-bake, 150°C, 30 min

5. Etch masking oxide

etchant, Micro-image SiO_2 etch, room temperature, time as per test-piece + 10% (approx 0.1 μm/min)

6. Strip photo-resist

strip, fuming HNO_3, room temperature, 20 min
wash, DI H_2O, 5 min
blow dry

7. Phosphorus pre-deposition

1050°C, N_2 main, 800 cc/min. O_2 through PO Cl_3, 50 cc/min
dope tube and boat prior to diffusion, 1 hour
load slices and introduce into furnace
pre-deposition, 45 min
N_2 main only, 3 min

8. Remove masking oxide

etchant, 10 parts 48% Aristar HF/90 parts DI H_2O

9. Clean wafer

oxidise, Analar HNO_3, 110°C, 15 min
remove oxide, 5% HF, 10 sec
wash, DI H_2O, 5 min
oxidise, Analar HNO_3, 110°C, 15 min
wash, DI H_2O, 5 min
spin dry, 5000 rpm

10. Grow thin oxide and drive-in phosphorus

950°C, gas flows as set
dry O_2, 15 min
wet O_2, 28 min (water at 95°C)

dry O_2, 10 min
N_2, 5 min
cool at neck of tube, N_2, 5 min

(nominal thickness, 0.2 μm)

11. High temperature anneal

1050°C, boil-off N_2, 3 ℓ/min
anneal, 30 min
cool at neck of tube, 10 min

12. Low temperature anneal

430°C, 60% N_2/40% H_2, 2 ℓ/min
anneal, 1 hour
cool at neck of tube, 10 min

13. Photolithography, mask 2 (contact holes)

as Stage 4

14. Etch contact holes and remove oxide from back of wafer

as Stage 5

15. Strip photo-resist

strip, fuming HNO_3, room temperature, 10 min
ditto, using fresh HNO_3
wash, DI H_2O, 5 min
spin dry

16. Metallise front of wafer

evaporate aluminium

(nominal thickness, 0.4 μm)

17. Photolithography, mask 3 (metallisation)

photo-resist, Shipley AZ 1350 H
spin on, 5000 rpm, 30 sec
air dry, 10 min
pre-bake, 80^{o}C, 20 min
expose
develop, Shipley developer, 45 sec
rinse, DI H_2O, 30 sec
post-bake, 150^{o}C, 30 min

18. Etch aluminium

etchant, Micro-image aluminium etch, room temperature

19. Strip photo-resist

as Stage 15

20. Metallise back of wafer

as Stage 16

21. Sinter aluminium

430^{o}C, 60% N_2/40% H_2, 2 ℓ/min
sinter, 25 min
cool at neck of tube, 10 min

APPENDIX 6: N-CHANNEL PROCESS EVALUATION

The ISFET devices described in Section 6.3 and Chapter 7 were fabricated using an n-channel MOS transistor process which was then being developed for the production of charge coupled devices. An extensive program of evaluation of IGFET devices which were produced using this process was carried out by the author[103,104]. Those aspects of the work which are relevant to the ISFET research will be briefly summarised here.

Test chips were specially designed for this purpose. They incorporated the following features:

- metal contacts to both 'front' and 'back' sides of the wafer to permit the assessment of the quality of contacts to the silicon substrate.
- metal contacts to diffused n-regions (which form the sources and drains of transistors), again for the evaluation of contact quality.
- p-n junction diode for the measurement of junction breakdown effects.
- thin oxide capacitor to allow the measurement of the capacitance-voltage (C-V) characteristics of the metal-oxide-silicon structure[88], as an indication of the threshold voltage (V_T) of the process. These capacitors were also used for the measurement of oxide breakdown voltages.
- conventional IGFET transistor structures having different geometries and aspect ratios ($^{W}/_{L}$).

Two silicon wafers were processed for the purposes of this work. The first was produced at the same time as the ISFET devices. The second wafer was manufactured several weeks later, to investigate the reproducibility of the fabrication process. Measurements were carried out on several chips from each wafer in order to obtain an indication of the 'yield' of the process and of the variation of parameters across the wafer. It was not possible to test sufficient devices to carry out a rigorous statistical analysis of the yield but the results for at least 50% of the measurements lay within the ranges quoted in Table A6.1. Devices for which the results lay outside these ranges were, in many cases, obviously 'faulty' (having very low breakdown voltages for example). In some cases however, threshold voltages of up to 10 V were observed in otherwise normally operating devices. Furthermore, the variations in V_T were observed over small dimensions, of the order of the size of a transistor. The values of the process constant, β, deduced from measurements on IGFET devices, lay within the range of 3 to 12 $\mu A/volt^2$ in the majority of cases. The median value was around 7 to 8 $\mu A/volt^2$ but the measured data were fairly well spread over the quoted range. These values for β were derived from measurements on devices of different geometries and aspect ratios and from measurements in both the 'triode region' and the 'saturation region'. There was some systematic relationship between these factors and the observed values of β, but random variations were dominant.

The threshold voltage, V_T, is a function of factors such as the density of electronic energy states at the silicon-oxide interface and the concentration of ionic impurities in the oxide[88]. These factors cannot be predicted from theoretical calculations. The value

metal-substrate contact:	non-rectifying[†]
metal-diffusion contact:	non-rectifying
p-n junction reverse breakdown voltage, V_B:	80 to 140 V
thin oxide breakdown voltage:	100 to 140 V
threshold voltage, V_T	
from C-V measurements:	-1 to -2 V
from IGFET measurements:	-1 to -2 V
process constant, β	
from IGFET measurements:	3 to 12 $\mu A/volt^2$
thin oxide capacitance, C_{ox}:	60 pF

[†]*The current-voltage characteristic of the wafer 'back contact' was somewhat non-linear, probably because the oxide was removed from this side of the wafer prior to the diffusion stage of the process and it was therefore doped n-type. The 'front contact' was non-rectifying however and front contacts were used in the ISFET work.*

Table A6.1 Summary of n-channel MOS characteristics

of β however is given by the equation[125]

$$\beta = \frac{\mu_e \varepsilon_{ox} \varepsilon_o}{t_{ox}} \qquad \text{(A6.1)}$$

where μ_e is the effective surface mobility of electrons (for an n-channel device), ε_{ox} and t_{ox} are respectively the dielectric constant and thickness of the oxide and ε_o is the permittivity of free space. Commonly used values for these constants are

$$\mu_e = 6.5 \times 10^{-2} \text{ m}^2 \text{ V}^{-1} \text{ s}^{-1}$$

$$e_{ox} = 3.9$$

$$e_o = 8.85 \times 10^{-12} \text{ Fm}^{-1}$$

The predicted oxide thickness for this process was 0.2 μm. Using these values in Equation A6.1, a value of 11 μA/volt^2 is obtained for β. The values of μ_e and t_{ox} used in this calculation are subject to considerable uncertainty however. The calculation of β from the measured IGFET characteristics involves the value of the aspect ratio, W/L, of the transistor. The latter quantity is also subject to uncertainties, which originate in the photolithographic and diffusion stages of the process. In view of these uncertainties, the agreement between the measured and calculated values of β is reasonable, although its variation across the wafer was greater than expected. The capacitance per unit area of the thin oxide can be predicted by the equation[125]

$$C_{ox} = \frac{\varepsilon_{ox} \varepsilon_o}{t_{ox}} \qquad \text{(A6.2)}$$

The capacitance of one of the thin oxide capacitors on the test chip was calculated, using Equation A6.2, as 57 pF which is in close agreement with its measured value of 60 pF, obtained from C-V data.

It was concluded that the important process parameters were reproducible between batches and reasonably consistent with their predicted values and that the process was adequate for the production of ISFET and conventional IGFET devices. It must be remembered however that the spread of β values across the wafer was rather large and that the yield was such that about 50% of devices had threshold voltages outside the range quoted in Table A6.1.

APPENDIX 7: TEMPERATURE CONTROLLER CIRCUIT

Figure A7.1 is a circuit diagram of the temperature controller referred to in Section 8.6. It is a 'proportional band' closed loop controller which delivers the maximum possible power to the heater element (R16 and R17) until the temperature of the oil bath, sensed by thermistor R(T), closely approaches the required set-point temperature, determined by VR2. The heater power is then progressively reduced to zero.

It can be easily shown that the resistances R4, R(T), R5, VR2 and R6 may be regarded as a bridge network, as a consequence of the action of the high gain, high input impedance amplifier, A2. Voltage V2 is therefore zero when the ratio of R4 to R(T) is equal to the ratio determined by R5, R6 and the 10 turn potentiometer, VR2, which is used to set the required temperature. It follows that V2 is independent of V1 when the set-point temperature is reached and the effect on circuit operation of small variations in V1 is minimised. When the temperature is below the set-point however, V2 has a positive value related to the difference between the required and actual temperatures. Voltage V1 is the driving voltage for the bridge network and must be sufficiently small to eliminate self-heating effects in the thermistor. It was set, by means of VR1, to a value of 770 mV in order to limit power dissipation in the thermistor to a maximum of 50 μW at 30^{o}C. The amplifier A3, together with its associated resistor network, provides a means of altering the gain of the controller, in the proportional

Components list

R1	220 Ω, ½W	VR1	2.2 KΩ preset
R2	10 KΩ, ¼W	VR2	1 KΩ w/w, 10 turn
R3	2.2 KΩ, ¼W	VR3	100 KΩ carbon, lin
R4	2.95 KΩ } thick film	C1	1 µF
R5	2.45 KΩ } matched resistor	C2	1 µF
R6	2.45 KΩ } network	C3	10 µF, electrolytic
R7	1 KΩ, ¼W	C4	10 µF, electrolytic
R8	1 KΩ, ¼W	C5	4.7 µF, electrolytic
R9	82 KΩ, ¼W	Z1	BZY88, 5.6 V
R10	1 KΩ, ¼W	Z2	BZY88, 2.7 V
R11	1 KΩ, ¼W	Z3	BZY88, 5.6 V
R12	10 KΩ, ¼W	D1	1N914
R13	1 MΩ, ¼W	A1	µA741
R14	10 KΩ, ¼W	A2	µA741
R15	1 KΩ, ¼W	A3	µA741
R16	100 Ω, 10 W } heater	A4	µA741
R17	100 Ω, 10 W } resistors	T1	BFY51
		T2	BFY51
		T3	2N3055
		R(T)	thermistor, ITT type F53D

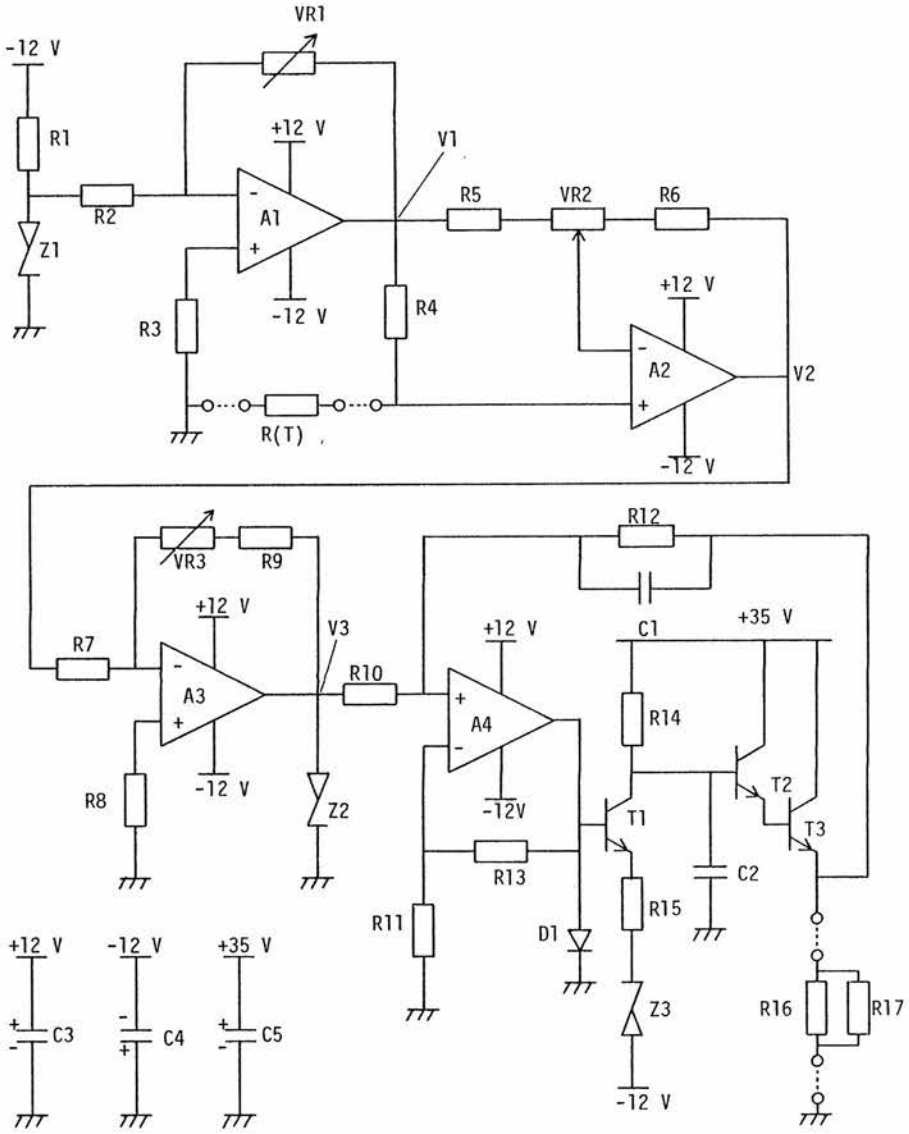

Figure A7.1 Temperature controller circuit

band. The setting of the front-panel control, VR3, was adjusted empirically to give optimum response time of the controlled temperature, without excessive overshooting. The remainder of the circuit provides the necessary power amplification to drive the heating element itself. The power rating of R16 and R17 (10 W each) dictates a maximum heater voltage of approximately 30 V, corresponding to a total current in T3 of 0.6 A. Amplifier A4 gives a large voltage gain and its output is further amplified by T1 to the voltage level required by the heater. The Darlington pair, T2 and T3, provide the necessary current driving capability. Overall negative feedback, via R12, is used to define a voltage gain of 10 between V3 and the heater. Capacitors C1 and C2 were added to stabilise the high gain feedback loop and diode D1 is required to prevent a 'latch-up' condition which can occur if the base of T1 becomes sufficiently positively biassed. The Zener diode, Z2, determines the maximum negative value of voltage V3 and hence limits the maximum voltage applied to the heater. The proportional band is entered when the actual temperature is between approximately 3 deg C and 5 deg C below the set-point temperature, depending on the setting of the gain control, VR3.

The circuit was constructed on a copper clad circuit board and housed in a cast aluminium box. Transistor T3 was attached to a substantial heat sink which was directly bolted to the box. The set-point and gain controls, VR2 and VR3, were made available as front-panel controls. A 4-wire cable was used to make connection between the control unit and the thermostat, separate earth returns

being used for the thermistor and the heater circuits. Connection was simplified by using a 4-way plug and socket where the cable entered the screened experimental enclosure. Power for the circuit was derived from standard laboratory power supplies.

REFERENCES

1 Light T S, 'Ion Selective Electrodes', Durst R A (ed), NBS Special Pub 314, Washington DC, 1969, Chapter 10.

2 Whitfield M, 'ASMA Handbook No 2', Australian Marine Sciences Association, Sydney, 1971.

3 Eisenman G (ed), 'Glass Electrodes for Hydrogen and Other Cations', Dekker, 1967, Chapters 15-19.

4 Warner T B, Marine Technology Soc J, 6 (2), 1972 pp24-33.

5 McClure J E and Rechnitz G A, Analyt Chem, 38 (1), 1966 pp136-139.

6 Durst R A, 'Ion Selective Electrodes', Durst R A (ed), NBS Special Pub 314, Washington DC, 1969, Chapter 11.

7 Cremer M, Z Biol 47, 1906 p562.

8 Haber F and Klemensiewicz Z, Z Physik Chem (Leipzig), 67, 1909 p385.

9 Durst R A (ed), 'Ion Selective Electrodes', NBS Special Pub 314, Washington DC, 1969.

10 Covington A K, 'Ion Selective Electrodes', CRC Critical Rev in Analyt Chem, Jan 1964 pp355-406.

11 Koryta J, 'Ion Selective Electrodes', Cambridge University Press, 1975.

12 'Orion Research Analytical Methods Guide', 7th ed, May 1975.

13 Beale J R A, Emms E T and Hilbourne R A, 'Microelectronics', Taylor and Francis, London, 1971.

14 Topfer M L, 'Thick Film Microelectronics', Van Nostrand, 1971.

15 Stern L, 'Fundamentals of Integrated Circuits', Pitman, 1968.

16 Bates R G, 'Determination of pH - Theory and Practice', Wiley, 1964 p299.

17 Zemel J N, Analyt Chem 47 (2), 1975 pp255A-268A.

18 Simpson R J, private communication.

19 Eisenman G, 'Advances in Analytical Chemistry and Instrumentation, Vol 4', Reilly C N (ed), Wiley, 1965 pp213-369.

20 Bockris J O'M and Reddy A K N, 'Modern Electrochemistry, Vol 2', MacDonald, London, 1970 p901.

21 Mattock G, 'Advances in Analytical Chemistry and Instrumentation, Vol 2', Reilly C N (ed), Wiley, 1963 pp35-121.

22 Bockris J O'M and Reddy A K N, 'Modern Electrochemistry, Vol 1', MacDonald, London, 1970.

23 Frant M S and Ross J W, Analyt Chem, 40 (7), 1968 pp1169-1171.

24 Mattock G and Band D M, 'Glass Electrodes for Hydrogen and Other Cations', Eisenman G (ed), Dekker, 1967, Chapter 1.

25 Covington A K, 'Ion Selective Electrodes', Durst R A (ed), NBS Special Pub 314, Washington DC, 1969.

26 Ives D J G and Janz G J (eds), 'Reference Electrodes', Academic Press, London, 1961 p55.

27 Bates R G 'Determination of pH - Theory and Practice', Wiley, 1964 p311.

28 Eckfeldt E L and Perley G A, J Electrochem Soc, 98 (2), 1951 pp37-47.

29 Buck R P, J Electroanal Chem, 18, 1968 pp363-380.

30 Buck R P, J Electroanal Chem, 18, 1968 pp381-386.

31 Buck R P and Krull I, J Electroanal Chem, 18, 1968 pp 387-399.

32 Brand M J D and Rechnitz G A, Analyt Chem, 41 (13), 1969 pp1788-1793.

33 Hinke J A M, 'Glass Electrodes for Hydrogen and Other Cations', Eisenman G (ed), Dekker, 1967, Chapter 17.

34 Diamond J J and Hubbard D, J Res Nat Bur Std, 47 (6), 1951 pp443-448.

35 Bates R G, 'Determination of pH - Theory and Practice', Wiley, 1964 pp319-322.

36 ibid, pp315-319.

37 ibid, pp299-302.

38 Eisenman G, Rudin D O and Casby J U, Science, 126, 1957 pp831-834.

39 MacInnes D A and Dole M, J Am Chem Soc, 52 (1), 1930 pp29-36.

40 Isard J O, 'Glass Electrodes for Hydrogen and Other Cations', Eisenman G (ed), Dekker, 1967, Chapter 3.

41 Disteche A and Dubuisson M, Rev Sci Instr, 25, 1954 pp869-875.

42 Rechnitz G A and Kugler G C, Analyt Chem, 39 (14), 1967 ppl682-1688.

43 Isard J O, Phys Chem Glasses, 17 (1), 1976 ppl-6.

44 Eisenman G, 'Glass Electrodes for Hydrogen and Other Cations', Eisenman G (ed), Dekker, 1967, Chapter 5.

45 Portnoy H D, ibid, Chapter 8.

46 Bates R G, 'Determination of pH - Theory and Practice', Wiley, 1964 p297.

47 Khuri R N, 'Glass Electrodes for Hydrogen and Other Cations', Eisenman G (ed), Dekker, 1967, Chapter 18.

48 Ross J W, 'Ion Selective Electrodes', Durst R A (ed), NBS Special Pub 314, Washington DC, 1969, Chapter 2.

49 Orion Research Newsletter, 4 (3 and 4), 1972.

50 Wyatt P A H, 'Energy and Entropy in Chemistry', Macmillan, 1967.

51 Koryta J, 'Ion Selective Electrodes', Cambridge University Press, 1975 p9.

52 Sparkes J J, 'Junction Transistors', Pergamon, 1966 p18.

53 Doremus R H, J Phys Chem, 68 (8), 1964 pp2212-2218.

54 Bockris J O'M and Reddy A K N, 'Modern Electrochemistry, Vol 2', MacDonald, London, 1970 p811.

55 Koryta J, Dvorak J and Bohackova V, 'Electrochemistry', Methuen, 1970 p145.

56 Koryta J, 'Ion Selective Electrodes', Cambridge University Press, 1975 p20.

57 Teorell T, 'Progress in Biophysics and Biophysical Chemistry, Vol 3', Butler J A V and Randall J T (eds), Pergamon, 1953.

58 Teorell T, J Gen Physiol, 19, 1936 p917.

59 Meyer K H and Sievers J F, Helv Chim Acta, 19, 1936 pp649-664.

60 Meyer K H and Sievers J F, Helv Chim Acta, 19, 1936 pp665-677.

61 Meyer K H and Sievers J F, Helv Chim Acta, 19, 1936 pp987-995.

62 Meyer K H, Helv Chim Acta, 20, 1937 pp634-644.

63 Koryta J, 'Ion Selective Electrodes', Cambridge University Press, 1975 p12.

64 Teorell T, Z Elektrochem, 55, 1951 p460.

65 Conti F and Eisenman G, Biophys J, 5, 1965 pp247-256.

66 Eisenman G, Biophys J, 2 (2), 1962 pp259-323.

67 Karreman G and Eisenman G, Bull Math Biophys, 24, 1962 pp413-427.

68 Conti F and Eisenman G, Biophys J, 5, 1965 pp511-530.

69 Dole M, 'The Glass Electrode', Wiley, 1941 pp272-274.

70 Koryta J, 'Ion Selective Electrodes', Cambridge University Press, 1975 p108.

71 Nicolsky B P, Shultz M M and Belijustin A A, 'Glass Electrodes for Hydrogen and Other Cations', Eisenman G (ed), Dekker, 1967, Chapter 5.

72 Buck R P, Analyt Chem, 45 (4), 1973 pp654-665.

73 Buck R P, Boles J H, Porter R D and Margolis J A, Analyt Chem, 46 (2), 1974 pp255-261.

74 Thompson M R, Bureau of Standards J Res, 9, 1932 pp 833-853.

75 U S Patent 2 117 596.

76 Friedman S M, 'Glass Electrodes for Hydrogen and Other Cations', Eisenman G (ed), Dekker, 1967, Chapter 16.

77 Gebert G and Friedman S M, J Appl Physiol, 34 (1), 1973 pp122-124.

78 Guignard J-P and Friedman S M, J Appl Physiol, 29 (2), 1970 pp254-257.

79 U K Patent 1 018 024.

80 U S Patent 3 306 837.

81 U K Patent 1 260 065.

82 Koebel M, Analyt Chem, 46 (11), 1974 pp1559-1563.

83 Buck R P and Rogers-Shepard V, Analyt Chem, 46 (14), 1974 pp2097-2103.

84 Freiser H, Research/Development, December 1976 pp28-33.

85 James H, Carmack G and Freiser H, Analyt Chem, 44 (4), 1972 pp856-857.

86 Smith M D, Genshaw M A and Greyson J, Analyt Chem, 45 (9), 1973 pp1782-1784.

87 Zemel J N, Analyt Chem, 47 (2), 1975 pp255A-268A.

88 Sze S M, 'Physics of Semiconductor Devices', Wiley, 1969.

89 Cobbold R S C, 'Theory and Applications of Field Effect Transistors', Wiley, 1970.

90 Moss S D, Janata J and Johnson C C, Analyt Chem, 47 (13), 1975 pp2238-2243.

91 Janata J and Moss S D, Biomed Eng, July 1976 pp241-245.

92 Buck R P and Hackleman D E, Analyt Chem, 49 (14), 1977 pp2315-2321.

93 Bergveld P, IEEE Trans Biomed Eng, BME-19 (5), 1972 pp342-351.

94 Graf R and Graf H, Helv Odont Acta, 15, 1971 pp42-50.

95 Wilde P and Rodgers P W, Rev Sci Inst, 41 (3), 1970 pp356-359.

96 Garrels R M, 'Glass Electrodes for Hydrogen and Other Cations', Eisenman G (ed), Dekker, 1967, Chapter 13.

97 Linzell J L, personal communication.

98 Dole M, 'The Glass Electrode', Wiley, 1941, p89.

99 Donaldson P E K, IEEE Trans Biomed Eng, BME-23 (4), 1976 pp281-285.

100 Mackay R S, 'Biomedical Telemetry', Wiley, 2nd ed, 1970, Chapter 4.

101 White M L, Proc IEEE, 57 (9), 1969 pp1610-1615.

102 Licari J J and Brands E R, 'Handbook of Materials and Processes for Electronics', Harper C A (ed), McGraw Hill, 1970, Chapter 5.

103 Kelly R G, 'Microelectronics Unit - MOS N-Channel Process Evaluation', Univ Edin Dept Elect Eng internal report, September 1974.

104 Kelly R G, 'Microelectronics Unit - MOS N-Channel Process Evaluation (Continued)', Univ Edin Dept Elect Eng internal report, February 1975.

105 Raider S I, Gregor L V and Flitsch R, J Electrochem Soc, 120 (3), 1973 pp425-431.

106 Burger R M and Donovan R P, 'Fundamentals of Silicon Integrated Device Technology, Vol 1', Prentice-Hall, 1967.

107 Berg H, personal communication.

108 Crawford R H, 'MOSFET in Circuit Design', McGraw Hill, 1967 p34.

* 109 Camoes M F G F C and Covington A K, Analyt Chem, 46 (11), 1974 pp1547-1551.

110 Keithley Instruments Inc, 'Model 610C Solid State Electrometer Instruction Manual'.

111 Bates R G, 'Determination of pH - Theory and Practice', Wiley, 1964 pp327-330.

112 Perley G A, Analyt Chem, 21 (5), 1949 pp559-562.

113 Eckfeldt E L and Proctor W E, Analyt Chem, 47 (13), 1975 pp2307-2309.

114 Eckfeldt E L and Proctor W E, Analyt Chem, 43 (3), 1971 pp332-337.

115 Janz G J, 'Reference Electrodes', Ives D J G and Janz G J (eds), Academic Press, London, 1961, Chapter 4.

116 Ives D J G and Janz G J (eds), 'Reference Electrodes', Academic Press, London, 1961.

117 Hills G J and Ives D J G, ibid p130.

118 Mattock G and Band D M, 'Glass Electrodes for Hydrogen and Other Cations', Eisenman G (ed), Dekker, 1967 p18.

119 Mattock G, 'Advances in Analytical Chemistry and Instrumentation, Vol 2', Reilly C N (ed), Wiley, 1963 p54.

120 Koryta J, 'Ion Selective Electrodes', Cambridge University Press, 1975, Chapter 2.

121 Haffeman D R, J Phys Chem, 69 (12), 1965 pp4226-4231.

122 McGillivray A D, J Chem Phys, 48 (7), 1968 pp2903-2907.

123 Okongwu D A, Lu W-K, Hamielec A E and Kirkaldy J S, J Chem Phys, 58 (2), 1973 pp777-787.

124 Cooper A R, J Non-Crystalline Solids, 14, 1974 pp65-78.

125 Mavor J (ed), 'MOST Integrated Circuit Engineering', Peter Peregrinus Ltd, Stevenage, 1973.

* ERRATUM

Throughout the text, reference 109 is incorrectly ascribed to 'Filomena et al'.